Predictors of cognitive recovery in paediatric autoimmune encephalitis

Charly Billaud

Doctor of Philosophy

ASTON UNIVERSITY

March 2023

Aston university

Predictors of cognitive recovery in paediatric autoimmune encephalitis

Charly Billaud

Doctor of Philosophy

March 2023

Thesis Abstract

Paediatric autoimmune encephalitis (AE) is an inflammatory brain disease associated with acute cognitive and behavioural difficulties, seizures, magnetic resonance imaging (MRI) and electroencephalography abnormalities. Some children with AE experience difficulties years after acute illness, but identifying those at high risk is difficult; factors able to predict them are needed. Advanced neuroimaging methods including magnetoencephalography (MEG) and quantitative measures of structural magnetic resonance imaging (MRI; for example cortical thickness) are promising tools with which to predict neurobehavioural outcome. This thesis developed and investigated the ability of these techniques to predict cognitive and behavioural outcome in children with AE. Children with autoimmune encephalitis (including anti-NMDA and ADEM) were recruited at least 18 months after initial presentation; along with typically developing children. Participants underwent MRI scans; MEG recordings at rest and during an auditory oddball task; and completed neuropsychological assessments. Through a series of experiments, long-term psychological outcomes were examined, and brain structure and function interrogated. Overall, the thesis found that behavioural assessments highlighted long-term difficulties in children with AE. MRI analyses showed brain cortical thinning in the left superior occipital and parietal gyri, and orbitofrontal cortex. Functional network analyses highlighted alterations within the delta frequency, with lower efficiency in information transmission within local connections. However, network measures, cortical thickness and auditory evoked responses did not predict neurobehavioural outcomes. The present findings show that these neuroimaging approaches are applicable in paediatric AE and enhance our understanding of long-term alterations, however, it is not established whether they can predict long-term difficulties. The findings highlight opportunities to further develop neuroimaging approaches that can potentially uncover clinically useful findings, and will be relevant for approaches that will better identify children with AE who warrant ongoing surveillance and early intervention to ameliorate long-term consequences of early life brain inflammation.

Keywords: autoimmune encephalitis; paediatric; magnetoencephalography; cortical thickness; cognition; behaviour; outcome; magnetic resonance imaging

Acknowledgements

I would like to acknowledge my supervisors who have supported me throughout the making of this thesis and gave me guidance and invaluable scientific insights. Thank you for helping me go through the tumultuous times and stoking my enthusiasm in pursuing this work. Thanks to Professor Amanda Wood, Dr. Elaine Foley and Dr. Sukhvir Wright who were there from the very beginning, and also Professor Klaus Kessler, Dr Evangeline Wassmer and Professor Gavin Woodhall who joined the supervision team over time. I am grateful to have received mentorship of such esteemed academic. The fact I am eager to pursue scientific research speaks for itself.

I also want to thank funders at the Encephalitis Society without whom this project would not have been possible. Thanks for giving me personal support as well as a chance to communicate and share my work with the great community of scientists and clinicians involved in helping survivors of encephalitis.

Furthermore, many talented people have supported me from the Institute of Health and Neurodevelopment, particularly Dr. Daniel-Griffiths King who has helped with recruitment, ethics application and data collection. Dr Elaine Foley also assisted my programming of the auditory-oddball paradigm. Credit is also due to radiographers Shaheen Lateef, Elisabeth Squire and Pratibha Price for their support with MRI images acquisition. Dr. Sukhvir Wright, Lydiah Makusha, and Dr Evangeline Wassmer also helped with recruitment at the Birmingham Children's Hospital. Additionally, Shaheen Lateef, Dr Sian Worthen, Dr Hongfang Wang, Rachel Green have all kindly helped with a number of MEG recordings. Lynette Looi Ling has also helped with a number of face-to-face assessments. I thank all of them for their support and kindness.

Even though I feel uncomfortable with intimate name-dropping, I would still like to thank my partner, my friends that stayed in touch from abroad and the friends that I have made in Birmingham. You have made this journey much more enjoyable for me and I cannot thank you enough. I can say the same of Aston University's chaplain priest, the parish community at St Chad's Cathedral and the Saint Vincent de Paul society who were a good spiritual support over the years. My experience would not have been the same without all of you.

Je finirai par un grand merci à ma famille qui m'a soutenu dans ce parcours malgré la distance, mes parents, mon frère, mes grands-parents, oncles et tantes et mes amis que je considère également comme une seconde famille.

Table of content

List of abbreviations

Abbreviation	Definition
Ab	Antibody
ADEM	Acute Disseminated Encephalomyelitis
ADHD	Attention deficit hyperactivity disorder
AE	Autoimmune Encephalitis
AEC	Amplitude Envelope Correlation
AMPA	α-amino-3-hydroxy-5-methyl-4-isoxazolepropionic
AMPAR	α-amino-3-hydroxy-5-methyl-4-isoxazolepropionic Receptors
AQP4	Aquaporin-4
ASD	Autism Spectrum Disorder
AUC	Area-Under-the-Curve
BCH	Birmingham Children's Hospital
CASPR	Contactin associated protein
CBCL	Child Behavior Checklist
CNR	Contrast-to-Noise Ratio
CSF	Cerebrospinal Fluid
DMN	Default Mode Network
DPPX	Dipeptidyl-peptidase-like protein-6
EDB	Extreme Delta Brush
EDSS	Expanded Disability Status Scale
EEG	Electroencephalography
ERF	Event-related Fields
FC	Functional Connectivity
fMRI	Functional Magnetic Resonance Imaging
FSIQ	Full-Scale Intelligence Quotient
GABA	Gamma-aminobutyric Acid
GAD	Glutamic Acid Decarboxylase Autoantibodies
GRDA	Generalised Rhythmic Delta Activity
IED	Interictal Epileptiform Discharges
IHN	Institute of Health and Neurodevelopment
IQ	Intelligence Quotient
LCMV	Linearly Constrained Minimum Variance
LGI1	Leucine-rich glioma-inactivated 1
LOFC	Left Orbitofrontal Cortex
MEG	Magnetoencephalography
MGluR5	metabotropic glutamate receptor 5
MOG	Myelin Oligodendrocyte Glycoprotein
MRI	Magnetic Resonance Imaging
mRS	Modified Rankin Scale
MS	Multiple Sclerosis
MTPC	Multi-Threshold Permutation Correction
MTL	Medial-Temporal Lobe
NMDA	N-methyl-D-aspartate
NMDAR	N-methyl-D-aspartate Receptor
PCPC	Pediatric Cerebral Performance Category Scale
PSI	Processing Speed Index
ROFC	Right Orbitofrontal Cortex
ROI	Region-Of-Interest
SDQ	Strengths and Difficulties Questionnaire
SQUID	Superconducting Quantum Interference Device
TBI	Traumatic Brain Injury
VIF	Variance Inflation Factor
WISC	Wechsler Intelligence Scale for Children
WMI	Working Memory Index

List of tables and figures

Chapter I. General introduction

Autoimmune encephalitis (AE) is an inflammatory brain disease with multiple autoimmune mechanisms, associated with seizures, movement disorders, psychiatric symptoms and cognitive deficits (Cellucci et al., 2020; Dalmau et al., 2019; Graus et al., 2016; Titulaer et al., 2013). Cerebral abnormalities, including brain lesions, but most commonly altered brain activity, are a prominent feature of the disease course (Dalmau et al., 2019; Gillinder et al., 2019; Heine et al., 2015; Peer et al., 2017). Children with AE may have specific clinical profiles (Granerod et al., 2010; Titulaer et al., 2013). Childhood brain damage may alter long term anatomical cerebral development; this phenomenon has been reported in paediatric brain injuries (Aubert-Broche et al., 2017; Burton et al., 2017; Deery et al., 2010; Donders & Warschausky, 2007). Recent research has shown that after acute medical recovery, residual cognitive and behavioural deficits persisted in a substantial proportion of paediatric AE patients (De Bruijn et al., 2018; Heine et al., 2021; McKeon et al., 2018; Tan et al., 2018). The need for an efficient identification of children at risk of long-term difficulties will help improve future interventions (McKeon et al., 2018). Given the predominant findings linking AE to abnormal brain function activities (Gillinder et al., 2019), this project aimed at investigating predictors of long-term deficits using magnetoencephalography, a sophisticated method which can localise functional brain activity with high temporal precision (da Silva, 2013; Hari et al., 2018).

1.1 Characteristics and symptoms of autoimmune encephalitis

1.1.1 Antibodies and treatment of autoimmune encephalitis

A definite diagnosis may be established when specific antibodies are detected in the cerebrospinal fluid (CSF) and the blood serum (Cellucci et al., 2020; Graus et al., 2016): that includes antibodies acting against intracellular antigens (such as Hu, Ma2, GAD antibodies), synaptic receptors (NMDA, AMPA, $GABA_A$, $GABA_B$, mGluR5, Dopamine 2 receptors) ion channels and various cell-surface proteins (LGI1, CASPR2, DPPX, MOG, AQP4, GQ1b). The action mechanisms of all these antibodies are not entirely known: anti-NMDAR antibodies bind on the GluN1 subunit of NMDARs, causing their internalization inside the cellular membrane (Moscato et al., 2014). They also indirectly act on AMPA receptor (AMPAR) antibodies on the GluA1 or GluA2 of AMPARs, causing the clusters of receptors to decrease in numbers (Bataller et al., 2010; Moscato et al., 2014). AMPARs and NMDARs play a role in synaptic regulation and remodelling of neuronal circuits, facilitating learning and memory by mediating synaptic potentiation (Huganir & Nicoll, 2013; Lau & Zukin, 2007). LGI1 antibodies, associated with limbic encephalitis, prevent the action of LGI1 proteins which modulate the excitability and morphology of neurons (Irani et al., 2011). Myelin Oligodendrocyte Glycoprotein (MOG) antibodies are observed in multiple demyelinating syndromes, with up to 68% antibody positive patients fulfilling the criteria for Acute Disseminated Encephalomyelitis (ADEM, Armangue et al., 2020; Baumann et al., 2016). MOG antibodies have been shown to damage oligodendrocytes in cell-based and mice studies: MOG would be associated with loss of microtubule cytoskeleton of oligodendrocytes, myelin changes, altered expression of axonal proteins, axonal loss and neuronal or astrocyte death (Wells et al., 2018). The alteration of synaptic function caused by antibodies, which has been observed in mice and cell cultures studies, explain how memory, behaviour in cognition are in turn affected (Leypoldt, Armangue & Dalmau, 2015).Pathological autoimmune responses in the brain and the increase in antibody levels are mediated by mechanisms involving B cells and T cells, i.e. immune cells that can infiltrate the central nervous system (CNS) and the CSF, and produce pathogenic antibodies within. When a loss of immune tolerance to self-antigens happens, self-antigen specific immune cells are no longer prevented from escaping, thereby causing the inflammation (Ramanathan et al., 2023). Genetic factors may contribute to such mechanisms: for example, monogenic mutations of proteins involved in clearing material from dead cells and regulating T cells, have also been associated with NMDA, LGI1, CASPR2 and GAD neuroinflammation;

and HLA class II molecules (which help B cells activate T cells) have risk alleles associated with CNS inflammation (Ramanathan et al., 2023).

Antibodies may *not* be detected in the CSF, and new antibodies are still being identified: the disease phenotypes remain the gold standard for diagnosis (Cellucci et al., 2020; Graus et al., 2016). Although specific antibodies can be used as a definite signature, there may be more immune mechanisms involved and whether all of them have a direct causal role in the pathology is unknown (Wells et al., 2018). Probable AE can therefore be diagnosed when no antibody is detected (*antibody negative* patients), based on common neurologic and/or psychiatric symptoms, cognitive difficulties, movement disorders, seizures not explained by previously known seizure disorder/related condition, CSF-specific features of inflammation (such as pleocytosis, oligoclonal bands, high Immunoglobulin G index), electroencephalography (EEG) recording with slowing or epileptiform activity, magnetic resonance imaging (MRI) abnormalities characteristic of encephalitis, or inflammatory cells found in biopsy (Cellucci et al., 2020; Graus et al., 2016). Since immunotherapy is still able to improve the course of antibody-negative diseases, it is probable that immune factors present in the body have not been identified (Hacohen et al., 2013; Wells et al., 2018).

Immunotherapy (and tumour removal when applicable) generally results in a good outcome in AE (Graus et al., 2016; Macher et al., 2018). First line immunotherapy aims at either removing circulating antibodies via plasma exchange or suppressing of the immune system; second line immunotherapy aims at reducing the production of any antibodies in the immune system (Wright & Vincent, 2019; Wells et al., 2018). Antibody removal can reverse the decrease of NMDA receptors in cell surfaces (Dalmau et al., 2008). For up to 81% of patients with anti-NMDAR encephalitis, immunotherapy led to a gradual decrease of clinically reported symptoms over 4 to 24 months with milder relapses (Titulaer et al., 2013). Most patients with ADEM recover with no new demyelinating event following immunotherapy, although relapses occur in a minority of patients (Pohl et al., 2016). The improvement can be explained by the decrease in levels of antibodies that are responsible for the synaptic dysfunction previously mentioned, as well as by the interference with B cell expansion and maturation into plasma cells (Leypoldt, Armangue & Dalmau, 2015). These studies did not report specific neuropsychological measures of cognitive or behavioural functions, which limits clinical findings.

1.1.2 Clinical signs and types of autoimmune encephalitis

Autoimmune encephalitis is an inflammatory neurological disorder characterized by a rapid onset of encephalopathy (altered mental states and functions), with symptoms like memory impairment, altered personality, decreased level of consciousness, seizures, associated with the presence of specific antibodies (see section 1.1.1), or cerebrospinal fluid (CSF) pleocytosis (Cellucci et al., 2020; Graus et al., 2016). As opposed to encephalitis with viral aetiologies, such as *herpes simplex* infection, AE stems from an endogenous immune response in the central nervous system, although viral infections or tumours can be susceptibility factors (Dalmau et al., 2019). Several types of AE have been defined in recent guidelines (Graus et al., 2016), with distinct criteria for children (Cellucci et al. 2020). An outline of these guidelines is given in Table 1.1.

Table 1.1

Types of auto-immune encephalitis (adapted from Cellucci et al., 2020; Graus et al., 2016)

Type	Diagnostic criteria	Specificities for children
Limbic encephalitis	Rapid onset (<3 months progression) of working memory deficits, seizures or psychiatric symptoms likely to involve the limbic system; Structural MRI abnormalities specifically in the medial temporal lobe; either CSF pleocytosis or temporal EEG abnormalities; exclusion of alternative causes	Uncommon in children. Commonly occur with GAD65: Unspecific memory loss, cognitive impairment, cerebellar ataxia is also considered, multifocal EEG epileptiform discharges, oligoclonal bands, personal or family history of autoimmunity, often resistant to immunotherapy
Acute Disseminated Encephalomyelitis	Multifocal clinical sign of inflammatory demyelination in the CNS; encephalopathy unexplained by fever; diffuse white matter lesions possibly with gray matter abnormalities observed with MRI; no new findings after 3 months from onset	Commonly associated with MOG antibodies (35% in Probstel et al., 2011; 40% in Brilot et al., 2009; 48.7% in Bauman et al., 2015): nonspecific EEG slowing, high titers of antibodies in younger children
Anti-NMDA receptor encephalitis	Rapid onset (<3 months) of at least four symptoms among: abnormal psychiatric behaviour or cognitive dysfunction, speech dysfunction, seizures, movement disorders or dyskinesias or abnormal postures, decreased consciousness, autonomic dysfunction or central hypoventilation; with either EEG abnormalities or CSF pleocytosis/oligoclonal bands	Children are more likely to present neurologic symptoms rather than psychiatric symptoms, with movement disorders and autonomic dysfunction appearing earlier. Other criteria: reduced verbal output/mutism, developmental regression in younger children, sleep dysfunction (mainly insomnia); may have T2/FLAIR brain lesions; increased association with tumours in females and patients above 12 years old
Bickerstaff's brainstem encephalitis	Rapid onset (<4 weeks) of decreased consciousness, bilateral external ophthalmoplegia and ataxia; definite diagnosis if there is a presence of IgG anti-GQ1b antibodies (regardless of the two previous symptoms and onset duration)	MOG may also be associated with paediatric brainstem encephalitis
Hashimoto's encephalopathy	Seizures, myoclonus, hallucinations, or stroke-like episodes; subclinical or mild overt thyroid illness; without established antibodies	Normal MRI in over 70% of children, normal thyroid function despite antithyroid antibodies, rare CSF pleocytosis, often EEG shows generalized or focal slowing without seizures

Note. MRI = Magnetic Resonance Imaging; CSF = Cerebrospinal Fluid; CNS = Central Nervous System; EEG = Electroencephalography. All these diagnoses also include the reasonable exclusion of an alternative diagnosis (cf. Cellucci et al., 2020; appendix in Graus et al., 2016)

The common phenotype explains why types with different MRI presentations and/or antibody negative CSF can be included under the umbrella of AE (Graus et al., 2016; Leypoldt, Armangue & Dalmau, 2015). ADEM, for example, is distinguished with predominant diffuse white matter lesions, but similarly includes encephalopathy (involving behavioural changes such as irritability and/or altered consciousness); CNS events caused by inflammation; and can also involve headaches, seizures, elevated pleocytosis which are common symptoms to other types of AE (Graus et al. 2016; Paolilo et al., 2020).

The clinical symptoms associated with different sub-types of AE vary above and beyond the core diagnostic criteria (Graus et al., 2016). ADEM can result in attention deficits, memory deficits and coordination problems detected 8 months to 4 years after the last demyelinating episode (Baumann et al., 2016). ADEM with anti-MOG antibodies is associated with a higher risk of seizures requiring antiepileptic treatments two years and more after onset (Rossor et al., 2019). Anti-NMDAR encephalitis is associated with headache, fever, positive psychotic symptoms (visual or auditory hallucinations, delusional thoughts) at onset (Dalmau et al., 2008; Dalmau et al., 2019; Titulaer et al., 2013). Some cases in the acute stage of anti-NMDAR encephalitis also had symptoms of autism or loss of social and communication skills similar to an autistic regression (Creten et al., 2011; Gonzalez-Toro et al., 2013; Hacohen et al., 2016), but symptoms related to autism spectrum disorder (ASD) are rarely assessed in AE, especially in long-term studies, which calls for further investigation. Limbic encephalitis with LGI1 antibodies can be observed in patients with faciobrachial dystonic seizures (Irani et al., 2011), and can involve deficits in memory, executive functions and attention at onset (Finke et al., 2017). Limbic encephalitis with antibodies against $GABA_A$ receptors was also linked to persisting epileptic activity weeks to years after recovery (Petit-Pedrol et al., 2014); patients with antibodies acting on $GABA_B$ and AMPA receptors present with memory deficits, confusion or behavioural abnormalities at onset (Onugoren et al., 2015). This highlights a variety of symptoms associated with AE, both at onset and in the long term.

1.1.3 Autoimmune encephalitis during childhood

The majority of studies have reported outcomes in adult patients, but up to 37% of patients with anti-NMDAR encephalitis are children (Titulaer et al., 2013). ADEM is also predominant in children (Granerod et al., 2010; Graus et al., 2016). However, children have a different clinical course compared to adults (Cellucci et al., 2020; Granerod et al., 2010; Graus et al., 2016). It is also remarkable that specific antibodies such as NMDA may be more frequent in younger adults below 40 years, while MOG are more frequent in children, and AQP4,

CASPR2 and LGI1 antibodies are more frequent in adults (Hacohen & Vincent, 2018; Ramanathan et al., 2023). It may therefore be informative to study adults and children separately.

Paediatric AE has more chance to present with multifocal neuropsychiatric symptoms; is less associated with tumours; may not be associated with stiff-person syndrome or cerebellar degeneration in GAD65 encephalitis (Cellucci et al., 2020); is more associated with movement abnormalities, agitation, speech deficits, insomnia or seizures in anti-NMDAR encephalitis (Cellucci et al., 2020). In 577 patients with anti-NMDAR encephalitis, movement disorders (such as orofacial dyskinesias and choreoathetosis) were more frequent under twelve years (Titulaer et al., 2013). In a sample of 53 adults and children, autonomic symptoms (such as salivation, urine/faeces incontinence), were more common in children (Zhang et al., 2018). Another study in NMDA encephalitis observed that patients whose disease onset started before 12 years of age had worse behavioural outcome compared to their peers whose onset was after 12 years (Yeshokumar et al., 2022). Early childhood onset of ADEM (before 5 years of age) is associated with lower global intellectual functioning compared to healthy controls, as well as lower reading and spelling performance compared to children with later disease onset (Jacobs et al., 2004). This shows that AE may have a specific impact when it occurs early in life.

Symptoms and deficits specific to children may be explained by the fact that their brain is in an early stage of brain development, and it is known that early brain inflammation can leave long-term damage on this development (Burton et al., 2017; Deery et al., 2010; Donders & Warschausky, 2007). Cellucci and colleagues suggest the evolution of children's neuronal circuits, receptor densities and myelination also likely explain the difference between adults and children with AE (Cellucci et al., 2020). Longitudinal studies suggest that children with ADEM (Aubert-Broche et al., 2017; Bartels et al., 2023), and anti-NMDAR encephalitis (Bartels et al., 2020) show impaired expected brain growth compared to age-matched normative samples. NMDA or AMPA receptors affected by antibodies play a role in neural development, supporting synaptic formation and dendritic arborisation, which could explain developmental dysfunction (Huganir & Nicoll, 2013; Lau & Zukin, 2007; Ewald & Cline, 2011). AE may therefore prevent the brain from developing normally during childhood, and result in brain abnormalities. This may go some way towards explaining why a younger age at onset is associated with poorer outcome (Jacobs et al., 2004; Yeshokumar et al., 2022).

1.2 Brain abnormalities in autoimmune encephalitis

1.2.1 Structural abnormalities

Brain structures in AE are conventionally visualised using structural *Magnetic Resonance Imaging* (MRI). The principles of MRI and how it functions will be described in Chapter 2. In samples with both children and adults, conventional assessment using structural MRI scans reported abnormalities in anti-NMDAR encephalitis with variable frequency (from 11% to 83% in a review from Bacchi et al., 2018; 33% in a large study, Titulaer et al., 2013). Specific details of such abnormalities are given in Chapter 2. Cohorts of anti-LGI1 encephalitis patients also had variable proportions of MRI abnormalities at onset (46% in Irani et al., 2011; 34.7% at onset and 67.7% in subsequent scans in Navarro et al. 2016). Some patients with anti-$GABA_A$ receptor antibodies show multifocal MRI abnormalities in cortical and subcortical regions (Petit-Pedrol et al., 2014), while cases with anti-$GABA_B$ and anti-AMPAR antibodies were associated with hippocampal features of acute oedema, medio-temporal atrophy, features similar to sclerosis, or hyperintensities in different brain regions (Onugoren et al., 2015). Cases with MOG antibodies-related encephalitis had lesions in cortical and/or subcortical gray matter (Bartels et al., 2021). White matter abnormalities are most commonly found in ADEM, affecting the frontal and temporal lobes, the optic nerves, basal ganglia and the thalamus (Armangue et la., 2020; Hamid et al., 2018; Ogawa et al., 2017). These studies show that patterns of abnormalities may differ between patients, and that they can also have a normal MRI.

Patients who present with macroscopic lesions or signal abnormalities on routine MRI, commonly go on to show apparent normalisation of MRI changes after recovery: In adult cases with unilateral cortical encephalitis, all brain abnormalities (unilateral cortical lesions, T1/FLAIR (Fluid Attenuated Inversion Recovery) hyperintensities) had disappeared after more than two years (Ogawa et al., 2017). In anti-NMDAR encephalitis, widespread superficial white matter damage could not be found in patients that recovered from acute illness, even though they kept residual deficits in working memory and attention (Phillips et al., 2018). Years after being diagnosed with ADEM during childhood, despite resolution of lesions and MRI abnormalities, studies still report cognitive deficits (Hahn et al., 2003; Kuni, Banwell & Till, 2012). This demonstrates that routine MRI may not give the full picture of underlying long-term effects of AE on the brain.

It should be noted that the above papers only reported conventional observations and did not produce specific advanced MRI analyses, like quantitative measures of cortical thickness or volumes (which are described in Chapter 2). An adult case report with anti-

NMDAR encephalitis and a normal MRI presentation showed a volume reduction of frontal cortices when quantitative measures were examined in a long-term follow up (Laurikainen et al., 2019). In a cohort of 23 adult and child patients, volume losses were more frequently detected with quantitative measures than abnormalities observed through qualitative assessment (Bassal et al., 2021). Other patients with LGI1 encephalitis had decreased hippocampal and intracranial volumes even when their routine MRI scans were considered normal (Irani et al., 2013). This gives support for deeper analyses of MRI scans, since patients may be affected by subtle alterations in the absence of visible abnormalities.

1.2.2 Functional connectivity

Structural changes may not give the full picture of AE's effects on the brain. Findings from *functional* brain imaging methods such as functional Magnetic Resonance Imaging (fMRI) suggest that patients with AE have reduced "functional connectivity", an indicator of neural activity shared between brain areas and interpreted as connections (Peer et al., 2017; Finke et al., 2013; Heine et al., 2018; Li et al., 2021). Reduced connectivity (or "dysconnectivity") reflects disruptions in neural connections between brain regions and impaired integration of neuronal information (Catani & Mesulam, 2008). In a study using structural MRI and resting-state fMRI, 72% of 43 patients (41 adults, 2 adolescents) had structural MRI scans that were reported as normal, but functional connectivity between bilateral hippocampi and the medial prefrontal cortex was decreased compared to controls (Peer et al., 2017). A study in 21 adults highlighted a lower group fMRI connectivity in the left insula compared to age/gender/education status matched healthy controls (Li et al., 2021).

Dysconnectivity in AE may provide an explanation of deficits: in adult patients, decreased fMRI functional connectivity between the anterior default mode network and bilateral anterior hippocampi was correlated with poorer verbal memory performance (Finke et al., 2013). In addition to a correlation between lower memory and hippocampal dysconnectivity, symptoms similar to schizophrenia and psychosis (such as hallucinations, delusions, anhedonia, avolition, flat affect, mutism, and catatonia) were also associated with fMRI network activity specific to patients (Peer et al., 2017). Lower connectivity in fMRI brain networks related to salient stimuli detection and processing was associated with decreased memory performance in another study in LGI1 encephalitis (Heine et al., 2018). Conversely, alterations also manifest as increases in fMRI connectivity, which correlate to higher performance in cognitive functions including verbal memory, working memory and processing speed, even if performance remains lower than healthy peers, which may reflect network

dysregulation (Chen et al., 2022; Heine et al., 2018; Peer et al., 2017). Increased activations suggest that those connections are being used more to compensate for other network damage (Heine et al., 2018). In conclusion, research shows that AE may cause alterations in functional connectivity in various neural networks.

1.2.3 Abnormal electrical activity and its clinical significance

Electroencephalography is a tool which can precisely measure electrical activity in time, and it shows abnormalities at the onset of AE (Dalmau et al., 2019; Fridinger & Alper, 2014; Irani et al., 2011). Common abnormalities are focal and diffuse slowing, which are formations of abnormal waveforms in the brain's electrical signal, with no specific etiology (Donnelly & Blum, 2007; Britton et al., 2016). Focal types include arrhythmic polymorphic or rhythmic monomorphic frequency patterns; the former usually suggests a structural lesion in the underlying subcortical white matter, disordered intracortical connectivity, or transient disturbances such as migraine or post-seizure state; while the latter is commonly tied to underlying gray matter lesions (Donnelly & Blum, 2007). Diffuse slowing can suggest CNS insults, including metabolic encephalopathy, toxic encephalopathy, and cerebral infections such as meningoencephalitis (Donnelly & Blum, 2007; Britton et al. 2016). In AE, EEG abnormalities are more likely to involve the temporal lobes predominantly in adults while it tends to be more generalized in children (Cellucci et al., 2020).

In anti-LGI1 limbic encephalitis, EEG abnormalities were found in 62.5% (Irani et al., 2011) to 70% of patients (Navarro et al., 2016). In cases with anti-$GABA_A$ receptor antibodies, generalised slowing was reported (Petit-Pedrol et al., 2014), while encephalitis with anti-$GABA_B$ receptor antibodies was linked to focal slowing in the temporal lobe (Onugoren et al., 2015). In paediatric cohorts with ADEM, a majority of patients had general slowing: 65% in 25 children (Fridinger & Alper, 2014) and 78% in 84 children (Tenembaum, Chamoles & Fejerman, 2002). In both children and adults with anti-NMDAR encephalitis, large proportions of patients had abnormalities: 96% had focal, diffuse slowing, or abnormal rhythmic delta activity (1-4 Hz) in 53 patients (Van Sonderen et al., 2018), 50 to 71% had excessive beta activity (14-30 Hz), extreme delta brushes and generalized rhythmic delta activity in 24 participants (Jeannin-Mayer et al., 2019), 77% had predominantly frontotemporal slowing or disorganized delta-theta activity (1–7 Hz) in 92 patients (Dalmau et al., 2008). This shows that AE is highly sensitive to EEG abnormalities (more details on delta and other frequency bands are given in 1.3.4).

EEG findings have a clinical significance. For example, extreme delta brushes are thought to play a role in cerebral development (Schmitt et al., 2012; Jeannin-Mayer et al.,

2019), and were associated with longer hospitalization in adult patients (Schmitt et al. 2012). Generalized rhythmic delta activity is also common in anti-NMDAR encephalitis: it is described as a repetition of a uniform oscillation without varying frequency or location, lasting minutes to hours, and is associated with abnormal movements (Jeannin-Mayer et al., 2019). In a systematic review, 373 out of 446 patients with anti-NMDAR encephalitis (aged 8 months to 84 years) had EEG abnormalities, and these were strongly correlated with admission in intensive care unit, while delta range abnormalities (such as extreme delta brush and generalized delta rhythmic activity) were highly associated with later better recovery (Gillinder et al., 2019). Indirect EEG markers of synaptic plasticity (slow brain waves during non-rapid eye movements stage of sleep) have also been found to be reduced in children with NMDAR encephalitis compared to healthy controls (Gefferie et al., 2021). The absence of abnormal EEG posterior rhythm in children and adults predicted a better clinical outcome and shorter hospital stay in a larger cohort, while severely abnormal EEG predicted a worse outcome (Van Sonderen et al., 2018). This shows that precise assessment of neural activity gives a deeper account of alterations in AE.

1.3 Magnetoencephalography

Magnetoencephalography (MEG) is an excellent non-invasive tool for the analysis of functional abnormalities because it provides a direct measure of neuronal activity (Proudfoot et al. 2014). This neuroimaging method may contribute to the gaps in MRI research which finds limited correlates of outcome in AE (Iizuka et al., 2016; Beatty et al. 2016; Tenembaum, Chamoles & Fejerman, 2002; Loane et al., 2019). MEG also has advantages over other functional neuroimaging methods like fMRI and EEG, with greater temporal and spatial resolution respectively (da Silva, 2013; Hari et al., 2018; Tewarie et al., 2013). MEG remains almost unused in research in AE (Miao et al., 2021; Gao et al., 2016). Given the benefits of gaining a direct measure of functional activity with excellent temporal resolution and superior source resolution to EEG, the present project proposes to use MEG to investigate brain activity and neuropsychological outcomes.

1.3.1 How magnetoencephalography can contribute to research in AE

Although structural MRI abnormalities can predict poor outcomes (Bartels et al., 2020), such prediction is limited and atrophy is often unrelated to clinical outcome in patients with anti-NMDAR encephalitis (Bassal et al., 2021; Iizuka et al., 2016). In 23 ADEM patients, the

volume of diffuse lesions predicted psychosocial symptoms but not deficits in cognitive measures like attention, memory or psychomotor speed (Beatty et al., 2016). In 84 children with ADEM, the presence of lesions was not associated with disability in the long term (Tenembaum, Chamoles & Fejerman, 2002). In 24 patients with limbic encephalitis, hippocampal atrophy was not associated with memory performance, as opposed to decreased fMRI connectivity (Loane et al., 2019). Given the observed alterations in functional connectivity with fMRI and their association with cognitive deficits (Finke et al., 2013; Heine et al., 2018; Peer et al., 2017), as well as the high occurrence of EEG abnormalities (Dalmau et al., 2008; Gillinder et al., 2019; Jeannin-Mayer, et al., 2019; Van Sonderen et al., 2018), functional imaging may be better able to predict cognitive outcomes.

MEG has a higher temporal resolution than fMRI (Tewarie et al., 2013): fMRI signals are detected over hundreds of milliseconds at best while MEG's precision is in milliseconds (Proudfoot et al., 2014). Both fMRI and MEG provide information about functional connectivity based on the coupling of neuronal events in time (Tewarie et al., 2013). Because fMRI is based on the BOLD (Blood Oxygen Level Dependent) response, it is an indirect measure of neuronal activation with limited temporal resolution, whereas MEG provides a direct measure of neuronal activity and connectivity (Schölvinck et al., 2013; Singh, 2012). Using MEG can therefore contribute to the current research regarding functional dysconnectivity in AE.

Magnetoencephalography can also complement past EEG findings in patients with AE described in section 1.2.3, because MEG is technically close to EEG. While the latter measures the electrical potential generated from neuronal activations, MEG measures the magnetic field which is generated during the same process (da Silva, 2013). MEG has several advantages over EEG, such as minimizing the influence of the meninges, the skull and the scalp on its signals; benefiting from a better spatial resolution when localising the source of magnetic signals (da Silva, 2013; Hari et al., 2018). Practically speaking, research in paediatric neuroimaging has shown MEG to elicit better compliance in children than EEG because of its shorter preparation time (Witton, Furlong & Seri, 2019). MEG is therefore expected to add greater information on brain activity in AE by assessing it more precisely in space and time.

MEG has demonstrated its potential in clinical research: in Multiple Sclerosis (MS), another demyelinating syndrome (Reindl et al., 2013), MEG measures could be correlated to cognitive impairment, suggesting that localized brain magnetic activity has clinical implications (Schoonhoven et al., 2018). MEG research in paediatric epilepsy has been fruitful in localizing sources of seizures, often concordant with MRI lesions (Frauscher et al., 2017), and showed how signals were related to intellectual deficits depending on their localization (Magara et al.,

2019). But literature investigating MEG data in AE is greatly lacking. One study used MEG on two adult patients with anti-LGI1 limbic encephalitis: interictal spike-wave dipoles were found in the temporal lobe, linking this region to faciobrachial dystonic seizures, and this was concomitant with abnormal general slowing observed with EEG (Gao et al., 2016). Another study used MEG to identify extreme delta brushes in a 16-year-old patient with anti-NMDAR encephalitis (Miao et al., 2021). No cohort study in paediatric AE is available to date. By employing this method, this project thus contributes to research in functional characteristics of paediatric AE.

1.3.2 Principles of Magnetoencephalography

MEG measures the magnetic field which is produced around the axis of an electric current: it can be detected when an assembly of neurons coordinated in space and time activate to perform a mental function (da Silva, 2013). MEG captures the magnetic field produced by post-synaptic currents flowing in pyramidal neurons and its post-synaptic dendritic neurons (Proudfoot et al., 2014). Because magnetic fields project radially from the current flow, MEG sensors are especially sensitive to cortical columns oriented tangentially to the skull, that is, perpendicular to the walls of cortical sulci, since its magnetic field projects beyond the surface (Hari et al., 2018; Proudfoot et al., 2014). The majority of cortical columns are positioned in this orientation (Proudfoot et al., 2014).

MEG's basic component is the Superconducting Quantum Interference Device (SQUID) which can have up to 300 magnetic-field sensors placed around the head: it is used non-invasively like a helmet above the head of the participant (Hari et al., 2018; Proudfoot et al., 2014). Each of the sensors contain gradiometers and magnetometers: they detect magnetic fields emerging outside the skull (passing through pick-up coils) and couple them to a superconductor (with an input coil) in order to generate a current proportional to the field (Hari et al., 2018). The SQUID thus converts magnetic flux to voltage, which results in a frequency measure that can be analysed in a similar way to EEG data (Hari et al., 2018).

MEG sensors are very sensitive, which means that they also pick up electromagnetic signals elicited by the body, such as head movements, eye movements and eye blinks, skeletal and cardiac muscles (physiological noise); as well as interfering magnetic material such as jewellery or dental amalgam (Hari et al., 2018; Proudfoot et al. 2014). Participants are therefore asked to sit still, and no metallic component should be on them (Proudfoot et al., 2014). The MEG system is also placed in a magnetically shielded room that limits the interference of environmental noise (such as elevators); and in the event of remaining artefacts in the

recording, these can be suppressed in post-processing (Hari et al., 2018). The objective of this is to keep only the electric signals produced by the neurons, and to localize them in the brain using *source estimation* (Hari et al., 2018), where MEG signals can be coregistered with structural MRI images (Hillebrand et al., 2005).

1.3.3 Analysis of evoked responses

A common use of MEG in research is the analysis of brain signals in a specific time span recorded at the moment of an experimental event ("time-locked"), called event-related fields (ERF; Proudfoot et al., 2014). Evoked responses, i.e. neuronal activities elicited in response to stimuli, can be measured at the time following the onset of a stimulus, so that the extent of change in frequency can be determined as the brain's response to an event of interest (David, Kilner & Fristron, 2006). Care is commonly taken to minimize the influence of factors such as external stimuli, repetition rates, and variables like the participant's vigilance, height, and age (Hari et al., 2018). Event-related potentials, the equivalent of ERF in EEG, have been shown to match cognitive functions (Proudfoot et al., 2014). Abnormal auditory evoked responses have been associated with cognitive deficits in MS: an explanation was that disruption of neuronal networks slowed or blocked neural conduction (Lori et al., 2011), which suggests event-related responses may have clinical implications.

1.3.4 Analysis of brain oscillations

Because assembled neurons compose a loop system with interneurons and pyramidal neurons, it is possible to detect constant brain oscillations, which are purported to play a role in information coding and modulation (da Silva, 2013). Depending on the frequency of the signals, different types of normal "rhythms" have been identified within the brain (Hari et al., 2018). There are infraslow frequencies (inferior to 0.2 Hz), delta (δ, from 0.2 to 3.5 Hz), theta (θ, from 4 to 7.5 Hz), alpha (α, from 8 to 13 Hz), beta (β, from 14 to 30 Hz) gamma (γ, from 30 to 90 Hz), and high-frequency oscillations (HFO; superior to 90 Hz), which are all linked to different cognitive functions, behaviours and mental states (da Silva, 2013; Hari et al., 2018). EEG has shown abnormalities within specific frequency bands in AE and has linked them with clinical findings (Dalmau et al., 2008; Gillinder et al., 2019; Jeannin-Mayer, et al., 2019; Van Sonderen et al., 2018). It may therefore be important to investigate frequency bands with MEG in AE. Using brain oscillations coupled in time, it is possible to measure how they are functionally connected across different brain locations (da Silva 2013; Hari et al., 2018). This has been done in MS: altered MEG functional connectivity in different networks were found, and this was associated with cognitive outcomes and disability (Tewarie et al., 2013).

Frequency oscillation analysis with MEG could thus improve the assessment of children with AE and their possible long-term cognitive correlates.

1.4 Outcomes of autoimmune encephalitis

Up to 81% of patients with AE have a 'good' clinical outcome in a long-term follow up (Titulaer et al., 2013). However, the measures used to define the clinical outcome in AE have been mostly limited to the assessment of physical disability (Gordon-Lipkin et al., 2017), but it appears that residual long-term effects on cognition and behaviours have not been assessed in detail (Armangue et al. 2020; Heine et al, 2021; Phillips et al., 2018).

1.4.1 Standard clinical outcome assessments and their limitations

Previously cited studies in anti-NMDAR encephalitis have investigated the clinical outcome using the *modified Rankin Scale* (mRS; Gordon-Lipkin et al., 2017), which measures the extent of disability caused by a disease in a score from 0 to 5 (it is often used for stroke, Banks & Marotta et al., 2007). However, studies have shown that this scale only partially assessed patients with a "good" outcome (scored 0 to 2, Titulaer et al., 2013), who frequently displayed residual cognitive and/or behavioural deficits in the long term (De Bruijn et al., 2018; Gordon-Lipkin et al., 2017; Matricardi et al., 2016; Yeshokumar et al., 2017). Even in patients with a "full" recovery (score of 0), decreased working memory and executive function could be found (Phillips et al., 2018). The inaccuracy of mRS for the measurement of cognitive impairment was therefore highlighted (Armangue et al. 2020; Heine et al., 2021). In a similar way, the *Expanded Disability Status Scale* (EDSS, initially built for MS, Kurtzke, 1983), was used in ADEM and other MOG related conditions (Baumann et al., 2016; Kornbluh et al., 2020), but the little focus on cognition of the EDSS was pointed (Kornbluh et al., 2020). This shows the importance of measuring neuropsychological outcomes even when there is initial recovery from acute symptomatology.

1.4.2 Long-term deficits in adulthood

Research in AE shows that cognitive deficits may remain in the long term: in a longitudinal study of 40 adult patients, moderate to severe cognitive impairment (including working, verbal, visuospatial memory, attention and/or executive functions) affected 85% of them at 2.3 years after onset; while deficits persisted in 65% of the cohort at 4.9 years, and some patients in their cohort did not follow an improvement trajectory (Heine et al., 2021). In a systematic review covering mostly adult studies in NMDA encephalitis, long-term deficits in episodic memory, executive functions (such as problem solving and visuo-spatial planning),

processing speed, language (such as word retrieval or auditory processing) and reduced global intellectual functioning (McKeon et al., 2018).

The review highlighted the need for a deeper study of predictive factors in order to improve interventions and possible cognitive rehabilitation for at-risk patients (McKeon et al., 2018). In the above cited cohort of 40 adults, worse cognitive outcome was predicted by delayed onset of first-line immunotherapy, long duration of hospitalization, disease severity, and admission in intensive care unit; while a younger age of onset predicted a better executive performance at last follow-up (Heine et al., 2021). While this suggests there is room for improvement in younger people, the cohort was mostly composed of adults (mean 25.9 ± 7.1, range 15–44), and it remains to be established whether age of onset matters for children.

1.4.3 Long-term deficits in children

Mckeon and colleagues (2018) suggest long-term outcome in paediatric population may differ because of the involvement of NMDA in brain development: "unexplored factors may be related to neuropsychological outcomes in this population. Given developmental changes in NMDAR expression […] hypofunction of this system during critical periods such as childhood and adolescence may affect normal CNS function more so than adult-onset episodes." (Mckeon et al., 2018, p.235). Other authors also emphasized that "Neuropsychological deficits can seriously affect participation and career choices as transition into adulthood might call for full cognitive abilities" (De Bruijn et al., 2018, p.e1998). This highlights the importance of paediatric studies.

Many small studies report cognitive deficits in long-term follow-up after childhood onset of AE: More than one year after onset, various deficits in intellectual abilities were found in 9 adolescent and paediatric cases of anti-NMDAR encephalitis (Matricardi et al., 2016), three children also suffered from deficits in executive functions (phonemic verbal fluency), attention shifting abilities, visuo-motor abilities (coding) and behavioural regulation (Cainelli et al., 2019). In a study looking at a follow-up of 5 months to 8 years following childhood onset of anti-NMDAR encephalitis, 22 children had persistent deficits growing up into adolescence, affecting sustained attention, long-term verbal memory, and processing speed, despite a "good" clinical recovery as per mRS (De Bruijn et al., 2018). Small samples of children and adolescents with ADEM also showed global cognitive impairment up to more than two years after onset (Deery et al., 2010; Kuni, Banwell & Till, 2012). A systematic review showed that persistent deficits were found in children with ADEM, but that sample size was often limited, although 15.8–22% of children are suggested to be at risk of long-term cognitive impairment (Tan et al., 2018).

Long-term deficits also seem to impact the behaviours of children: More than two years after disease onset, behavioural problems were observed in four children with ADEM, including irritability, hyperactivity, impulsivity and apathy (Cainelli et al., 2019). A meta-analysis reported long-lasting internalizing behavioural difficulties in a subset of patients with ADEM, supporting the need to identify risk factors leading to such worse outcome (Burton et al., 2017). In a small study of NMDA encephalitis patients with a good mRS outcome, two to three years after diagnosis, children had more behavioural difficulties compared to adults (Gordon-Lipkin et al., 2017). Lower scores on average adaptive behaviour scales, which is an indicator of poorer adaptation to changes in daily life, was also observed to a similar extent in paediatric and adult patients with anti-NMDAR encephalitis, including patients with a "good" mRS outcome (Yeshokumar et al., 2017).

While it remains unclear how children and adults specifically differ in long-term cognitive or behavioural difficulties, the above studies highlight the residual long-term difficulties experienced in patients with childhood onset AE.

1.5 Summary and hypotheses

1.5.1 Summary of the research to date

AE has been described with brain alterations at onset: Routine structural MRI shows a varying proportion of patients with brain abnormalities (Irani et al., 2011; Navarro et al. 2016; Ogawa et al., 2017), and several morphometric measures reveal underlying changes in brain volumes (Finke et al., 2017; Laurikainen et al., 2019; Loane et al., 2019). Abnormal electrical activity in EEG was reported in a large proportion of patients, with clinical and cognitive correlates (Irani et al., 2011; Onugoren et al., 2015; Petit-Pedrol et al., 2014; Van Sonderen et al., 2018; Dalmau et al., 2008; Gillinder et al., 2019). Similarly, reduced functional connectivity has been observed with fMRI and linked to cognitive impairment (Finke et al., 2013; Heine et al., 2018; Peer et al., 2017). In spite of immunotherapy being effective in managing acute symptoms in most patients (Titulaer et al., 2013), persistent long-term cognitive deficits are observed, and a better prediction of these should improve intervention (De Bruijn et al., 2018; Gordon-Lipkin et al., 2017; Matricardi et al., 2016; McKeon et al., 2018; Phillips et al., 2018). This is especially the case in children who may suffer more from the impact of AE on early brain development (Baumgartner et al., 2019; Burton et al., 2017; Deery et al., 2010). MEG is an efficient tool for the analysis of functional abnormalities and their clinical correlates

(Frauscher et al., 2017; Magara et al., 2019; Tewarie et al., 2013). It is therefore relevant to use MEG to identify predictors of long-term cognitive outcome in paediatric autoimmune encephalitis, as no such investigation has been conducted to date.

1.5.2 Aims and hypotheses

This project aims to investigate neuroimaging features of encephalitis and the predictors of long-term cognitive outcome in paediatric AE. It will have the strength of using a sophisticated non-invasive neuroimaging technique, MEG, coupled with structural MRI, in order to examine functional brain activities (da Silva, 2013; Hari et al., 2018; Proudfoot, 2014). To date, no research using MEG in paediatric AE has been carried out: the project thus represents a major contribution to the field by assessing this clinical condition with MEG and with a study of specific cognitive outcomes. The main axes are depicted in Figure 1.1.

The following hypotheses were tested:

1. There are MRI features in patients previously diagnosed with AE which differ from controls.
2. When MRI features are present, they predict long-term cognitive deficits.
3. Auditory evoked responses differ between patients and controls.
4. MEG resting-state functional connectivity is lower in patients with AE compared to controls.
5. MEG evoked responses and functional connectivity can predict long-term cognitive deficits.

1.5.3 Implications

Identifying predictors of long-term deficits would significantly improve treatment of children with AE and help anticipate cognitive rehabilitation for children at risk (McKeon et al., 2018). Because early treatment was found to be associated with better outcome (Finke et al., 2012; Titulaer et al., 2013), an appropriate identification of children at risk will potentially ensure a better recovery.

1.5.4 Planning of the research and COVID-19

The thesis project started in October 2019 and was significantly disrupted by the COVID-19 pandemic. Delays included the impossibility to safely do participant MRI scanning, MEG recording and face-to-face neuropsychological assessment at the Institute of Health and

Neurodevelopment (IHN), as well as the suspension and delays in running studies not related to COVID at the Birmingham Children's Hospital:

- From the first lockdown on the 23rd of March 2020, it became impossible to do participant scanning (MRI or MEG) or face-to-face cognitive assessment at the IHN as it was closed until the 4th of July 2020. Even after that date, recruitment was not possible as the Birmingham Children's Hospital, from where participants were recruited, halted studies not related to COVID-19.
- The second lockdown stopped participant facing research at Aston University on the 5th of November 2020. Birmingham entered Tier 4 restrictions on the 21st of December 2020, which meant the IHN had to pause all participant facing research which had no direct clinical benefit. This restriction included the present study.
- A further delay was encountered with the approval of electronic "permission to contact" forms being sent to patients. Therefore, data collection was only able to go ahead on the 23rd of August 2021.

Chapters 3 and 4 are the result of adaptations made possible by analyses of previously acquired data (chapter 3) as well as data collected as part of a planned audit / quality improvement project at the Hospital (chapter 4). While the original plan was to recruit both prospective and retrospective AE cohorts, only a retrospective cohort could be recruited and assessed.

Figure 1.1

Summary of the thesis research questions

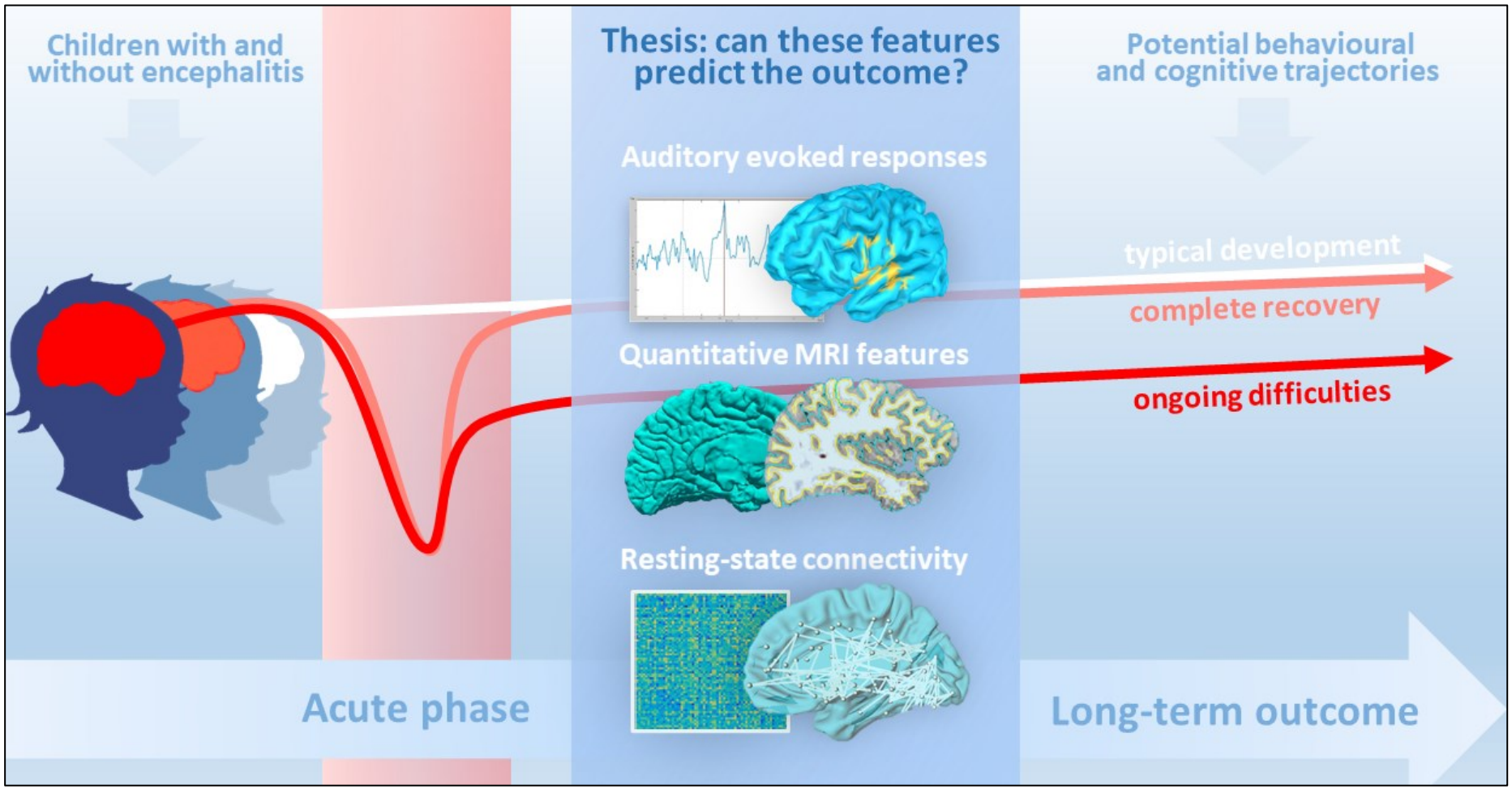

Note. 3D brain images have been generated with FreeSurfer (*v.* 6.0, https://surfer.nmr.mgh.harvard.edu/fswiki/ReleaseNotes), Brainstorm (*v.* 3.210818, 18 August 2021; Tadel et al., 2011) in Matlab R2017a (Matlab, 2017), and the NeuroMArVL web app (Dwyer et al., 2017). Note that the white arrow is only slightly higher for the purpose of visualization, the end trajectories of typical and fully recovering children are theorized to be equal

Chapter II. Structural MRI features in paediatric auto-immune encephalitis

2.1 Introduction

Brain abnormalities are reported in MRI scans in varying proportions of children with AE (Bacchi et al., 2018; Titulaer et al., 2013). The inflammation caused by antibodies likely contributes to these abnormalities: Volume reductions in the thalamus or the precuneus and posterior cingular cortices were suggested to be caused by an inflammatory degeneration expanding from the hippocampus through limbic circuitry (Loane et al., 2019). Hyperintensity in the basal ganglia was suggested to reflect damage of inflammation and immune-mediated swelling (Flanagan et al., 2015). MOG antibodies contribute to the damage of oligodendrocytes (Wells et al., 2018) and may be a cause of associated demyelinating syndromes (Armangue et al., 2020). However, many antibody-positive patients present with normal MRI scans (Titulaer et al., 2013). An explanation for this may be that routine MRI scans are not able to show the whole picture of AE's effects on brain structures, as algorithm-based morphometric measurements of subtle cortical changes can still be found in standard MRI scans that are considered normal through conventional assessment, i.e., visual inspections of MRI scans (Laurikainen et al., 2019).

2.1.1 Principles of structural MRI

Structural MRI is based on physical principles of nuclear magnetic resonance, characterized by detectable radiofrequency (RF) waves produced by atoms nuclei. Since brain tissues contain hydrogen atoms, it is possible to measure the signal they emit. When a patient is placed inside an MRI scanner *magnet* (a cylinder around them), hydrogen protons react by spinning up or down, producing a static "magnetic field" (McRobbie et al., 2006; Sprawls, 2000). Spinning protons are synchronized when the MRI scanner generates RF pulses: once a pulse stops, protons take a specific time to return to their individual spinning rates and axis (McRobbie et al., 2006). Signal intensity of the protons will depend on their density in the tissue and react to modifications of the magnetic field differently depending on their distance from the coils, and therefore allow the scanner to localise and distinguish, for example, white matter and grey matter in the brain: MRI scans are thus an estimation (in a 3D image) of where hydrogen signals are located and what tissue they result from (Ballester, 1999; McRobbie et

al., 2006). “FLAIR”, “T1” and “T2” weighted images are ways to estimate signal intensity, which create visual contrasts of white matter (depicted as brighter in T1, with higher intensity; the opposite in T2), grey matter (darker in T1, lower intensity; the opposite in T2) and of the CSF (FLAIR is used to suppress its signal; McRobbie et al., 2006; Ballester, 1999; Sprawls, 2000). The contrast allows to observe brain lesions where tissue will be disrupted and therefore, their signal intensity (McRobbie et al., 2006).

2.1.2 MRI abnormalities in auto-immune encephalitis

Through conventional clinical neuroradiological inspection, studies have reported abnormalities in MRI scans of patients with AE with a variable frequency, as a proportion of children, a majority in some studies, had normal MRI scans (Dalmau et al., 2008; Iizuka et al., 2013; Titulaer et al., 2013). Common abnormalities observed in routine MRIs of patients with AE are T2/FLAIR hyperintensities (interpreted as lesions; Venkatesan & Jagdish, 2019), leptomeningeal contrast enhancement (considered to reflect inflammation and loss of cortical tissue; Bergsland et al., 2019) visible gray and white matter alterations, and regional signs of atrophy (Bacchi et al., 2018; Venkatesan & Jagdish, 2019). Quantitative analyses also show altered gray matter volumes or white matter integrity in multiple regions (Finke et al., 2013; Wagner et al., 2015). Evidence suggests that the different types of AE impact widespread brain structures, commonly affecting frontal lobes and the hippocampus (Heine et al., 2018), but also the brainstem and the cerebellum (Venkatesan & Jagdish, 2019). Brain abnormalities associated with AE therefore seem to impact a diverse range of regions.

Anti-NMDAR encephalitis affects widespread brain structures: in the acute phase of anti-NMDAR encephalitis, 56 studies reported MRI abnormalities in 37.7% of patients, most frequently in the temporal lobes (Bacchi et al., 2018). The latter review highlighted, however, a lack of systematic indication of the exact duration between the MRI scan and the onset of symptoms, labelled “at onset”. Abnormalities are also frequently found in the frontal lobes, the hippocampus, the periventricular region, the cerebellum, the brainstem and subcortical regions such as the basal ganglia and the thalamus (Bacchi et al., 2018; Dalmau et al., 2008; Zhang et al., 2018). In a cohort of 15 patients, diffuse cortical atrophy was reported in 33% of patients at onset, affecting the cerebellum of 13% (Iizuka et al., 2016). In 53 patients, unspecified lesions were found in 47% of them in a 2-year follow-up, in various areas including the frontal, temporal and subcortical gray matter areas as well as white matter (callosal, or in the internal capsule, Zhang et al., 2018). Long-term hippocampal atrophy for severe cases was reported in other cohorts, the hippocampus being suggested to be a predominantly affected region in the

disease (Heine et al., 2015). However, some patients followed-up after the acute stage had no difference in hippocampal volumes compared to controls, but widespread white matter decreases, predominantly in bilateral cingular tracts, anterior thalamic radiations, superior and inferior longitudinal fasciculi, uncinate fasciculi, and major and minor forceps (Finke et al., 2013).

Limbic encephalitis is described as highly restricted to the bilateral medial temporal lobes, which is a criterion for the diagnosis (Graus et al., 2016). A high proportion of abnormalities in the hippocampus is reported at the acute stage (83% of patients in Loane et al., 2019; 73% in Finke et al., 2017; 77.7% in Heine et al., 2018) which frequently develops into hippocampal atrophy (Heine et al., 2015; Heine et al., 2018; Irani et al., 2011; Navarro et al., 2016). The cerebellum and the fusiform gyrus can also be affected in patients with the behavioural symptom of high levels of tearfulness five years after onset on average (Argyropoulos et al., 2020). In addition to bilateral hippocampal atrophy and T2 hyperintensity, patients with anti-LGI1 and anti-CASPR2 limbic encephalitis had decreased gray matter volumes in the thalamus and the precuneus-posterior cingulate cortices in the post-acute phase (Loane et al., 2019). Limbic encephalitis with anti-GABAB and anti-AMPA receptor antibodies has also shown abnormalities in the septum, insula, the frontal cortex, and the temporal lobes at onset (Heine et al., 2015; Onugoren et al., 2015). Enlargement of the amygdala and atrophy in the left cerebellar hemisphere, as well as long-term gray matter volume loss in the amygdalae, the basal ganglia, the thalamus, the parietooccipital cortex, the thalamus and the cerebellum were also reported in adult limbic encephalitis (Wagner et al., 2015). This shows that limbic encephalitis may have extended effects in the brain, beyond limbic structures.

At onset, ADEM is most characterized by multifocal lesions which can affect widespread brain regions, including the cerebral cortex, subcortical areas, the cerebellum, the brainstem and also the spinal cord (Baumann et al., 2016; Graus et al., 2016; Venkatesan & Jagdish, 2019). Diffuse and large lesions (over 1 to 2 cm) predominantly in cerebral white matter are part of the diagnostic criteria (Graus et al., 2016). Children with MOG related ADEM had deep gray matter lesions affecting the thalamus, the caudate and putamen nuclei, as well as the cerebellum and the spinal cord at onset (Deiva et al., 2020). Two cases with ADEM also presented at onset medial with temporal MRI abnormalities resembling limbic encephalitis, which shows that patterns of brain abnormalities can overlap (Sakai et al., 2011; Uchigami et al., 2020). This justifies evaluating different types of AE together, which may reveal a common pattern.

2.1.3 Limitations of standard clinical MRI

MRI abnormalities can last in some patients: diffuse cortical atrophy only partially recovered in patients with anti-NMDAR encephalitis, and others had remaining cerebellar atrophy at follow-up of 20 months after symptoms onset (Iizuka et al., 2016). In a 2-year follow-up of 53 patients with anti-NMDAR encephalitis, 13% had only hippocampal lesions, 21% both hippocampal lesions and lesions other areas (Zhang et al., 2018). In LGI1 encephalitis, unilateral and bilateral hippocampal atrophy were reported in 33 to 56% of another sample around 25.9 months after disease onset (Heine et al., 2018). In long-term follow up T1 scans, persisting abnormalities in the basal ganglia were reported of in 6 out of 11 patients with LGI1 encephalitis-associated faciobrachial dystonic seizures (Flanagan et al., 2015). In MOG-Ab related ADEM, MRI scans 3 to 13 months after the last demyelinating event show that the size and number of lesions decrease but may not completely disappear (Baumann et al., 2016). Although routine MRI scans are also reported to come back to normal at follow-up in other patients (Ogawa et al. 2017, Phillips et al., 2018), subtle brain alterations may remain nonetheless (Heine et al., 2015; Laurikainen et al., 2019). Furthermore, delayed MRI abnormal findings are found in some patients with ADEM, whose scans only showed observable demyelination days to weeks after the onset of the disease (Honkaniemi et al., 2001; Lakhan, 2012; Murray, Apetauerova & Scammell, 2000). This suggests AE affects the brain in a long-term, possibly progressive pattern.

Most studies have only reported abnormalities observed in conventional neuroradiological visual inspections of MRI scans (Bacchi et al., 2018; Heine et al., 2015; Titulaer et al., 2013). However, increasing evidence shows that patients with unremarkable standard clinical MRI do reveal brain atrophy in volumetric analyses (which aim at measuring brain volumes in MRI scans through computerized programs, e.g. volumes of gray matter, white matter, globally or in specific areas): reduced hippocampal and intracranial volumes was found in LGI1 encephalitis patients with “normal” MRI (Irani et al., 2013). Following a similar approach, an adult with anti-NMDAR encephalitis also had reduced volumes of superior frontal, rostral middle frontal, right lateral orbitofrontal and left anterior caudal cortices despite having a “normal” routine MRI (Laurikainen et al., 2019). In a cohort of 24 adults with anti-NMDAR encephalitis, 10 had a “normal” MRI in routine clinical inspection, but group analyses revealed reductions in cortical volumes and thickness affecting the precentral, superior parietal, supramarginal, temporal and hippocampal cortices (Xu et al., 2022). Volume reductions, especially in frontal and occipital lobes, were found in 4 scans over 14 months for a 20-months old child with anti-NMDAR encephalitis after a normal MRI at initial presentation (Nillo et al.,

2021). In a sample of 15 children and 8 adults with anti-NMDAR encephalitis, quantitative analyses revealed volume losses undetected with qualitative assessment (Bassal et al., 2021). In their review of MRI findings in different types of autoimmune encephalitis, Heine and colleagues concluded that quantitative and observer-independent analyses "provide more robust and reliable measures and allow for a better comparison between patient populations" (Heine et al., 2015, p.80).

MRI abnormalities observed with conventional visual assessment have limited statistical associations with cognitive difficulties: In anti-NMDAR encephalitis, bad clinical outcome (mRS >= 3) was only associated to cerebellar atrophy in one study (Iizuka et al., 2016), and with hippocampal lesions in another one (Zhang et al., 2018). However, volumetric analyses have found several cognitive correlates: Lower memory performance was associated with volume reductions in specific *cornu ammonis* subfields of the hippocampus in different cohorts (Finke et al., 2017; Miller et al., 2017; Miller et al., 2020). In ADEM, psychosocial symptoms were effectively predicted by the volume of diffuse lesions (Beatty et al., 2016). These findings support the need to use quantitative MRI analyses, since they have the potential to deepen our understanding of how the brain is affected by AE, even if it is not apparent in radiological inspections.

2.1.4 Relevance of quantitative analyses in a paediatric context

2.1.4.1 Impact of encephalitis on brain development

Neuroimaging features at onset could have important implications for future child development: It was hypothesized that children with a relatively lower brain size may be more vulnerable to the impact of demyelinating syndromes on brain growth (Aubert-Broche et al., 2017). This makes sense in view of the fact that some receptors attacked by antibodies in AE play a role in the development of neuronal networks and synapses, their impairment may consequently lead to a developmental impairment (Huganir & Nicoll, 2013; Lau & Zukin, 2007; Ewald & Cline, 2011). ADEM was also suggested to disrupt the cerebral development of children and cause long-term deficits in environmental information processing (Jacobs et al., 2004). Furthermore, ADEM children under 10 years with MOG antibodies had significantly more lesions in the putamen and the spinal cord than their older peers (Deiva et al. 2020), which makes demyelination an important problem for young children. However, research on the key regions involved in general paediatric AE remains limited.

2.1.4.2 Longitudinal volumetric studies

Research focused on paediatric AE is limited but indicates that the disease impairs brain growth: as mentioned in Chapter 1, recent studies have investigated MRI volumetric changes in children with AE and the differences in developmental trajectory compared to age-matched healthy peers (Aubert-Broche et al., 2017; Bartels et al., 2020; Bartels et al., 2023). In a retrospective study, Bartels and colleagues have produced measures of brain volumes in 38 children with anti-NMDAR encephalitis: at onset, the average whole brain volume, as well as volumes of gray matter, the brainstem, ventricles, and subcortical structures (hippocampus, thalamus, caudate and putamen nuclei) were significantly lower compared to healthy controls; despite clinical MRI scans being "normal" for 60.5% of the patients (Bartels et al., 2020). Furthermore, longitudinal measures over a two-year follow-up demonstrated that the patient group, and its interaction with time were significant predictors of whole brain and gray matter volume decrease, which means that AE predicts a volume decrease during brain development (Bartels et al., 2020). Aubert-Broche and colleagues longitudinally investigated brain growth in a range of monophasic demyelinating conditions including 18 children with ADEM, compared to age-normative MRI volumes based on a large database from a typically developing population (Aubert-Broche et al., 2017; Evans, 2006). The ADEM group had significantly lower white matter volumes at first presentation. Furthermore, the duration of the disease significantly predicted lower white matter and cortical gray matter volumes, as well as normalized thalamic volume over time, compared to the age-expected trajectory, which shows that demyelination may also impact gray matter development (Aubert-Broche et al., 2017). In 24 children with ADEM, a similar approach has shown whole-brain volume and white matter volume loss, as well as a failure to reach an age-expected brain growth compared to a normative healthy control cohort. Gray matter was specifically lower in MOG antibody negative patients (Bartels et al., 2023). Longitudinal studies therefore suggest that paediatric AE impairs brain development in the long term.

2.1.4.3 Measuring cortical thickness

The measure of cortical thickness, which is limited in research about AE, is a relevant indicator of brain atrophy: for example, a study in adult amyotrophic lateral sclerosis demonstrated that cortical thinning, showed whole brain differences compared to controls, while cortical volume did not (Verstraete et al., 2012). Traumatic brain injuries (TBI) in children are also associated with widespread cortical thinning (Koerte et al., 2016). A child with Rasmussen's encephalitis had widespread decrease in the left hemisphere's thickness (Boes et al., 2016). In 24 adults with anti-NMDAR encephalitis, cortical thickness was reduced in the

right superior temporal gyrus and right superior parietal lobule compared to controls, which was correlated with cognition measured with the Mini-Mental State Examination (Xu et al., 2022). Thickness represents the microstructure of neuronal columns of the cortex, particularly the extent of neuropils (axons, dendrites, synapses), which is thought to support internal connectivity and functional specialization (Wagstyl & Lerch, 2018). Cortical volume is thought to be a composite measure of both thickness and surface area: however, the two have been shown to follow different developmental trajectories and to be determined by different genetical factors (Winkler et al., 2010). Cortical thickness can be measured using an estimation of the white and gray matter surfaces and computing the distance separating the two (Fischl & Dale, 2000; Greve & Fischl, 2018 ; Wagstyl & Lerch, 2018). Cortical thickness is therefore an accessible and relevant morphometric measure for research in conditions associated with atrophy, such as AE.

2.1.5 Temporal poles and orbitofrontal microstructures

Even though the various types of AE follow relatively different volumetric courses (Heine et al., 2015), common findings make it possible that they share patterns. The impact of the hippocampus and the related limbic circuitry (Heine et al., 2015) could result into degeneration affecting distant structures of the limbic system, as correlated atrophy was noted in limbic encephalitis (Loane et al., 2019). Furthermore, this circuitry may be a cause of spread of excitotoxic damage (seizure-related), an explanation suggested for cerebellar atrophy accompanying mesiotemporal atrophy in AE (Wagner et al., 2015). The excitotoxicity hypothesis already exists in epilepsy research (Raj & Powell, 2018), along with the suggestion that loss of input from hippocampal connections (*deafferentiation*) contributes to brain atrophy: one study in temporal epilepsy found an association between decreased hippocampal fibres and gray matter atrophy in extrahippocampal regions; including the basal ganglia, the amygdala, the cerebellum, as well as frontal, orbito-frontal, temporal, and parietal cortices (Bonilha et al., 2010). Similar case of atrophy beyond the ictal areas was found in opercular-insular epilepsy, with cortical thinning being found in bilateral regions including the orbito-frontal area and temporal poles (Obaid et al., 2018). Such mechanisms could therefore exist in AE.

If these mechanisms exist in AE, they will explain the concomitant alterations in temporal and frontal cortices observed in earlier research (Heine et al., 2015). Although studies focusing on these brain regions in AE are lacking, volumetric abnormalities (Laurikainen et al., 2019) and inflammation marks (Nahum et al., 2010) in the orbito-frontal cortices were reported

in two case studies, with NMDAR encephalitis and limbic encephalitis respectively. In an adult fMRI study in anti-NMDAR encephalitis, local connectivity in the right orbital gyrus was also found to be increased compared to controls, which has been interpreted as a potential adaptive compensation of brain networks (Wang et al., 2021). Positron emission tomography has also shown reductions in NMDA receptors in the temporal poles of five patients with anti-NMDA encephalitis, which shows it is a zone of impact (Galovic et al. 2021). In another cohort, medial temporal structural abnormalities were accompanied by metabolic alterations in the prefrontal cortex of a patient with limbic encephalitis, and a suggestion was made that the circuitry linking the two areas may be affected by inflammation in AE, which could be a factor of cognitive deficits (Kataoka et al., 2008). Investigating the thickness of prefrontal and lateral temporal regions could therefore inform us on microstructural damage in AE.

The interconnected orbitofrontal and temporal poles cortices (Fernández-Jaén et al., 2014) are worth investigating since they are linked to brain disorders: thinning in the left orbito-frontal cortices and the temporal poles were significantly predicted by depression in patients with multiple sclerosis; those regions being considered to be part of a network controlling emotion, mood and visceromotor processes (Pravatà et al., 2017). This suggests demyelinating syndromes contribute to emotional dysfunctions similar to those found in ADEM and other types of AE (Armangue et al., 2013; Burton et al., 2017). Emotional problems have been linked to orbitofrontal cortices in typically developing children, which supports the role of orbitofrontal cortices (Whittle et al., 2020). Attention deficit/hyperactivity disorder (ADHD) is associated with thinning of bilateral orbito-frontal cortices and the right temporal pole (Fernández-Jaén et al., 2014), so are attention problems in typically developing children (Ducharme et al., 2012): hyperactivity and attention deficits have been reported in AE (Beatty et al., 2016; Mckeon et al., 2018). Reduced volumes of the bilateral temporal pole and the orbitofrontal cortices were found in paediatric TBI, the latter region correlating with lower social cognition; both are also considered to be part of a network supporting social skills (Ryan et al., 2016); social skills have been found in deficits in some patients with AE (Bach, 2014; McKeon et al., 2016). All of this suggests orbitofrontal and temporal regions are worth investigating in AE in light of associated disorders.

2.1.6 Summary and hypotheses

The literature has often relied on conventional MRI inspections and reported variable proportions of patients with normal scans (Bacchi et al., 2018; Titulaer et al., 2013). However, some evidence shows that deeper volumetric analyses reveal structural alterations even when

the MRI scans do not show visible abnormalities in routine clinical assessments (Bassal et al., 2021; Irani et al., 2013; Laurikainen et al., 2019). The resulting problem is that little is known about what morphometric alterations generally occur in AE and whether there is a pattern overlapping across types of AE. Furthermore, sensitive measures such as cortical thickness (Verstraete et al., 2012; Wagstyl & Lercher, 2018) have received little attention in past research (Boes et al., 2016). Investigating these neuroimaging features could help understand how they impact brain development in children, since volumetric alterations have been shown to predict altered long-term brain growth in AE (Aubert-Broche et al., 2017; Bartels et al., 2020; Bartels et al., 2023).

Inflammation in AE impacts widespread brain structures, commonly including medial temporal areas, frontal cortices, but also multiple zones such as the cerebellum, the brainstem and subcortical regions (Argyropoulos et al., 2020; Bacchi et al., 2018; Bauman et al., 2016; Heine et al., 2015). A possible mechanism behind its spread could be excitotoxicity or deafferentiation effects from damages in limbic circuitry (Bonilha et al., 2010; Wagner et al., 2015), with damage in the hippocampus leading to distant atrophy (Kataoka et al., 2008; Wagner et al., 2015). In light of epilepsy research, damage in external regions including the temporal and prefrontal cortices including the orbitofrontal cortex result from these mechanisms (Bonilha et al., 2010; Obaid et al., 2018; Raj & Powell, 2018). In various neurology conditions, cortical thinning of both orbitofrontal cortex and temporal poles was related to emotional deficits (Fernández-Jaén et al., 2014; Pravatà et al., 2017) that are similar to those reported in AE (Armangue et al., 2013; Beatty et al., 2016; Burton et al., 2017; Dalmau et al., 2019). Furthermore, some cases of AE presented with abnormalities in these specific areas (Kataoka et al., 2008; Laurikainen et al., 2019; Nahum et al., 2010).

Following the above research, the present study tested the hypothesis that whole brain cortical thickness of children with AE is significantly different compared to age-matched healthy children. Furthermore, it also tested the exploratory hypothesis that children with encephalitis had thinner orbitofrontal and temporal polar cortices compared to age-matched healthy children.

2.2 Methods

2.2.1 Participants

Two cohorts were recruited: one cohort included children with AE recruited through contact from clinical neurologists at the Birmingham Children's Hospital, Birmingham, United Kingdom: parents were given a permission to contact form, if consent was signed and given, the neurologists would provide their contact details to a researcher associated with the study at Aston University, only so they can contact the parents and invite them over the centre where informed consent to take part in the study will be collected. If consent was given, previous child's MRI data at the Hospital would be accessed with consent (Ethics Reference #17/YH/0299; #IRAS 222771).

The control cohort was composed of typically developing children. A part of the cohort was recruited through the same steps described above (Ethics reference #18/LO/0990; #IRAS 233424). A second part of the cohort was recruited at Aston University's *Institute of Health* & *Neurodevelopment* (IHN), Birmingham, United Kingdom (under Ethics #HLS21011), through contact permission collected from families that took part in research projects at the centre, as well as advertisement via social media/community organisations and Aston University/IHN outreach events, where contact details to get in touch with the study researchers were given.

Informed assent to participate from children and informed consent of one of their respective parents or legal guardians were collected. Exclusion criteria for both cohorts included dissent of the child from participating and presence of contraindication for MRI scanning. AE children were included if they had a previous diagnosis of any type of AE (according to the standards established in Cellucci et al., 2020; Graus et al., 2016), and were recruited at least 2 years after disease onset. Inclusion criteria for typically developing controls included the absence of diagnosis of learning difficulty, or psychiatric, neurodevelopmental, or neurological disorder and absence of known or suspected cerebral abnormality.

Additionally, a dataset of 15 anonymized and unidentifiable preprocessed paediatric T1 MRI scans from healthy controls was acquired from a previous study conducted at Aston University's IHN (Aston University Ethics ID: #888; #HLS2140) and was added to the present control cohort.

2.2.2 Image acquisition

Each participant underwent structural T1-weighted MRI scans. They were acquired from different MRI scanners at the Aston University's IHN, or at Birmingham Children's Hospital, in Birmingham, UK (Table 2.1).

Table 2.1

List of scanners and parameters in the sample

N AE:C	Site	Scanner	TE (ms)	TR (ms)	Flip angle	Field strength	Dimension
1:0	BCH	Siemens Avanto	0.00337	1.900	15	1.5T	176x208x256
8:24	IHN_a	Siemens TrioTim	0.00337	1.900	15	3T	176x240x256
0:13	BCH	Philips Achieva	0.00375	0.008	8	3T	176x240x240
3:11	IHN_b	Siemens MAGNETOM Prisma	0.00341	1.960	15	3T	176x240x256

Note. AE = Autoimmune Encephalitis; C = Controls; TE = Echo Time; TR = Repetition Time; BCH = Birmingham Children's Hospital, Birmingham, UK; IHN_a = Aston *Institute of Health* & *Neurodevelopment*, Birmingham: Old scanner until Oct 2021; IHN_b = Aston *Institute of Health* & *Neurodevelopment*, Birmingham: New scanner from March 2022.

2.2.3 Preprocessing

Structural MRI preprocessing was done using automated pipelines from the *FreeSurfer* software (v6.0, https://surfer.nmr.mgh.harvard.edu/fswiki/ReleaseNotes): all scans underwent skull stripping, removing tissues of the skull, the neck, the cerebellum and the brainstem in order to create a mask of the brain. The brain masks were then segmented by detecting gray matter, white matter, and CSF boundaries of the Brain. Meshes based on the delimitation of white matter and gray matter were created to reconstruct the surfaces of the two matters (Fischl & Dale, 2000). Meshes are made of triangles, with vertices at the meeting of each neighbouring points, about 1 mm apart. Cortical thickness was obtained as an average of the distance separating each vertex in the white surface from the closest point in the pial surface; and of the distance separating the corresponding pial vertex to the closest point on the white surface (Fischl & Dale, 2000; Greve & Fischl, 2018). For scans that were acquired with a 3T scanner, intensity non-uniformity was corrected with non-parametric non-uniform intensity normalization (*N3*) to correct adapted to the 3T scanners by using the **"**-3T" flag (Fischl, 2012): N3 consists in incrementally decomposing the gaussian distribution of the observed signal intensities across the space (to account for non-normal distribution of non-uniformity), until no further changes in distribution of non-uniformity happen; the distribution of intensity is kept

within the values where non-uniformity has a zero mean, thereby rendering a homogeneous intensity across the image (Sled, Zijdenbos, & Evans, 1998). Both surfaces were also smoothed and aligned in order to improve inter-participant comparability (Wagstyl & Lerch, 2018).

Manual edits were done in FreeSurfer to remove segmentation errors, remaining unwanted tissues and to correct surface estimation errors when needed. Cases with excessive noise or artefacts were discarded. To support this judgement, the quality of the outputs was examined using the *Qoala-T* shiny-app (https://qoala-t.shinyapps.io/qoala-t_app/), an automated application which derives volumes and thickness data to assess quality of scans and give a replicable selection for analyses (Klapwijk et al., 2019). Scans for which exclusion was advised by the application were investigated in details and a decision was made to either apply manual edits when possible or to discard the scans (see Appendix 2.2 for the outputs).

2.2.4 Statistical analyses

2.2.4.1 Whole-brain comparison

Surface-based cortical thickness estimated across the whole brain was integrated as the independent variable of a general linear model. Group was selected as a predictor of thickness increase or decrease (*abs*). Age and Gender were included as control variables as standard practice (notwithstanding group differences, Xu et al., 2022), as well as Contrast-to-Noise Ratio (CNR) to account for the variability of quality from the different scanners. CNR reflects the extent to which grey and white matter tissue signals are separated (Magnotta & Friedman, 2006) and has an important impact on tissue classification (Tardif, Collins & Pike, 2009). It is an image quality metrics that helps identify interscan variance (Esteban et al., 2017; Garcia-Dias et al., 2020).

CNR was computed using the following equation (following Garcia-Dias et al., 2020 ; Magnotta & Friedman, 2006; for T1 contrast):

$$CNR = \frac{\mu_{WM} - \mu_{GM}}{\sigma_{background}}$$

Gray matter and white matter intensities were estimated in each hemisphere using the aseg.mgz (#2, #3, #41, #42) segmentation colour frames and background intensity was estimated using the T1.mgz #0 segmentation colour frame, both extracting intensity from the original scan.

The whole-brain general linear model was run with FreeSurfer using the mri_glmfit-sim command. A 3D statistical map was generated for each hemisphere to estimate significant

intercept differences in average cortical thickness at p = <.05, with a 10mm Gaussian surface-based smoothing. Cluster correction with Monte Carlo Z simulation was applied to account for the interdependence of neighbouring voxels and estimate clusters to control for multiple comparisons. The clusters were defined at a Z-threshold of 2.0 (p = <.01), adjusted for the two hemispheres (Bonferroni division of the p-value by two), to limit the probability of false positives according to the selected smoothing (Greve & Fischl, 2018). Supplement Figure S2 in the latter article for FreeSurfer 6.0 shows that 2.0 Z gives a comparably low false positive rate at 10 mm smoothing, despite not being the most conservative threshold. Good statistical power for a detection of 10% thickness difference, with 10mm surface-based smoothing, was estimated to be detectable in widespread areas with two groups of 10 participants each, controlling for age and sex (Pardoe et al., 2013; see also supplementary data of the latter). A size of ten per group was therefore aimed for recruitment, and a 10 mm smoothing will be applied.

2.2.4.2 Regional exploratory analysis

The region-of-interest (ROI) analysis was done by estimating cortical thickness of each separated ROI in the Destrieux atlas, which is composed of both gyral and sulcal surfaces (Destrieux et al., 2010). The analysis included the cortical thickness of the bilateral temporal poles and the bilateral orbitofrontal cortices (4 dependent variables). Each orbital gyrus in the atlas was assembled with its corresponding orbital sulci ("H shaped") into a single region using the tksurfer GUI in FreeSurfer. Label files were exported in the GUI for each ROI. The average thickness measures of the four regions were then computed using FreeSurfer's mris_anatomical_stats command. Average thickness of each region was exported in *SPSS* v24 for Windows (IBM Corp., 2016) and integrated as response variables of a MANCOVA, with group as a predictor (coded 0 for controls, 1 for AE), age, gender, and average CNR as control variables.

Considering past research in cortical thickness of these areas, moderate to large effect sizes in cortical thinning can be expected (Fernández-Jaén et al., 2014 with η^2_p=0.1 to 0.24; Kühn, Schubert & Gallinat, 2010 with Cohen's d = 1.14; Williams et al., 2018 with Cohen's d = 1.07). A priori analyses with G*Power (Faul et al., 2007) for MANOVA have shown that a sufficiently powered difference (1- β = 0.8) could be detected in a sample of 38 participants if a high-medium effect size is found, $f^2(V)$= 0.14 (medium being 0.0625, large being 0.16 in G*Power) with four predictors: group, age, gender, and CNR; and four response variables: cortical thickness of each ROI. Therefore, 20 per group is the sample size that was aimed for the ROI analysis.

Several assumptions were checked before running the analysis (Mayers, 2013): Participants with any value of cortical thickness three standard-deviations above or below the group mean were excluded as outliers (to limit data distribution abnormality and excessive changes due to noise in the image ROIs). Given there were two groups, with no specified equal size, Roy's Largest Root was selected as the multivariate statistic value, assuming variables did not have a platykurtic distribution. This assumption was checked using measures of kurtosis in SPSS (below z = -1.96 would be considered abnormally platykurtic). Moderate positive *r* correlations (0.3 to 0.9) between the dependent variables are recommended and was also tested using a Pearson *r* correlation. Shapiro-Wilk's test was used to verify the normal distribution of the covariates, and would be excluded if there were not. The assumption of between-groups univariate homogeneity of variance was tested using Levene's test; and the assumption of homogeneity of multivariate variance-covariance with Box's M test (meant to be below $p = .001$). For the assumption that association between the covariates and dependent variables do not differ across groups, the interaction effect of group and covariates was tested in separate MANCOVAs using custom building term models in SPSS.

2.3 Results

2.3.1 Demographics

MRI scans of 60 children were acquired. Demographic information is presented in Table 2.2. The AE group was composed of 1 anti-NMDAR, 1 antibody negative, and 10 ADEM cases. Specific clinical data (including antibodies, mRS scores at scan and medication at scan per individual) are reported in Appendix 2.1.

Table 2.2

Demographic and clinical characteristics of children with autoimmune encephalitis and typically developing children

Child characteristics	Controls (N=48)	AE (N=12)	Statistics	
			Test	*p* value
Gender (female:male)	23:25	8:4	χ^2 = 1.352	.245
Age in years (mean±sd) IQR	10.5 ± 2.5 3.8	10.7 ± 3.5 7.3	*t* = -0.128	.899
Age of onset IQR	NA	3.91 ± 2.2 3.5	NA	NA
mRS at scan IQR	NA	0.92 ± 0.9 1	NA	NA

Note. AE = Autoimmune Encephalitis. mRS = modified Rankin Scale.

2.3.2 Whole-brain comparison

The whole-brain general linear model significantly predicted differences in cortical thickness in the posterior left hemisphere accounting for age, gender and CNR; which can be seen in the cluster depicted in Figure 2.1. The cortical thickness of the cluster was significantly lower in the AE group (peak tailarach coordinates (X,Y,Z) = −17.9, −80.2, 39.4; cluster size = 681.55 mm^2; N vertices= 1182; corrected cluster-wise p = 0.00459; cluster-wise Cohen's d= -8.3773).

Accounting for the Destrieux atlas parcellation, the cluster covered the top part of the superior occipital gyrus, the bottom part of the superior parietal gyrus as well as bits of the intraparietal, transverse parietal and parietooccipital sulci (Figure 2.1), all in the left hemisphere.

Figure 2.1

Comparison of cortical thickness between children with autoimmune encephalitis and typically developing children

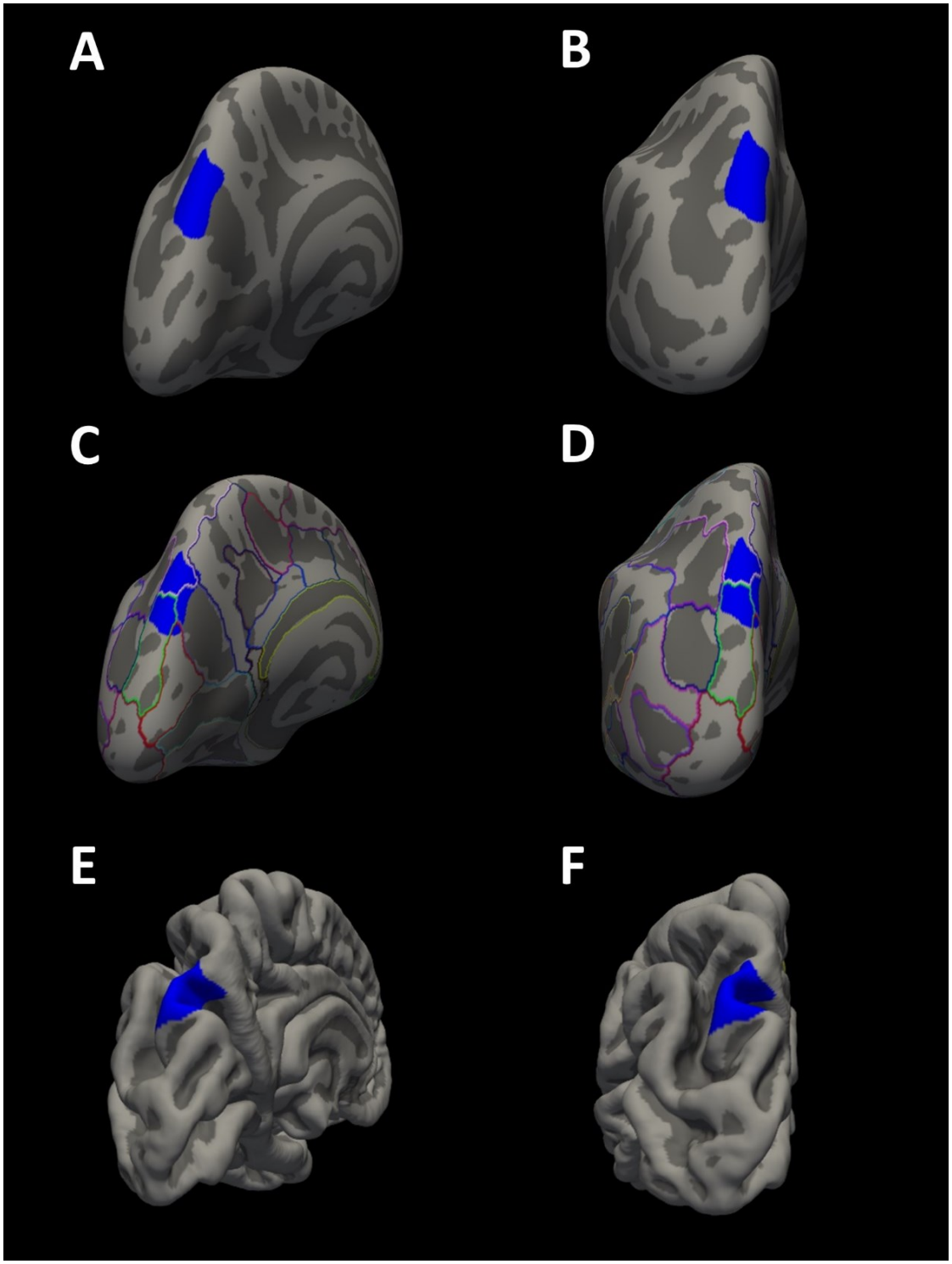

Note. A & B) Blue cluster showing lower cortical thickness in the AE group, from different angles; C & D) Same cluster superposed over the Destrieux Atlas parcellation. The cluster covers the superior occipital gyrus (bottom green of the cluster); the superior parietal gyrus (top pink); a slight part of the intraparietal sulcus and transverse parietal sulcus (left purple); the parietooccipital sulcus (right blue); E & F) Same cluster viewed on the fsaverage pial surface for more accuracy.

2.3.3 Regional exploratory analysis

Descriptive statistics for the cortical thickness of each individual ROI are shown in Figure 2.2.

Figure 2.2

Average cortical thickness of each region of interest across groups

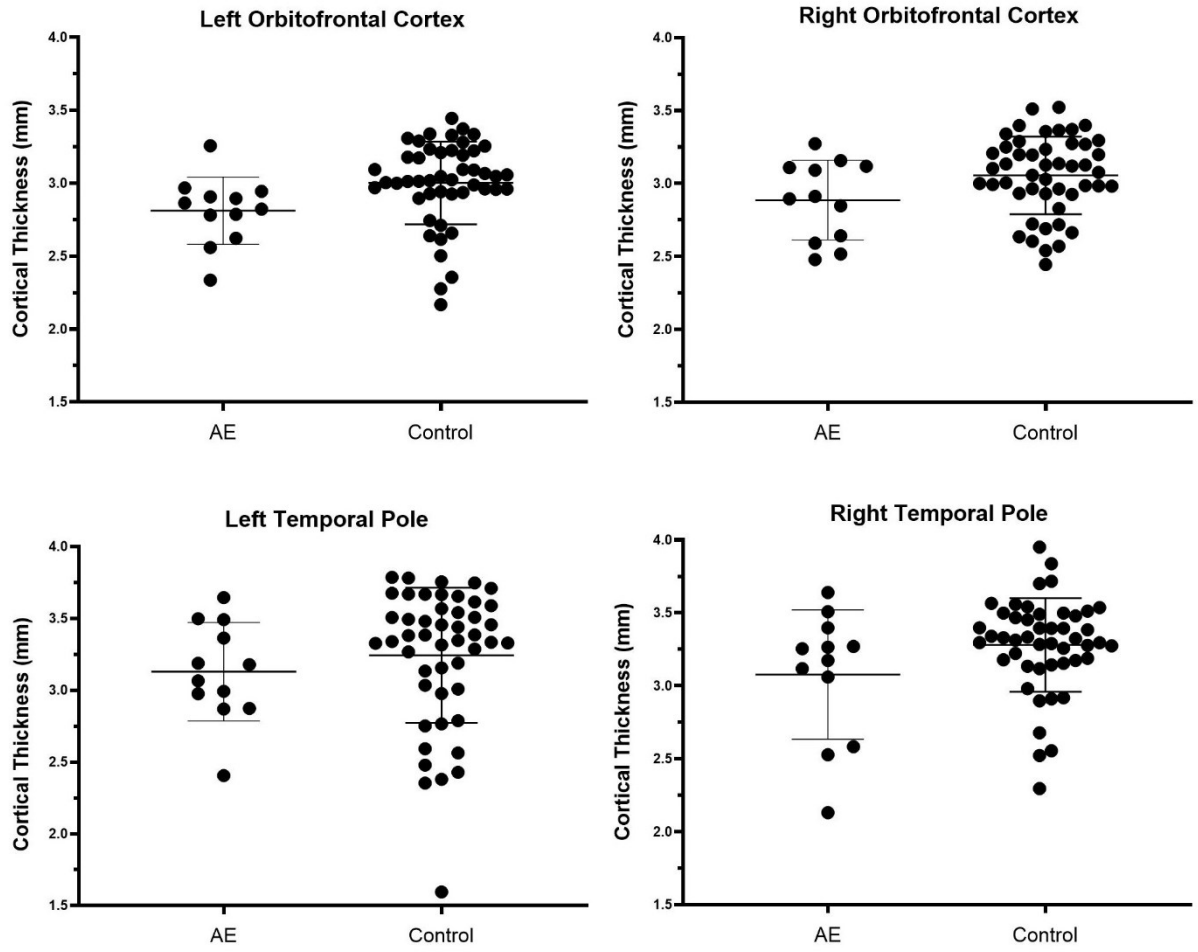

Note. AE = Autoimmune Encephalitis. In each graph: middle horizontal bars represent the group mean, bottom and top bars the standard deviations.

Two outliers (1 Control, and 1 Case, ID 6 in Appendix 2.1) were identified and excluded from the multivariate analysis. The distribution of dependent variables was not platykurtic, although 3 out of 4 ROIs were not normally distributed (Shapiro-Wilk test at p = <.05). These were acceptable as "reasonably normally distributed" (Mayers, 2013) given the robustness of multivariate models to abnormality and the lack of excessive skewness and kurtosis (z = ±1.96). Shapiro-Wilk's test, along with kurtosis and skewness measures, showed that CNR was not normally distributed in the control group and could not be included as a covariate. Age was normally distributed. No significant interaction between Group and Age or Group and Gender

was found, confirming their independence. Correlations between the dependent variables did not go above 0.9 or below 0.3. Levene's test confirmed the homogeneity of variance between groups and the Box's M test did not find a significant homogeneity of variance-covariance (p = .249). The above preliminary checks therefore ensured no violation of assumption prevented the MANCOVA from being run.

The MANCOVA did not detect any significant multivariate effect on the cortical thickness of the selected ROIs together. The multivariate outcome for Group was as follow: Roy's Largest Root = .095, F(df) = 1.207(4); p = .319; partial η^2 = .087; Observed Power: .351. The model's explanation of the variance in thickness was low in all ROIs: the adjusted R^2 was .039 for left orbitofrontal cortex, 0.134 for right orbitofrontal cortex, .049 for left temporal pole, and .045 for right temporal pole.

Nevertheless, among the univariate effects shown in Table 2.3, cortical thickness within the left orbitofrontal cortex was significantly predicted by Group with a small effect size. This suggests the encephalitis group may have a lower average cortical thickness in the left orbitofrontal cortex compared to controls, independently of age and gender. Age also had a significant effect on the right orbitofrontal cortex.

Table 2.3

Univariate outcome from the MANCOVA, using autoimmune encephalitis as a predictor of regional cortical thickness with age and gender as control variables

		Statistics			
Predictors	**ROI**	**F**	***p* value**	**Partial η^2**	**Observed power**
Group	LOFC	4.407	.040*	.075	.541
	ROFC	3.276	.076	.057	.428
	LTP	1.254	.268	.023	.196
	RTP	2.084	.155	.037	.294
Gender	LOFC	0.049	.826	.001	.055
	ROFC	0.231	.633	.004	.076
	LTP	0.032	.859	.001	.054
	RTP	0.696	.408	.013	.130
Age	LOFC	0.937	.337	.017	.158
	ROFC	5.123	.028*	.087	.604
	LTP	1.402	.242	.025	.214
	RTP	0.001	.976	<.001	.050

Note. LOFC = Left OrbitoFrontal Cortex; ROFC = Right OrbitoFrontal Cortex; LTP = Left Temporal Pole; RTP = Right Temporal Pole; * significant at p < .05, two-tailed.

2.4 Discussion

This chapter aimed to use advanced neuroimaging morphometric analyses of MRI scans to investigate whether subtle brain abnormalities can be identified in children with AE. Specifically, it aimed to assess cortical thickness, which has not received attention in previous research in paediatric AE. Comparison analyses with a control group of typically developing children were run at the level of the whole brain, along with an exploratory analysis assessing a specific effect of group on temporal poles and orbitofrontal cortices.

2.4.1 Summary of the results

The whole-brain comparison analysis found an effect of group on one posterior cluster in the left hemisphere, specifically covering the left superior parietal and superior occipital gyri. This suggests children with AE may have lower cortical thickness in this area compared to typically developing children. The area of difference is coherent with a previous adult limbic encephalitis study observing long-term gray matter volume loss in the parietooccipital cortex (Wagner et al., 2015) relatively close to the cluster observed. Similarly, occipital volume loss was found in a paediatric NMDAR encephalitis case study (Nillo et al., 2021). A cluster superior parietal lobule, although more lateral to the cluster found in the present analysis and in the right hemisphere was observed in adults with anti-NMDAR encephalitis, which was relevant to cognitive performance (Xu et al., 2022). These studies, along with the present findings, suggest brain gray matter thickness may be affected in posterior areas, although their association with symptoms and/or deficits has not been established in children with AE. It may also be relevant to note that thinning in the area of the cluster has been found in remitting-relapsing MS, which is also concerned by demyelination: given ADEM was common in the present cohort, they possibly share common damages (Nygaard et al., 2015). Using similar cluster-wise methods, part of the superior parietal lobule thickness was shown to be associated with global intellectual functioning in typically developing children (Menary et al. 2013), while global intellectual finding is impaired in some children with AE (Beatty et al., 2016; Jacobs et al., 2004; Mckeon et al., 2016; Mckeon et al., 2018); the area of difference found in the present study may thus be of interest for prediction of cognitive functions.

The exploratory analysis found a significant small group effect on the left orbitofrontal cortex, with a trend toward an effect on the right orbitofrontal cortex, which suggests children with AE may have lower cortical thickness in this area, independently of their age. An effect of age was also detected for the right orbitofrontal cortex, but not the left. This difference may be

explained by the fact that orbital regions do not correlate to age to the same extent across hemispheres, have different interindividual variability (Frangou et al., 2022) and are subject to laterality effect in children from 5 to 14 (Zhou et al., 2013). The discrepancy with the whole brain analysis, which failed to detect such effect, can be explained by the relatively conservative permutation correction, lack of statistical power to detect more than the cluster, surface smoothing, and the fact that CNR was not controlled for in the exploratory analysis. It is unknown whether the effect would appear in a whole-brain analysis with a higher statistical power, but possible given the difference in orbitofrontal thickness was slight and the effect size small. Nevertheless, lower cortical thickness in the orbitofrontal cortex is in conformity with previously reported abnormalities in case studies (Laurikainen et al., 2019; Nahum et al., 2010) and suggest this area may be of interest for research in AE. It was noted earlier that links between lower orbito-frontal cortical thickness and emotional networks, attention deficit/hyperactivity disorder, lower social cognition were reported in other populations (Fernández-Jaén et al., 2014; Pravatà et al., 2017; Ryan et al., 2016): this finding makes sense given emotional, social and attentional issues are also reported in paediatric AE (Armangue et al., 2013; Bach, 2014; Beatty et al., 2016; Burton et al., 2017; McKeon et al., 2016). However, the effect size was not large enough to reach the statistical power aimed originally (cf. Table 2.3), which calls for caution when interpreting the present results.

The MANCOVA did not find a significant multivariate group effect with regards to cortical thickness in the four regions of interest, nor significant univariate effects on the temporal poles. This suggests cortical thickness in the temporal poles may not be linked to that of the orbitofrontal cortices in AE as was hypothesized in this chapter. Even though they are interconnected (Fernández-Jaén et al., 2014; Kataoka et al., 2008), it could not be observed that AE had an impact on both pairs of regions. Despite previously reported alteration of limbic circuitry and temporal areas in AE (Galovic et al., 2021; Heine et al., 2015; Loane et al., 2019), the impact on temporal poles may also be more prevalent in *limbic* encephalitis, a specific type which was not diagnosed in any of our participants, as it is more frequent in adults (Cellucci et al., 2020). Alternatively, cortical thickness may simply not be affected in temporal poles at all, as it was never specifically investigated in the temporal poles in earlier AE research.

The hypothesis of damage caused through interconnection cannot be rejected altogether either. One study found that patients with anti-NMDAR encephalitis who had received second-line immunotherapy had a normal fMRI functional connectivity between the hippocampus and the medial prefrontal cortex compared to their peers with only first-line intervention (Wang et al., 2019). Second-line immunotherapy could therefore help preserve

extrahippocampal connections and therefore prevent distal damage which could result from the alteration of its circuitry, but immunotherapy was not controlled in the present study.

2.4.2 Limitations

FreeSurfer has a number of limitations that make the accuracy of morphometric analyses difficult: an example is lesion influencing the processing pipelines: they can distort voxel intensities, cause brain segmentation failures, mislabelling of tissue, and require manual corrections (King et al., 2020). Orbitofrontal and temporal cortices are also vulnerable to motion artefacts and ringing effect, which makes it difficult to obtain precise measures of cortical thickness: motion induces blurring of images which can make grey matter appear thinner in places, thus causing a systematic bias in morphometric estimates (Reuter et al., 2015), which means that a group with higher motion is susceptible to also have a spurious higher thinning. Furthermore, younger age is associated with lower MRI scan quality (Klapwijk et al., 2019). They may be even more susceptible to motion, and both higher motion and lower scan quality affect cortical thickness negatively (Ducharme et al., 2012; Reuter et al., 2015). Although motion correction methods were used for cases that had moved excessively (–motioncor method in FreeSurfer; Fischl, 2012; used for ID 14 across 4 runs; ID 7 across 4 runs cf. Appendix 2.1), and although motion was not more frequent in the AE group, it is uncertain how it may have affected the present findings. The Qoala-T tool was validated in a healthy cohort with 8 to 25 years (mean 14.05±3.67; Klapwijk et al., 2019), and was therefore chosen not to be fully relied on for inclusion decisions. Nevertheless, subjectivity involved in quality check remains an issue (as shown by the moderate inter-rater agreements, Klapwijk et al., 2019), and thus calls for caution when interpreting the present results.

The variability in protocols and/or parameters of the different MRI scanners is also an issue for accurate quantitative measurement: high variability can be found across scanners with different resolution, field strengths, image uniformity and tissue contrast (Biberacher et al., 2016; George et al., 2020; Tardif, Collins & Pike, 2009). While the present study attempted to control contrast-to-noise ratio, considered as one of the most important characteristics that impact tissue classification (Tardif, Collins & Pike, 2009), it remains a single aspect of interscanner variability, and it would therefore be more accurate across the same scanner. Tools of harmonization have been developed in the recent years to account for difference of scanners and parameters, such as *NeuroHarmony* (Garcia-Dias et al., 2020), and building validity for paediatric cohorts may help researchers account for multisite studies in the future. The present results may have been affected by the variability in scanners and will have to be

interpreted with caution until large sample and standardized analyses of cortical thickness in AE are done (George et al., 2020).

Variability may also exist within subtypes of autoimmune encephalitis, although establishing subgroups was not possible in the current sample. The current AE cohort was mainly composed of ADEM cases, among which 4 cases were MOG antibody positive (Appendix 2.1). ADEM is more characterized by lesions in white matter than other subtypes (Graus et al., 2016), and it is not clear how commonly affected is cortical thickness in children with ADEM compared to children with other AEs. The study may therefore be more representative of ADEM than of anti-NMDAR encephalitis and other types of AE.

Regarding the exploratory hypothesis, the methods used may not be the most appropriate to study damage related to brain circuitry. Cortical thickness can be useful to identify atrophic mechanisms but can be complemented using measures of white matter microstructures (King et al., 2019). More precise tools like diffusion tensor imaging are able to detect subtle white matter disruptions in AE (Chang, 2014; Finke et al., 2013; Finke et al., 2017). Alterations have been reported in functional connectivity with fMRI, which structural MRI is unable to measure (Finke et al., 2013; Heine et al., 2018), and disruption could be found in brains with no microstructural losses (Dalmau et al., 2008; Moscato et al., 2014). Functional MRI and diffusion tensor imaging may therefore be relevant tools to explore prefrontal-temporal circuits in the future.

2.4.3 Conclusion

Children with AE may have long-term alterations in their brain's cortical thickness, which has received limited attention up till then. This chapter gives support to the idea that advanced neuroimaging analyses may be relevant to investigations in paediatric AE as they add observations that are not visible in conventional MRI assessments. The present cohort had a relatively thinner gray matter thickness in left posterior and orbitofrontal areas compared to their typically developing peers. Larger studies with more statistical power will be needed to verify such differences and generate more reliable results. Furthermore, a longitudinal protocol such as what was accomplished in other studies (Aubert-Broche, 2017; Bartels et al., 2020; Bartels et al., 2023), but focused on cortical thickness, may give clearer information on how these structures evolve across the development of children with AE. Given cortical thinning has been linked to symptoms and deficits in other clinical populations (Fernández-Jaén et al., 2014; Pravatà et al., 2017; Ryan et al., 2016), and has been linked to cognition in adult NMDAR encephalitis (Xu et al., 2022), it may be worth investigating whether such differences are

associated with difficulties in paediatric AE. Furthermore, structural brain abnormalities may be present, but functional brain abnormalities, measured with MEG, may also inform us on the long-term impact of AE.

Chapter III. Epileptic functional networks relevant to autoimmune encephalitis

3.1 Introduction

3.1.1 Altered connectivity of brain networks in autoimmune encephalitis

The previous chapter looked at structural brain abnormalities using advanced neuroimaging techniques. Modern neuroimaging analysis methods can also look at how the brain makes connections across its different regions, and how these connections interact in real-time by recording brain activity (Chang, 2014, Finke et al., 2013; Finke et al., 2017; Wang et al., 2021). Alterations within brain activity across cerebral connections can be measured independently from structural changes using MEG, which has not been done in paediatric AE to date.

3.1.1.1 Structural abnormalities and dysconnectivity

Patients with AE may commonly have altered brain connections, structurally or functionally (Iype et al., 2018; Finke et al., 2017; Peer et al., 2017). Dysconnectivity is suggested in ADEM as it is characterized by white matter lesions, demyelination, and axonal loss (Beatty et al., 2016; Iype et al., 2018). Research in paediatric demyelinating syndromes suggests that immature brains recover less fully from early insult and result in delayed development: due to the interference in circuits, notably between frontal, posterior cortices and subcortical regions, information processing and response speed could be reduced (Deery et al., 2010). Disconnection syndromes are characterized by altered neural connections between brain regions: this results in impaired cognitive functions which rely on the transmission of signals through axonal tracts (Catani & Mesulam, 2008). In LGI1 and anti-NMDAR antibodies encephalitis, subtle white matter alterations have been detected (Chang, 2014; Finke et al., 2013; Finke et al., 2017; Wang et al., 2021). Thus, AE could be a condition involving neural disconnection.

Dysconnectivity can be observed without damaged neural structures, i.e., an “effective” form of dysconnectivity using functional neuroimaging when the transmission of information between regions is altered even when the structure of the pathways is preserved (Catani &

Mesulam, 2008). Abnormal synaptic mechanisms could be an explanation for why a large proportion of patients with anti-NMDAR encephalitis do not show structural MRI abnormalities (Dalmau et al., 2008; Titulaer et al., 2013; Iizuka et al., 2016), but functional dysconnectivity is generally found with fMRI nonetheless (Chang, 2014; Finke et al., 2013; Peer et al., 2017). Anti-NMDAR antibodies provoke the internalization of NMDA receptors and loss of receptors at the cell membrane surface (Dalmau et al., 2008) while anti-AMPA receptor antibodies cause a decrease in synaptic AMPA receptor clusters (Moscato et al., 2010). Mouse models have shown that anti-NMDAR antibodies altered excitatory connectivity and time constants in neurons, resulting in abnormal local field potential, which predicted EEG abnormalities in human paediatric patients (Rosch et al., 2018). Therefore, synaptic alteration caused by antibodies may not cause a loss of neurons but still affect connectivity.

3.1.1.2 Functional connectivity in autoimmune encephalitis

Using fMRI, multiple brain networks were altered in adult patients with anti-NMDAR encephalitis (Chen et al., 2022; Finke et al., 2013; Peer et al., 2017; Volz et al., 2016). In patients with the same condition, resting-state fMRI has shown decreased functional connectivity between the bilateral hippocampi and the medial prefrontal cortex compared to healthy controls (Peer et al., 2017). Decreased connectivity has been observed in resting-state fMRI in another adult anti-NMDAR cohort (Wang et al., 2021). In another adult cohort, increased fMRI connectivity compared to healthy controls was found between the dorsolateral-medial prefrontal cortices and the frontoparietal cortices (Chen et al., 2022). Using Transcranial magnetic stimulation paired with electric stimulation in the hand, evoked potential in the motor cortex was shown to increase in healthy participants but to decrease in patients with anti-NMDAR encephalitis; this was correlated to lower fMRI functional connectivity in the motor network (Volz et al., 2016). A similar difference was observed in the medial-temporal lobe (MTL) network in patients with a moderate disease course (mRS <2), while patients with the most severe symptoms (mRS >2) also had decreased fMRI connectivity in the sensorimotor, lateral-temporal and visual networks (Peer et al., 2017). In another study, a high mRS score was significantly associated with lower fMRI dynamic connectivity between the medial prefrontal cortex and the parahippocampal and angular gyri (von Schwanenflug et al., 2022a). fMRI dysconnectivity between the anterior parts of the hippocampi and of the default mode network (DMN) was reported in a cohort of 24 adults (Finke et al., 2013), and was also found in connections stemming from the left insula in 21 adult patients (Li et al., 2021). This shows anti-NMDAR encephalitis may cause widespread network dysfunction.

Limbic encephalitis is also related to dysconnectivity: fMRI connectivity analysis has shown impairments in autoimmune limbic encephalitis, such as decreased functional connectivity between the hippocampus and the parietal lobules (Argyropoulos et al., 2020); between the two hippocampi; or between the hippocampus and the medial prefrontal and posteromedial cortices (Loane et al., 2019). Patients with anti-LGI1 antibodies can also show an increased connectivity in multiple resting state fMRI networks such as the dorsal DMN (more connected to the frontal, cingulate and medial prefrontal cortices, the left precuneus, left temporal areas), the ventral DMN (frontal areas, inferior temporal and right occipital regions), the sensorimotor and visual networks (left cerebellum, right occipital cortex); while having a decrease in the salience network (with left parietal areas; Heine et al., 2018). The medial temporal subcomponent of the DMN may also be affected in anti-LGI1 encephalitis (Miller et al., 2020). As mentioned in Chapter 1, was suggested that increased activations may result from pathways being solicited as a compensation for concomitant damaged hippocampal structure (Heine et al., 2018). Limbic encephalitis is therefore linked to alterations in different networks, especially involved in temporal areas.

Functional connectivity research is lacking in ADEM. Although no functional network analysis has been done in ADEM to date, altered pathways may underlie functional dysconnectivity, because disrupted axons prevent the conduction of nervous signals (Beatty et al., 2016; Iype et al., 2018). Frequent abnormal brain activities are found with EEG, which may suggest functional alterations (Fridinger & Alper, 2014; Tenembaum, Chamoles & Fejerman, 2002). The studies outlined in this section do not give an account of brain functional connectivity in the paediatric population, which is to be investigated.

3.1.2 Assessing functional connectivity in neuroimaging

3.1.2.1 Functional connectivity across neuroimaging modalities

As introduced in Chapter 1, “functional connectivity” indicates the extent of neural activity shared between brain areas: in fMRI, it is considered that a functional connection is observed between a pair of areas when their respective BOLD signals (the oxygenated blood flow which accompanies neural activation) are statistically associated across time (Peer et al., 2017; Finke et al., 2013; Heine et al., 2018; Li et al., 2021). In EEG or MEG, a functional connection is considered to be observed based on temporal statistic association (or *coupling*) between neural electrical/magnetic signals; this can be the association of signal amplitudes concomitant in time, but also of the phase of the oscillations (Bullmore & Sporns, 2009). fMRI connectivity is thus an approximate indicator of neural transmission, with relatively low

temporal resolution, whereas MEG-based connectivity can look at the specific properties of the connections (e.g. at which frequency; da Silva, 2013) and in shorter periods of time (ms), therefore highlighting more precise aspects of the functional networks (Bullmore & Sporns, 2009). Furthermore, EEG connectivity studies are limited by their lower spatial resolution (da Silva, 2013; Hari et al., 2018) and commonly examine connectivity between signals at the level of the sensors (for example, Quraan et al., 2013; Sargolzaei et al., 2015); it can thus be argued that MEG source-located signals give a more precise account of the functional brain networks.

3.1.2.2 Connectomics

Graph theory studies the structure of complex networks and has been recently applied in neuroscience, based on the anatomical understanding that the brain is organised as networks of cortical regions connected by neuronal pathways (Bullmore & Sporns, 2009; Stam & Reijneveld, 2007). An abstract representation of brain networks is made in terms of *nodes*, which are points of connections, and *edges*, which are the connections between them (Bullmore & Sporns, 2009). A range of mathematical measures can be defined to determine the number of connections linking each node to the network (degree) or to neighbouring nodes (clustering coefficient), the average number of edges that separate them (path length) and so on; these measures are believed to reflect brain connectivity and its capacity to integrate and transmit information fast and efficiently (Bullmore & Sporns, 2009).

The common steps for resting-state functional connectivity analysis consist in defining nodes such as anatomical regions, quantifying functional connectivity between those nodes and deriving a network from them in the form of connectivity matrices (Fornito, Zalesky & Breakspear, 2015). In the case of MEG, edges can be determined with the temporal statistic association between signals (Bullmore & Sporns, 2009) which can be precisely located in coregistered MRI scans (Tewarie et al., 2013). Graph theoretical measures extracted from the networks can then be compared between groups for research in clinical conditions and correlated with cognitive performance (Bullmore & Sporns, 2009; Fornito, Zalesky & Breakspear, 2015). Such MEG network analysis has not been done in AE to date and may be valuable given alterations of connectivity discussed in section 1.1.2.

3.1.2.3 Anatomical implications

Research shows that structural connectivity and functional connectivity are interdependent to a certain extent: measures of structural network connectivity correlate with functional measures and show that an anatomically impaired brain network is associated with corresponding activity dysfunction (Bullmore & Sporns, 2009). Although the functional network

may be altered, it is possible that an adaptive response from other nodes compensates for structural damages and preserves task performance (Fornito, Zalesky, & Breakspear, 2015), while performance may still be impaired without structural damage (Catani & Mesulam, 2008). Whole brain functional imaging can show how focal lesions impact distant connected regions by altering their activation even if they are structurally intact (Fornito, Zalesky, & Breakspear, 2015). Maladaptive response such as diaschisis that inhibits connected regions, can then contribute to behavioural impairments (Fornito, Zalesky, & Breakspear, 2015).

It is possible that large brain networks undergo changes with time, related to aging or disease progression (Bullmore & Sporns, 2009; Fornito, Zalesky, & Breakspear, 2015). In healthy participants, functional connectivity can be subject to short term fluctuations, but global characteristics are found to be stable (Bullmore & Sporns, 2009), which allows scientists to define common networks (Peer et al., 2017; Heine et al., 2018). However, AE may be a cause of large network alteration: while this may not be associated with disease duration (Heine et al., 2018; Peer et al., 2017), inter-hippocampal fMRI functional connectivity has been found to decline with time after the acute stage (Loane et al., 2019). Furthermore, age of onset may be important because disruption in developing brain networks could have a clinical significance in AE (Beatty et al., 2016; Iype et al., 2018).

3.1.2.4 Important functional networks

Brain networks are known to support different cognitive functions. Attentional process is based on a balance of activated and deactivated regions during tasks (Anticevic et al., 2012; Fox et al., 2005): An activated network, including the intraparietal sulcus, inferior parietal lobule, the precentral sulcus, the dorsolateral prefrontal cortex and the middle temporal region; concomitant with the deactivated DMN, involving the posterior cingulate, the medial and lateral parietal cortex, and the medial prefrontal cortex (Fox et al., 2005). It was suggested that an over activation of the DMN may lead someone to exceedingly focus on thoughts and feelings, altering the integration of external information (Anticevic et al., 2012). Research shows that when the DMN is not appropriately suppressed, working memory performance decreases, and it is thought to obstruct goal-directed cognition (Anticevic et al., 2012; Fox et al., 2005). These are networks that likely explain cognitive deficits in AE (Finke et al., 2013; Heine et al., 2018). Networks also support visual perception, with the visual network (connecting to the occipital cortices, occipito-parietal and occipito-temporal regions), movements with the sensorimotor network (connecting primary somatosensory and somatosensory cortices); which are altered in AE (Heine et al., 2018; Peer et al., 2017; Volz et al., 2016). The MTL network, involving the hippocampus and parahippocampal cortex is associated with memory process and can be

altered in AE (Peer et al., 2017; Miller et al., 2020). The processing of salient stimuli, events relevant to behavioural responses, is associated to the *Salient network* which includes the insula, and has also been found to be altered in AE (Heine et al., 2018).

3.1.3 Dysconnectivity and epileptic abnormalities

3.1.3.1 Brain networks in Epilepsy

Epilepsy is a chronic brain disorder which is characterized by epileptic seizures (Geis et al., 2019). Seizures are "a transient occurrence of signs and/or symptoms due to abnormal excessive or synchronous neuronal activity in the brain" (Fisher et al., 2017, p.539). Epilepsy is now recognized as an archetypical hyperexcited neural network disorder (Xu et al., 2021): it is characterized by network dysfunction, commonly in the temporal lobes, impacting limbic regions related to emotions as well as stress response circuits, which is thought to increase psychiatric comorbidities (Colmers & Maguire, 2020). Epileptogenic zones, regions which produce epileptic seizures, are highly connected during ictal (seizure-related) phases, which led to the suggestion that seizures spread in network (Haneef & Chiang, 2014). Research in fMRI has shown specific circuits involved in epileptogenic zones of patients with Mesial Temporal Lobe epilepsy, especially in temporal and limbic structures such as the hippocampus and the thalamus (Englot, Konrad, & Morgan, 2016a). MEG, which has a higher capacity for localization of epileptiform activity (Xu et al., 2021), helped observe connections between absence seizures in anterior cerebellar regions, posterior and middle areas of the cingulum, bilateral precunei and the left thalamus of 16 children with absence epilepsy (Youssofzadeh et al., 2018). Discharges observed with MEG outside of seizures (*interictal epileptiform discharges,* IED) in theta and delta waves are also associated with fMRI network disruption; especially in children with a higher occurrence of such discharges (Ibrahim et al., 2014). MEG helped detecting and localizing epileptiform events called "spikes" discharges: during these, the network activity involves regions concordant with cognitive deficits, although the relevance of spikes to epilepsy outcome is unclear (Malinowska et al., 2014; van Mierlo et al., 2019).

Connectivity analyses at resting-state provide relevant information about network functioning in epilepsy: fMRI has showed decreased connectivity in the DMN (Englot, Konrad, & Morgan, 2016a), but the slow hemodynamic response from fMRI measures is considered to be a limited indicator of neural dynamics in time (Quraan et al., 2013). Electrophysiological responses are specifically relevant to epileptic activities: activating networks measured with EEG can discriminate children with epilepsy from healthy controls (Sargolzaei et al., 2015), and

higher synchronization likelihood in theta activity was shown to predict the diagnosis of any type of epilepsy (Douw et al., 2010a). Compared to controls, epileptic patients had increased clustering coefficient (connections forming local modules) in EEG theta oscillation networks, and decreased clustering coefficient in beta oscillation networks (Quraan et al., 2013). MEG, which performs direct high-resolution measures of brain activity reference-free along with a good source localization of epileptogenic zones, makes it an "ideal tool for investigating the resting-state functional connectivity in epilepsy" (Xu et al., 2021, p.2).

For example, MEG was more efficient in detecting lateralized delta activity in epilepsy (Englot et al., 2016b). Delta and theta band connectivity of the middle temporal and anterior cingular gyri in the DMN was higher in adults with temporal lobe epilepsy compared to controls (Hsiao et al., 2015). An adult MEG study reported increased global nodal strength (a measure of network efficiency) in theta, alpha and beta1 bands in a group with genetic generalized epilepsy; theta and beta1 for another group with non-lesional focal epilepsy; both compared to healthy controls (Li Hegner et al., 2018). At a regional level, individual clusters across delta, theta and beta bands were also found to be increased compared to healthy controls, affecting frontal, temporal, parietal and/or occipital regions (Li Hegner et al., 2018). In a cohort of 26 patients with juvenile myoclonic epilepsy, increased MEG theta connectivity in posterior brain regions and decreased beta connectivity in sensorimotor cortices was found in comparison to controls (Routley et al., 2020). All of this provides support for MEG as a tool that can identify precise patterns of dysconnectivity at resting state (Xu et al., 2021).

There is some evidence that there may be a relationship between MEG-detected functional disconnections and epileptic seizures: Looking at alpha and beta bands with MEG, a study of 12 post-surgery epilepsy patients found a higher alpha functional connectivity between regions generating IED and other brain regions for patients with seizures compared to seizure-free patients (Aydin et al., 2020). In an adult cohort with epilepsy due to low-grade glioma, MEG was used to show that theta band alterations in synchronous states were correlated with higher frequency of seizures, although not in the epileptic group with no glioma (van Dellen et al., 2012). Another study including 20 adults with epilepsy found an association between theta & alpha MEG connectivity and frequency of seizures although the significant association with theta did not survive correction; seizure frequency was also significantly associated with network efficiency in 4-10Hz frequency band (van Dellen et al., 2014). Another MEG study found a significant relationship between alpha connectivity and frequency of seizures in adults with mesial temporal lobe epilepsy and focal neocortical epilepsy; they did not test such analysis for slower frequencies although delta and theta connectivity values were

also lower than controls (Englot et al., 2015). In adult tumour-related epilepsy, MEG detected an association between theta-band connectivity and higher number of seizures (Douw et al., 2010b). The above evidence suggests that MEG functional connectivity and features of epilepsy are related. It remains to be tested whether networks measured with MEG directly relates to the frequency of seizures in children.

3.1.3.2 Epileptic features in autoimmune encephalitis

An immune etiology of epilepsy is recognized, as "immune epilepsies" has long been included in the *International League Against Epilepsy* classification of epilepsies, and was recently developed into two distinct phenomena: an "acute symptomatic seizures secondary to autoimmune encephalitis" that is characteristic of seizures during the acute phase of AE, and an "autoimmune-associated epilepsy" characterized by chronic seizures that are characteristic to autoimmune brain diseases (Steriade et al., 2020).

Seizures are one of the common features included in the diagnosis of autoimmune encephalitis, and it usually appears in the first 3 months after the disease onset (Graus et al., 2016; Titulaer et al., 2013). In 153 patients with anti-LGI1, anti-NMDAR and anti-$GABA_B$ receptor encephalitis, 110 had epileptic seizures, among whom 89% were seizure-free in a median of 59 days after onset (De Bruijn et al., 2019). Specifically, in anti-NMDAR encephalitis, seizures develop in 57% to 82% of patients at onset (Dalmau et al., 2019). This feature is most frequent in anti-NMDA and anti-LGI1 antibody positive patients between 12 and 17 years, and was suggested to be more likely to happen in immature brains because of an enhanced excitability following injury (Yeshokumar et al., 2021). A review reported that 66% to 89% of patients with anti-LGI1 encephalitis experienced temporal lobe seizures; 71% to 89% in CASPR2 antibodies encephalitis (Vogrig et al., 2019). A study of 74 children with ADEM has found that those with MOG antibodies were more likely to develop epilepsy (Rossor et al., 2020). Another systematic review reported that across different types of autoimmune encephalitis, seizures were present in 69.9% of patients (Yeshokumar et al., 2021). This makes seizures a prominent feature of AE.

Various types of seizures are being observed: Tonic-clonic seizures (involving muscle stiffening followed by muscle jerking; Fisher et al., 2017), focal seizures (in one area of the brain) with and without impaired awareness, and status epilepticus (abnormally prolonged seizures beyond 5 minutes, Trinka et al., 2015) were found in patients with anti-LGI1, anti-NMDAR, and anti-$GABA_B$ encephalitis (De Bruijn et al., 2019). Focal, bilateral tonic clonic and generalized epilepsy are also found in encephalitis with $GABA_A$ and MOG antibodies,

accompanied with status epilepticus and/or movement disorders (Vogrig et al. 2019). Faciobrachial dystonic seizures, which cause sustained contractions in muscles and abnormal postures (Fisher et al., 2017), are commonly observed in limbic encephalitis associated with anti-LGI1 antibodies (Irani et al., 2011; Vogrig et al., 2019). Temporal lobe seizures are a common sign of anti-NMDAR (with impaired awareness, orofacial and manual automatisms, or status epilepticus), anti-AMPAR (involving limbic areas), anti-LGI1 (with vegetative symptoms, intrapsychic hallucinations, or ictal fear), anti-CASPR2 (sometimes associated with severe anterograde amnesia or frontal lobe dysfunction), and anti-GAD65 encephalitis (with altered short-term memory, executive functions or mood; Vogrig et al., 2019).

Abnormalities during EEG recordings were present in 84.8% of 2025 patients with AE (Yeshokumar et al., 2021). Interictal discharges are also reported with routine EEG scans, commonly in the temporal lobe, unilaterally or bilaterally, as well as abnormal beta and delta activity, and diffuse slowing (Vogrig et al., 2019). Limited data exists with MEG, but it should be an efficient tool for assessing such abnormalities: one study observed interictal spike-waves in the temporal lobes of two patients with anti-LGI1 encephalitis, and it was associated with general EEG slowing as well as faciobrachial dystonic seizures (Gao et al., 2016). Another study on one patient with anti-NMDAR encephalitis showed that MEG could detect delta abnormalities and localize them in the brain (Miao et al., 2021). The role of interictal discharges in epileptic seizures is still unclear, but they may be functionally connected. Investigating the connectivity of such networks with MEG may provide a more detailed understanding of ictogenesis in AE (Heine et al., 2018; Peer et al., 2017).

3.1.3.3 Frequency oscillations and seizures

Constant brain oscillations are generated by circuits of assembled neurons activating and transmitting information through the brain (da Silva, 2013). These oscillations reflect processes during different states, including information processing, levels of vigilance, as well as seizures and other pathological states (Hari et al., 2018). Specific frequency bands may be affected in AE: EEG research has reported excessive beta activity and abnormal delta activity in anti-NMDAR encephalitis (Vogrig et al., 2019), with lower delta-theta power compared to other types of encephalopathy and higher beta-gamma power compared to neurological patient controls (Symmonds et al., 2018). Excessive beta activity appearing first in predominantly frontal regions, followed by extreme delta brushes and generalized delta activity, was suggested to reflect disease progression into subcortical regions, possibly in the basal ganglia, which is involved in motor and epileptic abnormalities (Vogrig et al., 2019). In 92

patients with anti-NMDAR encephalitis, 77% had predominantly frontotemporal slowing or disorganized delta-theta activity (Dalmau et al., 2008). A review reports that EEG slowing was found in 51% of patients with anti-NMDAR and LGI1 encephalitis (Yeshokumar et al., 2021). This suggests low frequency oscillations are especially of interest when investigating AE.

Extreme Delta Brush (EDB) is one of the EEG abnormalities used in the diagnosis of anti-NMDAR encephalitis (Graus et al., 2016). EDB is an event of delta activity with superimposed bursts of beta frequency, riding on each delta wave, which happens both at sleep and awake with high or low level of arousal (Miao et al., 2021; Schmitt et al. 2012): in 24 patients with anti-NMDAR, 58% had EDBs (7 of them were under 18 years of age; Jeannin-Mayer et al., 2019). Antibodies disrupting NMDAR-mediated currents was suggested to alter electrographic patterns (Schmitt et al. 2012). EDB's resemblance with delta brushes observed in premature infants also led to the suggestion that it was involved in cerebral development (Schmitt et al., 2012; Jeannin-Mayer et al., 2019). While EDBs were found to be more pronounced in frontal regions, it also appears diffusely (Jeannin-Mayer et al., 2019), suggesting the involvement of a network that may connect the affected regions. Using MEG, a study identified EDB components in different brain areas of a patient with anti-NMDAR encephalitis: the delta activity originated from the superior and middle temporal gyri, the inferior frontal gyrus, the left parietal lobe; and the beta activity originated in the bilateral superior parietal lobes (Miao et al., 2021). While EDBs may be a marker of severe outcome, as it is associated with longer hospitalization (Schmitt et al., 2012), it remains unknown whether EDBs share a common underlying neuronal dysfunction with epileptic seizures, particularly in children undergoing cerebral development and if delta activity is specifically relevant.

Generalised rhythmic delta activity (GRDA) is also a common observation in anti-NMDAR encephalitis (Jeannin-Mayer et al., 2019). As mentioned in the Chapter 1, GRDA is a repetition of a uniform oscillation without varying frequency or location, which lasts minutes to hours (Jeannin-Mayer et al., 2019). GRDA is included in the EEG abnormalities that were determined to be statistically associated with later better recovery (Gillinder et al., 2019). Delta frequency oscillations may therefore be relevant to brain networks in AE.

3.1.4 Summary and hypotheses

Evidence in fMRI studies shows that AE is impacted by functional dysconnectivity (Chang, 2014; Finke et al., 2013; Peer et al., 2017). This affects well-known brain networks, such as the motor network (Volz et al., 2016) the MTL network, the sensorimotor, lateral-temporal networks, visual networks (Peer et al., 2017) and the default mode network (DMN;

Finke et al., 2013; Miller et al., 2020). These network disruptions are associated with worse clinical outcome, lower verbal, episodic and working memory, and higher mood lability (Argyropoulos et al., 2020; Finke et al., 2013; Heine et al., 2018; Miller et al., 2020; Peer et al., 2017; Volz et al., 2016). However, connectivity analyses in paediatric AE are lacking, which is needed when alteration may have a long-term impact on childhood development (Beatty et al., 2016; Iype et al., 2018). Network topology of the brain has important implications for cognitive functions and brain development, making its investigation clinically meaningful (Bullmore & Sporns, 2009; Fornito, Zalesky, & Breakspear, 2015). MEG, which has not been used for such analysis in AE to date, gives an enhanced account of neural dynamics with its higher temporal resolution compared to fMRI (Quraan et al., 2013; Tewarie et al., 2013).

MEG has been established as a clinically relevant tool in epilepsy, providing important insights into seizure dynamics and network interactions through connectivity analyses (Douw et al., 2010b; Youssofzadeh et al., 2018). Epilepsy is a condition that has common symptoms with AE, such as seizures, interictal discharges or status epilepticus (Graus et al., 2016; Titulaer et al., 2013; Vogrig et al., 2019). IEDs in theta and delta frequency bands detected with MEG were shown to be associated with network disruption in epilepsy (Ibrahim et al., 2014), and interictal spike-wave discharges could be linked to seizures (Gao et al., 2016). IEDs were also found to increase delta and theta long range EEG connectivity and node degree (Lee et al., 2017). EEG studies have shown that theta-band connectivity and the number of seizures are associated in epilepsy (Douw et al., 2010b). This is relevant for AE which involves abnormalities related to delta and theta frequency bands in routine EEG (Vogrig et al., 2019), and it possibly shows an underlying network disruption (Jeannin-Mayer et al., 2019). While associations between MEG connectivity and seizure frequency have been found in adults (van Dellen et al., 2014), no analysis was conducted for these specific signals in children. Studying low-frequency connectivity in paediatric epilepsy with MEG may therefore provide useful insights into abnormal neuronal activity that generates seizures, which may be relevant to other neurological conditions involving seizures like AE.

Considering the current research, the following hypotheses will be tested here:

1. Network connectivity in theta frequency does not significantly differ between Epilepsy and AE
2. Network connectivity in delta frequency does not significantly differ between Epilepsy and AE
3. The frequency of epileptic seizures is predicted by network efficiency in theta frequency in Epilepsy and AE.

4. The frequency of epileptic seizures is predicted by network efficiency in delta frequency in Epilepsy and AE.

3.2 Methods

3.2.1 Participants

Anonymized clinical information, MEG recordings and MRI scans were obtained from a sample of 32 children with refractory epilepsy, whose data was previously acquired at the Aston University's IHN, as part of their work up for surgical evaluation. Diagnosis of AE was rejected for all of them. Children were aged 5 to 17 years (IQR 5.75), 15 females and 17 males (Ethics application #1715). Out of the 32 children, 18 were selected for analysis, because they had been recorded at rest with eyes open.

A control cohort was also recruited at the IHN, through contact permission from families that took part in research projects at the centre, as well as advertisement via social media/community organisations and Aston University/IHN outreach events. It included typically developing children from 6 to 16 years of age. Inclusion criteria included the absence of diagnosis of learning difficulty, or psychiatric, neurodevelopmental, or neurological disorder and absence of known or suspected cerebral abnormality. Their informed assent to participate and informed consent of one of their respective parents or legal guardians were collected.

Another cohort composed of paediatric patients with AE was recruited at the Birmingham Children's Hospital, Birmingham, United Kingdom, Birmingham, UK (Ethics Reference #17/YH/0299; #IRAS 222771). Inclusion criteria for all participants were an age range from birth to 6 to 16 years at point of recruitment. AE children were included if they had a previous diagnosis of any type of AE (according to the standards established in Cellucci et al., 2020; Graus et al., 2016), and were recruited at least 2 years after disease onset.

3.2.2 Image acquisition

Epilepsy participants had been scanned with the same MEG scanner which was used for the control participants, with the same parameters and protocol described in the following: the MEG scanner was an Elekta Neuromag® TRIUX MEG system, comprising 306-channels, including 102 magnetometers, coils that measure broadly any orthogonal magnetic field, and 204 planar gradiometers, that measure the maximum signal directly above the cortical source and subtract magnetic field external to the brain (Hari et al., 2018; Proudfoot et al., 2014). The channels are located in a single-shell magnetically shielded room equipped with MaxShieldTM technology. Scans were acquired with a sampling rate of 2000Hz and a low-pass filter of 660 Hz. Additionally, five head position indicator coils were added, three on the forehead and one

on each mastoid. In order to facilitate co-registration between the MEG and the MRI scans, a *Polhemus Fastrak* motion tracker device was used to digitize coordinates around the shape of each participant's head, starting from three main fiducials coordinates (located on the nasion, and bilateral preauricular points).

Control and AE participants took part in a 6-minutes resting state recording, where they had to sit still in the scanner and look at a black fixation cross on a white background. Epilepsy participants had been spontaneously recorded or specifically at rest with fixation cross during the recording from 4 to 12 minutes, eyes open with no movie or form of activity/entertainment.

MRI T1-weighted scans were acquired with a *Siemens TrioTim* scanner for the Epilepsy group; and with *Siemens TrioTim* and *Siemens MAGNETOM Prisma* scanners for the Control group and the AE group (both 3T, flip angle 15, dimension 176x240x256).

3.2.3 Preprocessing

3.2.3.1 MEG data processing

Each recording was filtered using the MaxFilter software (Elekta Neuromag Oy; version 2.2.10), which removes artefacts using spatiotemporal signal space separation (tSSS). tSSS is an algorithm that removes the signals that it estimates to be outside the spatial range of the brain and signals correlated in time to external (non-cortical) signals (Taulu & Simola, 2006). Filtered recordings were epoched into non-overlapping 10 second trials and DC component was removed using the *Fieldtrip* toolbox (*v*. 22 January 2021; Oostenveld et al., 2011) in Matlab R2017a (Matlab, 2017). A zero-phase butterworth 4th-order low-pass filter was also applied at 70 Hz (as in Vogrig et al., 2019). Channels and epochs were manually toggled through and rejected when containing excessive artefacts caused by muscle activity and SQUID jumps, and subsequently imported in the *BrainStorm* toolbox (*v.* 3.210818, 18 August 2021; Tadel et al., 2011), which is documented and freely available for download online under the GNU general public license (http://neuroimage.usc.edu/brainstorm). Segments with epileptiform spikes were identified based on their morphology in the time series data and manually removed in Brainstorm. The number of 10 second epochs that remained after processing were distributed as follows: 23.5±7.8 (IQR = 13) for the Epilepsy group; 37.5±1.6 (IQR = 1) for the Encephalitis group and 37.33±1.1 (IQR = 3) in the Control group.

3.2.3.2 MRI co-registration and source reconstruction

Source models were created using *FreeSurfer'*s preprocessing default pipelines (*v*. 6.0, https://surfer.nmr.mgh.harvard.edu/fswiki/ReleaseNotes). The software recreates 3D surfaces

of white matter and gray matter by segmenting them, while extracting the brain from tissues of the skull and of the neck (Despotović, Goossens & Philips, 2015). Skull-stripping, gray matter and white matter surface artefacts were manually corrected with FreeSurfer. When an MRI scan contained too many artefacts to generate FreeSurfer meshes, an age-matched paediatric symmetric MRI template preprocessed with the same FreeSurfer pipeline was used as a substitute for MEG modelling (Fonov et al., 2009; Fonov et al., 2011). An MRI template was needed for two participants in the Epilepsy group (ID 8 and 18 in Appendix 3.1), one in the Encephalitis group (ID 8 in Appendix 3.1), and one in the Control group. The templates were preprocessed again in order to keep the same parcellation atlases across participants.

The surfaces generated with FreeSurfer were imported to Brainstorm in order to align MEG channels of each participant's recording to its respective MRI head surfaces using the head position indicator coordinates. The number of vertices was downsampled to 15000 in order to optimize source projection. The imported surfaces were used in Brainstorm to generate three-shell realistically shaped head models for each participant, using the *OpenMEEG* plug-in (Gramfort et al., 2010; Kybic et al., 2006), using scalp/skull/brain layers with default settings for layer conductivities, vertices and skull thickness. The latter plug-in worked with the boundary element method, which can improve localization of source signals better relative to sphere-based methods (Stenroos, Hunold & Haueisen 2014). Data covariance (median eigenvalue, as recommended by Tadel et al., 2021) matrices were estimated from the whole recording files to reconstruct sources using the linearly constrained minimum variance (LCMV) beamformer (Van Veen et al., 1997; as in Youssofzadeh et al., 2018). LCMV beamforming is a "spatial filtering" algorithm that discriminates signals in space, by passing signals that originate in a specified location and attenuating signals from other locations. Based on the signal variance or strength across the sensors, normalized by background noise, it estimates the localization (within a head model) of the underlying neural activity by relating it to the spatial distribution of magnetic fields captured at the surface (Van Veen et al., 1997).

3.2.4 Connectivity analysis

3.2.4.1 Connectivity matrices computation

For each participant, each trial was transformed in the time-frequency domain using Hilbert transformation, keeping delta (1 to 4 Hz) and theta (4 to 8 Hz) frequency bands (classified as in Englot et al., 2016b; Hsiao et al., 2015; Wu et al., 2017). The Desikan-Killiany

parcellation atlas (processed in FreeSurfer) was selected to apply Brainstorm's scout function: this computed the mean power of the time-frequency (of each frequency of interest band-pass filtered separately) within each parcellated region before estimating connectivity. Connectivity between regions was computed for the two frequency bands of interest using *Amplitude Envelope Correlation* (AEC), which measures correlated envelopes (temporal evolutions of the amplitude of signals) between pairs of orthogonalized regional signals (Hipp et al., 2012). The orthogonalization of the pairs of signal ensures that they do not share the co-variability in power due to measuring the same source activity (which would then not represent a true connection but simply the same, common source activation). This consists in identifying a linear relation between a first source time-frequency power and a second source at each parallel time-point: the orthogonalized signal can be derived by subtracting the linear signal component to the source signal (Hipp et al., 2012, Supplementary information). The AEC method therefore avoids common source biases and was shown to produce a highly consistent network estimation (Colclough et al., 2016; Liuzzi et al., 2017). This measure was successfully used in a recent study in epilepsy (Aydin et al., 2020). Two connectivity matrices (for delta and theta connectivity) were generated for each epoch and averaged for each individual participant (resulting in two average connectivity matrices per participant).

3.2.4.2 Graph measures computation

The average matrices were exported in Matlab and negative correlations were excluded (set to zero). For graph measures, the weights of the matrices were normalized (ranging 0 to 1) with the Brain Connectivity Toolbox (Rubinov & Sporns, 2010), and thresholded with proportions of the 10% to 30% highest connections, in intervals of 4%, deriving 6 matrices per frequency band. The range was selected because networks at a threshold of 30% remained significantly different in an epilepsy cohort across measures of global efficiency, clustering coefficient and network topology in the theta band (EEG study from Quraan et al., 2013, Figure 5). Based on past studies in adult epilepsy cohorts (Chapter 5 will explore other metrics based on research in AE), the following graph network measures were extracted in each of the delta and theta frequency bands:

- *Characteristic path length* (*L*), as in Douw et al., 2010b; which is the average shortest path length between all pairs of nodes in the network, computed by converting the weighted matrices into connection-length matrices, higher connections being interpreted as shorter paths (*Dijkstra's algorithm*; Rubinov & Sporns, 2010), a measure for global integration of the network (Bullmore & Sporns, 2009); similar to *Diameter*

which was relevant to seizure frequency using the Minimum Spanning Tree method (van Dellen et al., 2014).

- Mean *Clustering coefficient* (*C*), as in Douw et al. (2010b) and Li Hegner et al. (2018); the average fraction of triangles around each node (or fraction of each node's neighbours that are also neighbours of each other; Rubinov & Sporns, 2010), indicating local segregation of "clusters" within the network (Bullmore & Sporns, 2009). Matrices were binarized for this specific measure.

Figure 3.1

Example of a MEG resting-state network topology measured in a child with autoimmune encephalitis

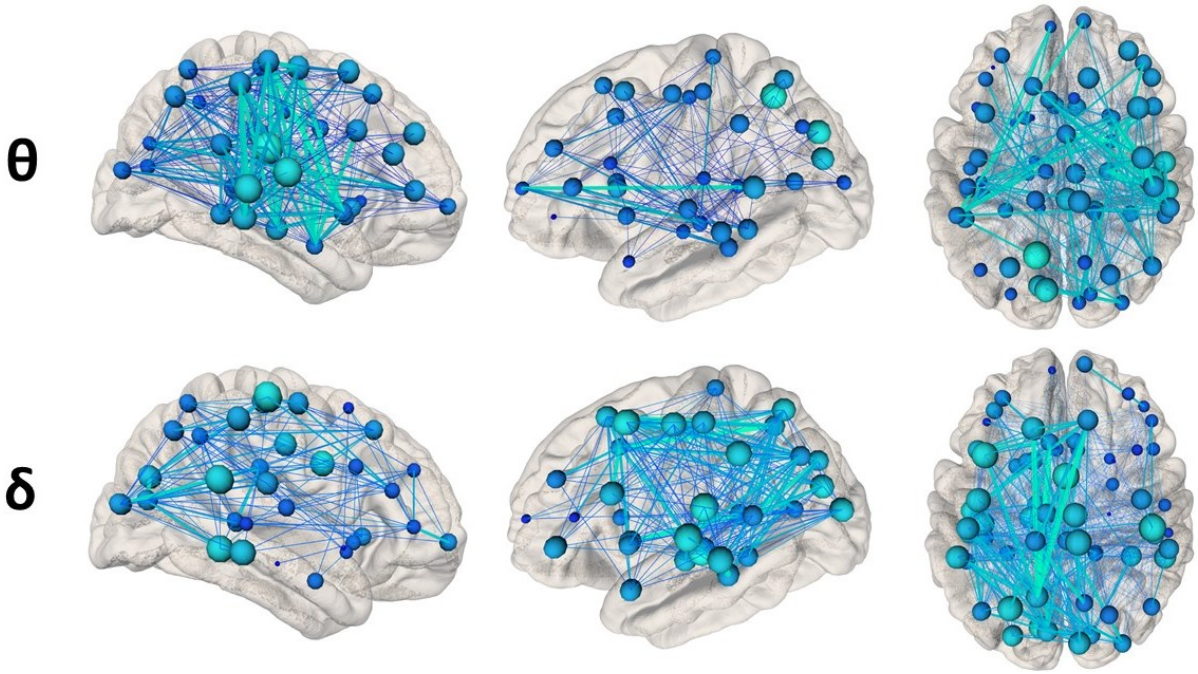

Note. The figures were produced using the NeuroMArVL web app (Dwyer et al., 2017). Node size and brightness represent the clustering coefficient per region, and Edge thickness and brightness represent the strength of the connectivity. The network was thresholded at 30%.

3.2.4.3 Multi-threshold permutation correction

To identify a threshold potentially relevant for seizures, the epilepsy group's graph measures were compared to the control group and to the AE group, and the AE group's graph measures to the control group at each threshold. In order to avoid the issue of multiple comparisons produced by the multiplication of thresholds, as each group difference was assessed for 2 frequency bands * 6 thresholds * 2 graph measures, the "multi-threshold permutation correction" (MTPC) was used. It was implemented in the *brainGRAPH* package (*v*.3.0.0; Csardi & Nepusz, 2006; Watson et al., 2020) in *R* (*v*.4.2.1; R Core Team, 2022). This approach allows the identification of a group difference that is stable across thresholds and controls for multiple comparison through permutation correction. The MTPC was successfully applied in other clinical populations with structural diffusion-weighted imaging networks (Cheng et al., 2019; Drakesmith et al., 2015; Watson, DeMaster, & Ewing-Cobbs, 2019; Spilling et al., 2019), and can be replicated in MEG-derived networks as they are represented in the same mathematical graph pattern. The Desikan-Killiany atlas in brainGRAPH was reordered in order to match the labels of the matrices in Brainstorm. The MTPC computes a test-statistic (here, *t*) on graph measures across groups for each threshold, and permutes group

assignments (here, 5000 times). The maximum *t* across all permutations for each threshold are used to establish a critical value at a desired confidence level (here at α = .05). For each threshold, an area-under-the-curve (AUC) is computed for significant "clusters" where the true *t* is higher than the critical value. A critical AUC is determined from the mean of the super-critical AUCs of the permuted tests: the output of the MTPC is significant if the AUC of the significant clusters exceeds the critical AUC (Drakesmith et al., 2015). In the present study, the MTPC model was two-sided.

To account for the multiple MTPC analyses (3 group comparisons * 2 frequency bands * 2 graph measures), the *p* values corrected across all six thresholds in each MTPC (p.fdr values), were corrected again for false discovery rate against the p.fdr values of the other MTPC analyses (12 * 6 p.fdr in total).

According to the output of the MTPC in comparison to controls, graph measures for each participant were extracted for the threshold where the group difference was the highest, regardless of statistical significance, and used for further statistical analyses.

3.2.4.4 Network comparison in alpha and beta bands

Multimodal findings show that typical resting-state connectivity in MEG is largely composed of alpha and beta activations, with high spatial concomitance to networks established in fMRI resting state data (Brookes et al., 2011). Because of this, network comparisons analyses were also produced in the alpha and beta bands and were reported in Appendix 3.2 to give potentially informative studies for further studies in AE that may explore other frequency bands in the future.

3.2.5 Statistics

3.2.5.1 Power analysis

Associations run between network measures and frequency of seizures in past studies produced moderate to strong effect sizes (τ = 0.538 in Douw et al., 2010b; τ = −0.448 in van Dellen et al., 2012; τ = 0.545 in van Dellen et al., 2014; R^2 = 0.121 in Englot et al., 2015). Kendall's tau's equivalent in Pearson's *r* can be computed using the following formula (Walker, 2003): $r = sin(\pi \times \tau \times .5)$. A τ of 0.538 is equivalent to *r* = 0.748; a τ of -0.448 to *r* = –0.647; a τ of 0.545 to *r* = 0.755. Using G*Power (Faul et al., 2007), it was determined that a multiple regression with a power of 1- β = 0.65 at *p* = .05 could be obtained with the 18 cases provided that a large effect size (f^2 =.035, *r* = .05) is found. However, adding predictors would require an

even larger effect size, which means the sample is underpowered for appropriately reliable multiple regressions.

3.2.5.2 Regression analysis

Graph measures for each frequency band (delta and theta) at the selected highest-difference thresholds were extracted and included in an ordinal logistic regression model, predicting reported frequency of seizures contemporary to the time of MEG (not during the MEG recording), controlling for age and epilepsy duration in *SPSS* (*v*.26 64-bit for Windows; IBM Corp, 2019). Such analysis was not run for the AE group as only two children of that group had seizures contemporary to the MEG recordings (ID 2 and 11 in Appendix 3.1). Seizure frequency was coded ordinally as such: "<1 a month", "1 to 30 a month", "31 to 120 a month", ">120 a month". Epilepsy duration was included as a covariate because it has also been found to be linked to MEG delta and theta connectivity in patients with temporal lobe epilepsy (Zhang et al., 2021). The assumption of no multicollinearity between independent variables was checked by looking at variance inflation factor (VIF) values and collinearity diagnostics in a separate linear model; and the assumption of proportional odds was tested using the Test of Parallel Lines.

In summary, the ordinal regressions testing the effects of network measure in the epilepsy group were as follows: Seizure frequency ~ Graph measure + Age + Epilepsy duration. This amounted to four linear models: 2 for delta (effect of clustering coefficient, effect of path length), 2 for theta (effect of clustering coefficient, effect of path length). Resulting significant *p* values for the graph measure effect were corrected across the four outputs for false discovery rate.

3.3 Results

3.3.1 Demographics

Demographic information of the sample is shown in Table 3.1. Age at MEG did not significantly differ between Epilepsy and Control groups (t = -1.747, p = .092), between Epilepsy and AE groups (t = 1.205, p = .238), or between AE and Control groups (t = -0.503, p = .620). Gender distribution did not significantly differ between the three groups (χ^2 = 1.575, p = .455). The Epilepsy and AE groups had a similar disease duration (t = 0.829, p = .414). Specific clinical data and antiepileptic medication is shown in Appendix 3.1. The patients with epilepsy in the AE group had controlled seizures.

Table 3.1

Demographic and clinical characteristics of children with epilepsy, autoimmune encephalitis and typically developing children

Child characteristics	Epilepsy N=18	Controls N=12	AE N=12
Gender (female:male)	9:9	4:8	7:5
Age at MEG in years (mean±sd) IQR	12.9±3.8 6	10.6±3.2 6	11.2 ± 3.5 7
Disease duration in years (mean±sd) IQR	8.11±4.5 8	NA	6.75±4.2 8
Seizure lateralisation (left:right)	13:5	NA	NA
MOG antibody positive (%)	NA	NA	5/12 (41.6%)

Note. AE = Autoimmune Encephalitis. MOG = Myelin Oligodendrocyte Glycoprotein.

Etiologies of epilepsy diagnoses and types of autoimmune encephalitis in the cohort, along with information about medication at the time of MEG, are described in Appendix 3.1.

3.3.2 Connectivity compared across groups

The MTPC analysis returned a significant difference between the Epilepsy group and the Control group in theta characteristic path length and clustering coefficient, but not in the delta frequency. The output is depicted in Figure 3.2., showing a lower theta characteristic path length across five thresholds and a higher clustering coefficient across all thresholds in the Epilepsy group compared to the Control group.

The MTPC analysis returned a significant difference between the Epilepsy group and the AE group in both delta and theta frequency characteristic path length and clustering coefficient. The output is depicted in Figure 3.3., showing a lower theta and delta characteristic path length and a higher theta and delta clustering coefficient across all thresholds in the Epilepsy group compared to the AE group.

The MTPC analysis did not return a significant difference between the AE group and the Control group in the theta frequency, or in delta characteristic path length. However, delta clustering coefficient was significantly lower in AE compared to Controls across all thresholds. The output is depicted in Figure 3.4. All significantly different thresholds remained significant at $p < .05$ after all the p values (corrected across thresholds) of the MTPC analyses were corrected again for false discovery rate across all twelve comparison analyses.

Figure 3.2

Comparison of network measures between Epilepsy and Control groups

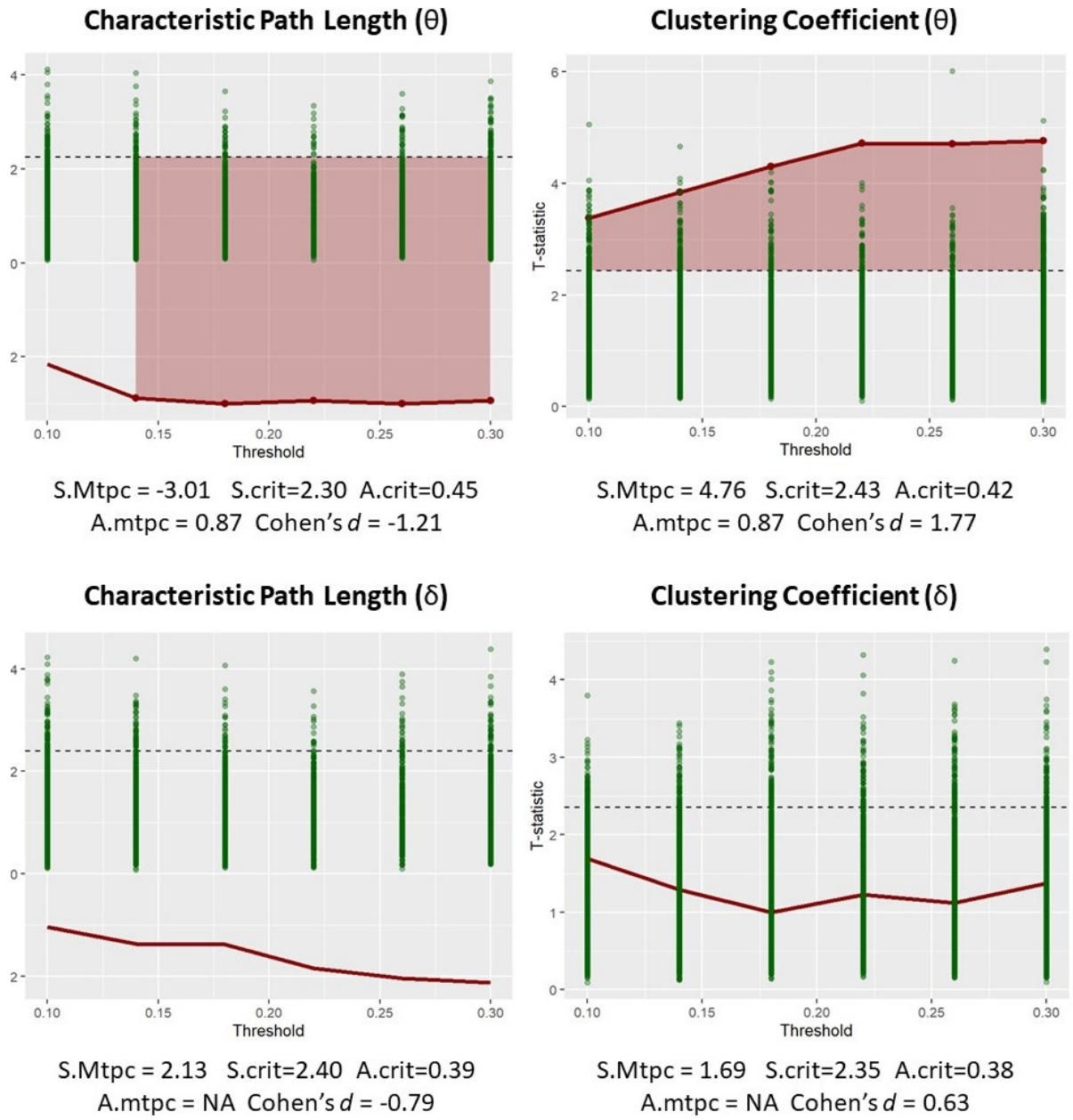

Note. S.mtpc = maximum observed statistic; S.crit = critical value of the null max. statistic; A.crit = mean of the supra-critical null AUCs; A.mtpc = AUC value of supracritical cluster.
Each graph depicts the network contrast of the Epilepsy group in reference to the Control group. The green dots are the maximum null *t* statistics of the 5000 permutations. Red dots are the observed *t* statistics. The dashed line is the critical null statistic (S.crit, top 95th percentile of the null distribution of maximum *t* statistics). The red shaded areas represent clusters of observed statistics above the critical value, whose area-under-the-curve (A.mtpc) is also greater than the mean areas-under-the-curve of the supracritical permuted statistics (A.crit). This means that a lower shaded red bar is a significantly lower network measure compared to the Control group and a higher shaded red bar is a significantly higher network measure compared to the Control group (at $p < .05$). Non-shaded bars are non-significant. The effect size *d* is only that of the threshold with the largest difference.

Figure 3.3

Comparison of network measures between Epilepsy and Autoimmune Encephalitis

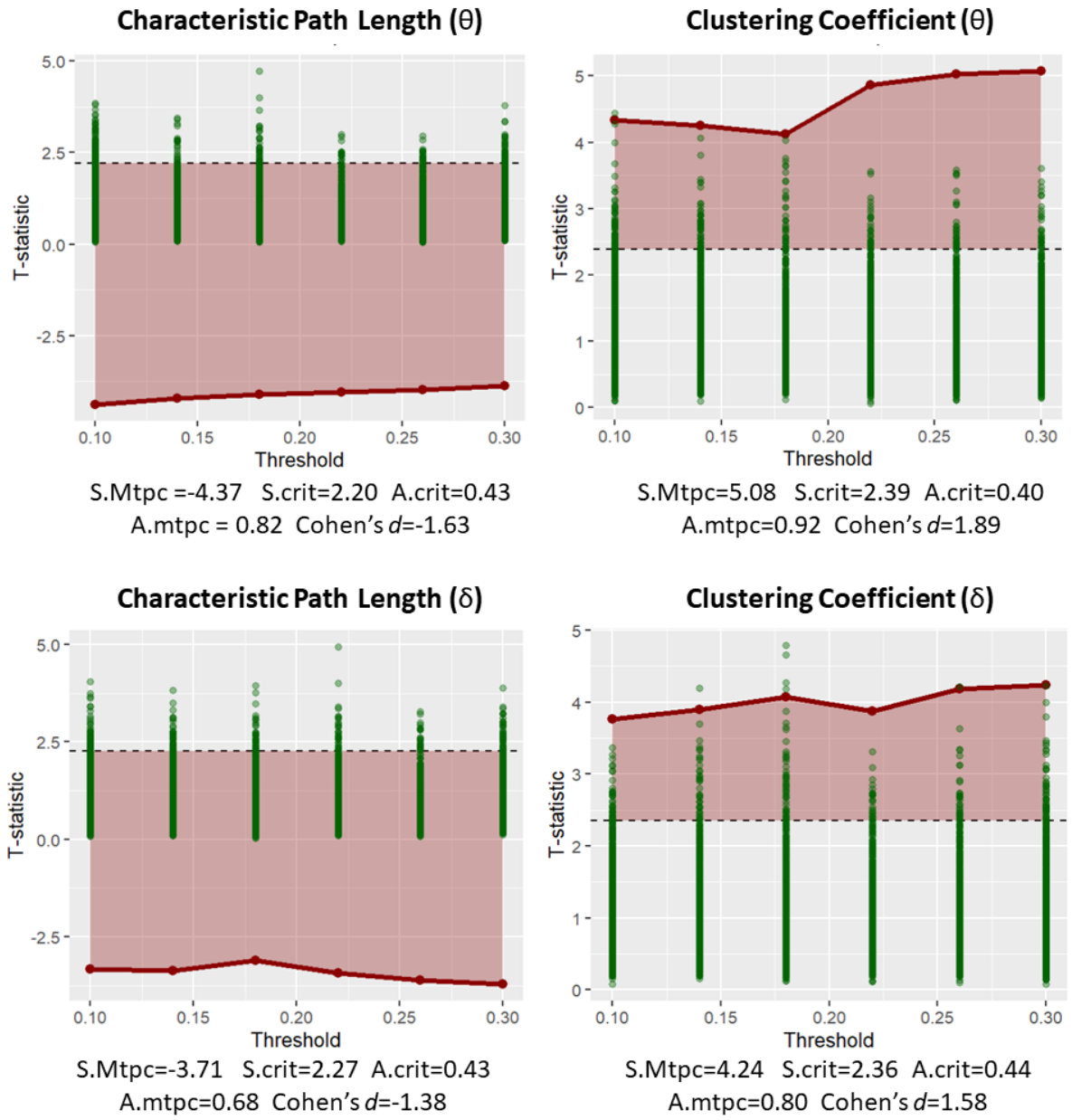

Note. S.mtpc = maximum observed statistic; S.crit = critical value of the null max. statistic; A.crit = mean of the supra-critical null AUCs; A.mtpc = AUC value of supracritical cluster.
Each graph depicts the network contrast of the Epilepsy group in reference to the AE group. The green dots are the maximum null *t* statistics of the 5000 permutations. Red dots are the observed *t* statistics. The dashed line is the critical null statistic (S.crit, top 95th percentile of the null distribution of maximum *t* statistics). The red shaded areas represent clusters of observed statistics above the critical value, whose area-under-the-curve (A.mtpc) is also greater than the mean areas-under-the-curve of the supracritical permuted statistics (A.crit). This means that a lower shaded red bar is a significantly lower network measure compared to the AE group and a higher shaded red bar is a significantly higher network measure compared to the AE group (at $p < .05$). The effect size *d* is only that of the threshold with the largest difference.

Figure 3.4

Comparison of network measures between Autoimmune Encephalitis and Control groups

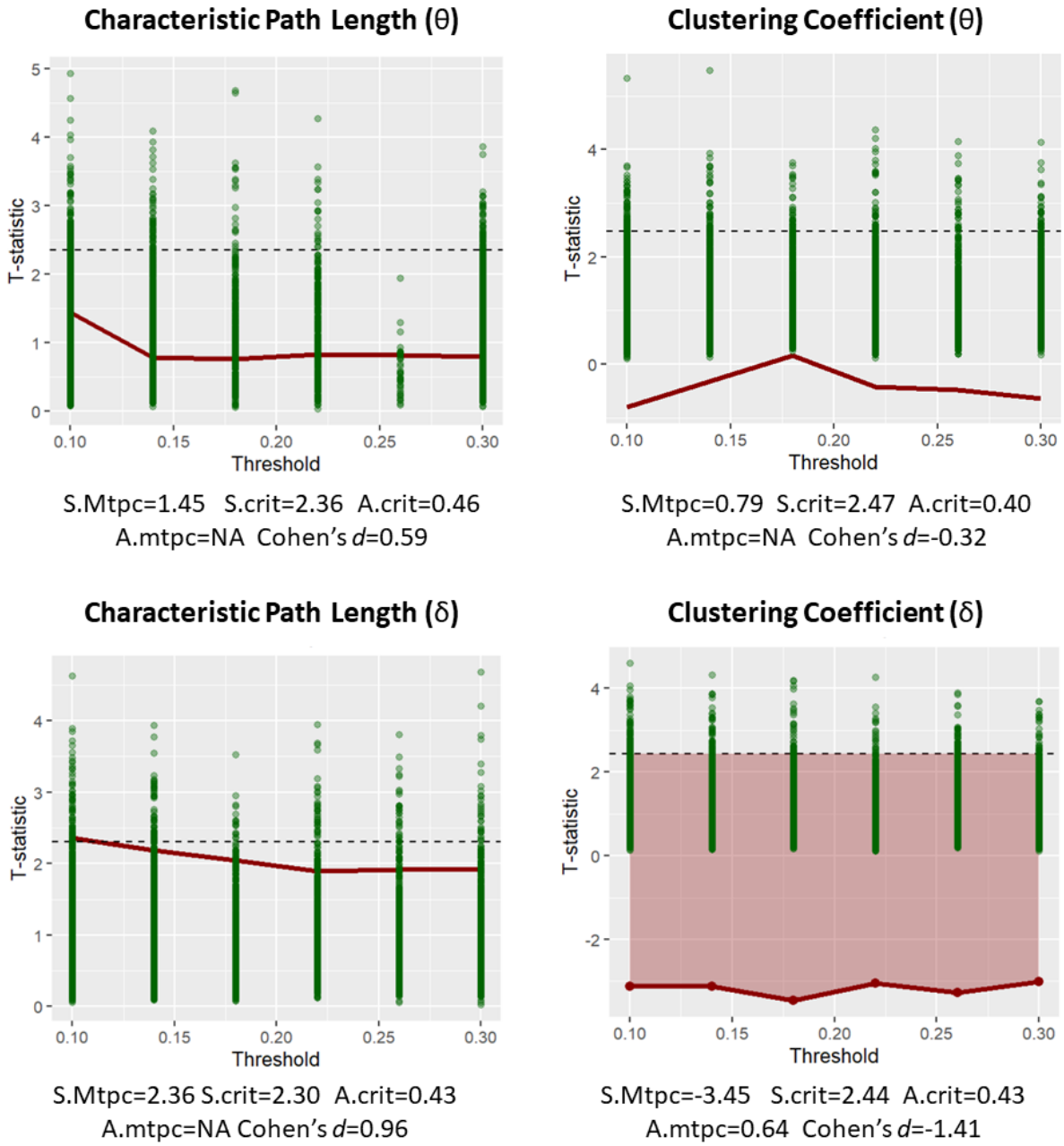

Note. S.mtpc = maximum observed statistic; S.crit = critical value of the null max. statistic; A.crit = mean of the supra-critical null AUCs; A.mtpc = AUC value of supracritical cluster.
Each graph depicts the network contrast of the AE group in reference to the Control group. The green dots are the maximum null *t* statistics of the 5000 permutations. Red dots are the observed *t* statistics. The dashed line is the critical null statistic (S.crit, top 95th percentile of the null distribution of maximum *t* statistics). The red shaded areas represent clusters of observed statistics above the critical value, whose area-under-the-curve (A.mtpc) is also greater than the mean areas-under-the-curve of the supracritical permuted statistics (A.crit). This means that a lower shaded red bar is a significantly lower network measure compared to the Control group (at $p < .05$). Non-shaded bar is non-significant. The effect size *d* is only that of the threshold with the largest difference.

3.3.3 Connectivity in relation to seizure frequency

Seizure frequency was distributed in the epilepsy group as depicted in Figure 3.5. In the AE cohort, two children had less than 1 seizure a month at the time of MEG (ID 2 and 11 in Appendix 3.1) and the rest had none, which prevented predictions to be tested for their group as previously stated.

Figure 3.5

Epilepsy cohort frequency of seizures at the time of MEG

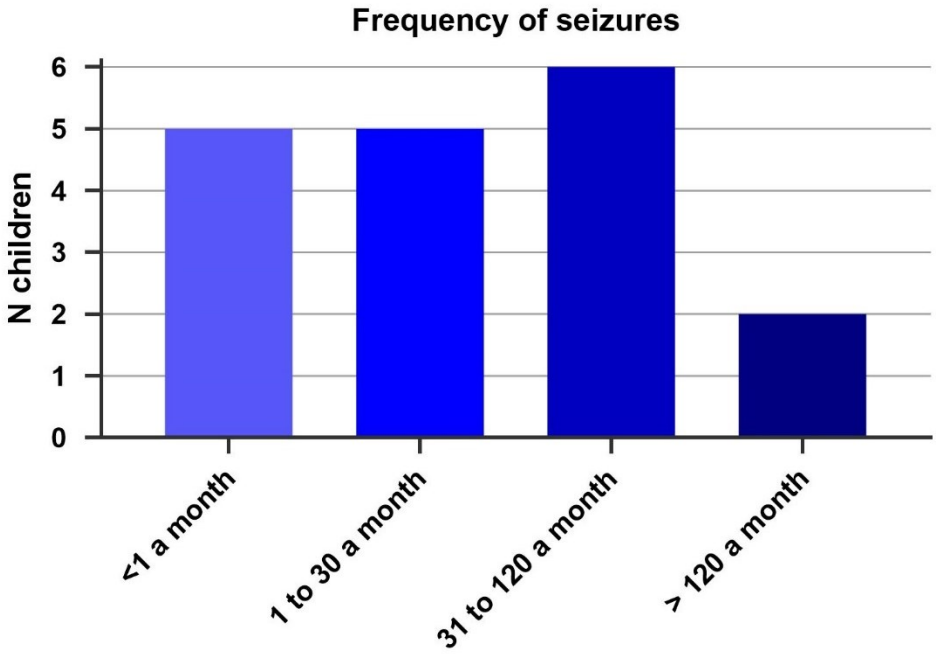

Based on the threshold at which group difference had the lowest p-value, the following graph measures were selected for prediction of seizure frequency: theta clustering coefficient at threshold 0.3; theta path length at threshold 0.18; delta clustering coefficient at threshold 0.1, delta path length at threshold 0.3. Given none of the Goodness of Fit or Parallel Lines test was significant, none of the linear models violated assumptions of no multicollinearity or of proportional odds.

No regression model significantly predicted frequency of seizures.

The regression model for theta clustering coefficient did not significantly predict frequency of seizure (χ^2 = 2.998; df = 3; p = .392; Nagelkerke's R^2 = .165). Individual effects are depicted in Table 3.2.

Table 3.2

Effect of theta clustering coefficient on seizure frequency

Predictor	Estimate (sd error)	Wald (df)	*p* value	Confidence interval 95%	
				Lower	Upper
Theta C	16.43 (11.1)	2.209 (1)	.137	-5.235	38.092
Age at MEG	-0.95 (.142)	0.454 (1)	.500	-0.373	0.182
Disease duration	0.14 (.121)	1.270 (1)	.260	-0.101	0.373

Note. C = Clustering coefficient.

The regression model for theta characteristic path length did not significantly predict frequency of seizure (χ^2 = 1.593; df = 3; p = .661; Nagelkerke's R^2 = .091). Individual effects are depicted in Table 3.3.

Table 3.3

Effect of theta characteristic path length on seizure frequency

Graph measure	Estimate (sd error)	Wald (df)	*p* value	Confidence interval 95%	
				Lower	Upper
Theta L	1.03 (1.0)	1.033 (1)	.309	-0.951	3.000
Age at MEG	-0.21 (.138)	0.023 (1)	.880	-0.291	0.250
Disease duration	0.14 (.128	1.230 (1)	.267	-0.109	0.392

Note. L = Characteristic Path Length.

The regression model for delta clustering coefficient did not significantly predict frequency of seizure (χ^2 = 2.639; df = 3; p = .451; Nagelkerke's R^2 = .147). Individual effects are depicted in Table 3.4.

Table 3.4

Effect of delta clustering coefficient on seizure frequency

Graph measure	Estimate (sd error)	Wald (df)	*p* value	Confidence interval 95%	
				Lower	Upper
Delta C	7.74 (5.7)	1.680 (1)	.195	-3.961	19.436
Age at MEG	0.50 (.152)	0.109 (1)	.741	-0.248	0.348
Disease duration	0.50 (.117)	0.183 (1)	.669	-0.179	0.278

Note. C = Clustering coefficient.

The regression model for delta characteristic path length did not significantly predict frequency of seizure (χ^2 = 1.016; df = 3; p = .781; Nagelkerke's R^2 = .062). Individual effects are depicted in Table 3.5.

Table 3.5

Effect of delta characteristic path length on seizure frequency

Graph measure	Estimate (sd error)	Wald (df)	*p* value	Confidence interval 95%	
				Lower	Upper
Delta L	0.81 (1.1)	0.568 (1)	.451	-0.286	2.920
Age at MEG	0.19 (.156)	0.015 (1)	.901	-0.286	0.324
Disease duration	0.09 (.116)	0.639 (1)	.424	-0.134	0.319

Note. L = Characteristic Path Length.

No measure of clustering coefficient and characteristic path length individually predicted seizure frequency in either theta or delta frequency bands. No effect of age or epilepsy duration covariates was observed.

3.4 Discussion

This chapter aimed to use measures of connectivity analyses with Magnetoencephalography to examine resting-state functional brain networks in children with refractory epilepsy, and to explore how those brain networks relate to seizure frequency. The point is that seizures are a common symptom in paediatric AE and that MEG network analyses could potentially provide useful information on the relationship between seizure activity and the underlying neural networks. A cohort of children diagnosed with refractory epilepsy were recorded at rest and their brain activity assessed for connectivity between regions in theta and delta frequency bands. More specifically, network topology was assessed using graph measures and compared to a cohort of typically developing children and children with AE. Where the graph measures differed the most compared to the control group, it was tested whether they predicted frequency of seizures in the epilepsy cohort.

3.4.1 Summary of the results

3.4.1.1 Differences in network topology

The preliminary group comparison between the Epilepsy group and the Control group detected differences in brain networks across thresholds, specifically in the theta frequency band (5 to 8 Hz magnetic activity), with an increased clustering coefficient and a lower characteristic path length. The absence of difference in delta connectivity is incongruent with the findings of three MEG adult epilepsy studies (Englot et al., 2015; Hsiao et al. 2015; Li Hegner et al., 2018), two of which were at regional level. It is possible that global delta networks of resting state activity are not specific to epilepsy in children, and it is important to note that it was a heterogeneous group of patients who were referred for pre-surgical evaluation. The difference in theta activity is coherent with previous findings in adult epilepsy studies, that linked epileptiform discharges to MEG theta waves (Ibrahim et al., 2014), or a higher theta synchronization likelihood in EEG to a diagnosis of epilepsy (Douw et al., 2010a). An average increase in nodal strength, that is weights of connectivity linked to a region/node, was also detected in the theta band of an adult epilepsy cohort with MEG (Li Hegner et al. 2018). More precisely, clustering coefficient was found to be increased in the present cohort compared to controls: this corresponds to a finding of increased theta clustering coefficient in an adult epilepsy cohort using resting-state EEG (Quraan et al. 2013). The present findings suggest this clustering pattern in theta activity may be true to children with epilepsy as well.

The clustering coefficient gives an idea of the extent to which brain connection patterns form clusters between adjacent nodes, which translates to an efficiency in local information transfer (Bullmore & Sporns, 2009; Douw et al., 2010b). The characteristic path length gives an idea of the number of connections that have to be crossed, on average, to go from a node to another: the less steps to take, the higher the global efficiency (Bullmore & Sporns, 2009). The observed shorter characteristic path length suggests theta connectivity networks transmit neural activity "faster" in epilepsy, more efficiently, across the whole network. This means the resting theta activity measured in the present cohort reaches more efficiently widespread areas while stimulating more distinct clusters. This is known as small-world topology, and is tied to the modularity of the brain (Bullmore & Sporns, 2009). It is unclear whether this contributes to seizures or epilepsy.

It may also be possible that the seizures affect the formation of resting state brain networks in local "clusters", especially if interictal discharges tend to stimulate this frequency band: interictal discharges have been associated with increased clustering and lower in characteristic path length in fMRI networks, therefore showing a similar pattern (Ibrahim et al. 2014), although IEDs were removed for the present analysis. While a small sample would be unlikely to yield sufficiently powered results, it may be interesting to investigate network differences at node (regional) level, which would give an idea of the location of the cluster network differences: increased MEG theta connectivity was detected in middle temporal and anterior cingular gyri in an adult epilepsy study (Hsiao et al. 2015). It is possible that such nodes would relate to the source of the epileptic activity (e.g., specific to the temporal lobe in Mesial Temporal Lobe epilepsy) and heterogeneity of epilepsy aetiologies would have to be controlled when looking at local nodes. An increase in posterior MEG theta connectivity was found in another adult cohort (Routley et al., 2020). It was also hypothesized that surgery could remove "pathological hubs" of connections, which would help decentralize the networks and result in seizure freedom (van Dellen et al. 2014). A regional approach was not investigated in the present study and could be relevant to future paediatric studies, as the increased clustering coefficient suggests there are local "clusters" of brain activations.

With regards to AE, it seems that paediatric epilepsy has its own pattern of resting-state network, despite the common symptomatic features both conditions share. While abnormal delta and theta activity is detected in AE (Dalmau et al., 2008; Symmonds et al., 2018; Vogrig et al. 2019), the epilepsy group had a significantly higher level of "small-worldness" than the AE group (Bullmore & Sporns, 2009): lower characteristic path length and higher clustering coefficient in both delta and theta frequency. Interestingly, this difference in delta frequency

was not found in Epilepsy compared to the control group; and the AE group had a lower delta clustering coefficient compared to controls. This suggests global delta networks of resting state activity is distinct in paediatric AE and may involve a less efficient brain activity network pattern than in epilepsy. It is possible that the abnormal delta and theta activity reported in EEG studies (including EDB, GRDA, or disorganised theta-delta activity) are responsible for such network topology difference in AE (Dalmau et al., 2008; Jeannin-Mayer et al., 2019; Symmonds et al. 2018; Vogrig et al., 2019). Children with AE and children with Epilepsy may therefore have different functional network connectivity patterns.

3.4.1.2 MEG networks and seizure frequency

None of the above graph measures did, however, significantly predict frequency of seizure, and they may not be directly linked to this specific symptom. The present finding is incongruent with the previously reported relationship between MEG theta connectivity and frequency of seizures in adult epilepsy, but the sample differed in that it included specifically lesional epilepsy, intractable or tumour-related (van Dellen et al., 2014). It is possible that it does not apply to general (and therefore heterogeneous) groups with paediatric epilepsy. Furthermore, the latter study had reported a positive correlation between seizure frequency and theta networks "with higher average distance between nodes" (supplementary material; van Dellen et al., 2014): although with a slightly different measure, the present cohort was found to have a significantly *lower* distance between nodes, which reinforce the possibility that children with epilepsy have different brain activity patterns. Given the size of the sample and its heterogeneity in etiologies, seizure frequency or medication, larger and more specific data will help verify such activity patterns.

Another reason for the incongruency may indeed be the type of epilepsy: a MEG study only found a correlation between theta activity and seizure frequency in a subgroup with low-grade glioma (van Dellen et al., 2012), and another detected a relationship between theta connectivity and number of seizures in adult tumour-related epilepsy (Douw et al., 2010b); 15 out of 20 patients in another similar study had low-grade glioma (van Dellen et al. 2014); all of which suggest that effect may also be more specific to a certain type of epilepsy, although this was not verified in children. As mentioned in the demographic information, no child had an established and graded glioma in the present cohort. This may be another reason why no prediction was detected.

Finally, the MEG study that tested correlations with number of seizures also lost significance over the two time periods (separated from six months), despite similar functional

connectivity (Douw et al., 2010b), which suggests such association may decrease over time. Although it was not verified in the present study, MEG graph network measures may be unstable across time in epilepsy cohorts: a study in fMRI paediatric epilepsy has shown that although high repeatability is found in graph measures for resting state recordings, there is an existing level of intra-participant variability introduced with normalization and thresholding (Paldino et al., 2017). The proportional thresholding, which was used here, appears to produce more stable measures than absolute thresholding in fMRI (Garrison et al., 2015). It is not known how much these problems may affect MEG networks. Replication of similar analyses is therefore required.

3.4.2 Limitations

Due to the size of the sample and of the detected effect sizes, replication will need to be done in larger samples (Button et al., 2013) in order to reliably establish or reject a relationship between MEG networks and seizures. As mentioned in the method section, 18 cases provided a limited statistical power, and the analyses did not reach a large enough effect to report reliable association effects. A conclusion cannot be drawn for the time being and the results are to be interpreted with caution as they also have a higher chance of being false negatives. This also applies to the limited MEG data samples available: the number of post-processed 10 second epochs to analyse was lower in the epilepsy group because of the variability in the duration of recordings and therefore subject to less stable activity patterns. A stable resting-state paradigm with a similar duration for all participants will be ideal in future research.

It is difficult to determine whether the study design could provide a marker of seizure frequency as it is not a prospective design: MEG recordings were acquired in a period where patients may have had little seizures compared to the extent of their occurrence in earlier medical records. Therefore, the network topology observed in the present sample could be the long-term impact of the syndrome rather than a factor which could help predict the course of the disease. Furthermore, the network dynamics observed could be the result of anti-epileptic medication, as it is known to affect brain connectivity (Haneef, Levin & Chiang, 2015). Due to the size of the sample, this study was lacking power to control for possible confounding factors (age of onset and medication) as statistical covariates. Further investigation in a longitudinal setting could allow to test whether similar functional networks are found at onset and remain stable across time, with a more detailed assessment of medication taken at each time point.

While AE and Epilepsy have overlapping symptoms as seizures is a common feature of AE (Graus et al., 2016), the present results suggest their resting-state brain networks differ in slow wave frequencies, and that changes in delta activity may be more specific to paediatric AE. With regards to seizure frequency, we are unable to make an inference about AE, as it remains to be investigated in that specific group whether the same mechanics of dynamic networks are involved when seizures happen. Network disruptions potentially caused by brain inflammation and antibodies (Finke et al., 2013; Peer et al., 2017; Volz et al., 2016) may result in different frequency or patterns of epileptic features in AE.

3.4.3 Conclusion

Paediatric AE may be subject to specific functional brain network alterations in the long term. Connectivity analyses using MEG identified distinct network topologies in children with AE compared to children with paediatric epilepsy or with a typically developing brain, which demonstrates its potential benefit in investigating the impact of AE on brain activity. While epileptiform activity and seizures manifest in AE, they may not be directly linked to such brain activity patterns, as no evidence was found that seizure frequency was predicted by network topology in paediatric epilepsy. In the present cohort, epilepsy brain networks differed from controls specifically within the theta band, with an increase in network efficiency and small-worldness, while in AE, networks differed from controls in the delta bands, with a decrease in network clustering. Altered delta brain activity patterns make sense in light of delta abnormalities previously reported in adult AE (Dalmau et al., 2008; Jeannin-Mayer et al., 2019; Symmonds et al. 2018; Vogrig et al., 2019), as well as fMRI functional abnormalities (Finke et al., 2013; Peer et al., 2017; Wang et al., 2021). It appears that theta band brain activity may tend to be more diffuse at rest in AE, with less segregation between neighbouring regions of the brain. It remains to be established whether this plays a role in cognitive or behavioural issues.

Chapter IV. Emotional and behavioural features in children with autoimmune encephalitis

4.1 Introduction

4.1.1 Clinical reports of emotional and behavioural problems

Beyond structural or functional brain changes in the long-term, auto-immune encephalitis is also associated with behavioural and emotional problems, which may be a common phenotype: a cohort of mostly adult patients, both antibody negative and positive, reported emotional lability, lower adaptive behaviour and concentration difficulties many years after diagnosis (Gordon-Lipkin et al., 2017; Yeshokumar et al., 2017). Forty-eight children with various types of paediatric AE reported 63% of behavioural changes at presentation, while 35% had remaining behavioural problems in a 1 to 5 years follow-up (Hacohen et al., 2013). Furthermore, according to parental reports, the social and emotional wellbeing of children with encephalitis can be affected by the attitude and support of others, lack of available resources; support from individuals or organisational environment was seen to impact learning and suffering (Lemon et al., 2019).

Patients with anti-NMDA receptor encephalitis show abnormal behaviours like aggression, irritability, agitation, impulsivity, hyperactivity, and catatonia (Dalmau et al., 2019; De Bruijn et al., 2018). One review stated that irritability was “more frequently identified in children” (Dalmau et al., 2019). Children can present with agitation, aggression, anxiety, negativism, and autolytic thoughts (Armangue et al., 2013). A clinical report on 27 children also mentions abnormal behaviour or psychosis in half of the group (Shim et al., 2020). Among 38 children, 23 had signs of behavioural disorder at a first presentation, 31 had them develop over the course of the disease in total, and "behavioural problems” had the highest incidence rate among other clinical symptoms at follow up (Bartels et al., 2020), suggesting this could be a central concern for anti-NMDAR encephalitis. One study even found abnormal behaviours in 96% of 382 patients with the disease, including a subset that had a “good outcome” using the modified Rankin scale (Balu et al., 2019): adding behavioural data may therefore give more specificity to the assessment of outcome.

Patients with limbic encephalitis also present behavioural changes: a recent review on LGI1 limbic encephalitis included reports of apathy, anxiety, depression, irritability, aggression,

agitation, and less precise observations including “behavioural problems” or being “less interactive” (Griffith et al., 2020). At onset, a child with anti-Ma2 encephalitis had behavioural disturbance including agitation, episodes of crying, expressions of terror, as well as mood disturbances (Mrabet et al., 2015). Previous cases of children and adolescent with limbic encephalitis had reported unspecified “behavioural changes”, depression, anxiety, fear, and concentration difficulties (Haberlandt et al., 2011). Cases of children and adolescents with anti-LGI1 and anti-CASPR2 antibodies encephalitis also reported “behavioural changes”, anxiety, emotional lability, and kleptomania (López-Chiriboga et al., 2018; Schimmel, Frühwald & Bien, 2018).

In ADEM, a meta-analysis reported a trend toward internalizing symptoms (like depression and anxiety) lasting in the long term, reported in 23% to 62% of patients (Burton et al., 2017).

4.1.2 Neuropsychological assessment of emotions and behaviours

Data outlining and measuring specific behavioural difficulties in children with AE is needed. This information could give clinical information that helps understand the impact of AE in children’s behaviours. Quantitative assessments could also help detect such problems which are often not identified until children return to the educational system (Hacohen et al., 2013). In a cohort of a majority of adults, a standardized assessment (*Adaptive Behaviour Assessment System-III*) has shown that more than half of patients with encephalitis had a score below average in all three domains, concerning a range of skills including communication, self-direction, social skills, and practical skills such as self-care, life at home, at work, health and safety etc., but no specific sub-group analysis was done for children (Yeshokumar et al., 2017). However, a small study using the same assessment found that, as opposed to their 6 adult peers, children with anti-NMDAR encephalitis had lower median score in their general adaptive composite measures and lower practical skills in a long-term follow-up (Gordon-Lipkin et al., 2017), which suggests children may be specifically at risk of having behavioural problems. In ADEM, increased psychosocial problems (including emotional and behavioural regulations) years after the start of the disease were correlated with an earlier age of onset, suggesting the disease may cause worse outcomes in younger children (Beatty et al., 2016). Using neuropsychological measures, a study including 19 patients (mean age 5.4) with ADEM detected a higher proportion of clinically elevated scores in internalizing problems and overall

behavioural symptoms compared to controls (Kuni, Banwell & Till, 2012), which demonstrates that quantitative assessments can also help identify children with worse behavioural outcome.

Measures of behavioural difficulties in paediatric ADEM have been used to identify difficulties in emotional, social, and school functioning, including depression, atypicality, anxiety, hyperactivity (Beatty et al., 2016; Cainelli et al., 2019; Jacobs et al., 2004). However, these studies have often used assessments that are arguably time consuming due to the number of details collected and they required specific qualifications, both being elements that can be inconvenient for day-to-day clinical practice. The *Strengths and Difficulties Questionnaire* (SDQ) is a shorter and accessible tool commonly used in research to assess behavioural problems in children: its validity was demonstrated in a longitudinal study involving 3,375 children from the general population, with consistent factors across childhood in specific measures of emotional and behavioural characteristics (Sosu & Schmidt, 2017). In a sample of 1,028 looked-after children, the SDQ was shown to have a strong specificity and sensitivity (above 80%) when used to predict various psychiatric disorders in attention, hyperactivity, anxiety and depression; especially when screened by multiple informants; it was thus recommended in a clinical context (Goodman et al., 2004).

Studies have used the SDQ for conditions with similar phenotypes to paediatric AE. For example, one study in children with epilepsy reported that behavioural difficulties were higher than for normal controls; and focal EEG abnormalities were associated with higher scores in Total difficulties, Hyperactivity and Prosocial behaviour (Tanabe et al., 2013). It was also noted that hyperactivity and total difficulties scores were negatively correlated with the age of epilepsy onset, suggesting that children affected early may have more difficulties (Tanabe et al., 2013). Given that EEG abnormalities are commonly found at the onset of AE (Graus et al., 2016), it is relevant to assess whether similar behavioural difficulties are found in this group of children.

Investigations have found that parents of children with encephalitis cared a lot about how their children reintegrated into everyday life: among priority concerns mentioned were their ability to join activities with their peers, make and maintain friendships, their general happiness and wellbeing (Lemon et al., 2019). These are aspects that the SDQ gives information about (Goodman et al., 2004), which makes it very relevant for parents. One long-term study in paediatric anti-NMDAR encephalitis reported that patients had substantial difficulties in performing daily activities, with additional uncorrected SDQ results showing significantly higher total difficulties and conduct problems compared to healthy controls (table e-7 in supplemental material of De Bruijn et al., 2018). It may therefore be helpful to use the

SDQ in other types of paediatric AE such as ADEM or Limbic encephalitis, which has not been done to date.

4.1.3 Impact of emotional and behavioural problems

Emotional and behavioural problems may have important implications for children's future lives, for example, difficulties found in adaptive behaviours may result in higher dependence and elevated requirement of support at home and at school compared to neurotypical children (Gordon-Lipkin et al., 2017). Behavioural difficulties in children are also known to predict future academic underachievement: externalizing difficulties (such as antisocial behaviours, aggression, misconduct) have a negative impact on performance at school (Van der Ende, Verhulst, & Tiemeier, 2016) and this may in turn increase internalizing problems later in young adulthood (Masten et al., 2005). A longitudinal study found an increase in internalising and externalising problems from 7 to 11 years of age. This was suggested to be caused by a feedback loop effect of academic poor performance, which would both be caused and cause the increase of symptoms (DeVries, Gebhardt, & Voß, 2017).

This is relevant to patients with AE as difficulties may already impact their future academic careers. In 61 patients aged 15 to 77 years with anti-NMDAR encephalitis, 31.1% of patients did not return to school or work as a result of their disease (Blum et al., 2020). In younger patients (aged 0 to 18 years, median age 14), 36% of 28 patients did not resume their previous school level after hospital admission or rehabilitation, with reports of attention and concentration deficits, anxiety, impulsiveness (De Bruijn et al., 2018). The authors observed five children with passivity and apathy, among whom 3 had dropped out of school because of fatigue or anxiety (De Bruijn et al., 2018). Recent research reported that ADEM positive to myelin-oligodendrocyte-glycoprotein (MOG) antibodies was associated with increased academic difficulties, especially when the age of onset was 10 years and younger (Deiva et al., 2020). All of this shows the importance of having a detailed understanding of the behavioural problems associated with paediatric AE to inform parents and clinicians.

Academic progress when coming back to school, the children's future independence and employment were important highlights of parents' concerns regarding paediatric AE (Lemon et al., 2019). Given this is a major concern for families, identifying behavioural and emotional problems will be important in the management of children following autoimmune encephalitis, and may consequently give guidance for helping such aspects of children's lives in a long-term follow up.

4.1.4 Hypotheses

According to the above research, we expected children with AE to have higher emotional and behavioural difficulties than the population norm, with levels of difficulties and proportions of abnormally high difficulties similar to children with general neurological disorders.

4.2 Methods

4.2.1 Participants

A cohort of 12 patients with AE and 26 disease control children with general neurology diagnoses (without AE) was recruited at the Birmingham Children's Hospital, Birmingham, United Kingdom from August 2019 to February 2020. Patients were identified from an existing clinical database of neuroinflammatory disease paediatric cases and controls from neurology outpatient lists. Inclusion criteria was a diagnosis of AE (according to the standards established in Graus et al., 2016) in the first group and distinct general neurology diagnoses in the second group, both with a disease onset below the age of 16.

Data was anonymised for analysis and collected as part of a planned audit/quality improvement project of the use of the SDQ in everyday clinical practice to identify behavioural problems in children with AE. Due to the COVID-19 pandemic psychology support for the patients was disrupted: the use of this questionnaire was therefore piloted as a 'screening tool' to identify patients most in need of support. The details of this project were registered with the Birmingham Children's Hospital CARMS department.

4.2.2 Neuropsychological assessment

The behavioural characteristics of all participants were assessed using the SDQ for 4–17-year-olds, which can be completed by the child, a related parent, or a related teacher (Goodman et al., 2004). The questionnaires were completed during routine clinical care and data was received for analysis in the anonymised format with the agreement of families. The scoring was thus blinded to the identities of participants and was confirmed by two independent scorers. The SDQ is composed of 25 statements about the child regarding four psychological difficulty dimensions (emotional problems, conduct problems, hyperactivity, and peer problems) and one dimension of strengths (prosocial behaviours). They can be analysed as five separate factors or as three factors (*externalising* score grouping conduct and hyperactivity problems; *internalising* score grouping emotional and peer problems; and a *prosocial* score, Goodman et al., 2004). Each statement is scored with a scale of 3 points, 0 being "not true", 1 "somewhat true" and 2 "certainly true" and is generally completed by both the child and her/his parent/teacher/other carer. The final scores can be classified in terms of normality cut-points based on a UK community sample (Youthinmind, 2016): the four-bands

categorisation was used in this study, coded *Close to average*, *Slightly raised (/Slightly lowered for the prosocial scale*), *High* (/*Low*), Very High (*very low*).

4.2.3 Descriptive statistics

All statistical analyses were performed using SPSS v24 for Windows (IBM Corp., 2016). Descriptive analyses were computed for the five scales scores (Emotional problems, Conduct problems, Hyperactivity, Peer problems, Prosocial) and the Total difficulties score (total of all the scores). Outliers were removed if their score was higher or lower than three standard deviations from the mean of their respective group. The assumption of normality was assessed using the Shapiro-Wilks normality test, and comparison tests were performed accordingly for each component of the SDQ: non-parametric Mann-Whitney U tests for not normally distributed variables and t tests for normally distributed variables. A Chi-square test was used to determine differences in gender distribution across groups.

4.2.4 Binary logistic regression analysis

In order to assess the observation ratio of having abnormal scores with a confidence interval of 95%, a binary logistic regression was conducted for each scale score and the Total difficulties score by setting a group independent variable (AE = 1, Control = 0) in prediction of a normality dependant variable set from the cut-points classification for Parent informants (*Close to Average* to *Slightly raised/lowered* score = 0; *High/Low* to *Very High/Low* score = 1).

4.3 Results

4.3.1 Demographics

Of the overall cohort, one child had only a self-assessed SDQ and so was excluded from analyses. In the remaining 37 children (97%) who were assessed by their parent, 19 (51%) also gave a self-assessment. Two statistical outliers were identified among control participants for the conduct problems scale; and two had an autoimmune demyelinating disease (optic neuritis and multiple sclerosis) which limits the distinction with the AE/ADEM group; they were therefore excluded from the final sample, in which 33 participants remained. Only parent assessments were retained for the current analyses.

Descriptive statistics about the sample's demographic and clinical characteristics are shown in Table 4.1. Gender distribution across the healthy control and the patient groups did not significantly differ (Table 4.1). Specific clinical data is given in Appendix 4.

Table 4.1

Demographic and clinical characteristics of autoimmune encephalitis patients and disease controls

Child characteristics	**Disease controls (n=21)**	**AE (n=12)**	**Statistics**	
			Test	***p* value**
Gender (female:male)	14:7	9:3	$\chi^2 = 0.251$	.616
Age	9.19±4.51	10.50±5.3	$t = -0.754$	.457
Age of onset	4.57±5.4	6.95±4.5	$U = 78$	.071
Abnormal MRI scans/Total scans	6/17	11/12	$\chi^2 = 9.216$	.002
mRS	1.90±1.2	1.25±1.5	$U = 82.5$	.090

Note. AE = Autoimmune Encephalitis. mRS = Modified Rankin Scale.

In the patient group, 10 were diagnosed with ADEM, 6 of which were MOG positive and 4 MOG negative, 1 was diagnosed with anti-NMDAR encephalitis and 1 with Hashimoto's Encephalopathy. The disease control group was composed of various neurological disorders such as epilepsy (4); developmental delay (3), headache (2); genetic syndromes (3); functional movement disorder (1); cerebral palsy (2); ASD (1); focal seizures (1); Guillain Barré syndrome (1); Benign tremor (1); Cerebrovascular disease (2).

4.3.2 Strengths and Difficulties Questionnaire scales

According to the non-normality of their respective distributions, non-parametric Mann-Whitney U tests were used to compare Conduct problems, Peer problems and Prosocial scales scores across groups; the Emotional problems, Hyperactivity and the Total difficulties scores were compared between groups using parametric t-tests (Table 4.2).

Table 4.2

Strengths and Difficulties Questionnaires scores in autoimmune encephalitis patients compared to disease controls

Scales	Disease controls (n=21)	AE (n=12)	Statistics		
			Test	*p* value	Effect size
Emotional problems	4.62 ± 2.42	4.25 ± 2.42	t = 0.422	.676	d = 0.153
Conduct problems	2.14 ± 1.65	1.92 ± 1.51	U = 121	.849	η^2 = 0.001
Hyperactivity	6.29 ± 2.83	5.25 ± 3.08	t = 0.980	.335	d = 0.355
Peer problems	2.90 ± 1.61	1.92 ± 1.78	U= 81	.084	η^2 = 0.086
Prosocial	6.67 ± 2.22	7.33 ± 2.87	U = 96	.253	η^2 = 0.038
Total difficulties	15.95 ± 5.02	13.33 ± 6.24	t = 1.320	.196	d = 0.478

Note. AE = Autoimmune Encephalitis.

No mean score reaches the abnormality cut-points as defined in the four-band categorisation except the prosocial score for disease controls which is considered low below 7. The mean Total difficulties score of the whole sample was 15.00 (sd = 5.55) which stands as a *Slightly raised* score compared to the typically developing population, both groups being within the normal range (Figure 4.1). On average, the disease control group had a higher score in most scales except in prosocial behaviours, but no significant differences were found between groups for the different scales and the total difficulties scores (Table 4.2).

Figure 4.1

SDQ Total difficulties score of autoimmune encephalitis and disease control groups

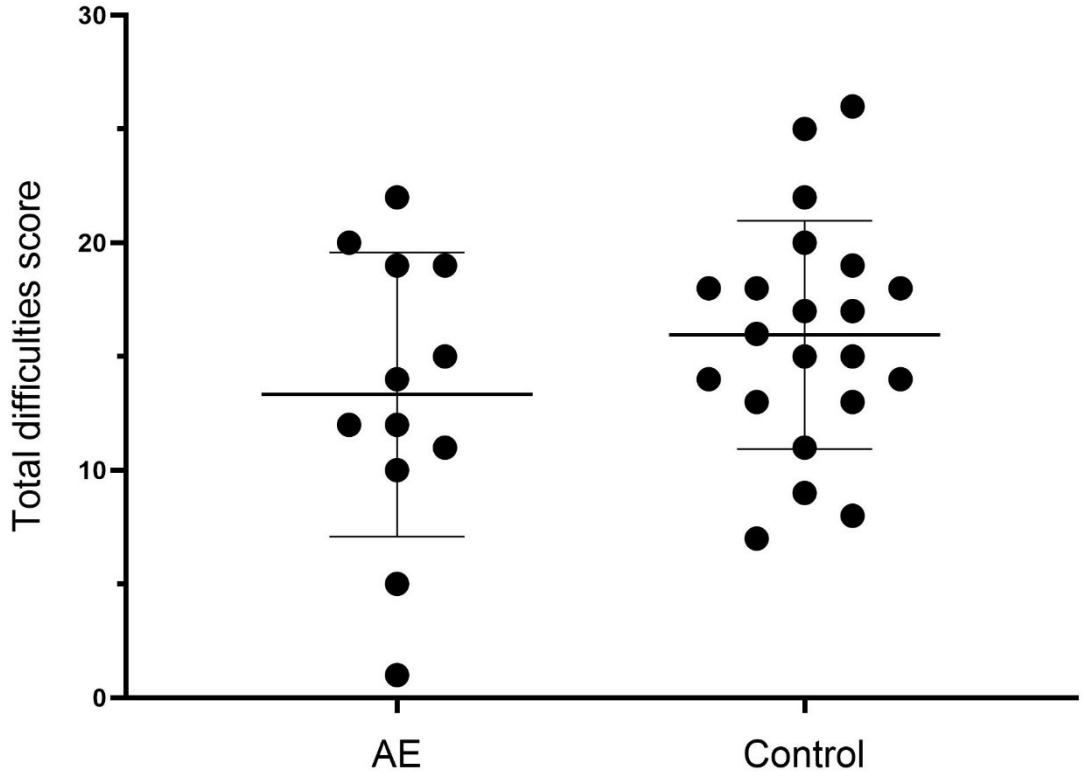

Note. SDQ = Strengths and difficulties questionnaire. AE = Autoimmune Encephalitis. Control = disease control group. According to the SDQ cut-points, an abnormal High to Very High score (parent informant) is 17 and above.

4.3.3 Abnormal scores in the sample

The proportions of patients with abnormal scores show that the AE group had a slightly larger proportion of children with abnormal conduct problems, while disease controls had more cases of emotional problems, hyperactivity, peer problems and prosocial problems. No difference reached statistical significance (Table 4.3).

Table 4.3

Participants with abnormal scores in autoimmune encephalitis patients compared to disease controls

	Disease controls n=21	**AE (n=12)**	**Statistics**		
Scale			**Test**	***p* value**	**Effect size**
Emotional problems	13 (61.9%)	4 (33.3%)	$\chi^2 = 2.496$	.114	$\varphi = -0.275$
Conduct problems	3 (14.3%)	2 (16.7%)	$\chi^2 = 0.034$	.854	$\varphi = 0.032$
Hyperactivity	9 (42.9%)	4 (33.3%)	$\chi^2 = 0.290$	.590	$\varphi = -0.094$
Peer problems	8 (38.1%)	2 (16.7%)	$\chi^2 = 1.660$	.198	$\varphi = -0.224$
Prosocial	9 (42.9%)	5 (41.7%)	$\chi^2 = 0.004$	.947	$\varphi = -0.012$
Total difficulties	10 (47.6%)	4 (33.3%)	$\chi^2 = 0.638$	.424	$\varphi = -0.139$

Note. AE = Autoimmune Encephalitis.

The odds of obtaining scores with High to Very High abnormality were not significantly different across groups (Table 4.4).

Table 4.4

Binary logistic regression of autoimmune encephalitis diagnosis in prediction of abnormal scores

	Statistics				
Scale	**B(SE)**	**Wald's χ^2**	**Exp(B)**	***p*-value**	**95% Confidence interval**
Emotional Problems	-1.179(0.76)	2.408	0.308	.121	0.690-1.363
Conduct Problems	0.182(0.99)	0.034	1.200	.855	0.171-8.426
Hyperactivity	-0.405 (0.76)	0.289	0.667	.591	0.152-2.926
Peer problems	-1.124(0.90)	1.575	0.325	.209	0.056-1.880
Prosocial	-0.049(0.73)	0.004	0.947	.952	0.226-4.006
Total difficulties	-0.598(0.75)	0.632	2.182	.427	0.126-2.403

4.3.4 Profiles of AE children with abnormalities

Patients with AE who had multiple abnormal scores are outlined in Table 4.5. Patients with abnormally high Total Difficulties all had abnormal Prosocial behaviours, but no overall pattern was notable for the group.

Table 4.5

Normal and abnormal SDQ scores found in patients diagnosed with autoimmune encephalitis

	Scale					
P. N°	**Total Difficulties**	**Emotional Problems**	**Conduct problems**	**Hyperactivity**	**Peer problems**	**Prosocial**
1	**Abnormal**	Normal	**Abnormal**	**Abnormal**	**Abnormal**	**Abnormal**
2	Normal	**Abnormal**	Normal	Normal	Normal	Normal
3	Normal	Normal	Normal	Normal	Normal	Normal
4	Normal	Normal	Normal	Normal	Normal	Normal
5	Normal	Normal	Normal	**Abnormal**	Normal	Normal
6	Normal	Normal	Normal	Normal	Normal	**Abnormal**
7	Normal	Normal	Normal	**Abnormal**	Normal	Normal
8	Normal	**Abnormal**	Normal	Normal	Normal	Normal
9	**Abnormal**	Normal	**Abnormal**	**Abnormal**	Normal	**Abnormal**
10	**Abnormal**	**Abnormal**	Normal	Normal	Normal	**Abnormal**
11	**Abnormal**	**Abnormal**	Normal	Normal	**Abnormal**	**Abnormal**
12	Normal	Normal	Normal	Normal	Normal	Normal

Note. P. N° = Patient number

Among the ten AE children with a good mRS outcome, 3 had abnormal emotional problems, 2 had abnormal conduct problems, 3 had abnormal hyperactivity, 1 had abnormal peer problems and 4 had abnormal prosocial scores.

4.4. Discussion

4.4.1 Summary of the results

The aim of this preliminary study was to determine whether children with AE were more likely to have abnormal behavioural difficulties measured by the Strengths and Difficulties Questionnaire, compared to children with other neurological diagnoses. The use of the SDQ is a strength for this study as it gives a valid and consistent assessment of the extent of behavioural difficulties that are faced by children (Goodman et al., 2004; Sosu & Schmidt, 2017). The study also gives data that is lacking in previous research in children with different types of AE.

The average difficulties across domains varied between children with AE and children with general neurological diagnoses but none of the average scores were significantly different: more statistical power would be needed to verify whether the patterns differ. The current data suggests children with AE may have a similar level of difficulties in emotional, conduct and peer problems, as well as hyperactivity and prosocial behaviours compared to that found in children with general neurological disorders. Emotional and behavioural difficulties may therefore be an under-recognised sequela of paediatric AE. Furthermore, the group had a relatively low mRS score which is considered to reflect a "good" outcome: it is possible that the current measures of clinical outcome that focus on neurologic disability are unable to capture residual behavioural difficulties (Gordon-Lipkin et al., 2017).

The proportion of patients with abnormal scores found in both groups appeared to be higher than the proportions of abnormal scores found in a large-scale study with a large population of 6-year-old children in Scotland, being 4.8% for Emotional problems; 10.4% for Conduct problems; 12.3% for Hyperactivity; 6.6% for Peer problems; 6.8% for Prosocial behaviours (Sosu & Schmidt, 2017). The present AE group shows an increased proportion of +28.5% for Emotional problems, +6.3% for Conduct problems, +21% for Hyperactivity, +10.1% for Peer problems and +34.9% for Prosocial behaviours (Figure 4.2). This makes sense because abnormal behaviours are a significant feature in clinical studies about paediatric AE (Beatty et al., 2016; Tan et al., 2018), and a diagnostic factor for anti-NMDAR encephalitis (Graus et al., 2016). It remains to be confirmed with larger studies whether comparison of SDQ scores with healthy controls would show higher difficulties in AE, given the recruitment bias that may have affected findings in the present sample. The study from Sosu and Schmidt (2017) used the three bands categorisation while this study used the four bands. The

assessment of abnormalities differs slightly and made this study more conservative for hyperactivity (abnormal score from 7 and above for the three bands system, 8 for the four bands system) and less conservative prosocial behaviours (abnormal from 4 and below for the three bands system, 6 for the four bands system; Goodman et al., 2004). Finally, it not clear whether our cohort from England can be accurately compared to a population of Scotland in Sosu et al. (2017): the absence of an established baseline "rate" of abnormalities within the English child population limits the reliability of this parallel. A recruitment of age-matched healthy controls in subsequent investigations using the exact same measures may therefore provide more information about the abnormal behaviours of concern that are specific to children with AE.

Figure 4.2

Proportions of children with abnormal scores across SDQ scales

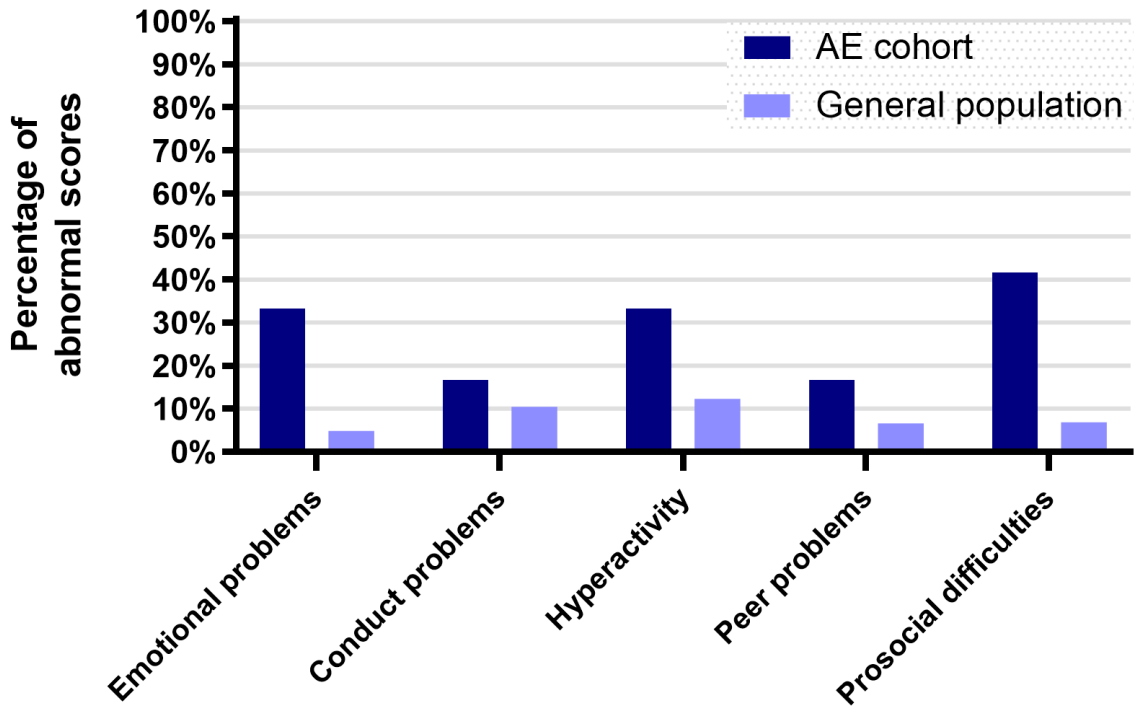

Note. SDQ = Strengths and difficulties questionnaire. AE = Autoimmune Encephalitis. The general population group is based on 6-year-old children from a large Scotland-based study (Sosu et al., 2017).

The largest proportions of abnormalities found among children with AE regarded emotional problems, hyperactivity, and most frequently prosocial behaviours. With regards to the SDQ items, abnormal scores in emotional problems suggest that they are more concerned with complaints of headaches, worrying, unhappiness, nervosity, fear. Abnormal hyperactivity score is determined with occurrence of restlessness, fidgeting or squirming behaviours,

difficulties in concentrating, thinking before acting, and/or going through tasks entirely. Prosocial behaviours were linked to considering other people's feelings, sharing with other children, helping when someone's hurt, being kind to younger children and often volunteering to help, which means that low-scoring children tended not to adopt these behaviours.

It is possible that emotional problems are linked to the anxiety and depression that was previously reported in AE (Beatty et al., 2016). Hyperactivity was also reported in children with ADEM (Beatty et al., 2016), as well as commonly associated attention deficits (Tan et al., 2018). Reduced social cognition may be linked to the prosocial scale, especially the item regarding "considering other people's feelings": such reduction was reported in several adult patients with AE (Bach, 2014; Dodich et al., 2016; McKeon et al., 2016). Social cognition is impaired in ASD, and it is interesting to note it may have common symptoms with AE (Creten et al., 2011; Gonzalez-Toro et al., 2013; Hacohen et al., 2016). This would therefore require further investigation.

4.4.2 Limitations

The main limit of this study is that the sample was relatively small, the results of the present data may therefore not give a good representation of the overall population. A sample bias seems unlikely since the recruitment was based on series in clinic. Increasing the sample size in future analyses may yield additional important insights regarding the nature and magnitude of behavioural difficulties following AE in childhood.

Another limit is that the SDQ scores included in the study were only completed by parents, which means that the study is based on their own observations. It was shown that parents and teachers significantly differed in rating children's impairments as parents tend to miss symptoms that are reported by teachers, which can be explained by the situational specificity of behavioural problems (Brown et al., 2006). Psychological disorders were predicted with higher sensitivity using questionnaires completed by both a parent and a teacher (75 to 100%), while being relatively lower with only one informant (54 to 87%) and much lower with only self-report (7 to 47%), supporting multi-informant screening (Goodman et al., 2004). Our sample did not include teacher ratings and only parent ratings were kept for the sake of homogeneity, which limits the accuracy of the assessment.

Although this was not investigated here, the stage of the disease may also impact how parents perceive their children's problems: some of their concerns are more subject to focus depending on whether children with AE are in the acute stage, in the course of recovery or

trying to reintegrate the social world, when biomedical concerns are more apparent to them at the onset of the disease while broader social outcomes would be more addressed after recovery (Lemon et al., 2019).

Furthermore, there was an unavailability of information on socioeconomic status, that can account for behavioural problems to some extent: a lower socioeconomic background was associated with higher hyperactivity, emotional problems and total difficulties scores in a longitudinal study (Becker et al., 2015). Environmental factors could contribute to emotional and behavioural difficulties, such as lack of social and material support faced by some children; the creation of social bounds can also be impeded by inabilities to join various activities (Lemon et al., 2019). However, network disruption in areas commonly associated with emotion were suggested to be a plausible explanation of emotional troubles in AE (Wang et al., 2021). It remains to be investigated whether these difficulties are best explained by environmental issues or by the neurological disease itself.

4.4.3 Conclusion

Paediatric AE may involve a risk for long-term emotional behavioural difficulties, independently from conventional clinical outcome measures. The present findings suggest children with AE may have levels of difficulties that are comparable to their peers affected by general neurological disorders. This includes hyperactivity, emotional, conduct and peer-related problems, and difficulties in engaging in prosocial behaviours. Across these domains, the largest proportions of AE children with abnormally high difficulties were found for problems with emotional, hyperactivity, and prosocial behaviours. While the study is small and subject to recruitment bias, the fact that proportions of difficulties in children with AE appeared to be higher than in the general population of 6-year-old children (Sosu & Schmidt, 2017) suggests such problems represent a relevant feature of long-term outcome that will need more focus in larger studies. Whether emotional and behavioural issues are related to long-term alterations in brain structures or activity also remains to be established.

Chapter V. Predictors of cognitive outcome in paediatric auto-immune encephalitis

5.1 Introduction

Research in AE has highlighted the clinical relevance of identifying children at risk of a bad long-term outcome: being able to predict a worse disease course would help clinicians make treatment decisions in anticipation of impairments, and also give guidance to carers and families (Bartels et al., 2020). Predictive factors of neuropsychological outcome would also improve clinical interventions or rehabilitation in patients with AE at-risk of cognitive difficulties (McKeon et al., 2018). Furthermore, routine clinical outcome assessments have been considered insufficiently specific as they often focus on physical abilities while missing independent subtle cognitive deficits (Armangue et al. 2020; Heine et al., 2021; Kornbluh et al., 2020; Shim et al., 2020). The previous chapter suggests such assessments also overlook residual emotional and behavioural difficulties. While modern neuroimaging methods can identify long-term differences in brain structures and activities, as supported in chapters 2 and 3, the present chapter aims to establish a preliminary study exploring whether such methods have the potential to predict long-term cognitive-behavioural outcome in paediatric AE.

5.1.1 Structural neuroimaging as a predictor of long-term outcome

Structural MRI abnormalities and structural alterations were discussed in Chapter 2. The present chapter describes how these may be relevant for the prediction of clinical and neuropsychological outcomes.

5.1.1.1 Structural MRI and clinical outcome

Research in paediatric TBI has shown successful attempts at using structural MRI to assess long-term cognitive development (Mayer, Hanlon & Ling, 2015). Altered cortical thickness compared to controls also correlated with symptoms in emotional control and behavioural regulation (Wilde et al., 2012). It has been suggested that critical stages may exist during childhood where the brain is most vulnerable to insult and the neuropsychological consequences are worse (King et al., 2019). Given the observation of an altered brain-volume

growth over time in paediatric AE (Aubert-Broche et al., 2017; Bartels et al., 2020; Bartels et al., 2023), a similar phenomenon could be verified. A recent review noted that although they may not be disease-specific, neuroimaging biomarkers fulfil several criteria for an "ideal biomarker": minimal invasiveness, cost-effectiveness, and reproducibility (Ciano-Petersen et al., 2021). Investigating neuroimaging features of AE is therefore relevant for clinical follow-up.

In AE, abnormal structural MRI (with findings consistent with or suggestive of encephalitis, Graus et al., 2016) predicted poorer functional status (measured by the modified Rankin scale) 1 year after diagnosis in a study involving 382 patients with anti-NMDAR encephalitis (Balu et al., 2019), which suggests MRI could be relevant to predict future difficulties, although the study did not assess specific cognitive and behavioural outcome. The latter is relevant because the study noted abnormal behaviours in children that had a "good" clinical outcome in the mRS (Balu et al., 2019). MRI quantitative analyses also seem to have a predictive potential: reduced whole brain and hippocampal volumes at a first presentation were significantly associated with persistent deficits and lower clinical outcome at follow-up using the *Pediatric Cerebral Performance Category* Scale (PCPC), a measure of disability (Bartels et al., 2020). Lower whole brain volumes and altered hippocampus at the first scan were predictors of maximum PCPC score, while MRI abnormalities at any time (such as T2/FLAIR hyper-intensities, gray/white matter lesions, meningeal enhancement, and global/regional brain atrophy) were also significantly correlated with maximum scores (Bartels et al., 2020). This shows that the identification of children at risk of a poor clinical outcome is possible with MRI.

5.1.1.2 Structural MRI and psychometric measures

This predictive ability of structural neuroimaging may not only be true for measures of functional ability, but also for psychometric measures that have received limited attention in AE. Deep gray matter lesions were a significant predictor of academic difficulties assessed in an average follow up of 1 to 7 years after a first presentation of demyelinating syndromes including ADEM. Presentation of the latter diagnosis and an age under 10 years was also a significant predictor of decrease in academic performance (Deiva et al., 2020). Exploring other outcome domains such as cognition and behaviour could therefore be done with similar methods.

As discussed in Chapter 2, cortical thickness is an advanced neuroimaging measure that was shown to be statistically associated with behavioural, emotional and cognitive outcome in various neurological conditions (Fernández-Jaén et al., 2014; Pravatà et al., 2017; Ryan et al., 2016). In adult anti-NMDAR encephalitis, lower cortical thickness was correlated with the

score at the Mini-Mental State Examination (Xu et al., 2022), showing that cortical thickness is potentially relevant to cognitive outcome in AE. This has not been verified in paediatric AE research to date, while cognitive impairments can also be found in children (De Bruijn et al., 2018; Tan et al., 2018): cortical thickness could therefore be a relevant predictor of outcome for children with AE.

5.1.2 Functional neuroimaging as a predictor of long-term outcome

Observable changes in brain structures can also be complemented by functional neuroimaging approaches, as discussed and detailed in Chapters 1 and 3. Such approaches have been associated with cognitive performance in adult AE (Peer et al., 2017; Finke et al., 2013; Heine et al., 2018), making them a potentially relevant marker of cognitive outcome in children.

5.1.2.1 Functional dysconnectivity and clinical outcome

Network dysconnectivity, as previously described in Chapter 1, likely contributes to cognitive deficits in anti-NMDAR encephalitis and was observed in fMRI studies where verbal memory performance was correlated with hippocampal functional dysconnectivity in two studies (Finke et al., 2013; Peer et al., 2017). Lower fMRI functional connectivity was also linked to higher disease severity (mRS score; Finke et al., 2013; Peer et al., 2017; Volz et al., 2016). Large fMRI networks were shown to be involved: connectivity in the frontoparietal control network, was a discriminant factor and was correlated to psychiatric symptoms close to psychosis and schizophrenia after the acute stage of the disease (Peer et al., 2017). Local fMRI network features such as lower clustering coefficient and lower nodal local efficiency were found in adult NMDA encephalitis (Li et al., 2021). Anti-NMDAR antibodies may be the cause of such dysconnectivity, as a study in schizophrenia showed that administrating a NMDAR antagonist (ketamine) disrupted the activity of task-based and default-mode networks which predicted lower performance in working memory tasks (Anticevic et al. 2012).

Other antibodies may also disrupt functional connections: in patients with anti- LGI1 and CASPR2 antibodies, lower episodic memory in the post-acute phase correlated with lower fMRI inter-hippocampal connectivity and lower connectivity between the hippocampus and the posteromedial cortex (Loane et al., 2019). In another cohort with limbic encephalitis, higher mood lability in the post-acute phase was associated with decreased fMRI connectivity between the right hippocampus and right ventral posteromedial cortex (Argyropoulos et al.,

2020). In a long-term follow-up of patients with anti-LGI1 limbic encephalitis, higher fMRI connectivity between the ventral DMN and temporal, frontal, and occipital regions correlated with higher mRS score; higher connectivity between the ventral DMN and the insula correlated with lower verbal memory; the salience network's connectivity with the insula and parietal default mode regions was correlated to lower working and verbal episodic memory (Heine et al., 2018). Reduced fMRI connectivity in the medial temporal subcomponent of the DMN also predicted lower remembrance of internal episodic details in the chronic phase of LGI1 encephalitis (Miller et al., 2020). Another study suggested that damaged brain structures can provoke compensatory changes in connectivity which may lead to deficits, highlighting insular involvement in neuropsychiatric symptoms in dementia and schizophrenia (Heine et al., 2018). All of this indicates that functional disconnections are present in AE and that they are associated with cognitive deficits.

5.1.2.2 Network analysis with magnetoencephalography

MEG data is lacking in research about AE, and previously cited evidence of functional dysconnectivity was only reported using fMRI. MEG is able to show widespread changes in functional connectivity with higher temporal resolution than fMRI (Englot, Konrad, & Morgan, 2016a), and is considered to provide a better spatial resolution than EEG, as it avoids the biases caused by tissue layers around the brain (Quraan et al., 2013). MEG may also be useful in predicting clinical outcome. For example, research conducted in paediatric epilepsy found an association between change in clustering coefficient following a following interictal discharges and lower full-scale IQ: MEG functional connectivity may help predict development of intellectual functioning in children (Ibrahim et al., 2014). Looking at specific brain oscillation bands (cf. Chapter 1) is also relevant: reduced attention and working memory in adults with multiple sclerosis was also significantly predicted by reduced alpha band clustering coefficient using MEG (Schoonheim et al., 2013). Advantages of EEG biomarkers correspond to those of MEG (cost-effective, non-invasive, reproducible; Ciano-Petersen et al. 2021); This supports the idea that MEG is a relevant tool to contribute to research in paediatric AE.

Research in epilepsy may give guidance for hypotheses in AE, seizures being a common feature of the latter (Graus et al., 2016; Titulaer et al., 2013; Vogrig et al., 2019). EEG findings already suggested that low frequency signals (including theta and delta frequency) were linked to spike-wave discharges (Lee et al., 2017), and underlined network differences in epilepsy compared to controls (Douw et al., 2010a; Horstmann et al., 2010; Quraan et al., 2013). Some studies using MEG in epilepsy have found that abnormal low frequency brain activity was associated with network disruption (Ibrahim et al., 2014) as well as occurrence of seizures

(Douw et al., 2010b). Asymmetric interictal delta slow activity was also observed using MEG in epileptic patients (Englot et al., 2016b). Given that epileptic activity is found in AE (Graus et al., 2016; Titulaer et al., 2013; Vogrig et al., 2019), we may expect MEG to highlight network abnormalities within low frequency signals of children with AE.

5.1.3 Functional brain features of interest

5.1.3.1 MEG resting state networks

A method commonly used in research is the recording of the brain when the participant is "resting" in the scanner (e.g., sitting eyes closed or eyes open to a blank screen or a fixation cross), which is convenient for children with reduced compliance or difficulties engaging in tasks. Functional connectivity can be inferred from measuring resting-state networks using MEG (da Silva, 2013; Johnson & He, 2019), in a similar way to fMRI resting-state research in AE (Peer et al., 2017). Chapter 1 and 3 described a range of resting-state fMRI studies conducted in patients with AE and highlighted observed altered connections between widespread regions and their statistical association with clinical or cognitive outcome. This method has also been used in MEG to show the development of connectivity between brain regions across age and was suggested to reflect enhanced functional integration (Johnson & He, 2019), which makes it a relevant protocol for paediatric research.

Resting state analyses in MEG have highlighted brain network dysconnectivity in MS, affecting delta, theta and alpha activity, with correlations to different cognitive scores (Khan, Sami, & Litvak, 2021). For example, a longitudinal MEG study in MS has found more integrated beta network and less integrated delta network to predict cognitive decline after five years (Nauta et al., 2021). In paediatric temporal lobe epilepsy, MEG resting-state data was used to compute brain connectivity and identify patterns of connections across different frequency oscillations that significantly correlated with measures of visual and verbal memory, working memory and global intellectual functioning: children with more bilateral connectivity across frequency bands had lower scores in all cognitive tasks compared to their peers with epilepsy (Arski et al., 2022). As research in AE has reported altered theta-delta activity using EEG (Dalmau et al., 2008; Symmonds et al., 2018): lower frequency bands are therefore of interest for MEG and were selected to assess their potential in predicting cognitive outcome.

With regards to cognition, theta brain networks have been linked to attention and stimulus processing (sensation and perception), encoding and consolidation of information in memory, and executive functions including working memory (Karakaş, 2020). Delta networks

are also associated with attention and concentration and working memory (Harmony, 2013). That makes them both relevant candidate markers of cognition.

5.1.3.2 Auditory P300 and information processing

MEG can be used to assess brain activities involved in information processing: some studies have highlighted the association of these activities with functional and cognitive outcome (Hahn et al., 2012; Mamashli et al., 2017). The *Auditory Oddball Paradigm*, in which participants hear infrequent sounds among frequent sounds is appropriate for paediatric populations: It can be passive and has the advantage of not requiring cognitively demanding tasks, considering the fatigue of children with AE and intellectual difficulties (McKeon et al., 2018; Tan et al., 2018). Using this paradigm, specific signal patterns related to target information processing are well documented in EEG and MEG (P300, Polich, 2012). MEG was also successful in detecting M100 signal abnormalities using this paradigm in ASD, interpreted as linked to auditory sensitivity and NMDAR dysfunction (Matsuzaki et al., 2017). This makes the auditory oddball paradigm relevant to research in paediatric AE: if alterations exist in auditory evoked responses, they may reflect difficulties reported in information processing tasks (Beatty et al., 2016; Cainelli et al., 2019; Matricardi et al., 2016; Mckeon et al., 2016; Mckeon et al., 2018).

The event-related signal P300 (*M300* in MEG) is the evoked response of the brain in reaction to a target stimulus discriminated from background information, thought to reflect the updating of mental schema in a context with new stimuli (Polich, 2012). It is usually defined as the largest positive peak in the evoked response between 250 ms and 500 ms following the stimulus of interest (Boucher et al., 2010; Hahn et al., 2012; Salmond et al., 2007), ranging from 290.0–447.5 ms in healthy populations according to a meta-analysis (van Dinteren et al., 2014). Two subcomponents were described. P3b in response to targeted stimuli and P3a in response to novel stimuli (Polich, 2012; Salmond et al., 2007). P300's *amplitude* (mV/fT signal from baseline) is commonly considered as indicating the extent of neuronal activity or cognitive resources and was suggested to support memory encoding and storage (Polich, 2012; van Dinteren et al., 2014). Some studies have found positive association of amplitude with working memory (Boucher et al., 2010; Roca et al., 2014) and processing speed (Boucher et al., 2010; Yang et al., 2013) in both children and adults.

P300's *latency* (the time from stimulus onset to the peak) is thought to reflect stimulus evaluation time and processing speed (Polich, 2012; van Dinteren et al., 2014). Some studies

have reported negative correlations between latency and neuropsychological measures of processing speed (Boucher et al., 2010; Yang et al., 2013) as well as working memory performance (Boucher et al., 2010; Polich, Howard, & Starr, 1983; Whelan et al., 2010; Yang et al., 2013). A meta-analysis has found that P300 latency decreased progressively from childhood to adolescence before a slow increase during the rest of the lifespan. In contrast, amplitude increased until approximately 21 years of age before a slow decrease throughout life. Combined P300 latency and amplitude are therefore thought to reflect brain development in childhood and degeneration with aging (van Dinteren et al., 2014). Attempts at localizing sources of auditory P3b have suggested it is generated in auditory cortices, in addition to the bilateral mesiotemporal lobes, the superior temporal lobes and also the parietal lobes (Giani et al., 2015; Uohashi et al., 2006).

The auditory P300 has been measured in various neurological conditions in children (Riggins & Scott, 2020), and associated with brain abnormalities and reduced cognitive abilities (Lori et al., 2011; Salmond et al., 2007; Roca et al., 2014). Accordingly, P3b alteration was hypothesized to reflect slower processing caused by disruption of brain networks (Lori et al., 2011). It was suggested that the P300 neurophysiological response during an oddball task could be a useful tool to assess paediatric populations with atypical development, and guide clinical assessments of cognitive markers in the future (Riggins & Scott, 2020). For example, in children with ASD, a correlation between P3b amplitude and hippocampal gray matter density was found (Salmond et al., 2007), which suggests features of this signal also reflects structural differences. Furthermore, this amplitude was correlated with verbal IQ; while being significantly lower in children that had intellectual impairment (Salmond et al., 2007). A similar study in paediatric ASD used MEG to highlight region-specific lower brain response in the inferior frontal gyrus compared to typically developing controls when the paradigm was accompanied by noise, while this regional response was negatively correlated to disease severity (Mamashli et al., 2017). In a cohort of 6 children with MS, individuals with cognitive impairment had decreased P3b amplitude and increased P3b latency; the two being respectively strongly correlated with the number of failures in cognitive tests (under the 5th or the 95th percentile of healthy control's performance in tests of visual memory, verbal memory, attention and executive function; Lori et al., 2011). In a sample of 31 adolescents with ADHD, P300 amplitude was correlated with the working memory's subscale of the *Behavior Rating Inventory of Executive Function* (BRIEF) questionnaire for parents (Roca et al., 2014). The above literature thus indicates that P300 could be a relevant marker of cognitive deficits in paediatric AE.

Data about P300 in AE is limited, but it may be of interest, as increased latency compared to healthy controls was shown in 14.9% of an adult cohort mostly affected by viral encephalitis (including two ADEM; Hahn et al., 2012). In a cohort of 30 patients with encephalitis (12 of which had an unspecified aetiology), 20% had a longer latency in the P300 signal compared to age-matched healthy controls (Kalita, Misra, & Srivastava, 2009). A longer P300 latency was also associated with abnormal MRI, abnormal score in the *Mini Mental state examination* (Kalita, Misra, & Srivastava, 2009) and correlated to unfavourable functional outcome (mRS score) in a long-term follow-up (Hahn et al., 2012). It can also be noted that the hippocampi are known to play a role in P300 functioning (Polich, 2012; Salmond et al., 2007): AE being commonly associated with hippocampal alterations (Heine et al., 2015), it is therefore likely that P300 is altered in this population.

5.1.4 Summary and hypotheses

5.1.4.1 Structural MRI cortical thickness

Assessing structural MRI measures has been shown to be relevant to functional clinical outcome in AE (Balu et al., 2019). Morphometric analyses, which can measure grey or white matter volumes, have also been associated with long-term functional outcome in AE (Bartels et al., 2020). Predicting psychometric measures may also be possible, despite limited research in paediatric AE. For example, deep gray matter lesions were a significant predictor of long-term academic difficulties in ADEM (Deiva et al., 2020). This supports the probability that structural MRI assessments could help predict cognitive and/or behaviour difficulties in AE. One under-investigated measure, cortical thickness, has been associated with behavioural, emotional, cognitive outcome in other conditions (Fernández-Jaén et al., 2014; Pravatà et al., 2017; Ryan et al., 2016) and correlated with cognition in adult anti-NMDAR encephalitis (Xu et al., 2022). Cortical thickness may therefore be a potentially relevant predictor of cognitive difficulties, which remains to be tested in children with AE.

The findings presented in Chapter 2 suggest children with AE may have lower cortical thickness in the left posterior region (superior parietal lobule and superior occipital gyrus) as well as in orbitofrontal cortices, which corresponded to brain alterations observed in those areas in AE cases (Laurikainen et al., 2019; Nahum et al., 2010; Nillo et al., 2021; Wang et al., 2021). Research in other populations links lower cortical thickness in those areas to behavioural and cognitive domains (Ducharme et al., 2012; Fernández-Jaén et al., 2014; Menary et al., 2013 ; Ryan et al., 2016; Whittle et al., 2020) that can be impaired in children

with AE (Armangue et al., 2013; Bach, 2014; Cainelli et al., 2019; Beatty et al., 2016; Burton et al., 2017; Jacobs et al., 2004; Mckeon et al., 2016; Mckeon et al., 2018).

The *Child Behaviour Checklist*, which has been used in paediatric anti-NMDAR AE (Cainelli et al., 2019), and linked to bilateral orbital cortical thickness in typically developing children (Ducharme et al., 2012; Whittle et al., 2020), covers such domains of interest with the Attention problems and Internalizing problem scales. Therefore, the present chapter aimed at investigating whether cortical thickness is relevant to these domains in paediatric AE, via the following hypotheses:

- Cortical thickness in the cluster covering the superior-parietal lobule and the superior occipital gyrus predicts general intellectual functioning in paediatric AE
- Cortical thickness in the left orbitofrontal cortex predicts internalizing problems and attention problems in paediatric AE
- Cortical thickness in the right orbitofrontal cortex predicts internalizing problems and attention problems in paediatric AE

5.1.4.2 Resting-state functional connectivity

Given that functional neuroimaging analyses provide complementary information to structural analyses, functional connectivity was aimed to be explored. Altered fMRI functional connectivity has been observed in AE and statistically associated with outcome measures including mRS disease severity (Heine et al., 2018; Peer et al., 2017; von Schwanenflug et al., 2022a), lower verbal memory (Finke et al., 2013; Heine et al., 2018), lower episodic memory (Heine et al., 2018), lower working memory (Heine et al., 2018) or occurrence of psychiatric symptoms (Peer et al., 2017). EEG studies in AE report abnormalities in the delta brain oscillation including extreme delta brushes and generalised rhythmic delta activity (Schmitt et al., 2012; Jeannin-Mayer et al., 2019) and these related to longer hospitalization and later better recovery (Gillinder et al., 2019; Schmitt et al., 2012). Because delta and theta abnormalities have been reported in previous research in AE (Miao et al., 2021; Symmonds et al., 2018; Vogrig et al., 2019; Yeshokumar et al., 2021), delta and theta frequency were selected in the present analysis to verify whether connectivity in these oscillations predicts cognitive performance, given their relevance to information processing, attention and working memory (Harmony, 2013 ; Karakaş, 2020).

Lower working memory (assessed with digit span test) and processing speed (using symbol digit modalities test) were reported in AE and linked to fMRI altered connectivity (Chen et al., 2022; Heine et al., 2018). However, it is unknown whether MEG-captured delta or theta

connectivity is associated with performance in these cognitive functions in AE. The working memory index has been shown to provide a summation of different tasks for working memory (digit span and letter-number sequencing) in relation to MEG resting-state theta and delta activity in healthy adults, and was therefore selected for a potential broader network association (Oswald et al. 2017). Using validated measures of these functions (Working Memory Index and Processing Speed Index from the WISC-V; Wechsler, 2014), the following hypotheses have been made:

- Theta network connectivity is lower in paediatric AE
- Delta network connectivity is lower in paediatric AE
- Theta network connectivity predicts working memory performance in paediatric AE
- Delta network connectivity predicts working memory performance in paediatric AE
- Theta network connectivity predicts processing speed performance in paediatric AE
- Delta network connectivity predicts processing speed performance in paediatric AE

5.1.4.3 Auditory oddball and M300

The amplitude of the auditory P300 (M300 in MEG) is considered an indicator of cognitive resources (Polich, 2012; van Dinteren et al., 2014) and may be reduced in children with cognitive impairments (Lori et al., 2011; Salmond et al., 2007). The auditory P300's latency, thought to be an indicator of information processing speed (Polich, 2012; van Dinteren et al., 2014), was found to be increased in children with cognitive impairments (Lori et al., 2011) and was associated with negative outcome in viral encephalitis (Hahn et al., 2012; Kalita, Misra, & Srivastava, 2009). It should be noted that it is possible that clinical populations differ in that association: for example, adults with remitting-relapsing multiple sclerosis had a *positive* association between longer P300 latency and domains of intellectual functioning (Sundgren et al., 2015). It remains unknown what directionality applies to children with auto-immune encephalitis.

In some studies that have assessed working memory, P300's amplitude was correlated with higher performance (Boucher et al., 2010; Roca et al., 2014), while P300's latency was correlated with lower performance in working memory (Boucher et al., 2010; Polich, Howard and Starr, 1983; Whelan et al., 2010; Yang et al., 2013). Deficits in working memory have been reported in AE, both in children and adults (Beatty et al., 2016; Heine et al., 2021; Phillips et al., 2018; Mckeon et al., 2018). The digit span test has been frequently used to highlight such deficits in AE (Beatty et al. 2016; Finke et al., 2017; Heine et al, 2018; Heine et al., 2021; Mckeon et al., 2016). Therefore, the following hypotheses have been made:

- M300 amplitude predicts digit span performance in paediatric AE
- M300 latency predicts digit span performance in paediatric AE

In some studies that have measured processing speed, P300's amplitude was correlated with higher performance, while P300's latency was associated with lower processing speed performance (Boucher et al., 2010; Yang et al., 2013). In paediatric AE, deficits in processing speed were reported (Matricardi et al., 2016; Cainelli et al., 2019; Beatty et al., 2016). Wechsler's global processing speed index (PSI) has been used to highlight such deficits (WISC-IV in Beatty et al., 2016; Matricardi et al., 2016) and was correlated to latency in older female populations (WAIS-III in Yang et al., 2013). Therefore, the following hypotheses have been made :

- M300 amplitude predicts processing speed score in paediatric AE
- M300 latency predicts processing speed score in paediatric AE

5.2 Methods

5.2.1 Participants

Two cohorts were recruited: one cohort included children with AE recruited through contact from clinical neurologists at the Birmingham Children's Hospital, Birmingham, United Kingdom. Parents were given a permission to contact form, if consent was signed and given, the neurologists provided their contact details to a researcher associated with the study at Aston University, who could then contact the parents and to obtain informed consent to take part in the study. Once consent was obtained, the child's MRI data were requested and retrieved from the hospital as part of the PROBIt study (Ethics Reference #17/YH/0299; #IRAS 222771).

The control cohort was composed of typically developing children, recruited at Aston University's Institute of Health & Neurodevelopment, Birmingham, United Kingdom (under Ethics #HLS21011), through contact permission collected from families that took part in research projects at the centre, as well as advertisement via social media/community organisations and Aston University/IHN outreach events, where contact details to get in touch with the study researchers were given.

Informed assent to participate from children and informed consent of one of their respective parents or legal guardians were collected. Inclusion criteria for all participants were an age range from birth to 6 to 16 years at point of recruitment. Exclusion criteria for both cohorts included dissent of the child from participating and presence of contraindication for MRI scanning. AE children were included if they had a previous diagnosis of any type of AE (according to the standards established in Cellucci et al., 2020; Graus et al., 2016), and were recruited at least 2 years after disease onset. Inclusion criteria for typically developing controls included the absence of diagnosis of learning difficulty, or psychiatric, neurodevelopmental, or neurological disorder and absence of known or suspected cerebral abnormality.

5.2.2 Neuropsychological assessment

Participants were examined with neuropsychological tests. In all participants, cognitive functions were assessed using the *Wechsler Intelligence Scale for Children, 5th Edition* (WISC-V) to assess general intellectual functioning in children from 6 years to 16 years and 11 months (Wechsler, 2014). The Wechsler scale uses a battery of psychometric tests that assess intellectual quotient (IQ) into separate indices (Wechsler, 2014). For the fifth edition of the

WISC, the subtests are classified into the following indices: Verbal Comprehension, Visual Spatial, Fluid Reasoning, Working Memory, and Processing Speed (Wechsler, 2014). *Full-scale Intelligence Quotient* (FSIQ) is the score summing the results of the indices.

Furthermore, parents completed the Child Behavior Checklist (CBCL) 6–18 questionnaire (Achenbach, 2001), which has been used in earlier research in paediatric anti-NMDAR encephalitis to highlight behavioural issues (Cainelli et al., 2019). It was validated in multiple paediatric populations (Nakamura et al., 2009; Pandolfi, Magyar & Norris, 2014). The questionnaire gives information about emotional and behavioural problems in children, across the following syndrome scales: social withdrawal, somatic complaints, anxiety/depression, social problems, thought problems, attention problems, rule-breaking behaviour, and aggressive behaviour. The questionnaire allows to conceptualize them into two broadband scales: externalizing problems and internalizing problems (Cainelli et al., 2019).

5.2.3 MRI image acquisition

Each participant had structural MRI scans (T1 and FLAIR), acquired using a 3T MRI scanner located at the Aston *Institute of Health* & *Neurodevelopment*, Birmingham. The scanner was Siemens TrioTim until Oct 2021; and Siemens MAGNETOM Prisma from March 2022 (for both: flip angle = 15; dimensions = 176x240x256). Three children with AE (ID 10, 11, 12, Appendix 5) and all controls were scanned using the Siemens MAGNETOM Prisma scanner. One child (ID 13, Appendix 5) was not scanned at the institute, instead a scan previously acquired at the Birmingham's Children Hospital was used for analyses (Siemens Avanto, Flip angle = 15, field strength = 1.5T, dimensions = 176x208x256).

T1 weighted structural MRI scans were preprocessed using automated pipelines in FreeSurfer (v6.0, Fischl, 2012): including segmentation of gray matter, white matter and CSF boundaries; brain extraction; quality check for segmentation or surface estimation errors; normalization and automated structural parcellation (Wagstyl & Lerch, 2018). Intensity correction was done with N3 (described in 2.2.3) adapted to scans acquired from 3T scanners using the "-3T" flag (Fischl, 2012); and pial surface estimation was improved with the contrasts from the FLAIR scans when a FLAIR scan was available ("-FLAIRpial" argument; Fischl, 2012). Every scan was quality-checked for skull-stripping, segmentation or normalization errors, with the assistance of the *Qoala-T* shiny-app (Klapwijk et al., 2019), as described in Chapter 2 (section 2.2.3).

5.2.4 Cortical thickness analysis

5.2.4.1 Data preprocessing

Cortical thickness was estimated from the average distance between the generated 3D surfaces of the white matter and the gray matter in FreeSurfer (Fischl & Dale, 2000; Wagstyl & Lerch, 2018). The surfaces were smoothed and aligned to a common reference group template supplied in FreeSurfer (*buckner40*) for inter-participant comparability (Fischl, 2012; Wagstyl & Lerch, 2018).

5.2.4.2 Regional cortical thickness estimation

Based on the findings from Chapter 2, three ROIs were selected for cortical thickness analyses: the superior posterior cluster and the two bilateral orbitofrontal cortices. As in Chapter 2, for each AE participant, the labels of the orbitofrontal cortices were first extracted by combining each orbital gyrus and corresponding orbital sulci ("H shaped") using the *Destrieux* atlas (Destrieux et al., 2010) with the tksurfer GUI in FreeSurfer. Then the average thickness for each label was computed using FreeSurfer's mris_anatomical_stats command. The cluster's average cortical thickness was obtained with the segmentation output of Chapter 2's group analysis ('cache.th20.abs.sig.ocn.mgh'). This allowed to extract the average thickness within the boundaries of the significant cluster, in each participant's whole-brain thickness values (smoothed and resampled on a common brain template with '-qcache': e.g., 'lh.thickness.fwhm10.fsaverage.mgh').

5.2.5 MEG protocol and processing

5.2.5.1 MEG acquisition parameters

MEG recordings were conducted with the Elekta Neuromag® TRIUX MEG system at the Institute of Health and Neurodevelopment, Birmingham, UK, comprising 306-channels (including 102 magnetometers and 204 planar gradiometers) located in a single-shell magnetically shielded room equipped with MaxShieldTM technology. Recordings were conducted with a 2000 Hz sampling rate, a high-pass filter of 0.1 Hz and a high-pass filter of 330 Hz; and included a bipolar electrocardiography electrode to control for heartbeats. Five head position indicator coils were used on children, three on the forehead and one on each mastoid to track head movements (the information being then used to estimate head movement and coregister the MEG recording to the estimated head surface in brainstorm). Co-registration between the MEG and the MRI scans was prepared using a *Polhemus Fastrak* motion tracker which digitizes the coordinates of each participant's head shape, starting with

three fiducial coordinates (nasion, and bilateral preauricular points), followed by the head position coils and the rest of the head.

5.2.5.2 Resting state

During the MEG recordings, all participants underwent a recording at resting state, in which they had to sit still in the scanner for 6 minutes and look at a black fixation cross on a white background.

5.2.5.3 Auditory oddball

Participants went through an auditory oddball paradigm programmed in *Presentation* (v. 15.1, Build 04.03.12). The task presented a set of auditory tones to participants with different occurrence: a standard tone appearing 80% of the time, and a target deviant tone appearing 20% of the time. Frequent tones had a sound frequency of 1000 Hz and deviant tones had a frequency of 2000Hz (occurrence and frequency as in Boucher et al., 2010; Lori et al., 2011; Uohashi et al., 2006). Each sequence was presented randomly, with rare tones not appearing twice in succession. The sounds were presented binaurally through a plastic tube with ear inserts. Participants were asked to passively listen while the stimuli were presented. The duration of all tones was 80ms. Each patient heard 100 stimuli with an inter-stimulus interval of 2,500-3,000 ms, for approximately five to six minutes, including 20 target trials (an experiment found that this number was enough to gather reliable and statistically stable P300 measures: Cohen & Polich, 1997).

5.2.5.4 MEG co-registration and source modelling

Each individual's MRI scan was co-registered to their MEG recording using *BrainStorm* (*v.* 3.210818, 18 August 2021; Tadel et al., 2011), which is documented and freely available for download online under the GNU general public license (http://neuroimage.usc.edu/brainstorm). The coregistration was done using fiducial points manually defined on the MRI scans and refined using the head position indicator coordinates. Anatomy models were imported individually for each participant's MRI preprocessed with the FreeSurfer pipeline described in section 5.2.3. The number of vertices of the whole cortex surface generated in FreeSurfer was downsampled to 15000 in order to optimize source projection.

When an MRI scan contained too many artefacts to generate FreeSurfer meshes or could not be preprocessed, an age-matched paediatric symmetric MRI template preprocessed with the same FreeSurfer pipeline was used as a substitute for the MEG models described in

the next paragraph (Fonov et al., 2009; Fonov et al., 2011). The templates were preprocessed with FreeSurfer again in order to keep the same parcellation atlases across participants. Template models were used for one AE case (ID 8, Appendix 5) and one in the control group.

Three-shell realistically-shaped head models were generated for each participant based on their respective imported surfaces, with adaptive integration in *BrainStorm* and the *OpenMEEG* plug-in (Gramfort et al., 2010; Kybic et al., 2006), using scalp/skull/brain layers with default settings for layer conductivities, vertices and skull thickness. The boundary element method (BEM) was used, as it supports accurate localization of signal sources compared to sphere-based methods (Stenroos, Hunold & Haueisen, 2014). The source of the signal was reconstructed in each anatomy model using LCMV beamformer, accounting for external background noise: it was assumed to be captured in a data covariance matrix, regularized with the median eigenvalues (as recommended by Tadel et al., 2021) extracted from the whole recording for resting state recording, and extracted from the 500ms prestimulus baseline for the auditory recordings.

5.2.6 Resting state network analysis

Raw resting state recordings were epoched into non-overlapping trials of 10 seconds using *Fieldtrip* (*v*. 22 January 2021; Oostenveld et al., 2011). Signals were filtered with a 4th-order Butterworth zero-phase low-pass filter for better visualization (cut-off: 70 Hz, as in Vogrig et al., 2019). An independent component analysis (ICA) was run (keeping the number of components equal to the number of included channels), to reject heartbeats, eye blinks and eye movement artefacts. An ICA is a method that extracts individual signals from mixtures of signals by decomposing the recording data in statistically independent components (assumed to be produced by different sources, Stone, 2002). Here, components were visually identified using an in-built script that allows toggling through the components, plotting their topography and signal time-course in all trials. Each trial was toggled manually in order to reject trials and channels that contained excessive artefacts caused by muscle activity and SQUID jumps. The cleaned data was then imported into *BrainStorm* (*v.* 3.210818, 18 August 2021; Tadel et al., 2011) to facilitate connectivity analysis. The number of 10 second epochs that remained after processing were distributed as follows: 37.5±1.6 (IQR = 1) for the Encephalitis group and 37.33±1.1 (IQR = 3) in the Control group.

Before computing connectivity, each trial was transformed in the time-frequency domain using Hilbert transformation. Frequency bands of interest were delta (1 to 4 Hz) and theta (5 to 8 Hz). Using the Desikan-Killiany atlas, Brainstorm's scout function was applied to

produce the mean power (average of the square of all the signals) of the time-frequency (of each frequency of interest band-pass filtered separately) within each parcellated region *before* estimating frequency connectivity (instead of *after* estimating connectivity for each dipole in order to reduce processing time). Connectivity between these regions was computed for each frequency band of interest using Amplitude Envelope Correlation, a measure of temporal evolution of spectral power (envelope), correlated between pairs of orthogonalized signals within separate regions (Hipp et al., 2012). This method avoids common source contamination and has also been shown to have a superior between-sessions network estimation consistency compared to other measures of connectivity (Colclough et al., 2016; Liuzzi et al., 2017). This method has also previously been used to explore connectivity patterns relevant to epileptic brain activity (Aydin et al., 2020). Two 68x68 connectivity matrices were generated for each epoch and then averaged for each participant; resulting in one average delta connectivity matrix (example given in Figure 5.1) and one average theta connectivity matrix per participant).

Figure 5.1

Delta connectivity matrix estimated in a participant

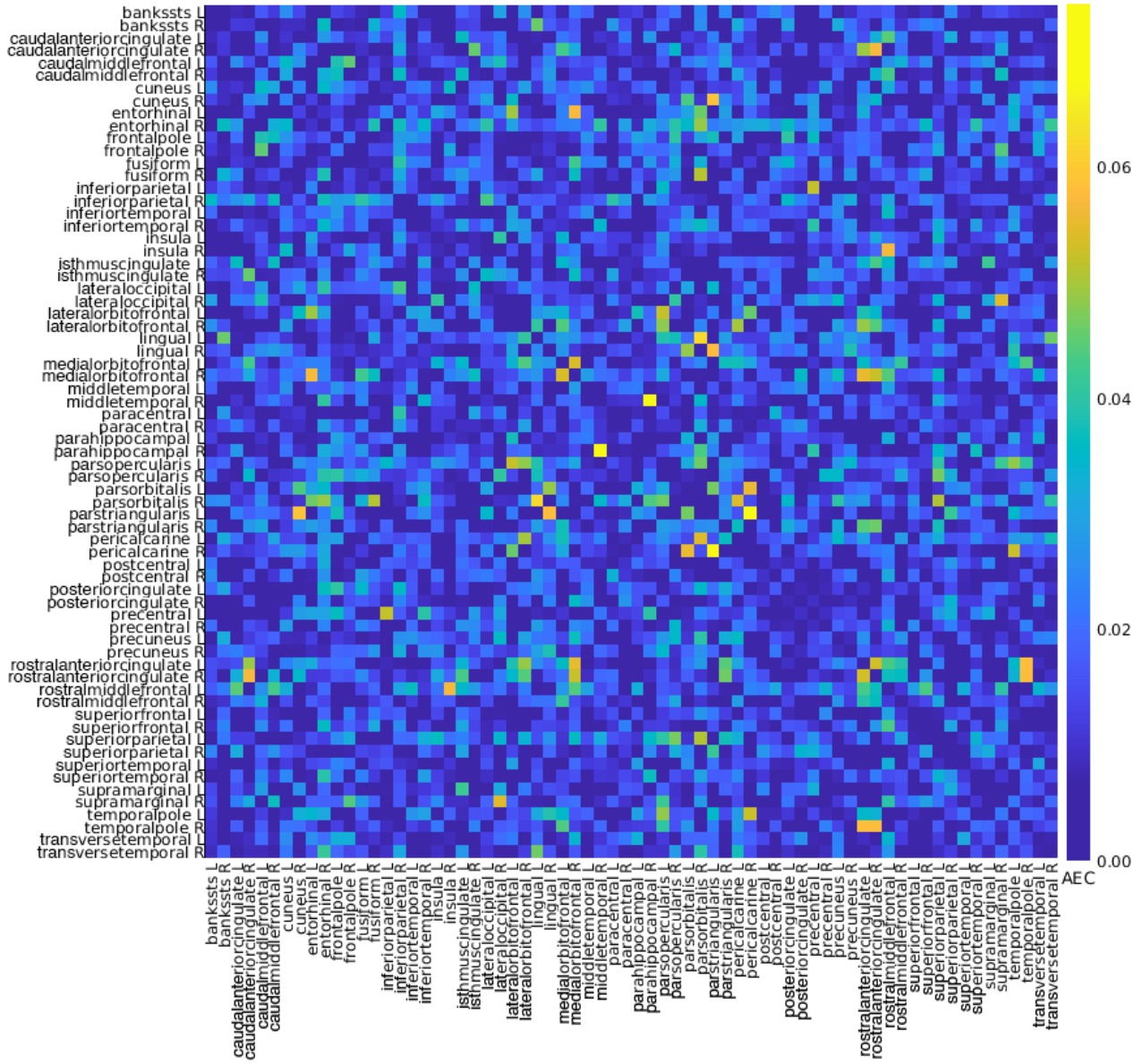

Note. AEC = Amplitude Envelope Correlation. The figure was produced with *Brainstorm* (Tadel, 2011). The matrix depicts the level of connectivity between each of the 68 brain regions parcellated with the Desikan-Killiany atlas.

The average connectivity matrices were exported individually for each participant in Matlab. Negative correlations were transformed into zeros. The Brain Connectivity Toolbox (BCT *v*. 2019-03-03; Rubinov & Sporns, 2010) was then used to normalize the matrices' weights into a range from 0 (no connection) to 1 (maximum connectivity). Proportional thresholds were chosen for their higher stability within graph measures (Garrison et al., 2015); and applied to keep 10% to 30% strongest connections for each frequency matrix (as in previous paediatric MEG research, Takahashi et al., 2017), in intervals of 4%, thus 6 matrices per frequency band. The purpose of looking at the networks with different thresholds is to

control for the instability of graph measures across threshold and the arbitrariness of selecting one threshold (Drakesmith et al., 2015).

Measures of efficiency and modularity, that reflect how well brain networks are able to integrate and segregate distinct modules to transmit efficiently neuronal information, were chosen as they were investigated in previous encephalitis fMRI research (Li et al., 2021; Wang et al., 2021). Note that these measures complement the measures used in Chapter 3 (involving the same control and AE cohorts). The latter had been selected based on epilepsy literature while the present study follows AE literature (Li et al., 2021; Wang et al., 2021). For each thresholded matrix, were measured:

- *Modularity* (*M*), the degree to which the network can be subdivided into non-overlapping groups, maximizing within-group edges, and minimizing between-group edges (Rubinov & Sporns, 2010, using *Q* maximized modularity).
- *Global efficiency* (E_{glob}), the average inverse shortest path length between all pairs of nodes (Rubinov & Sporns, 2010).
- Mean *Local efficiency* (E_{loc}), the global efficiency computed for neighbouring nodes at the level of each node (Rubinov & Sporns, 2010, with the recommended 2017 BCT function)

In order to avoid the issue of multiple comparisons produced by the multiplication of thresholds, as the group difference would need to be assessed for 2 frequency bands * 6 thresholds * 3 graph measures, the MTPC was used. It was implemented in the *brainGRAPH* package (*v*.3.0.0; Csardi & Nepusz, 2006; Watson et al., 2020) in *R* (*v*.4.2.1; R Core Team, 2022). This method allows the identification of a group difference that is stable across thresholds and controls for multiple comparison through permutation correction. The MTPC was successfully applied in other clinical populations with structural diffusion-weighted imaging networks (Cheng et al., 2019; Drakesmith et al., 2015; Watson, DeMaster, & Ewing-Cobbs, 2019; Spilling et al., 2019), and can be replicated in MEG-derived networks as they are represented in the same mathematical graph pattern. The Desikan-Killiany atlas in brainGRAPH was reordered in order to match the labels of the matrices in Brainstorm. The MTPC computes a test-statistic (here, *t*) on graph measures across groups for each threshold, and permutes group assignments (here, 5000 times). The maximum *t* across all permutations for each threshold are used to establish a critical value at a desired confidence level (here at $\alpha = .05$). For each threshold, an area-under-the-curve is computed for significant "clusters" where the true *t* is higher than the critical value. A critical AUC is determined from the mean of the super-critical AUCs of the permuted tests: the output of the MTPC is significant if the AUC of the

significant clusters exceeds the critical AUC (Drakesmith et al., 2015). In the present study, the MTPC model was one-sided and verified lower ("less") connectivity in the AE group.

To account for the multiple MTPC analyses (2 frequency bands * 3 graph measures), the *p* values corrected across all six thresholds in each MTPC (p.fdr values), were corrected again for false discovery rate against the p.fdr values of the other MTPC analyses (6 * 6 p.fdr in total).

For significant differences, a post-hoc exploratory analysis was run to verify a potential difference in overall raw functional connectivity (overall FC, i.e. average of the AEC across all connections of a network), compared across groups using nonparametric permutation tests (t-test with threshold 3.1, two-tailed, 5000 permutations, significant at $p = .05$, component size = extent) in the *Network Based Statistic* toolbox (Zalesky, Fornito & Bullmore, 2010). The point of such post-hoc analysis is to verify whether the network organization differences may simply be explained by the overall difference in FC or, on the contrary, remain different regardless of this overall connectivity contrast. That is because low overall FC can introduce spurious connections within proportional thresholds and in turn influence network metrics (Hallquist & Hilary, 2018; van den Heuvel et al., 2017). If overall FC differed between groups, a strategy proposed by van den Heuvel et al., 2017 was followed if applicable to the data, by establishing overall FC-matched subgroups and rerunning the graph metrics analyses.

5.2.7 Auditory Oddball analysis

Auditory recordings were filtered with MaxFilter (Elekta Neuromag Oy; version 2.2.10), using temporal extension of signal space separation (tSSS) to detect and remove external noise artefacts. Bad channels detected by MaxFilter were removed and the amount of movement was estimated from the head position indicators (extracting goodness of fit, rotation velocity and drifting from the initial position values, as described in *MRC Cognition and Brain Sciences Unit*, 2013). When the estimation suggested a lot of movement happened during the recording (at least one value extracted being above 0.5 cm), Maxfilter's movement compensation was applied along with the tSSS filter.

Using Fieldtrip, each recording was segmented in epochs time-locked for 1500 ms after each target deviant tone (as in Salmond et al., 2007), using a prestimulus baseline of 500 milliseconds, with a 4^{th}-order Butterworth zero-phase low-pass filter (30 Hz cut-off, as in Bianchi et al., 2010; Giani et al., 2015; Kheirkhah et al., 2021). A principal component analysis (PCA) was used here for faster processing (it is a transformation that reduces/compresses the data

to a determined number of components instead of separating it in components on the basis of independence as in ICA; Stone, 2022). Here the PCA was used reducing the data to 30 components, in order to reject heartbeats, eye blinks and eye movement. After the PCA, trials and channels were manually checked separately for standard and odd stimuli, and rejected if too many artefacts caused by muscle activity and SQUID jumps were found (none of the 20 odd trials per participant were rejected). The cleaned data was then imported into *BrainStorm* (*v.* 3.210818, 18 August 2021; Tadel et al., 2011); in which weighted mean amplitude was obtained separately for the two sets of trials (following odd or standard tones) in each participant; and then source analyses were computed following the protocol in section 5.2.5.4. The number of standard trials that remained after processing were distributed as follows: 77.75±1.9 (IQR = 3) for the AE group and 78.27±2.5 (IQR = 3) in the Control group.

To look at the auditory response specific to odd stimuli, the absolute difference between the sources of the two averages (|odd|-|standard|) was obtained, to look at the strength of the response and avoid the ambiguity in the sign of the source (Tadel et al., 2019; Tadel et al., 2021). The source-space signal was looked in areas proximate to the bilateral auditory cortices including: transverse temporal/heschl gyri, transverse temporal sulci, planum polare, planum temporale and superior lateral temporal areas (with guidance from the Destrieux atlas parcellations in FreeSurfer: *G_temp_sup-G_T_transv*, S_temporal_transverse, *G_temp_sup-Plan_tempo, G_temp_sup-Plan_polar, G_temp_sup-Lateral*; cf. Destrieux et al., 2010).

The M300 was identified as the strongest brain response (compared to standard response) between 250 and 500 ms after the stimulus in either of the two hemispheres (time-window as in Boucher et al., 2010; Hahn et al., 2012; Salmond et al., 2007), displayed visually at 70% highest difference threshold. When identified, a 15 vertices region-of-interest was manually created in the surface to extract an average source-space time-series of the signal. Amplitude (positive difference in absolute *Pseudo Neural Activity Index*, as per Brainstorm's LCMV, standardized with normalization to the prestimulus 500ms baseline) and Latency (ms) values of the peak response were respectively extracted and exported to an SPSS database (SPSS *v*.26 64-bit for Windows; IBM Corp., 2019) for further statistical analyses. An example of a M300 region-of-interest is shown in Figure 5.2.

Figure 5.2

M300 auditory response identified at source-level activity in a participant

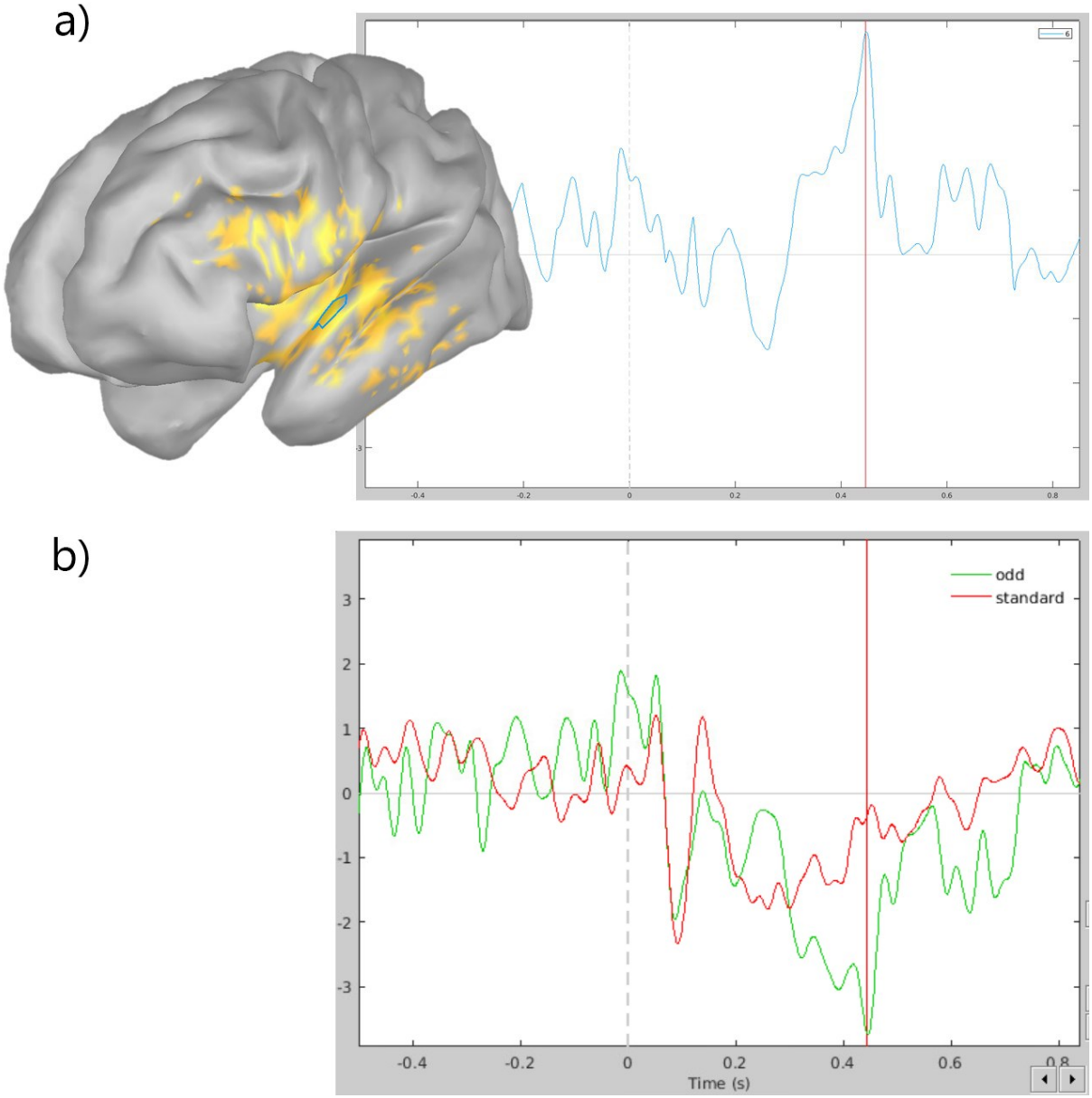

Note. The figures were produced with *Brainstorm* (Tadel, 2011). A) The yellow activity is the absolute difference in average brain response to odd stimuli compared to standard stimuli. The blue parcel on the 3D model is the region-of-interest (in this case extending on the planum polare and lateral superior temporal areas). The amplitude of the response difference within the region is shown on the right. B) The same odd and standard average responses plotted separately, showing a negative magnitude for the odd response (in green) stronger than the standard response (in red) (note that the sign of the magnitude, in a constrained source estimation, is dependent on the orientation of the source signal, Tadel et al., 2021).

5.2.8 Statistical analyses

Note that because the study design was not longitudinal, "predictors" tested in the study designate variables that statistically contribute to the variance of a defined outcome (Mayers, 2013). They are statistical associations rather than an early anticipation of an outcome in time.

5.2.8.1 Multiple regressions for cortical thickness measures

Statistical analyses for the cortical thickness of the three ROIs were run using (SPSS *v*.26 64-bit for Windows; IBM Corp., 2019). Cluster-of-interest cortical thickness, left orbitofrontal cortical thickness and right orbitofrontal cortical thickness, were extracted for each participant in the AE group. Both orbitofrontal values were then tested in separate multiple regression analyses, in prediction of CBCL Internalizing Scale score and CBCL Attention Problems score (one linear model per behavioural measure). Given that an international study (N= 56,665) reported very minuscule effects of age and gender on the above CBCL scores ($\eta^2 < 0.01$; Rescorla et al., 2012) they were not controlled for to preserve statistical power. An additional multiple regression was run for the cluster-of-interest in prediction of FSIQ, controlling for the potential effect of gender on WISC scores (Giofrè et al., 2022). The p-values across regression models were corrected for false discovery rate if significant.

A Shapiro-Wilk test was used to assess the normality of the distribution of the cognitive variables. Outliers were defined as three standard-deviations over or under the mean. The assumption of linearity between predictors and outcome variable was checked by plotting Residuals vs Fitted value scatterplots in SPSS; the assumption of multicollinearity was tested by computing collinearity diagnostics of the regressors and VIF values (below 10), and the assumption of independence of error residuals was tested with the Durbin-Watson test output considered acceptable between 1 and 3 (Mayers, 2013).

5.2.8.2 Multiple regressions for resting state networks

Given the graph measures were computed in *R* (*v*.4.2.1; R Core Team, 2022), regressions were run on the same software, with the *car* package (Fox & Weisberg, 2019). According to the output of the MTPC comparison analyses, graph measures for each participant in the AE group were extracted for the threshold where the group difference was the highest compared to controls. Graph measures were then separately included in multiple regression analyses predicting Processing Speed Index (PSI) and Working Memory Index

(WMI), controlling for gender as the latter may have an effect on these scores of the WISC (Giofrè et al., 2022). Age was not controlled for as the standard WISC scores are already standardized across age-range. Each linear model was defined as such in R: cognitive measure ~ graph measure + gender. This amounted to 12 linear models (2 frequency bands * 3 graph measures * 2 cognitive measures). The p-value output for individual graph measure coefficients were corrected for false discovery rate across all the regressions if significant.

A Shapiro-Wilk test was used to assess the normality of the distribution of the cognitive variables. Outliers were defined as three standard-deviations over or under the mean. The assumption of linearity was checked through Residuals vs Fitted scatterplots. The assumption of multicollinearity was tested by computing VIF values (below 10), and the assumption of independence of error residuals was tested with the Durbin-Watson test (non-significant *p* value).

5.2.8.3 Multiple regressions for the auditory oddball task

Statistical analyses for the auditory evoked response were run using (SPSS *v*.26 64-bit for Windows; IBM Corp., 2019). M300 amplitude and M300 latency values in the AE group were included in four multiple regression analyses (2 M300 measures * 2 cognitive measures), predicting Processing Speed Index (PSI) and Digit Span scale score, adjusting for gender as the latter may have an effect on these scores of the WISC (Giofrè et al., 2022). Age was not controlled for as the standard WISC scores are already standardized across age-range. The p-value output for individual graph coefficients were corrected for false discovery rate across all the regressions if significant.

A Shapiro-Wilk test was used to assess the normality of the distribution of the cognitive variables. Outliers were defined as three standard-deviations over or under the mean. The assumption of linearity between predictors and outcome variable was checked by plotting Residuals vs Fitted value scatterplots in SPSS; the assumption of multicollinearity was tested by computing collinearity diagnostics of the regressors and VIF, and the assumption of independence of error residuals was tested with the Durbin-Watson test output considered acceptable between 1 and 3 (Mayers, 2013).

5.3 Results

5.3.1 Demographics

25 children completed the study. Demographic information is presented in Table 5.1. Specific clinical data and diagnoses are shown in Appendix 5.

Table 5.1

Demographic and clinical characteristics of children with autoimmune encephalitis and typically developing children

Child characteristics	Controls N=12	AE N=13	Statistics	
			Test	*p* value
Gender (female:male)	4:8	8:5	$\chi^2 = 1.989$	.158
Age in years (mean±sd) IQR	10.5 ± 3.2 6.5	11.14 ± 3.32 7.0	$t = -0.455$	.653
Age of onset (mean±sd) IQR	NA	4.8 ± 3.22 4	NA	NA
mRS at scan IQR	NA	0.92 ± 0.86 1	NA	NA

Note. AE = Autoimmune Encephalitis.

5.3.2 Neuropsychological outcomes

One child with AE (ID 6 in Appendix 5) did not complete cognitive assessments and another (ID 12) did not complete the full assessment that leads to the FSIQ score. The scores of the WISC-V for each group are depicted in Figure 5.3. Groups did not significantly differ on average in Digit Span performance ($t = 1.410$; $p = .173$; Cohen's $d = -0.577$), in general Working Memory ($t = 1.751$; $p = .094$; Cohen's $d = -0.715$) or in general intellectual functioning ($t = 1.547$; $p = .137$; Cohen's $d = -0.646$). The AE group had a significantly lower average score in Processing Speed ($t = 2.735$; $p = .012$; Cohen's $d = -1.117$).

Children's scores based on WISC's age-normalized population categories are depicted in Figure 5.4. Due to low expected cell counts, proportions were compared binary-wise (Extremely low to Low average | Average to Extremely High) using Fisher's Exact Test: no significant difference in categories was observed between groups in Processing speed ($p = .414$), Working Memory ($p = .193$) or General Intellectual functioning ($p = .400$).

Figure 5.3

Cognitive outcome from the neuropsychological assessments across groups

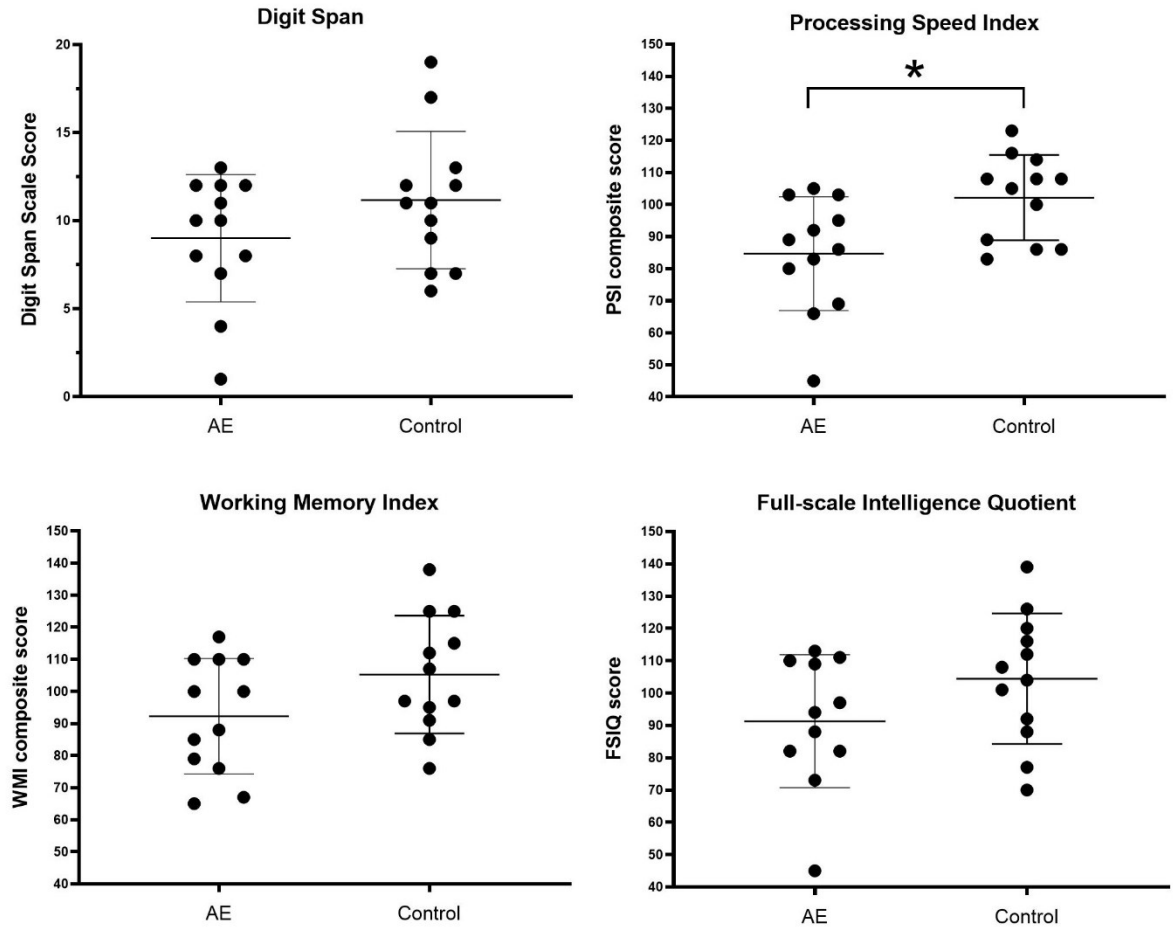

Note. AE = Auto-immune Encephalitis; PSI = Processing Speed Index; WMI = Working Memory Index; FSIQ = Full-Scale Intelligence Quotient; All measures were obtained with the WISC-V (Wechsler, 2014). * = significant difference at p = .012.

Figure 5.4

Population-norm cognitive score categories across groups

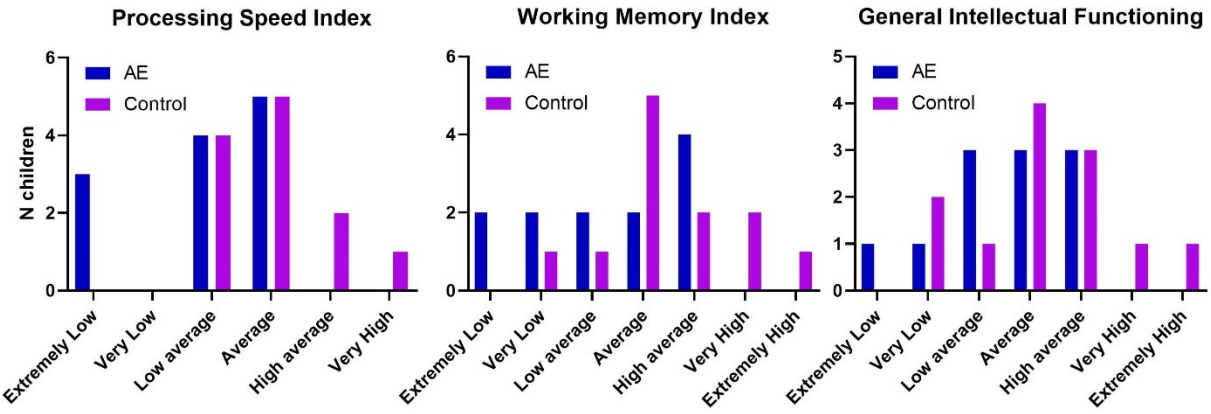

Note. AE = Auto-immune Encephalitis. Classification categories and measures were obtained with the WISC-V (Wechsler, 2014).

Regarding CBCL questionnaires, parents of 3 controls and 5 children with AE did not complete them at the time of the analyses (patient ID 3, 5, 6, 7, 12 in Appendix 5). Internalizing problems were significantly higher in the AE group (t = -2.449; p = .027; Cohen's d = 1.19) and Attention Problems did not significantly differ across groups (U = 16.5; p = .059; Cohen's d = 1.022). The t-scores are depicted in Figure 5.5. With regards to internalizing problems, three children were within the clinical range and two in the borderline range in the AE group, while all controls were within a normal range. For attention problems, two children were within the clinical range and two in the borderline range in the AE group, and one child within the control group was within the borderline range.

Figure 5.5

Internalizing and Attention Problems scores across groups

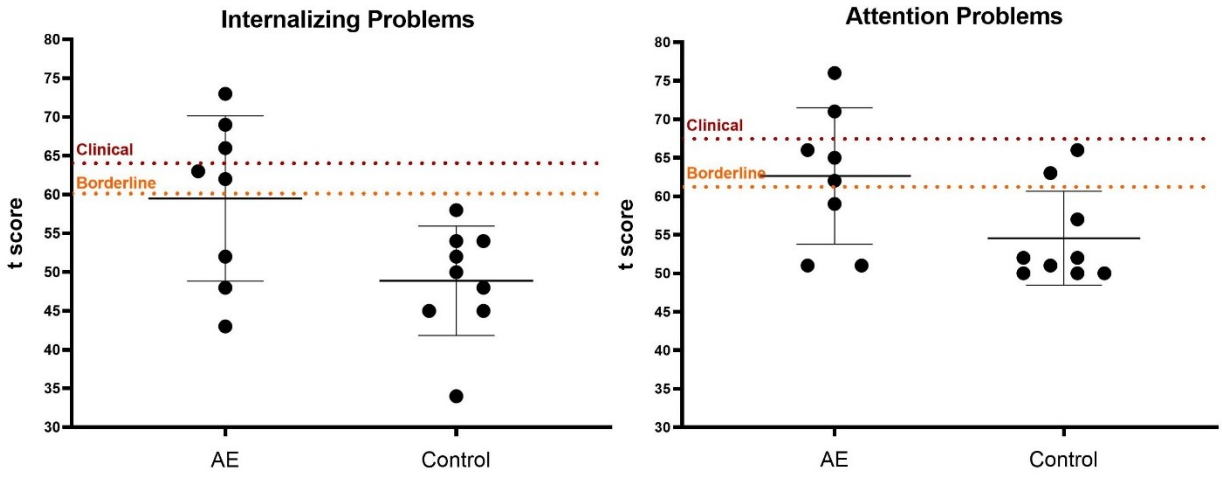

Note. AE = Auto-immune Encephalitis. Scores were separately measured and classified as per the Child Behavior Checklist 6-18 guidelines (Achenbach, 2001).

5.3.3 Cortical thickness analysis

For the analysis with the cluster-based cortical thickness, 10 children with AE were eligible as they had a usable T1 MRI for estimation of cortical thickness along with a full WISC assessment (unincluded cases were ID 6, 8, 12, in Appendix 5). Power for a regression analysis with two covariates is 1-β = .25 for the overall model, and 1-β = .37 for the main effect coefficient, assuming a large effect size is detected according to a post-hoc estimate in G*Power (Faul et al., 2007). No outliers were detected, and the distribution of the cognitive variables was normal. No multicollinearity between the predictors or significant dependence of error residuals was observed in the model. The relationship between predictors and the outcome variables was linear.

The regression model for the posterior Cluster's mean cortical thickness did not significantly predict general intellectual functioning (F(df) = .747(2); p = .508; adjusted R^2 = -.60). Individual effects are depicted in Table 5.2.

Table 5.2

Effect of Cluster mean cortical thickness on General intellectual functioning

						Confidence interval 95%	
Predictor	**B**	**sd error**	**β**	***t* value**	***p* value**	**Lower**	**Upper**
Cluster Thickness	-37.387	31.256	-.441	-1.196	.271	-111.296	36.523
Gender	-3.390	16.477	-.076	-.206	.843	-42.353	35.572

Note. General intellectual functioning was measured with the Full-Scale Intelligence Quotient from the WISC-V (Wechsler, 2014).

Regarding orbitofrontal cortical thickness and behavioural questionnaires, only parents of 7 children with AE could be used and tested in relation to available MRI data (patient ID 3, 5, 6, 7, 8, 12 in Appendix 5). Power for a regression analysis with one covariate is 1-β = .25 for the overall model, and for the main effect coefficient, assuming a large effect size is detected according to a post-hoc estimate in G*Power (Faul et al., 2007). No outliers were detected, and the distribution of the cognitive variables was normal. The relationship between predictors and the outcome variables was linear. VIF values were below 10 (3.25; Tolerance = .307), but collinearity diagnostics returned common dimensions with a Condition Index of 58.7, indicating multicollinearity. This was reinforced by the opposition of coefficient signs and inflation of their effect magnitude compared to separate individual regressions, an artificial phenomenon caused by multicollinearity (Kalnins, 2018; Kalnins, 2022). Because of this, four separate individual regressions are reported.

Internalizing problems were not significantly predicted either by left orbitofrontal (F(df)= .191 (1), adjusted R^2 = -.156) or right orbitofrontal (F(df)= .139 (1), adjusted R^2 = -.167) cortical thickness (Table 5.3 and Table 5.4). Similarly, attention problems were not significantly predicted either by left orbitofrontal (F(df)= .062 (1), adjusted R^2 = -.185) or right orbitofrontal (F(df)= 1.115 (1), adjusted R^2 = .019) cortical thickness (Table 5.5 and Table 5.6).

Table 5.3

Effect of left orbitofrontal cortical thickness on internalizing problems

						Confidence interval 95%	
Predictor	**B**	**sd error**	**β**	***t* value**	***p* value**	**Lower**	**Upper**
LOFC Cortical Thickness	9.782	22.390	.192	.437	.680	-47.772	67.336

Note. LOFC = Left OrbitoFrontal Cortex. Internalizing problems were measured with the Child Behavior Checklist 6-18 (Achenbach, 2001).

Table 5.4

Effect of right orbitofrontal cortical thickness on internalizing problems

						Confidence interval 95%	
Predictor	**B**	**sd error**	**β**	***t* value**	***p* value**	**Lower**	**Upper**
ROFC Cortical Thickness	-6.928	18.566	-.165	-.373	.724	-54.654	40.798

Note. ROFC = Right OrbitoFrontal Cortex. Internalizing problems were measured with the Child Behavior Checklist 6-18 (Achenbach, 2001).

Table 5.5

Effect of left orbitofrontal cortical thickness on attention problems

						Confidence interval 95%	
Predictor	**B**	**sd error**	**β**	***t* value**	***p* value**	**Lower**	**Upper**
LOFC Cortical Thickness	5.022	20.108	.111	.250	.813	-46.667	56.711

Note. LOFC = Left OrbitoFrontal Cortex. Attention problems were measured with the Child Behavior Checklist 6-18 (Achenbach, 2001).

Table 5.6

Effect of right orbitofrontal cortical thickness on attention problems

						Confidence interval 95%	
Predictor	**B**	**sd error**	**β**	***t* value**	***p* value**	**Lower**	**Upper**
ROFC Cortical Thickness	-15.943	15.095	-.427	-1.056	.339	-54.746	22.860

Note. ROFC = Right OrbitoFrontal Cortex. Attention problems were measured with the Child Behavior Checklist 6-18 (Achenbach, 2001).

5.3.4 Resting state network analysis

5.3.4.1 Brain networks across groups

Resting state recordings were obtained in 12 controls and 12 children with AE. The MTPC comparison analysis returned no significant difference between the AE group and the Control group in the theta frequency (Figure 5.6). In the delta frequency, modularity and global efficiency did not significantly differ, but the mean local efficiency of the AE group was significantly lower than in the control group (Figure 5.7). All significantly different thresholds remained significant at $p < .05$ after all the p values (corrected across thresholds) of the MTPC analyses were corrected again for false discovery rate across all twelve comparison analyses. No difference in overall FC was observed across groups in either frequency bands.

Figure 5.6

Comparison of theta network measures between Autoimmune Encephalitis and Control groups

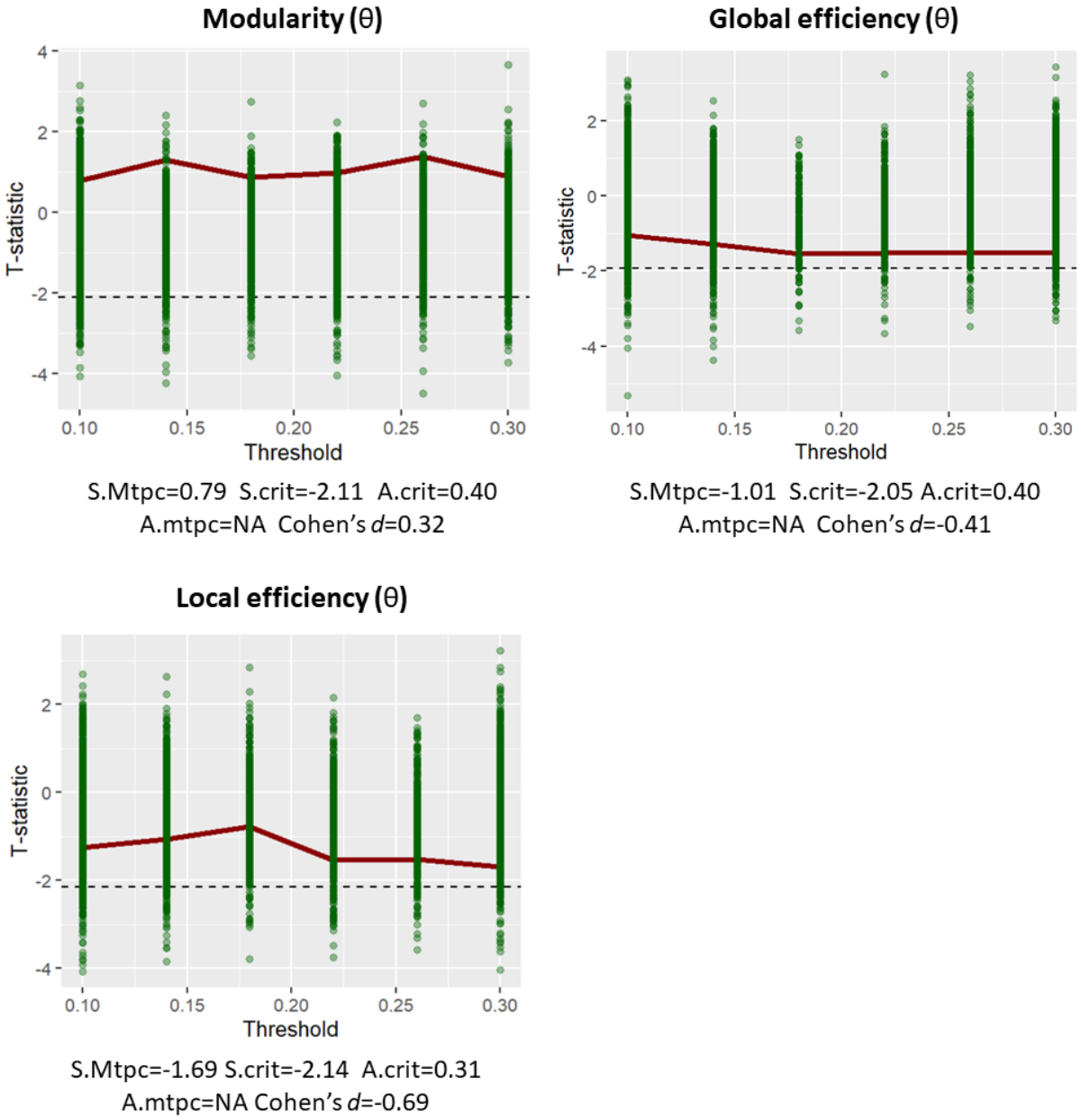

Note. S.mtpc = maximum observed statistic; S.crit = critical value of the null max. statistic; A.crit = mean of the supra-critical null AUCs; A.mtpc = AUC value of supracritical cluster.
Each graph depicts the network contrast of the AE group in reference to the Control group. The green dots are the maximum null *t* statistics of the 5000 permutations. Red dots are the observed *t* statistics. The dashed line is the critical null statistic (S.crit, top 95th percentile of the null distribution of maximum *t* statistics). The red shaded areas represent clusters of observed statistics above the critical value, whose area-under-the-curve (A.mtpc) is also greater than the mean areas-under-the-curve of the supracritical permuted statistics (A.crit). This means that a lower shaded red bar is a significantly lower network measure compared to the Control group (at $p < .05$). Non-shaded bars are non-significant. The effect size *d* is only that of the threshold with the largest difference.

Figure 5.7

Comparison of delta network measures between Autoimmune Encephalitis and Control groups

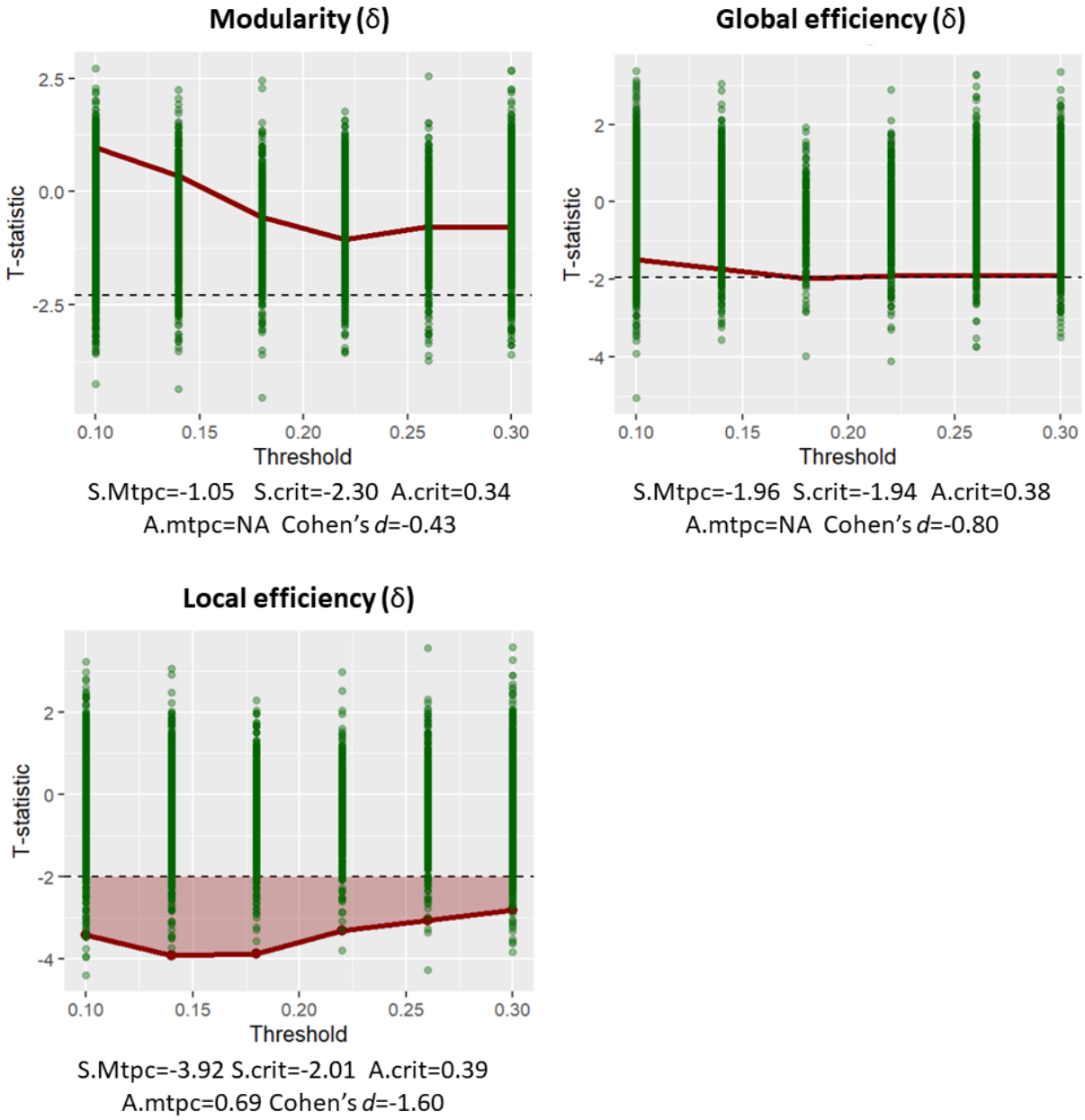

Note. S.mtpc = maximum observed statistic; S.crit = critical value of the null max. statistic; A.crit = mean of the supra-critical null AUCs; A.mtpc = AUC value of supracritical cluster.
Each graph depicts the network contrast of the AE group in reference to the Control group. The green dots are the maximum null *t* statistics of the 5000 permutations. Red dots are the observed *t* statistics. The dashed line is the critical null statistic (S.crit, top 95th percentile of the null distribution of maximum *t* statistics). The red shaded areas represent clusters of observed statistics above the critical value, whose area-under-the-curve (A.mtpc) is also greater than the mean areas-under-the-curve of the supracritical permuted statistics (A.crit). This means that a lower shaded red bar is a significantly lower network measure compared to the Control group (at $p < .05$). Non-shaded bars are non-significant. The effect size *d* is only that of the threshold with the largest difference.

Figure 5.8

Depiction of average delta networks in Autoimmune Encephalitis and Control groups

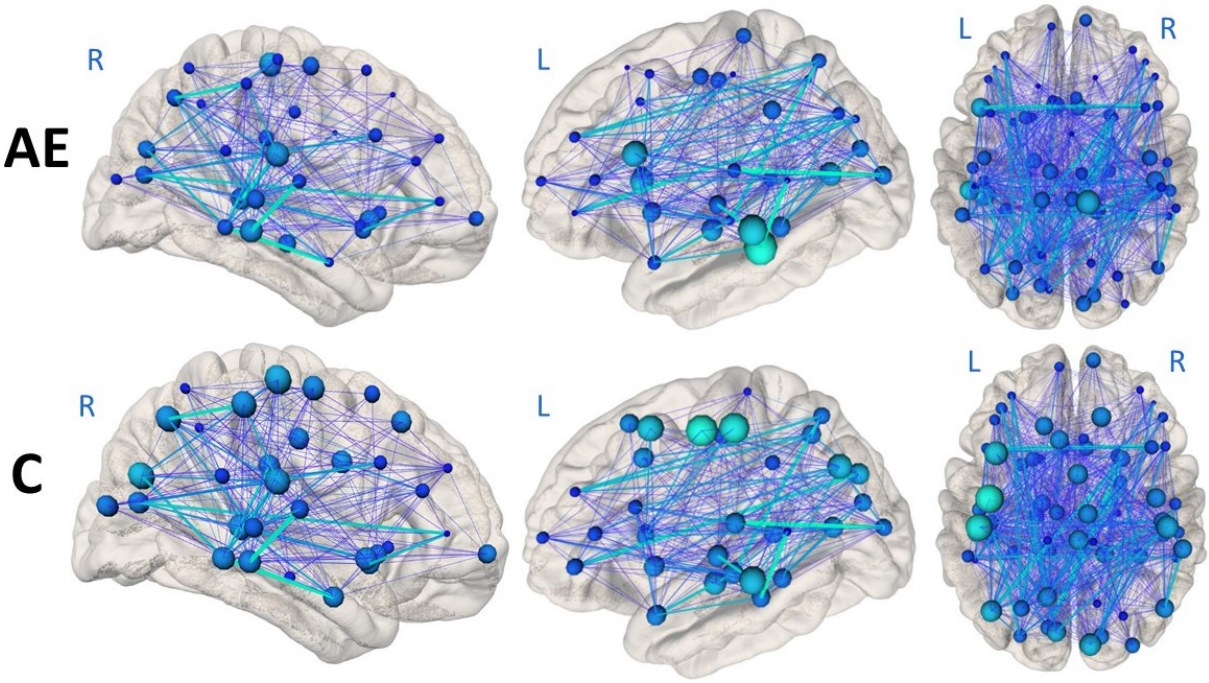

Note. AE= Autoimmune Encephalitis ; C = Controls. The figures were produced using the NeuroMArVL web app (Dwyer et al., 2017). 3D surfaces are based on the fsaverage FreeSurfer template. Node size and brightness represent the group average local efficiency per region, and edge thickness and brightness represent the group average strength of the connectivity (not relatively to the other group, on the same scale). The network was thresholded at 14%.

5.3.4.2 Multiple regression outcomes

Based on the threshold at which group difference had the lowest p-value, the following graph measures were selected for prediction of cognitive measures: theta modularity at threshold 0.1; theta global efficiency at threshold 0.3; theta local efficiency at threshold 0.3, delta modularity at threshold 0.22, delta global efficiency at threshold 0.18, delta local efficiency at threshold 0.14.

One AE case (F) was not included in the regression analyses because the neuropsychological assessments were not completed. This amounted to a group of 11 AE cases, which is underpowered for a regression analysis with two covariates (1-β = .29 for the overall model, and 1-β = .41 for the main effect coefficient, assuming a large effect size is detected according to a post-hoc estimate in G*Power, Faul et al., 2007).

No outliers were detected, and the distribution of the cognitive variables was normal. No multicollinearity between the predictors or significant dependence of error residuals was

observed in any model. Their relationship with predictors was linear except for 5 out of the 12 models. Respectively:

- Theta modularity did not have a linear relationship with PSI
- Theta global efficiency, theta local efficiency, delta global efficiency and delta local efficiency did not have a linear relationship with WMI.

This violation of linearity could not be solved using log, square root or square transformations of either dependent variables, independent variables or both. The above 5 regressions models were therefore not run.

The regression model for theta modularity did not significantly predict Working memory performance (F(df)= 3.348 (2); p = .088; adjusted R^2 = 0.320). Individual effects are depicted in Table 5.7. The effect of Modularity did not survive false discovery rate correction.

Table 5.7

Effect of theta modularity on Working Memory Performance

						Confidence interval 95%	
Predictor	**B**	**sd error**	**β**	***t* value**	***p* value**	**Lower**	**Upper**
Θ Modularity	-493.4	190.68	-.781	-2.588	.032*	-933.11	-53.69
Gender	-12.99	9.79	-.400	-1.327	.221	-35.56	9.597

Note. Working Memory was the Working Memory Index composite score from the WISC-V (Wechsler, 2014). * significant at $p < .05$ (fdr corrected = .224).

The regression model for theta global efficiency did not significantly predict Processing speed performance (F(df)= 0.085(2); p = .911; adjusted R^2 = -0.224). Individual effects are depicted in Table 5.8.

Table 5.8

Effect of theta global efficiency on Processing Speed Performance

						Confidence interval 95%	
Predictor	**B**	**sd error**	**β**	***t* value**	***p* value**	**Lower**	**Upper**
Θ E.Glob	-79.70	233.50	-0.152	-0.341	.742	-618.2	458.8
Gender	5.992	15.249	0.175	0.393	.705	-29.17	41.16

Note. E.Glob = Global efficiency. Processing speed was the Processing Speed Index composite score from the WISC-V (Wechsler, 2014).

The regression model for theta local efficiency did not significantly predict Processing speed performance (F(df)= 0.029 (2); p = .972; adjusted R^2 = -0.241). Individual effects are depicted in Table 5.9.

Table 5.9

Effect of theta local efficiency on Processing Speed Performance

						Confidence interval 95%	
Predictor	**B**	**sd error**	**β**	***t* value**	***p* value**	**Lower**	**Upper**
Θ E.Loc	12.22	176.9	0.028	0.069	.947	-395.9	420.3
Gender	2.308	13.76	0.067	0.168	.871	-29.42	34.05

Note. E.Loc = Local efficiency. Processing speed was the Processing Speed Index composite score from the WISC-V (Wechsler, 2014).

The regression model for delta modularity did not significantly predict Working memory performance (F(df)= 0.181(2); p = .837; adjusted R^2 = -0.196). Individual effects are depicted in Table 5.10.

Table 5.10

Effect of delta modularity on Working Memory Performance

						Confidence interval 95%	
Predictor	**B**	**sd error**	**B**	***t* value**	***p* value**	**Lower**	**Upper**
δ Modularity	-164.7	273.9	-0.225	-0.601	.564	-791.4	476.1
Gender	-3.090	12.17	-0.095	-0.254	.805	-31.15	24.97

Note. Working Memory was the Working Memory Index composite score from the WISC-V (Wechsler, 2014).

The regression model for delta modularity did not significantly predict Processing speed performance (F(df)= 0.049 (2); p = .952; adjusted R^2 = -0.234). Individual effects are depicted in Table 5.11.

Table 5.11

Effect of delta modularity on Processing Speed Performance

						Confidence interval 95%	
Predictor	**B**	**sd error**	**β**	***t* value**	***p* value**	**Lower**	**Upper**
δ Modularity	-62.78	293.4	-0.082	-0.214	.836	-739.3	613.7
Gender	1.690	13.03	0.049	0.130	.900	-28.36	31.74

Note. Processing speed was the Processing Speed Index composite score from the WISC-V (Wechsler, 2014). * = significant at $p < .05$.

The regression model for delta global efficiency did not significantly predict Processing speed performance (F(df)= 0.166 (2); p = .850; adjusted R^2 = -0.200). Individual effects are depicted in Table 5.12.

Table 5.12

Effect of delta global efficiency on Processing Speed Performance

						Confidence interval 95%	
Predictor	**B**	**sd error**	**B**	***t* value**	***p* value**	**Lower**	**Upper**
δ E.Glob	99.95	190.0	0.193	0.526	.613	-338.3	539.19
Gender	0.593	12.55	0.017	0.047	.963	-28.35	29.53

Note. E.Glob = Global efficiency. Processing speed was the Processing Speed Index composite score from the WISC-V (Wechsler, 2014). * = significant at $p < .05$.

The regression model for delta local efficiency did not significantly predict Processing speed performance (F(df)= 0.027 (2); p = .974; adjusted R^2 = -0.242). Individual effects are depicted in Table 5.13.

Table 5.13

Effect of delta local efficiency on Processing Speed Performance

						Confidence interval 95%	
Predictor	**B**	**sd error**	**β**	***t* value**	***p* value**	**Lower**	**Upper**
δ E.Loc	-5.172	171.6	-0.014	-0.030	.977	-400.0	390.6
Gender	3.057	15.43	0.089	0.198	.848	-32.53	38.64

Note. E.Loc = Local efficiency. Processing speed was the Processing Speed Index composite score from the WISC-V (Wechsler, 2014). * = significant at p < .05.

5.3.5 Auditory Oddball analysis

5.3.5.1 M300 amplitude and latency across groups

The auditory oddball task was completed by 11 controls and 12 children with AE. The descriptive statistics of the M300 amplitude and latency across groups are shown in Figure 5.8. There were no significant t-test differences between the groups in either M300 amplitude (t = 1.010, p = .324; Cohen's d = .422) or latency (t = 0.713, p = .484; Cohen's d = 0.298).

Figure 5.9

M300 amplitude and latency across groups

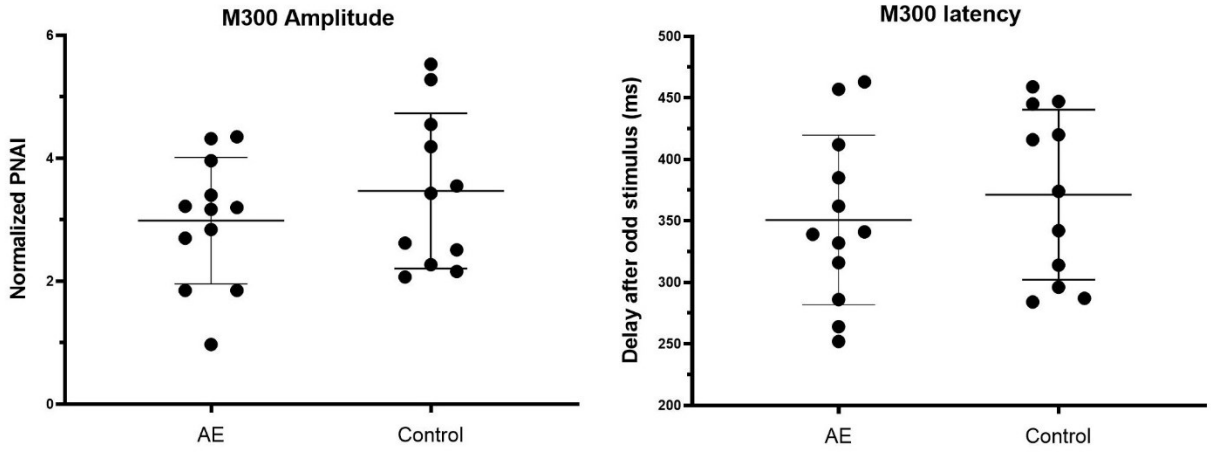

Note. AE = Autoimmune Encephalitis; PNAI = Pseudo Neural Activity Index, as per linearly constrained minimum variance beamforming parameters in Brainstorm (Tadel et al., 2021).

5.3.5.2 Multiple regression outcomes

One AE case (F, ID 6 in Appendix 5) was not included in the regression analyses because the neuropsychological assessments were not completed. This amounted to a group of 11 AE cases, which is underpowered for a regression analysis with two covariates (1-β = .29 for the overall model, and 1-β = .41 for the main effect coefficient, assuming a large effect size is detected according to a post-hoc estimate in G*Power, Faul et al., 2007).

No regression model significantly predicted cognitive outcome in the AE group. No outliers were detected, and no assumption was violated: the distribution of the cognitive variables was normal except for digit span in the AE group (Shapiro-Wilk's p = .035, but kurtosis and skewness were normal) and their relationship with predictors was linear. No multicollinearity between the predictors or dependence of error residuals was observed.

The regression model for M300 Amplitude did not significantly predict Digit span performance (F(df)= .253(2); p = .783; adjusted R^2 = -.176). Individual effects are depicted in Table 5.14.

Table 5.14

Effect of M300 Amplitude on Digit Span performance

						Confidence interval 95%	
Predictor	**B**	**sd error**	**β**	***t* value**	***p* value**	**Lower**	**Upper**
M300 Amplitude	-0.403	1.100	-.127	-.366	.724	-2.940	2.133
Gender	-1.254	2.264	-.192	-.554	.595	-6.475	3.966

Note. Digit Span performance was measured with the scale score from the WISC-V (Wechsler, 2014).

The regression model for M300 Amplitude did not significantly predict Processing Speed performance (F(df) = .262(2); p = .776; adjusted R^2 = -.173). Individual effects are depicted in Table 5.15.

Table 5.15

Effect of M300 Amplitude on Processing Speed performance

						Confidence interval 95%	
Predictor	**B**	**sd error**	**β**	***t* value**	***p* value**	**Lower**	**Upper**
M300 Amplitude	-3.929	5.745	-.236	-.684	.513	-17.177	9.319
Gender	-1.673	11.825	-.049	-.141	.891	-28.941	25.595

Note. Processing Speed performance was measured with the Processing Speed index composite score from the WISC-V (Wechsler, 2014).

The regression model for M300 Latency did not significantly predict Digit span performance (F(df) = .202(2); p = .821; adjusted R^2 = -.190). Individual effects are depicted in Table 5.16.

Table 5.16

Effect of M300 Latency on Digit Span performance

						Confidence interval 95%	
Predictor	**B**	**sd error**	**β**	***t* value**	***p* value**	**Lower**	**Upper**
M300 Latency	0.003	.017	.067	.192	.853	-0.035	0.042
Gender	-1.280	2.301	-.196	-.556	.593	-6.587	4.027

Note. Digit Span performance was measured with the scale score from the WISC-V (Wechsler, 2014).

The regression model for M300 Latency did not significantly predict Processing Speed performance (F(df) = .604(2); p = .570; adjusted R^2 = -.086). Individual effects are depicted in Table 5.17.

Table 5.17

Effect of M300 Latency on Processing Speed performance

						Confidence interval 95%	
Predictor	**B**	**sd error**	**β**	***t* value**	***p* value**	**Lower**	**Upper**
M300 Latency	-0.089	.083	-.360	-1.071	.315	-0.281	0.103
Gender	-5.178	11.495	-.151	-.450	.664	-31.685	21.329

Note. Processing Speed performance was measured with the Processing Speed index composite score from the WISC-V (Wechsler, 2014).

5.4 Discussion

This chapter aimed to use advanced neuroimaging analyses in MRI and MEG to investigate whether such complementary tools predict behavioural and cognitive outcome in paediatric AE. Considering the literature and findings from the previous chapters, three aspects of brain structure and activity were analysed in a cohort of children with AE: MRI cortical thickness, MEG resting-state theta and delta frequency network connectivity, and MEG auditory M300 evoked response. The neuroimaging measures were included in linear models to predict cognitive and behavioural outcomes of interest: outcomes which were previously associated with deficits in AE, and that have been linked with the above neuroimaging analyses in other populations. Cognitive-behavioural outcome measures included internalizing problems, attention problems, general intellectual functioning, processing speed and working memory. This is the first study to attempt such analyses in a cohort of children with AE.

5.4.1 Summary of the results

5.4.1.1 Neuropsychological outcome

With regards to cognitive outcome, a minority of children in the AE cohort had an identifiable cognitive impairment in processing speed, working memory and general intellectual functioning, which is coherent with longer-term reports in AE (Beatty et al., 2016; Mckeon et al., 2018). Impairment (Very low to Extremely low scores) makes up 8.9% of the child population according to the norm established in the WISC-V (Wechsler, 2014), while 16.7% of children in the present AE cohort fit those categories in working memory performance, 33% in processing speed performance, and 20% for the general intellectual functioning. This is higher than in some small studies in ADEM (Beatty et al., 2016; Hahn et al., 2003; Kanmaz et al., 2020) and comparable to studies in anti-NMDAR encephalitis (Mckeon et al., 2018), but may be the result of a recruitment bias. It could not be verified that the proportions of children with a lower performance were significantly higher than in the control cohort. On average, only processing speed was significantly lower in the AE cohort compared to the Control group (a trend towards significance was arguably present as well for working memory). Processing speed is one of the most common difficulties observed in anti-NMDAR encephalitis and ADEM (Beatty et al., 2016; Burton et al., 2017; Mckeon et al., 2018). This suggests children with auto-immune encephalitis may be more likely to struggle with responding rapidly to task-relevant information, even some years after onset, suggesting that these are persistent deficits.

With respect to behavioural outcomes measured in this study, on average, the group of children with AE had higher levels of internalizing problems compared to controls. Out of eight children for whom the questionnaire was completed, three had a clinically high level of internalizing problems, and two had a borderline level of problems. This highlights the presence of symptoms of depression including anxiety, feelings of sadness, guilt and fear, and behaviours of withdrawal. The score also includes somatic complaints such as headaches, tiredness, stomach problems etc. (Achenbach, 2001). This supports the findings of internalizing problems that have been commonly reported in paediatric ADEM (Burton et al., 2017) and is also present in children with anti-NMDAR encephalitis (Cainelli et al. 2019), months to years after the onset of the disease. Although attention problem scores were not significantly worse in AE on average (with a trend towards significance), two children had a clinically high level of such problems and two a borderline level, which also reinforces the idea that children with AE are specifically more vulnerable to difficulties in maintaining attention (Burton et al., 2017; Cainelli et al. 2019). This includes difficulties in finishing tasks, concentrating, a tendency to be confused or daydreaming, inattentive etc. (Achenbach, 2001). Such proportions of children with high levels of difficulties may be explained by recruitment bias and the possibility that the parents who did return questionnaires were also the most concerned about possible impairments.

However, regardless of this, it is relevant to note that the patient cohort would be said to have a "good" outcome on average (mRS score 0 to 2, Titulaer et al., 2013) when considering the Rankin scale's measure of disability, with only one child having an elevated score (cf. Appendix 5). This further confirms the points made in Chapter 1 about the limitations of conventional clinical outcome measures and the value of examining specific neuropsychological outcomes. It is also worth noting that the majority of children with AE were within the normal range in both cognitive and behavioural measures, suggesting only a small proportion of children may require long term follow-up in these specific areas.

5.4.1.2 Cortical thickness and cognitive-behavioural outcome

A number of key findings were reported and are reviewed here. Contrary to predictions, cortical thickness in the cluster covering the left superior occipital and parietal gyri did not significantly predict general intellectual functioning. Although an association was observed with general intellectual functioning in the superior parietal region in typically developing children (Manery et al. 2020), the discrepancy can be explained by the difference in cluster area, as the latter study's cluster and the present one extend to different spaces, despite both partially covering the superior parietal gyrus. It is, however, difficult to establish what the specific cluster

identified in Chapter 2 may be associated with: clusters of cortical thinning that also covered this area in the literature were variable in shape and cognitive correlates. For example, thinning in the left superior parietal gyrus correlated with lower visuospatial function in typical middle-aged adults, but not with Wechsler's block design test score (Ferreira et al., 2014). In a cohort of older adults with cerebrovascular diseases, cortical thickness in the same region was predicted by total score in the *Montreal Cognitive Assessment* and its "Attention" sub-score (Ozzoude et al., 2020). Because of the differences in populations, and the fact that the latter measure mainly concerns mild cognitive impairment (Nasreddine et al., 2005), it is not clear whether thinning in this brain area applies to cognition in paediatric AE.

Cortical thickness in the orbitofrontal cortices did not significantly predict measures of internalizing problems or attention problems. While this does not match what was found in healthy children with the same measure of attention (Ducharme et al., 2012) and internalizing problems (Whittle et al. 2020), this could be explained by the fact that children with AE simply have a different brain developmental pattern. For example, the right orbital gyrus was hypothesized to be subject to adaptive compensation in brain morphology in adult anti-NMDAR encephalitis (Wang et al., 2021). Furthermore, Whittle and colleagues (2020) focused specifically on children from lower socioeconomic populations, which has not been accounted for in the present study. Furthermore, no distinction was made between lateral and medial parts of the orbitofrontal gyri in the current study (as opposed to Ducharme et al., 2012; Whittle et al. 2020), averaging cortical thickness across the whole orbitofrontal gyrus may not be specific enough. It can also be noted that the left and right orbitofrontal cortices showed opposite patterns of association when separately predicting attention or internalizing problems, which may reflect studies highlighting how asymmetry (across both hemispheres) in orbitofrontal gray matter is associated with paediatric behavioural issues (Chen et al., 2021; Lam, Huang & Gao, 2021). Looking into how much the two bilateral areas *differ* in cortical thickness may be of relevance for behavioural prediction in future research.

5.4.1.3 Resting-state network connectivity and cognitive outcome

Resting-state network connectivity and topology were assessed within delta and theta frequency bands because of their relevance for cognition (Harmony, 2013; Karakaş, 2020) and their previously observed alterations in patients with AE (Miao et al., 2021; Symmonds et al., 2018; Vogrig et al., 2019; Yeshokumar et al., 2021). In the theta frequency, modularity, global efficiency and local efficiency were not significantly different in AE compared to controls. These measures estimate the extent to which the brain was efficient in transmitting information across the whole network while maintaining efficient and distinct local groups of brain activities. Theta

network topology may not be affected in paediatric AE, even if abnormal and decreased activity in EEG has been previously reported in this frequency band in adults (Dalmau et al., 2008; Symmonds et al., 2018). This incongruency is also reinforced by the fact that no overall functional connectivity decrease was observed in Theta, regardless of topology. Theta alterations could therefore be an adult phenomenon, although it has not been verified with MEG to date.

In the delta frequency, neither modularity nor global efficiency differed from controls, but local efficiency was significantly lower compared to controls. This suggests that while a global topology and modularity is preserved, activity in local neighbourhoods of regions does not transmit information across as efficiently as in typically developing brains on average. Decreased local efficiency confirms what has been observed in resting-state fMRI in an adult anti-NMDAR cohort (Wang et al., 2021). The reason why it was observed in delta bands specifically may be linked to the abnormalities that are commonly reported in EEG assessments: extreme delta brushes are a diagnostic criterion of anti-NMDAR encephalitis (Graus et al., 2016) and generalised rhythmic delta activity is also a common observation (Jeannin-Mayer et al., 2019), while slowing of brain activity in EEG is also reported in ADEM (McGetrick et al., 2021; Rossor et al., 2020). This suggests slow-wave delta activity may be affected in AE in the long-term and could represent a good candidate biomarker for future research.

With regards to cognitive outcome, only one graph measure returned a significant result, but did not survive correction for multiple comparisons: theta modularity significantly predicted lower working memory performance. While the failure to survive correction may be explained by lack of statistical power, such a result, if replicable in larger studies, suggests that the more brain theta activity tends to form individual and distinct modules within the network, the harder it is for children with AE to keep information in mind and manipulate it. Given working memory is one of the deficits that have been reported in AE (Beatty et al., 2016; Mckeon et al., 2018), theta modularity may be worth investigating in the future. Recent research has shown that MEG theta connectivity (diffuse and bilateral connections) was correlated negatively to lower working memory in paediatric temporal lobe epilepsy (Arski et al., 2022) which suggests theta activity, especially when increasing a distinction between neighbourhoods of regions, may interfere with working memory function in children. This may be because specific regions are involved in working memory (Constantinidis & Klingberg, 2016) and theta oscillation activates to sustain selective attention to stimuli (Karakaş, 2020): if irrelevant clusters of regions

also tend to produce theta activity, they may interfere with the relevant clusters solicited in working memory.

None of the other graph measures significantly predicted processing speed or working memory when a valid statistical model was feasible. Although adult studies did find association between fMRI connectivity in regionally defined networks with working memory and processing speed (Chen et al., 2021; Heine et al., 2018), the present approach may differ too much in many aspects (paediatric, MEG-based, global topology-based). The measures used in the present analyses focused on more global and average measures of network efficiency: none of them give an idea of the connectivity at a specific nodal level (that is, in specifically identified regions where that local efficiency could be affected). Previous fMRI studies in anti-NMDAR encephalitis observed a higher connectivity to neighbouring nodes in the right lateral orbital gyrus compared to controls (Wang et al, 2021), and lower clustering coefficient and local efficiency in the left insula (Li et al., 2021), which suggests differing local areas within a network could be identified in future studies.

5.4.1.4 Auditory M300 evoked response and cognitive outcome

Two aspects of the auditory M300 were explored (amplitude and latency) in relation to processing speed and working memory. None of the two M300 measures significantly differed in AE compared to controls, which suggests no alteration or abnormality in the signal could be identified. This does not match previous findings about P300 in adult cohorts mostly affected by viral encephalitis (Hahn et al., 2012; Kalita, Misra & Srivastava, 2009). AE may not affect the brain's odd-tone processing. Furthermore, M300 latency or amplitude measures did not predict either performance on processing speed or working memory tasks measured by this study. This is out of keeping with previous literature about the auditory P300, although focused on EEG recordings. P300 latency has been considered a marker of information processing speed (Polich, 2012), while P300 amplitude has been considered a marker of memory encoding and storage (Polich, 2012; van Dinteren et al., 2014). Furthermore, it has been statistically associated with working memory (Boucher et al., 2010; Roca et al., 2014) and processing speed (Boucher et al., 2010; Yang et al., 2013) in both children and adults. In the case of Processing Speed, it is worth noting that Boucher and colleagues (2010) found no association between P300 latency and the WISC's subtests of processing speed, but did with reaction time in the *Stewart Extended Continuous Performance Test* (which involves button-pressing when a target appears). Score in the WISC may relate more to fine motor abilities and visual scanning in children rather than "pure" processing speed (Boucher et al., 2010).

A probable explanation of these null associations is that MEG's M300 is of a different nature to EEG's P300 – despite both being an electrical brain response to odd auditory stimuli – and cannot be easily compared. M300 is far from having the established data that has been collected for decades for the P300; and it has been shown that MEG and EEG, possibly due to their different assessment of conductivity and orientation of electrical sources, produce different waveforms at sensor-level (Akimoto et al., 2014). The approach chosen in this Chapter for defining the M300 expanded common EEG approaches by localizing the signal response to a specific source (the auditory cortices). A "global" approach may be a more suitable one to assess the M300 in the future, more similar to a measure commonly done across central electrodes in EEG (van Dinteren et al., 2014). While the M300 was examined in a specific area, the P300 stems from different brain regions distributed in frontal, temporal and parietal networks, with amplitudes and latencies varying across brain regions (Polich, 2007; Riggins & Scott 2020). When studying the M300, it might thus be more relevant to look, similarly to EEG studies, at global areas rather than specific brain regions.

5.4.2 Limitations

The current study was characterised by several limitations. Given the low statistical power that could be attained in the present analyses, sample size can be considered the main limitation of the study. The present findings must be interpreted with caution and cannot be extrapolated to the population of children with AE; however they do offer compelling preliminary findings or indications for future large-scale investigations. Paediatric AE is a rare condition that makes it difficult to set up a large cohort. Furthermore, the cohort was heterogeneous in terms of subtypes of AE, and was too small to be subdivided. Future and larger studies will be needed to replicate and potentially reinforce the reliability of the present observations.

Several limitations in the analysis design are also worth noting, such as the fact that adult atlases were used for parcellation of the MRI acquired brain surfaces, because no atlas specific to the age-range of the cohort was available in FreeSurfer. The selected atlases were not standardized for children of that age range and therefore may lack accuracy. There were also manual processes, such as manual edits to correct for MRI artefacts, or manual fiducial positioning of the MEG coordinates along the MRI scans, which could not be automated with the *Neuromag* coordinate system. Manual intervention may have introduced a level of bias and to mitigate this, the guidance detailed in the FreeSurfer online resources was followed (https://surfer.nmr.mgh.harvard.edu/fswiki/FsTutorial/TroubleshootingData).

Although maxfiltering was not used on MEG resting state recordings, and no principal component analysis was used, an independent component analysis was deemed necessary to obtain a sufficiently clean data for further analysis. This involves the risk of the phase being distorted as documented in some EEG simulations (Montefusco-Siegmund, Maldonado & Devia, 2013; Thatcher et al., 2020). Because spurious changes in phase may occur, so do spurious indices of phase coherence when measuring connectivity (Montefusco-Siegmund, Maldonado & Devia, 2013). This was further demonstrated by phase distortion observed in segments that were specifically artefact-free after an ICA run on overall EEG recordings (Thatcher et al., 2020). Because the connectivity analysis of the present study relied on amplitude envelope correlation rather than phase-locking connectivity, it may be less affected by phase distortion (given the envelope is a broader measure of the signal). The extent to which such distortion impact MEG data is unknown, and if it exists, there is a risk that artificial correlations between signals appeared as a result of random distortions. Thresholding may have however minimized the likeliness of including spurious connections. Signal decomposition in paediatric MEG data still appears to be the most efficient way to address artefacts, given manual inspection and attempts to minimize motion during the recordings were not sufficient to produce clean data in the present paediatric cohorts.

A criticism may also be done for the use of the LCMV beamformer to estimate auditory sources: since the auditory stimuli were delivered in both ears during the MEG recording, it is expected that both brain hemispheres activate in reaction to their respectively connected ears. However, LCMV optimally locates signal sources when the individual signals are in small number of focal sources with uncorrelated time-series, while bilateral stimulus-locked brain responses are expected to correlate in synchrony, resulting in low signal-to-noise ratio for highly correlated responses (Kuznetsova, Nurislamova & Ossadtchi, 2021). Minimum norm imaging as opposed to beamforming (Tadel et al., 2021) might be more suited for that specific task, although there is evidence that the P300 response emerges with different latency and strength across the hemispheres (Giani et al., 2015; Polich, 2012; Uohashi et al., 2012), thus being potentially less affected by this bias. Rapaport and colleagues used LCMV successfully for a similar auditory paradigm (Rapaport et al., 2023).

Due to the novelty of the current adaptation of P300 to MEG, the approach chosen in the auditory M300 analysis lacks replicable standard approaches. Thus, the M300 was identified as the largest peak between 250 and 500 ms following earlier studies, but there are some studies which chose a wider window (250-550 ms in Uohashi et al., 2006; 300–650 in Yang et al., 2013) and others a narrower window (280-450 ms in Roca et al., 2014). There is

therefore a chance that different “peaks” would have been selected if they appeared outside the present range. Other studies chose a mean amplitude rather than a peak amplitude (Riggins & Scott, 2020), or defined amplitude as a difference between target response and prestimulus baseline (van Dinteren et al., 2014), as opposed to a difference between target response and regular response. This lack of standard makes it difficult to replicate or compare with certainty to findings relevant to neurophysiological deficits. It is also possible to investigate time-frequency based M300 response, with for example maximal theta response being specific in children (Riggins & Scott, 2020). There are therefore many ways to approach M300 and replication needs to be done in similar areas and assessment levels to establish a specific information-processing mechanism in MEG. This will be an interesting and important focus for future research where M300 is determined to be of theoretical relevance.

5.4.3 Conclusion

This study supports the idea that children with AE have ongoing residual cognitive and behavioural difficulties, with lower performance in processing speed and higher levels of internalizing and attention problems compared to typically developing children and in spite of “good” medical outcome. However, such difficulties may not reflect the specific structural and functional cerebral features investigated in the present study. However, this is the first study to investigate those features in a cohort of children with AE. While advanced neuroimaging techniques detected thinner gray matter in posterior and orbitofrontal cortices of children with AE, cortical thickness did not predict behavioural or cognitive outcome. Resting-state MEG recordings also proved able to observe lower local efficiency within delta frequency networks of children with AE: on average delta brain activity tended to make less efficient connections within neighbourhood of brain regions. That aspect did not, however, predict processing speed or working memory. Conversely, higher levels of modularity within the theta-frequency resting-state network predicted lower working memory. While the latter prediction did not survive correction for multiple comparison, the possibility of false negatives resulting from stringent corrections in a small sample is to be considered. Finally, the chosen approach in MEG to look at auditory M300 evoked responses was also not a predictor of processing speed or working memory in paediatric AE. Future studies will benefit from larger samples and reasonable selection of neuroimaging approaches will be guided by the measures investigated in the present study. The preliminary data presented gives support for advanced neuroimaging methods in children with AE as an appropriate means of investigation.

Chapter VI. General discussion

6.1 Summary of the thesis

6.1.1 Purpose of the thesis

This thesis aimed at identifying predictors of long-term outcome in children with auto-immune encephalitis. Past research has reported that months to years after onset of the disease, children can still experience a range of difficulties, affecting their attention, their memory, their executive functions, linguistic skills (Baumann et al., 2016; Cainelli et al., 2019; De Bruijn et al., 2018; Matricardi et al., 2016; McKeon et al., 2018; Tan et al., 2018), as well as their behaviour (Burton et al., 2017; Cainelli et al., 2019; Gordon-Lipkin et al., 2017; Yeshokumar et al., 2017). Optimal follow-up interventions and adapted rehabilitations for children with such difficulties require that they can be identified early on using predictive factors. Predictors are therefore needed for clinical care (Bartels et al., 2020; McKeon et al., 2018).

Such predictors may be identifiable using advanced neuroimaging methods. MRI measures of specific aspects of the brain, such as gray and white matter volumes, have pointed to long-term alterations in the development of brain structures in children with anti-NMDAR encephalitis and ADEM (Aubert-Broche et al., 2017; Bartels et al., 2020; Bartels et al., 2023). Measuring cortical thickness has also shown that alterations were statistically associated with cognition in an adult cohort with anti-NMDAR encephalitis (Xu et al., 2022), but this has not been tested in children to date. Functional neuroimaging using EEG suggests that abnormal brain activities at onset of the disease relate to the clinical outcome at later follow-up (Gillinder et al., 2019; Jeannin-Mayer et al., 2019; van Sonderen et al., 2018). Adult fMRI studies have reported altered connectivity in AE in association with cognition (Finke et al., 2013; Peer et al., 2017; Wang et al., 2021). MEG is an excellent non-invasive method of analysis of functional brain dynamics (Proudfoot et al., 2014), and has received little attention in AE research so far, despite being used to detect abnormalities in case studies (Gao et al., 2016; Miao et al., 2021).

Considering the above research, the thesis aimed at investigating for the first time whether analyses of MRI-measured cortical thickness, and of MEG-captured brain activities, could be used to predict long-term cognition and behaviour in a cohort of children with AE. The AE cohorts recruited and assessed throughout the chapters are depicted in Figure 6.1.

Figure 6.1

Cohorts of children with autoimmune encephalitis across the thesis chapters

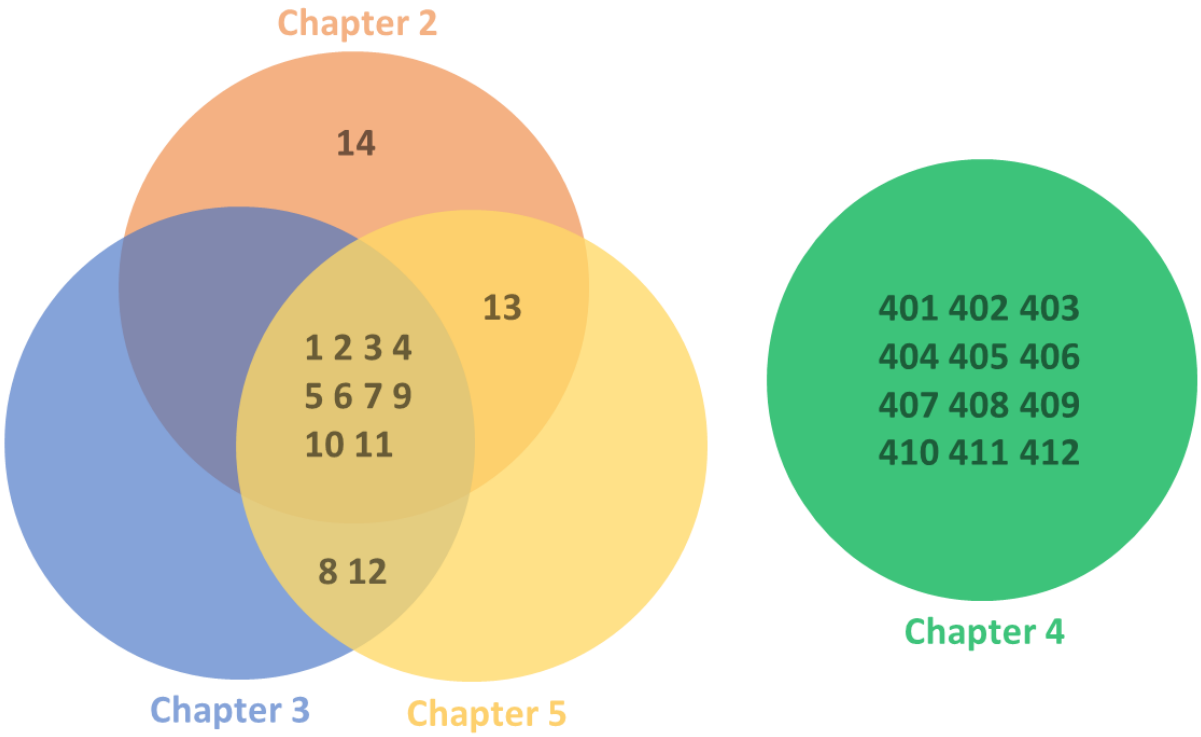

Note. Each number corresponds to a subject ID shown across appendices 2.1, 3, 4 and 5. ID 14 had an MRI scan and no neuropsychological assessment or MEG recording. ID 13 had an MRI scan and neuropsychological assessment, but no MEG. ID 8 did not have an MRI scan and the MRI scan of 12 did not pass quality check for thickness analysis. ID 401 to 412 only took part in the behavioural study.

6.1.2 Main findings

6.1.2.1 Advanced neuroimaging measures in paediatric auto-immune encephalitis

Chapter 2 focused on the analysis of gray matter cortical thickness in children with AE. Cortical thickness reflects the extent of neuropils in neural microstructure and is relevant to connectivity and functional specialization in brain regions (Wagstyl & Lerch, 2018). Thinner areas in the brain have been associated with lower cognitive performance in adult anti-NMDAR encephalitis (Xu et al., 2022), but had not been analysed in a cohort of children with AE to date. The analyses conducted in Chapter 2 have detected areas of the brain where cortices were significantly thinner on average: a cluster covering the superior parietal and occipital gyri, and the left orbitofrontal cortex. The measures were conducted on MRI scans which were acquired several years after onset, which supports the fact that AE may have a lasting impact on brain structures. This is in line with what has already been observed in longitudinal studies using

measures of brain volumes (Aubert-Broche et al., 2017; Bartels et al., 2020; Bartels et al., 2023). This supports the idea that measuring cortical thickness may be relevant to children with AE, and it remains to be established whether that impacts cognition in the long term.

6.1.2.2 Brain networks, epilepsy and auto-immune encephalitis

Chapter 3 has investigated parallel brain activity features between children with AE and children with epilepsy, considering both conditions share common symptoms including seizures and interictal epileptiform discharges (Graus et al., 2016; Titulaer et al., 2013; Vogrig et al., 2019). Using MEG recordings at rest, networks of delta and theta-band brain activity were investigated in order to determine differences between both patient groups and also in comparison to typically developing children. The analyses revealed distinct patterns between the three groups: the epilepsy group had a significantly more "efficient" theta network than the other two groups. This was defined by a shorter average length of connections needed to transmit information across brain regions (characteristic path length), and a higher tendency to form local clusters of connections (clustering coefficient, Bullmore & Sporns, 2009). Given theta features and delta path length did not differ between the AE group and controls, this suggests increase in network organization of theta brain activity is a pattern more specific to epilepsy.

In contrast, the encephalitis group had a lower network path length and clustering in delta activity compared to the epilepsy group. This implies that paediatric AE does not share similar network patterns to paediatric epilepsy in these frequency bands. As opposed to the epilepsy group, the AE group had a lower clustering coefficient in delta activity compared to the control group. This suggests brain networks affected by AE are specific and tend to form less clusters within delta frequency activations. Whether this is relevant to seizure formation could not be verified given the lack of available cases with contemporary seizures. Within the epilepsy group neither theta nor delta network measures predicted frequency of seizures. Altered clustering coefficient or characteristic path length in MEG network topology in resting-state slow-wave activity may thus not be relevant to frequency of seizures in children with epilepsy and also reflect a different pattern compared to AE.

6.1.2.3 Behavioural difficulties in paediatric auto-immune encephalitis

Chapter 4 shed light on the types of behavioural difficulties that patients with auto-immune encephalitis can experience years after onset. It appears that widespread areas of behaviour can be impacted, including problems related to conduct in daily life (children with difficulties may tend to disobey, fight, have hot temper, lie, cheat, or steal etc.), hyperactivity

(which involves restlessness, fidgeting, lack of concentration etc.), engaging in prosocial behaviours (lack of consideration for the feelings of others, sharing or helping behaviours, kindness with younger children etc.). Psychometric measures provided by the SDQ questionnaire seem to confirm earlier reports of irritable, aggressive, hyperactive or attention deficits in AE (Beatty et al., 2016; Graus et al., 2016; Tan et al., 2018), although specific difficulties in engaging in prosocial behaviours, which was the most frequent issue, lacks investigation in children. This finding supports the existence of long-term residual behavioural impairments in AE (Burton et al., 2017; Cainelli et al., 2019; Gordon-Lipkin et al., 2017; Yeshokumar et al., 2017).

Abnormally high difficulties in those areas, compared to a typical population-based cut-off, were similar in the encephalitis group compared to the disease control group which had a range of non-autoimmune brain disorders including epilepsy, genetic syndromes and learning difficulty, which means that they may not be specific to AE. Furthermore, the proportions of children with abnormal difficulties in AE appeared more frequent in the sample than earlier large-scale assessment in the general population of children in Scotland (Sosu & Schmidt, 2017). Behavioural issues, which are a particular feature at onset of the disease (Graus et al., 2016), may therefore be worsened by neurological alterations. What sorts of alterations specifically predict long-term behavioural issues remain to be identified.

6.1.2.4 Cortical thickness, brain networks and auditory evoked response in paediatric auto-immune encephalitis

Chapter 5 used MRI cortical thickness measures, MEG resting-state network analyses and MEG M300 auditory evoked responses to assess whether such measures can be used as predictors of cognitive and behavioural measures of interest in children with AE. In the cohort of children with AE, cognitive measures identified children with difficulties in general intellectual functioning, working memory and processing speed in proportions comparable to what has been found in anti-NMDAR encephalitis (Mckeon et al., 2018) and relatively higher than in some ADEM studies (Beatty et al., 2016; Hahn et al., 2003; Kanmaz et al., 2020). Similarly, a proportion of children reported high levels of internalizing problems and attention problems in a similar fashion to previous literature (Burton et al., 2017; Cainelli et al., 2019). These findings confirm that cognitive-behavioural problems may be lasting in the long-term, and are in line with Chapter 4, with regards to lasting behavioural problems in paediatric AE. They also confirm that the mRS score (which was “good”, i.e. 0-2, for the cohort except for one case) gives a

limited assessment of long-term outcome and that cognition and behaviour should also be considered.

In light of the differences observed in Chapter 2, the left posterior cluster, along the orbitofrontal cortices were selected to test whether cortical thickness in those areas predicted outcome measures which had been associated with the same brain regions in the other populations. Cortical thickness in the posterior cluster did not predict general intellectual functioning in children with AE; and cortical thickness in the orbitofrontal cortices did not predict internalizing or attention problems. Thinning in these areas of the brain may therefore not be relevant to these specific domains in paediatric AE.

Regarding resting-state MEG analyses, network measures of modularity, global efficiency and local efficiency were investigated in delta and theta frequency. Preliminary comparisons to controls showed that delta local efficiency was decreased in AE. This suggests that on average, networks within this frequency band transmit information less efficiently across neighbouring regions compared to networks in the typically developing brain. Local efficiency is related to clustering coefficient (Rubinov & Sporns, 2010), which was also reduced in Chapter 3. These findings support the idea that brain networks in AE may be affected locally, which was already suggested by fMRI network studies specifically at regional level in adult AE (Li et al., 2021; Wang et al., 2021). Nevertheless, delta local efficiency did not predict processing speed: whether such alteration in network is associated with altered cognitive functions remains to be verified in paediatric AE. While it did not differ from typically developing children, theta modularity in children with AE, which indicates the extent to which groups of brain regions within the network distinguish themselves by favouring within-group connections over between-groups connections, predicted lower performance in working memory. While the significance did not survive correction for multiple comparison, this may be considered a clue for future investigation in larger studies. A higher extent of local clustering in theta activity may affect negatively how children keep and manipulate relevant information in mind when performing an action or a task: because working memory relies on the activation of specific regions and involves theta oscillations (Constantinidis & Klingberg, 2016; Karakaş, 2020), irrelevant clusters of regions may interfere with clusters relevant to working memory if they also tend to activate. This would, however, need to be demonstrated in a MEG recording of a working memory task.

The auditory evoked responses in MEG, focusing on M300 amplitude and latency, did not differ in AE compared to the control group. None of these aspects of the M300 predicted performance in processing speed or working memory, despite past literature supporting

associations with EEG's P300, although mostly focused on adults (Boucher et al., 2010; Polich, 2012; van Dinteren et al., 2014; Roca et al., 2014; Yang et al., 2013). This suggests that auditory M300 evoked response in children, and the approach employed to measure it with MEG, could reflect a different aspect of the brain's information processing than that which was captured in adult EEG studies, despite both recording similar auditory tasks. MEG M300 may therefore not be a relevant predictor of cognitive outcome in the context of paediatric AE.

6.1.2.5 Predictors of outcome in neuroimaging analyses

Despite findings of differences in brain structures and dynamics compared to typically developing children, these differences in AE were not necessarily relevant to how these children performed in terms of cognition or behaviour. They could in theory be epiphenomenal and not be a cause or a marker of any real difficulty. However, this small data sample only gives a preliminary idea of such predictions. Furthermore, this does not mean that the measures which have not predicted cognition are not relevant to cognition at all: only a limited number of cognitive and behavioural measures were tested in the thesis. As already discussed in Chapter 1, there is a broad range of skills where long-term difficulties have been reported in paediatric AE, including phonemic verbal fluency, attention shifting, behavioural regulation, sustained attention, verbal memory (Cainelli et al., 2019; De Bruijn et al., 2018; Tan et al., 2018), which were not specifically covered in the present thesis. A similar statement can be made of neuroimaging analysis methods: for example, not every existing connectivity or network measure was investigated and there are multiple ways to examine brain networks (Bullmore & Sporns, 2009; Rubinov & Sporns, 2010). Future studies may be able to verify whether a relationship exists between such approaches and the deficits identified in children with AE, and this first preliminary study demonstrates that investigations of the sort can be successfully undertaken in paediatric AE.

6.2 Strengths and limitations

6.2.1 Main strengths of the thesis

The present thesis has several strengths. It made a unique contribution to research by using analyses of MRI cortical thickness and MEG networks and evoked responses in a cohort of children with AE for the first time. This demonstrated the feasibility of running such protocols in children and getting meaningful information about brain structures and neuronal dynamics following AE. This novel approach highlighted differences in gray matter cortical thickness and MEG networks in children with AE compared to typically developing children. Analyses also demonstrated differences in MEG network topology compared to children with epilepsy. These findings cannot be identified through conventional visual inspections of MRI scans and therefore give support to the use of advanced neuroimaging methods. Furthermore, the present results suggest AE can impact a child's brain structure and brain network activity years after the onset of the disease. The thesis also showed that clinical outcome measures focused on disability neglected cognitive-behavioural difficulties that can be found in children with a "good" outcome. Using specific cognitive and behavioural assessments, the thesis highlighted residual difficulties in children with AE. Finally, the thesis explored the predictive potential of novel neuroimaging analyses with regards to behavioural-cognitive domains, and offers preliminary insights about MEG network measures and potential markers of cognitive performance.

6.2.2 Difficulties and compromises that come with paediatric research

A common difficulty in the experiments of the thesis was the size of the MEG helmet, which was designed to work on adults and therefore bigger than average child-size heads. This leaves spare room for motion, reduced sensor coverage and reduced signal-to-noise ratio. Furthermore, because the helmet is bigger, smaller children cannot fully insert their head, or the upper side may obscure visual space and make them lean forward, which also risks losing sensor space coverage (Witton, Furlong & Seri, 2019). To compensate for that, efforts were made to add cushions to limit head movements (although they may compress with time), or to boost/elevate the seat as much as possible (Witton, Furlong & Seri, 2019). While it may reduce the accuracy of the recordings in small children, the present experiments nevertheless demonstrated that it is feasible to scan children with MEG and extract meaningful results.

Compliance is especially important in such protocols. This is why additional methods to control for artefacts such as eye movements and eye blinks using electrooculography were avoided. This allowed children not to be overwhelmed with electrodes, saved preparation time, and limited invasiveness, which can be detrimental to the children's compliance. Likewise, combining MEG and EEG may provide a more complete picture of the brain's activity, as shown in epilepsy (Hari et al., 2018), and it may give more information on auditory-evoked responses as they show different information across modalities (Hari et al., 2018). However, as pointed in the latter review, "it may be laborious to apply EEG electrodes to all subjects completing a MEG recording" (Hari et al., 2018), and it is especially true to paediatric AE. Combining MRI and MEG was already a burdensome experience for children. Combining modalities significantly increases scanning time and therefore, risks lower compliance and higher number of movements due to fatigue, thus defeating the point of getting precise data. Because of compliance, short duration of scanning sessions is a primary consideration in paediatric studies (Johnson & He, 2019). It was therefore beneficial to keep MEG short in the present study and will be in future studies.

Morphometric analysis of structural MRI scans is also sensitive to motion artefacts, such as ringing effects, which can significantly bias the estimation of cortical thickness (Reuter et al., 2015), and the cohorts of the thesis did suffer from that issue. Children from clinical populations, especially males, are prone to motion artefacts (Pardoe, Hiess, & Kuzniecky, 2016), however, the typically developing cohort in Chapter 2 was also affected by motion. Ideally, MRI scans of children that have noticeably moved would be repeated until a clean quality is reached or discarded: the latter was not a viable option because of the rarity of the cases, and repeating was not always feasible as the protocols were time consuming, especially when they included neuropsychological assessment and/or MEG recordings on the same day. While that does not guarantee an exact quality of scans across the whole sample, motion correction methods were used in the protocols for cases that had excessive motion. With children prone to moving in a MRI scan, especially for patients in a clinical context, the accuracy of the morphometric differences identified in Chapter 2 is limited. Statistical corrections were nevertheless able to identify stable cortical thickness differences, which indicates that relevant information may still be obtained from imperfect scans.

6.2.3 Interscanner variability and MRI cortical thickness

The multiplicity of scanners introduced an important bias in the estimation of cortical thickness, as MRI quality is sensitive to both scanner parameters and protocols, resulting in variable contrasts and tissue classifications (Biberacher et al., 2016). In a clinical context, scans are obtained in different sites, with different scanners and different protocols; this impacts group level measures like cortical thickness, increasing variability and decreasing statistical power (George et al., 2020). Controlling for the interscanner variability with a categorical variable limits the ability to extensively control these biases while keeping statistically meaningful results in terms of statistical power. Contrast-to-noise ratio was used in Chapter 2 as a quantitative alternative as it is a relevant factor of interscanner variability (Magnotta & Friedman, 2006; Tardif, Collins & Pike, 2009). This factor does not cover the totality of the metrics which vary across scanners, therefore future studies will ideally standardize scanner parameters and protocols.

6.2.4 Heterogeneity in MEG brain network analyses

MEG studies lack standardization, with heterogeneity in the parameters chosen to run analyses, including filtering, head modelling (Stenroos, Hunold & Haueisen, 2014), or source beamforming (Tadel et al., 2021). When it comes to the study of brain networks, the choice of connectivity metrics varies as well (Colclough et al., 2016; Liuzzi et al., 2017). Graph measures approaches come with heterogeneous aspects that are present in fMRI, including the choice of parcellation atlas or number of nodes (Hallquist & Hillary, 2018), choice of thresholding (Garrison et al., 2015; van den Heuvel et al., 2017), and choice of network measures (Rubinov & Sporns, 2010). These choices lead to different findings and make replicability difficult (Hallquist & Hillary, 2018). A review on MEG brain networks in paediatric studies pointed out that network measures suffer from lack of standard strategy with different choices of thresholds or weights in defining nodes and edges (Johnson & He, 2020). The present study selected connectivity parameters that were shown to provide more stable results (Colclough et al., 2016; Garrison et al., 2015; Liuzzi et al., 2017), which will help replication.

In graph networks, a common problem to address is the choice of thresholding for graph metrics, which consists in choosing a connectivity threshold from which connections are included in a network, as an attempt to preserve the strongest connections and discard weak and potentially spurious ones. The fact that an arbitrary choice has to be made adds to the heterogeneity of studies. Furthermore, the graph metrics resulting from these choices do not

remain stable across the thresholds (Garrison et al., 2015). Case-control studies are affected by this choice: if the groups differ in overall functional connectivity, choosing a standard threshold across groups can lead to very different numbers of connections included (with continuous threshold; Garrison et al., 2015) or risk including weaker and potentially spurious connections (with proportional threshold; van den Heuvel et al., 2017), which will both influence the graph measures that result from them. Overall functional connectivity was controlled for in Chapter 5 and helped ensure differences in graph measures were not due to variation in connectivity.

The difficulty in replicating the same choices across different research centres may be the main obstacle to overcome in order to produce robust and reliable results that could make connectivity analyses useful in a clinical context. Measures where relevant differences and associations were found in paediatric AE in the present novel findings could serve as guidance for future MEG network studies in the population.

6.2.5 Auditory M300 response and how to approach it

M300 was difficult to identify in the present sample. Although a standard range for the definition of the peak was chosen, it was sometimes not certain whether the peak selected at the individual level was the "true" peak of the M300, because other peaks often appeared beside and almost reached the criteria of selection. The main cause of this may be noise generated by the (head, eyes, limbs) movements during the scan. Six minutes may have not been enough to obtain a clear average time-locked evoked response, distinct from the baseline noise, as it involved a small number of target trials (20 odd targets for 80 regular tones). Multiplying the number of trials would give a more robust manifestation of the signal peak when averaging trials and 20 may therefore not be enough (Cohen, J., & Polich, J., 1997). In the present study, a balance was sought between duration of the paradigm and number of trials, because more trials extend the duration of the task. It thus avoided potentially making it harder for children to comply and remain still, especially those with neurological conditions. The inter-stimulus period of 2,500-3,000 ms seconds may have been much too long for the present protocol and reducing it will be beneficial. A recent study successfully multiplied target trials extensively within a span of 12 minutes using a multi-feature auditory oddball paradigm and reduced inter-stimulus interval, which may be the way forward in future studies (Rapaport et al., 2023).

Furthermore, the fact that the signal was specifically investigated in the auditory cortices at source level may only reflect a fraction of the information processing phenomenon

at stake. As mentioned in Chapter 5, previous research has often used central reference electrodes and averaged global brain signals to look at the P300 evoked response (van Dinteren et al., 2014). Looking at the M300 as a global brain response may therefore be a more reliable way to investigate auditory-oddball processing. Establishing standards for clearly identifying M300 using MEG, as in investigations of the optimal filtering of EEG's P300 (Bougrain, Saavedra & Ranta, 2012), with a focus on paediatric samples, would significantly help replicating such experiment.

A replication of the task in a larger cohort, accounting for the issues raised above, will shed light on the relevance of the MEG auditory oddball response in children with AE. Establishing a common definition of the M300 and how to measure it accurately in children, will help give it a stable meaning in a clinical context.

6.2.6 Statistical power

Another important issue of the current state of research in neuroscience is low statistical power, which reduces the likelihood that significant findings are "true" findings, as opposed to an effect of randomness (Button et al., 2013). This is a concern for the present results that were obtained from small samples and depend partly on the rarity of AE in the general population. Low power reduces the chance of discovering true effects. Small sampling and random error also run the risk of inflating effect sizes, effect sizes which may not be found in large cohorts. When calculating power a priori, the required sample size cannot be accurately estimated if it is based on effect sizes that were inflated in small studies as a reference (Button et al., 2013; Marek et al., 2022). For neuroimaging studies in AE, this means replication of small studies will be better done with larger cohorts in order to reliably confirm or infirm the truthfulness of the significant findings and their effect sizes, including the findings reported in the present thesis. This has not been accomplished with MEG and AE to date but always remains difficult given the relative rarity of the condition, and within-participant study designs (such as longitudinal designs) are recommended for small studies (Marek et al., 2022). Furthermore, increasing the sample size of the control cohort appears to only modestly increase statistical power (Aguinis & Stone-Romero, 1997).

Findings in neuroimaging are especially vulnerable to those issues. The inflation of effect size was demonstrated in a large-scale brain-wise association study in which it was shown that a large effect size (for a univariate correlation between cortical structure/function and cognitive ability/psychopathology) could be strongly inflated in one direction or another by chance with a small sample size (sampling variability); furthermore, the relation kept an amount

of inflation in thousands-large samples (Marek et al., 2022). To give a concrete example, the vibration effect in fMRI, which is also common in MEG, will have a wider impact in a small study because of the higher uncertainty, and the slightest change in sample size will make the findings fluctuate (Button et al., 2013). Preliminary findings of this thesis give an example of this fluctuation: the work-in-progress results presented at the Encephalitis Conference 2021 (Appendix 6), with an early (and therefore smaller) cohort, differed a lot from the final results (in a larger cohort) reported in Chapter 5.

The false positive rate in neuroimaging can also be inflated by the multiplicity of measures that can be computed in one analysis. This is a known problem for structural neuroimaging when a value is commonly assessed for each of tens of thousands of voxels or vertices in a single modelled brain. Different approaches exist to account for the multiple comparison problems, and the Monte Carlo Z cluster-wise simulation (Greve & Fischl, 2018) was used in Chapter 2, which reinforced the reliability of the findings. A similar problem exists when different MEG-measured values are tested for tens of atlas-parcellated regions for different frequency bands (which is an issue that was addressed in Chapter 5). Furthermore, correction for multiple comparison in small sample studies increases the rate of false negatives, especially with strict corrections such as Bonferroni, which runs the risk of focusing replication studies on inflated effects rather than true effects (Marek et al., 2022). In the current study, relatively less conservative statistical corrections were chosen to maintain statistical rigor while limiting the risk of false negatives.

6.3 Future directions

6.3.1 Expanding research in paediatric AE

Emerging neuroimaging methods provide complex information about brain development and give an opportunity for understanding how damage created by autoimmune encephalitis impacts the cognitive functions tied to brain structures and network dynamics. The wealth of possible investigations is paradoxically a weakness in the sense that it generates a large heterogeneity in the protocols, which produce variable results. MEG studies will therefore need standardized protocols to make sure results are replicated. If robust evidence is given, then MEG could be used in clinical settings. So far, the extent to which neuronal dynamics captured in MEG reflect cognitive or behavioural skills in AE is unknown and to date, it is not possible to conclude whether MEG is enough to predict concrete long-term difficulties in AE. Furthermore, the vast number of different types of brain activities in numerous brain areas that can be examined will introduce a level of randomness which must be controlled in case-control studies. Future investigations will be able to make analysis decisions based on what has or has not been found in the present study.

To improve reliability, it is important for research to be conducted in large samples (Button et al., 2013). However, it is practically difficult, if possible, to obtain large samples for the exact same protocols in AE, as it is a rare condition. A good alternative may be to refer to an age-matched norm instead of large average case-control comparisons, and instead of focusing on group trends, it may be more relevant to focus on individual children whose given age-expected measure could be compared to a normative reference. This approach has emerged with the concept of a “brain-predicted age”, patterns of neuroimaging data attributable to a typical chronological age, which could help predict individual cognitive and health trajectories, as opposed to disease-specific trends (Cole, 2018; Cole, Franke & Cherbuin, 2019). In paediatric studies, it is possible to identify children that diverge from a normative typically developing sample within an age-matched reference window, and test whether that divergence correlates with cognitive difficulties, as was done previously with executive functions in paediatric traumatic brain injury (King et al., 2020).

Quantitative measures of brain structures have been shown to diverge from age-matched norms in paediatric AE (Aubert-Broche et al., 2017; Bartels et al., 2020), which was moderately correlated with disability (Bartels et al., 2020). If a normative age-matched expectation in MEG can be established with magnetic brain activity in typical brain

development, such as evoked responses like the M300 or network connectivity, then it will be possible to test whether children outside of that norm have a predictable outcome trajectory, in specific regions and specific aspects of cognition or behaviour. MEG could thus provide individual-specific biomarkers in paediatric AE, suitable to a clinical context where patients are individually assessed and compared to a normative dataset.

6.3.2 Solving paediatric scanning issues

Limitations regarding MEG scanner and adaptation to children may require technological improvements. An obvious but costly solution to such limitations would be to acquire MEG scanners designed for children of a specific age range (Johnson & He, 2019). It is also possible to use head size as a confounding factor in group studies (Johnson & He, 2019) which nonetheless requires statistical power. Although it was not done for children, a recent study has successfully tested the improvements in reproducibility of MEG connectivity findings using foam head-casts, created with 3D printing, that would allow the head to be locked in place, improve coregistration and minimise motion (Liuzzi et al., 2017). Whether children would be compliant to such techniques remains to be verified, especially in the process of creating the head-cast, and the method may remain costly. Furthermore, it may miss the advantage of a simple MEG seat having a non-intimidating, more “child-friendly” appearance in a clinical context. This issue is likely to be fixed in the future with optically pumped magnetometers (OPM) MEG systems, which use sensor arrays flexible to head size variation (Johnson & He, 2019; Hill et al., 2020).

Lack of compliance was also discussed in Chapter 5, with a need for shorter scanning sessions, which is tied to the issues addressed above regarding the quality of the auditory oddball recording. The attempt to balance duration and the number of trials can be reconsidered in light of the fact that the scanning sessions conducted for this thesis included a resting state section and a visuomotor task (for a separate study) in addition to the auditory oddball. It may not be a problem to expand the duration of the auditory oddball per se, but rather to accumulate many tasks and make the overall session last longer. Presumably, the number of trials could be easily doubled or tripled in a paradigm that only involves auditory-oddball and nothing else, with stable compliance from a child. This will improve the quality of it at the expense of not imposing too many tasks.

6.3.3 Solving interscanner variability

Harmonization tools that calibrate image quality metrics to account for the scanner differences appear to be the way forward (Esteban et al., 2017; Garcia-Dias et al., 2020), and developing these within the paediatric population, which was not done to date, could support such analyses in the future. If the interscanner variability issues are resolved through calibration algorithms in further studies, it may then be possible to establish a reliable standard expectation across the brain development of children with AE while not being impeded by the multiplicity of sites and scanners involved. As discussed in the Chapter 2, this bias introduced by the diversity of scanners was one of the limitations of the MRI study conducted in the said chapter. Nevertheless, this diversity of MRI scanners is common to a realistic clinical setting and if a useful morphometric biomarker for clinician is to be found in AE, it will have to be robust across scanners and not limited to one selected model.

6.3.4 Functional connectivity analyses

6.3.4.1 Avoiding threshold selection in network analyses

Earlier in this chapter, the issue of the heterogeneity of MEG analyses was also raised, including the arbitrary choice of threshold for the assessment of topological networks in the brain. Emerging methods aim at avoiding the biases and instability in the thresholding of graph networks, by using permutation correction methods that identify stable network differences across thresholds ("multi-threshold permutation correction" (MTPC)). This is similar to an approach measuring differences based on the overall area-under-the curve across thresholds (AUC methods), while avoiding a dilution of effects specific to narrow ranges of thresholds (Drakesmith et al., 2015). As the algorithm functions with R-specific data structure and toolbox, it would be good to expand its implementation within the field, as in MATLAB toolboxes for example. Admittedly, choices remain to some extent: the range of the thresholds across which group difference is assessed, and the choice of permutation number (Drakesmith et al., 2015). This method remains nonetheless a great improvement as it avoids multiplying separate analyses with conservative post-hoc statistical corrections, and may get us closer to homogenous findings across studies. This is therefore a notable strength of the present MEG network analyses.

Alternatively, it was suggested that the use of the *minimum spanning tree* (MST) approach also avoided the standardization problem as it does not require thresholding (Johnson & He, 2020; Tewarie et al., 2015). Based on the Kruskal algorithm (Kruskal, 1956),

the MST orders the distance between nodes in an ascending way, constructing a "tree" starting with the shortest links until the nodes are connected in a loopless form (links are added only if no loop is created in the network Boersma et al., 2013; Johnson & He, 2020; Tewarie et al. 2015). MST produced stable results in different populations including epilepsy, strongly related to conventional graph measures, while being insensitive to arbitrary selection of thresholds (Johnson & He, 2020; Tewarie et al., 2015). Although it also comes with its variability across age and gender (Boersma et al., 2013), and does not prevent other sources of heterogeneity like choice of atlas (Tewarie et al., 2015), it may be a good contribution to more standardization in network-related research. MST will need more research to be established in MEG literature and also need more accessible tools as current algorithms including MST like *BrainWave* (http://home.kpn.nl/stam7883/brainwave.html) lack flexibility with data processed in other software.

6.3.4.2 Dynamic connectivity

An approach in the analysis of brain topological networks has been fruitful in identifying cognitive correlates in AE fMRI studies (von Schwanenflug et al., 2022a; von Schwanenflug et al., 2022b; von Schwanenflug et al., 2023). This method consists in looking at how functional networks captured in time ("brain states") change across time, how transition between brain states differ across groups, how long the brain remains in those states etc. In an adult cohort with anti-NMDAR encephalitis, differences in such brain dynamics were found compared to healthy controls, and these were correlated to mRS disease severity and unspecified negative/positive schizophrenia like symptoms (von Schwanenflug et al., 2022a). Alterations in brain-state transitions in another cohort of adults with anti-NMDAR encephalitis have also been correlated to disease severity as per the mRS score (von Schwanenflug et al., 2023). Given MEG can also compute network analysis, this same approach could be used with MEG in the future as only static connectivity was investigated in the present thesis. This data, along with the present findings, suggest that resting-state networks may effectively be relevant to AE and are worth investigating in further details.

6.4 Conclusion

Advanced analyses of MRI scans and MEG recordings are excellent tools for the investigation of subtle neural alterations in paediatric AE. While they highlight the existence of changes in the brain that are identifiable years after the onset of the disease, it still remains to be established whether such analyses can help define biomarkers for long-term deficits and difficulties in children. This thesis attempted to provide preliminary investigations and potential guidance for future research in paediatric AE: assessing functional brain networks with MEG may help estimate a child's cognitive performance in the long-term, while M300 auditory evoked response and cortical thickness may not, although more data is needed to confirm these observations. As discussed in the present chapter, there is a wealth of alternative approaches in MEG analyses that remain to be explored. Future studies will benefit from the generation of larger datasets and improved analysis techniques when trying to find statistical associations that are robust and reliable enough to translate into clinical practice. The potential is high: if the establishment of a marker using these modalities succeeds, it will be an "ideal biomarker" for paediatric care, given its non-invasiveness, cost-effectiveness and reproducibility.

References

Achenbach, T. M. (2001). Manual for ASEBA school-age forms & profiles. *University of Vermont, Research Center for Children, Youth & Families*.

Aguinis, H., & Stone-Romero, E. F. (1997). Methodological artifacts in moderated multiple regression and their effects on statistical power. *Journal of Applied Psychology*, *82*(1), 192.

Akimoto, Y., Nozawa, T., Kanno, A., Ihara, M., Goto, T., Ogawa, T., … & Kawashima, R. (2014). High-gamma activity in an attention network predicts individual differences in elderly adults' behavioral performance. *Neuroimage*, *100*, 290-300.

Anticevic, A., Gancsos, M., Murray, J. D., Repovs, G., Driesen, N. R., Ennis, D. J., … & Ramani, R. (2012). NMDA receptor function in large-scale anticorrelated neural systems with implications for cognition and schizophrenia. *Proceedings of the National Academy of Sciences*, *109*(41), 16720-16725.

Argyropoulos, G. P., Moore, L., Loane, C., Roca-Fernandez, A., Lage-Martinez, C., Gurau, O., ... & Butler, C. R. (2020). Pathologic tearfulness after limbic encephalitis: A novel disorder and its neural basis. *Neurology*, *94*(12), e1320-e1335.

Armangue, T., Olivé-Cirera, G., Martínez-Hernandez, E., Sepulveda, M., Ruiz-Garcia, R., Muñoz-Batista, M., ... & Villar-Vera, C. (2020). Associations of paediatric demyelinating and encephalitic syndromes with myelin oligodendrocyte glycoprotein antibodies: a multicentre observational study. *The Lancet Neurology*, *19*(3), 234-246.

Armangue, T., Titulaer, M. J., Málaga, I., Bataller, L., Gabilondo, I., Graus, F., ... & Anti-N-methyl-D-Aspartate, S. (2013). Paediatric anti-N-methyl-D-aspartate receptor encephalitis—clinical analysis and novel findings in a series of 20 patients. The Journal of paediatrics, 162(4), 850-856.

Arski, O. N., Martire, D. J., Young, J. M., Wong, S. M., Suresh, H., Kerr, E. N., ... & Ibrahim, G. M. (2022). Connectomic Profiles and Cognitive Trajectories After Epilepsy Surgery in Children. *Neurology*, *98*(22), e2233-e2244.

Aubert-Broche, B., Weier, K., Longoni, G., Fonov, V. S., Bar-Or, A., Marrie, R. A., ... & Banwell, B. (2017). Monophasic demyelination reduces brain growth in children. *Neurology*, *88*(18), 1744-1750.

Aydin, Ü., Pellegrino, G., Ali, O. B. K. B., Abdallah, C., Dubeau, F., Lina, J. M., ... & Grova, C. (2020). Magnetoencephalography resting state connectivity patterns as indicatives of surgical outcome in epilepsy patients. *Journal of neural engineering*, *17*(3), 035007.

Bach, L. J. (2014). Long term rehabilitation management and outcome of anti-NMDA receptor encephalitis. NeuroRehabilitation, 35(4), 863-875.

Bacchi, S., Franke, K., Wewegama, D., Needham, E., Patel, S., & Menon, D. (2018). Magnetic resonance imaging and positron emission tomography in anti-NMDA receptor encephalitis: a systematic review. *Journal of Clinical Neuroscience*, *52*, 54-59.

Ballester, M. Á. G. (1999). *Morphometric Analysis of Brain Structures in MRI* (Doctoral dissertation, University of Oxford).

Balu, R., McCracken, L., Lancaster, E., Graus, F., Dalmau, J., & Titulaer, M. J. (2019). A score that predicts 1-year functional status in patients with anti-NMDA receptor encephalitis. *Neurology*, *92*(3), e244-e252.

Banks, J. L., & Marotta, C. A. (2007). Outcomes validity and reliability of the modified Rankin scale: implications for stroke clinical trials: a literature review and synthesis. *Stroke*, *38*(3), 1091-1096.

Bartels, F., Baumgartner, B., Aigner, A., Cooper, G., Blaschek, A., Wendel, E. M., ... & Rostásy, K. (2023). Impaired Brain Growth in Myelin Oligodendrocyte Glycoprotein Antibody–Associated Acute Disseminated Encephalomyelitis. *Neurology-Neuroimmunology Neuroinflammation*, *10*(2).

Bartels, F., Krohn, S., Nikolaus, M., Johannsen, J., Wickström, R., Schimmel, M., Häusler, M., Berger, A., Breu, M., Blankenburg, M., Stoffels, J., Hendricks, O., Bernert, G., Kurlemann, G., Knierim, E., Kaindl, A., Rostásy, K. and Finke, C. (2020), Clinical and Magnetic Resonance Imaging Outcome Predictors in Pediatric Anti–N-Methyl-D-Aspartate Receptor Encephalitis. *Ann Neurol*, 88: 148-159. https://doi.org/10.1002/ana.25754

Bartels, F., Lu, A., Oertel, F. C., Finke, C., Paul, F., & Chien, C. (2021). Clinical and neuroimaging findings in MOGAD–MRI and OCT. *Clinical & Experimental Immunology*.

Bassal, F. C., Harwood, M., Oh, A., Lundberg, J. N., Hoffman, J., Cornejo, P., ... & Narayan, R. (2021). Anti-NMDA receptor encephalitis and brain atrophy in children and adults: A quantitative study. *Clinical Imaging*, *78*, 296-300.

Bataller, L., Galiano, R., Garcia-Escrig, M., Martinez, B., Sevilla, T., Blasco, R., ... & Dalmau, J. (2010). Reversible paraneoplastic limbic encephalitis associated with antibodies to the AMPA receptor. *Neurology*, *74*(3), 265-267.

Baumann, M., Hennes, E. M., Schanda, K., Karenfort, M., Kornek, B., Seidl, R., ... & Syrbe, S. (2016). Children with multiphasic disseminated encephalomyelitis and antibodies to the myelin oligodendrocyte glycoprotein (MOG): extending the spectrum of MOG antibody positive diseases. *Multiple Sclerosis Journal*, *22*(14), 1821-1829.

Baumann, M., Sahin, K., Lechner, C., Hennes, E. M., Schanda, K., Mader, S., ... & Rostásy, K. (2015). Clinical and neuroradiological differences of paediatric acute disseminating encephalomyelitis with and without antibodies to the myelin oligodendrocyte glycoprotein. *Journal of Neurology, Neurosurgery & Psychiatry*, *86*(3), 265-272.

Baumgartner, B., Bartels, F., Wendel, E., Marquard, K., Blaschek, A., Karenfort, M., ... & Leiz, S. (2019). Failure of Expected Brain Growth in Children with ADEM. *Neuropaediatrics*, *50*(S 02), GNP-PO04.

Beatty, C., Bowler, R. A., Farooq, O., Dudeck, L., Ramasamy, D., Yeh, E. A., ... & Parrish, J. B. (2016). Long-term neurocognitive, psychosocial, and magnetic resonance imaging outcomes in paediatric-onset acute disseminated encephalomyelitis. *Paediatric neurology*, *57*, 64-73.

Becker, A., Rothenberger, A., Sohn, A., & BELLA Study Group. (2015). Six years ahead: a longitudinal analysis regarding course and predictive value of the Strengths and Difficulties Questionnaire (SDQ) in children and adolescents. *European child & adolescent psychiatry*, *24*(6), 715-725.

Bergsland, N., Ramasamy, D., Tavazzi, E., Hojnacki, D., Weinstock-Guttman, B., & Zivadinov, R. (2019). Leptomeningeal contrast enhancement is related to focal cortical thinning in relapsing-remitting multiple sclerosis: A cross-sectional MRI study. *American Journal of Neuroradiology*, *40*(4), 620-625.

Bianchi, L., Sami, S., Hillebrand, A., Fawcett, I. P., Quitadamo, L. R., & Seri, S. (2010). Which physiological components are more suitable for visual ERP based brain–computer interface? A preliminary MEG/EEG study. *Brain topography*, *23*(2), 180-185.

Biberacher, V., Schmidt, P., Keshavan, A., Boucard, C. C., Righart, R., Sämann, P., ... & Mühlau, M. (2016). Intra-and interscanner variability of magnetic resonance imaging based volumetry in multiple sclerosis. *Neuroimage*, *142*, 188-197.

Blum, R. A., Tomlinson, A. R., Jetté, N., Kwon, C. S., Easton, A., & Yeshokumar, A. K. (2020). Assessment of long-term psychosocial outcomes in anti-NMDA receptor encephalitis. *Epilepsy & Behavior*, *108*, 107088.

Boersma, M., Smit, D. J., Boomsma, D. I., De Geus, E. J., Delemarre-van de Waal, H. A., & Stam, C. J. (2013). Growing trees in child brains: graph theoretical analysis of electroencephalography-derived minimum spanning tree in 5-and 7-year-old children reflects brain maturation. *Brain connectivity*, *3*(1), 50-60.

Boes, A. D., Caruso, P., Duhaime, A. C., & Fischl, B. (2016). FreeSurfer is useful for early detection of Rasmussen's encephalitis prior to obvious atrophy. *Developmental medicine and child neurology*, *58*(2), 209.

Bonilha, L., Edwards, J. C., Kinsman, S. L., Morgan, P. S., Fridriksson, J., Rorden, C., ... & Halford, J. J. (2010). Extrahippocampal gray matter loss and hippocampal deafferentation in patients with temporal lobe epilepsy. *Epilepsia*, *51*(4), 519-528.

Boucher, O., Bastien, C. H., Muckle, G., Saint-Amour, D., Jacobson, S. W., & Jacobson, J. L. (2010). Behavioural correlates of the P3b event-related potential in school-age children. *International Journal of Psychophysiology*, *76*(3), 148-157.

Bougrain, L., Saavedra, C., & Ranta, R. (2012, March). Finally, what is the best filter for P300 detection?. In *TOBI Workshop III-Tools for Brain-Computer Interaction-2012*.

Brilot, F., Dale, R. C., Selter, R. C., Grummel, V., Reddy Kalluri, S., Aslam, M., ... & Hemmer, B. (2009). Antibodies to native myelin oligodendrocyte glycoprotein in children with inflammatory demyelinating central nervous system disease. *Annals of Neurology: Official Journal of the American Neurological Association and the Child Neurology Society*, *66*(6), 833-842.

Brookes, M. J., Woolrich, M., Luckhoo, H., Price, D., Hale, J. R., Stephenson, M. C., ... & Morris, P. G. (2011). Investigating the electrophysiological basis of resting state networks using magnetoencephalography. *Proceedings of the National Academy of Sciences*, *108*(40), 16783-16788.

Brown, J. D., Wissow, L. S., Gadomski, A., Zachary, C., Bartlett, E., & Horn, I. (2006). Parent and teacher mental health ratings of children using primary-care services: interrater agreement and implications for mental health screening. *Ambulatory Pediatrics*, *6*(6), 347-351.

Bullmore, E., & Sporns, O. (2009). Complex brain networks: graph theoretical analysis of structural and functional systems. *Nature reviews neuroscience*, *10*(3), 186.

Burton, K. L., Williams, T. A., Catchpoole, S. E., & Brunsdon, R. K. (2017). Long-term neuropsychological outcomes of childhood onset acute disseminated encephalomyelitis (ADEM): a meta-analysis. *Neuropsychology review*, *27*(2), 124-133.

Button, K. S., Ioannidis, J., Mokrysz, C., Nosek, B. A., Flint, J., Robinson, E. S., & Munafò, M. R. (2013). Power failure: why small sample size undermines the reliability of neuroscience. *Nature reviews neuroscience*, *14*(5), 365-376.

Cainelli, E., Nosadini, M., Sartori, S., & Suppiej, A. (2019). Neuropsychological and psychopathological profile of anti-nmdar encephalitis: a possible pathophysiological model for paediatric neuropsychiatric disorders. Archives of Clinical Neuropsychology, 34(8), 1309-1319.

Catani, M., & Mesulam, M. (2008). What is a disconnection syndrome?. *Cortex*, *44*, 8, 911-913.

Cellucci, T., Van Mater, H., Graus, F., Muscal, E., Gallentine, W., Klein-Gitelman, M. S., ... & Dale, R. C. (2020). Clinical approach to the diagnosis of autoimmune encephalitis in the pediatric patient. *Neurology-Neuroimmunology Neuroinflammation*, *7*(2).

Chang, B. S. (2014). Paradox Lost: Exploring the Clinical-Radiologic Dissociation Seen in Anti-NMDA Receptor Encephalitis: Imaging Changes in Anti-NMDA Receptor Encephalitis. *Epilepsy Currents*, *14*(3), 127-128.

Chen, S., Guan, L., Tang, J., He, F., & Zheng, Y. (2021). Asymmetry in cortical and subcortical structures of the brain in children and adolescents with attention-deficit/hyperactivity disorder. *Neuropsychiatric Disease and Treatment*, 493-502.

Chen, Z., Zhou, J., Wu, D., Ji, C., Luo, B., & Wang, K. (2022). Altered executive control network connectivity in anti-NMDA receptor encephalitis. *Annals of Clinical and Translational Neurology*, *9*(1), 30-40.

Cheng, B., Schlemm, E., Schulz, R., Boenstrup, M., Messé, A., Hilgetag, C., ... & Thomalla, G. (2019). Altered topology of large-scale structural brain networks in chronic stroke. *Brain communications*, *1*(1), fcz020.

Ciano-Petersen, N. L., Cabezudo-García, P., Muñiz-Castrillo, S., Honnorat, J., Serrano-Castro, P. J., & Oliver-Martos, B. (2021). Current Status of Biomarkers in Anti-N-Methyl-D-Aspartate Receptor Encephalitis. *International journal of molecular sciences*, *22*(23), 13127.

Cohen, J., & Polich, J. (1997). On the number of trials needed for P300. *International Journal of Psychophysiology*, *25*(3), 249-255.

Colclough, G. L., Woolrich, M. W., Tewarie, P. K., Brookes, M. J., Quinn, A. J., & Smith, S. M. (2016). How reliable are MEG resting-state connectivity metrics?. *Neuroimage*, *138*, 284-293.

Cole, J. H. (2018). Neuroimaging studies illustrate the commonalities between ageing and brain diseases. *BioEssays*, *40*(7), 1700221.

Cole, J. H., Franke, K., & Cherbuin, N. (2019). Quantification of the biological age of the brain using neuroimaging. In *Biomarkers of human aging* (pp. 293-328). Springer, Cham.

Colmers, P. L., & Maguire, J. (2020). Network Dysfunction in Comorbid Psychiatric Illnesses and Epilepsy. *Epilepsy Currents*, *20*(4), 205-210.

Constantinidis, C., & Klingberg, T. (2016). The neuroscience of working memory capacity and training. *Nature Reviews Neuroscience*, *17*(7), 438-449.

Creten, C., van der Zwaan, S., Blankespoor, R. J., Maatkamp, A., Nicolai, J., van Os, J., & Schieveld, J. N. (2011). Late onset autism and anti-NMDA-receptor encephalitis. *The Lancet*, *378*(9785), 98.

Csardi, G., & Nepusz, T. (2006). The igraph software package for complex network research. *InterJournal, complex systems*, *1695*(5), 1-9.

Dalmau, J., Armangué, T., Planagumà, J., Radosevic, M., Mannara, F., Leypoldt, F., ... & Graus, F. (2019). An update on anti-NMDA receptor encephalitis for neurologists and psychiatrists: mechanisms and models. *The Lancet Neurology*, *18*(11), 1045-1057.

Dalmau, J., Gleichman, A. J., Hughes, E. G., Rossi, J. E., Peng, X., Lai, M., ... & Lynch, D. R. (2008). Anti-NMDA-receptor encephalitis: case series and analysis of the effects of antibodies. *The Lancet Neurology*, *7*(12), 1091-1098.

da Silva, F. L. (2013). EEG and MEG: relevance to neuroscience. *Neuron*, *80*(5), 1112-1128.

David, O., Kilner, J. M., & Friston, K. J. (2006). Mechanisms of evoked and induced responses in MEG/EEG. *Neuroimage*, *31*(4), 1580-1591.

De Bruijn, M. A., Aarsen, F. K., Van Oosterhout, M. P., Van Der Knoop, M. M., Catsman-Berrevoets, C. E., Schreurs, M. W., ... & Titulaer, M. J. (2018). Long-term neuropsychological outcome following paediatric anti-NMDAR encephalitis. *Neurology*, *90*(22), e1997-e2005.

De Bruijn, M. A., Van Sonderen, A., van Coevorden-Hameete, M. H., Bastiaansen, A. E., Schreurs, M. W., Rouhl, R. P., ... & Thijs, R. D. (2019). Evaluation of seizure treatment in anti-LGI1, anti-NMDAR, and anti-GABABR encephalitis. *Neurology*, *92*(19), e2185-e2196.

Deery, B., Anderson, V., Jacobs, R., Neale, J., & Kornberg, A. (2010). Childhood MS and ADEM: Investigation and comparison of neurocognitive features in children. Developmental neuropsychology, 35(5), 506-521.

Deiva, K., Cobo-Calvo, A., Maurey, H., De Chalus, A., Yazbeck, E., Husson, B., ... & Kidbiosep Cohort, K. (2020). Risk factors for academic difficulties in children with myelin oligodendrocyte glycoprotein antibody-associated acute demyelinating syndromes. *Developmental Medicine & Child Neurology*, *62*(9), 1075-1081.

Despotović, I., Goossens, B., & Philips, W. (2015). MRI segmentation of the human brain: challenges, methods, and applications. *Computational and mathematical methods in medicine*, *2015*.

Destrieux, C., Fischl, B., Dale, A., & Halgren, E. (2010). Automatic parcellation of human cortical gyri and sulci using standard anatomical nomenclature. *Neuroimage*, *53*(1), 1-15.

DeVries, J. M., Gebhardt, M., & Voß, S. (2017). An assessment of measurement invariance in the 3-and 5-factor models of the Strengths and Difficulties Questionnaire: New insights from a longitudinal study. *Personality and Individual Differences*, *119*, 1-6.

Dodich, A., Cerami, C., Iannaccone, S., Marcone, A., Alongi, P., Crespi, C., ... & Perani, D. (2016). Neuropsychological and FDG-PET profiles in VGKC autoimmune limbic encephalitis. *Brain and Cognition*, *108*, 81-87.

Donders, J., & Warschausky, S. (2007). Neurobehavioral outcomes after early versus late childhood traumatic brain injury. *The Journal of head trauma rehabilitation*, *22*(5), 296-302.

Donnelly, E. M., & Blum, A. S. (2007). Focal and generalized slowing, coma, and brain death. In *The Clinical Neurophysiology Primer* (pp. 127-140). Humana Press.

Douw, L., De Groot, M., Van Dellen, E., Heimans, J. J., Ronner, H. E., Stam, C. J., & Reijneveld, J. C. (2010a). 'Functional connectivity' is a sensitive predictor of epilepsy diagnosis after the first seizure. *PLoS One*, *5*(5), e10839.

Douw, L., van Dellen, E., de Groot, M., Heimans, J. J., Klein, M., Stam, C. J., & Reijneveld, J. C. (2010b). Epilepsy is related to theta band brain connectivity and network topology in brain tumor patients. *BMC neuroscience*, *11*(1), 103.

Drakesmith, M., Caeyenberghs, K., Dutt, A., Lewis, G., David, A. S., & Jones, D. K. (2015). Overcoming the effects of false positives and threshold bias in graph theoretical analyses of neuroimaging data. *Neuroimage*, *118*, 313-333.

Ducharme, S., Hudziak, J. J., Botteron, K. N., Albaugh, M. D., Nguyen, T. V., Karama, S., ... & Brain Development Cooperative Group. (2012). Decreased regional cortical thickness and thinning rate are associated with inattention symptoms in healthy children. *Journal of the American Academy of Child & Adolescent Psychiatry*, *51*(1), 18-27.

Dwyer, T., Fornito, A., Pham, T. N., Shi, M., Smith, N., Manley, J. & Klapperstueck, M. (2017). *NeuroMArVL*. https://immersive.erc.monash.edu/neuromarvl/

Englot, D. J., Hinkley, L. B., Kort, N. S., Imber, B. S., Mizuiri, D., Honma, S. M., ... & Tarapore, P. E. (2015). Global and regional functional connectivity maps of neural oscillations in focal epilepsy. *Brain*, *138*(8), 2249-2262.

Englot, D. J., Konrad, P. E., & Morgan, V. L. (2016a). Regional and global connectivity disturbances in focal epilepsy, related neurocognitive sequelae, and potential mechanistic underpinnings. *Epilepsia*, *57*(10), 1546-1557.

Englot, D. J., Nagarajan, S. S., Wang, D. D., Rolston, J. D., Mizuiri, D., Honma, S. M., ... & Kirsch, H. E. (2016b). The sensitivity and significance of lateralized interictal slow activity on magnetoencephalography in focal epilepsy. *Epilepsy research*, *121*, 21-28.

Esteban, O., Birman, D., Schaer, M., Koyejo, O. O., Poldrack, R. A., & Gorgolewski, K. J. (2017). MRIQC: Advancing the automatic prediction of image quality in MRI from unseen sites. *PloS one*, *12*(9), e0184661.

Evans, A. C., & Brain Development Cooperative Group. (2006). The NIH MRI study of normal brain development. *Neuroimage*, *30*(1), 184-202.

Ewald, R. C., & Cline, H. T. (2009). NMDA Receptors and Brain Development. In A. M. Van Dongen (Ed.), *Biology of the NMDA Receptor*. CRC Press/Taylor & Francis.

Faul, F., Erdfelder, E., Lang, A.-G., & Buchner, A. (2007). G*Power 3: A flexible statistical power analysis program for the social, behavioral, and biomedical sciences. *Behavior Research Methods*, *39*, 175-191.

Ferreira, D., Molina, Y., Machado, A., Westman, E., Wahlund, L. O., Nieto, A., ... & Barroso, J. (2014). Cognitive decline is mediated by gray matter changes during middle age. *Neurobiology of aging*, *35*(5), 1086-1094.

Fernández-Jaén, A., López-Martín, S., Albert, J., Fernández-Mayoralas, D. M., Fernández-Perrone, A. L., Tapia, D. Q., & Calleja-Pérez, B. (2014). Cortical thinning of temporal pole and orbitofrontal cortex in medication-naive children and adolescents with ADHD. Psychiatry Research: Neuroimaging, 224(1), 8-13.

Finke, C., Kopp, U. A., Prüss, H., Dalmau, J., Wandinger, K. P., & Ploner, C. J. (2012). Cognitive deficits following anti-NMDA receptor encephalitis. *J Neurol Neurosurg Psychiatry*, *83*(2), 195-198.

Finke, C., Kopp, U. A., Scheel, M., Pech, L. M., Soemmer, C., Schlichting, J., ... & Ploner, C. J. (2013). Functional and structural brain changes in anti–N-methyl-D-aspartate receptor encephalitis. *Annals of neurology*, *74*(2), 284-296.

Finke, C., Prüss, H., Heine, J., Reuter, S., Kopp, U. A., Wegner, F., ... & Deuschl, G. (2017). Evaluation of cognitive deficits and structural hippocampal damage in encephalitis with leucine-rich, glioma-inactivated 1 antibodies. *JAMA neurology*, *74*(1), 50-59.

Fischl, B. (2012). FreeSurfer. *Neuroimage*, *62*(2), 774-781.

Fischl, B., & Dale, A. M. (2000). Measuring the thickness of the human cerebral cortex from magnetic resonance images. *Proceedings of the National Academy of Sciences*, *97*(20), 11050-11055.

Fisher, R. S., Cross, J. H., D'souza, C., French, J. A., Haut, S. R., Higurashi, N., ... & Peltola, J. (2017). Instruction manual for the ILAE 2017 operational classification of seizure types. *Epilepsia*, *58*(4), 531-542.

Flanagan, E. P., Kotsenas, A. L., Britton, J. W., McKeon, A., Watson, R. E., Klein, C. J., ... & Boes, C. J. (2015). Basal ganglia T1 hyperintensity in LGI1-autoantibody faciobrachial dystonic seizures. *Neurology-Neuroimmunology Neuroinflammation*, *2*(6), e161.

Fonov, V. S., Evans, A. C., Botteron, K., Almli, C. R., McKinstry, R. C., & Collins, D. L. Group, BD C.(2011). Unbiased average age-appropriate atlases for pediatric studies. *NeuroImage*, *54*(1), 313-327.

Fonov, V. S., Evans, A. C., McKinstry, R. C., Almli, C. R., & Collins, D. L. (2009). Unbiased nonlinear average age-appropriate brain templates from birth to adulthood. *NeuroImage*, (47), S102.

Fornito, A., Zalesky, A., & Breakspear, M. (2015). The connectomics of brain disorders. *Nature Reviews Neuroscience*, *16*(3), 159-172.

Fox, M. D., Snyder, A. Z., Vincent, J. L., Corbetta, M., Van Essen, D. C., & Raichle, M. E. (2005). The human brain is intrinsically organized into dynamic, anticorrelated functional networks. *Proceedings of the National Academy of Sciences*, *102*(27), 9673-9678.

Fox J., & Weisberg S. (2019). *An R Companion to Applied Regression* (3rd ed.). Sage Publications. https://socialsciences.mcmaster.ca/jfox/Books/Companion/.

Frangou, S., Modabbernia, A., Williams, S. C., Papachristou, E., Doucet, G. E., Agartz, I., ... & Salvador, R. (2022). Cortical thickness across the lifespan: Data from 17,075 healthy individuals aged 3–90 years. *Human brain mapping*, *43*(1), 431-451.

Frauscher, B., Bartolomei, F., Kobayashi, K., Cimbalnik, J., van 't Klooster, M. A., Rampp, S., ... & Engel Jr, J. (2017). High-frequency oscillations: the state of clinical research. *Epilepsia*, *58*(8), 1316-1329.

Fridinger, S. E., & Alper, G. (2014). Defining encephalopathy in acute disseminated encephalomyelitis. *Journal of child neurology*, *29*(6), 751-755.

Galovic, M., Al-Diwani, A., Vivekananda, U., Torrealdea, F., Erlandsson, K., Fryer, T. D., ... & Koepp, M. J. (2021). In vivo NMDA receptor function in people with NMDA receptor antibody encephalitis. *medRxiv*.

Gao, L., Liu, A., Zhan, S., Wang, L., Li, L., Guan, L., ... & Wang, Y. (2016). Clinical characterization of autoimmune LGI1 antibody limbic encephalitis. *Epilepsy & Behavior*, *56*, 165-169.

Garcia-Dias, R., Scarpazza, C., Baecker, L., Vieira, S., Pinaya, W. H., Corvin, A., ... & Mechelli, A. (2020). Neuroharmony: A new tool for harmonizing volumetric MRI data from unseen scanners. *NeuroImage*, *220*.

Garrison, K. A., Scheinost, D., Finn, E. S., Shen, X., & Constable, R. T. (2015). The (in) stability of functional brain network measures across thresholds. *Neuroimage*, *118*, 651-661.

Gefferie, S. R., Maric, A., Critelli, H., Gueden, S., Kurlemann, G., Kurth, S., ... & Bölsterli, B. K. (2021). Altered EEG markers of synaptic plasticity in a human model of NMDA receptor deficiency: Anti-NMDA receptor encephalitis. *Neuroimage*, *239*, 118281.

Geis, C., Planagumà, J., Carreño, M., Graus, F., & Dalmau, J. (2019). Autoimmune seizures and epilepsy. *The Journal of clinical investigation*, *129*(3), 926-940.

George, A., Kuzniecky, R., Rusinek, H., Pardoe, H. R., & Human Epilepsy Project Investigators. (2020). Standardized brain MRI acquisition protocols improve statistical power in multicenter quantitative morphometry studies. *Journal of Neuroimaging*, *30*(1), 126-133.

Giani, A. S., Belardinelli, P., Ortiz, E., Kleiner, M., & Noppeney, U. (2015). Detecting tones in complex auditory scenes. *Neuroimage*, *122*, 203-213.

Gillinder, L., Warren, N., Hartel, G., Dionisio, S., & O'Gorman, C. (2019). EEG findings in NMDA encephalitis–a systematic review. *Seizure*, *65*, 20-24.

Giofrè, D., Allen, K., Toffalini, E., & Caviola, S. (2022). The Impasse on Gender Differences in Intelligence: a Meta-Analysis on WISC Batteries. *Educational Psychology Review*, 1-26.

Gonzalez-Toro, M. C., Jadraque-Rodríguez, R., Sempere-Pérez, Á., Martinez-Pastor, P., Jover-Cerdá, J., & Gómez-Gosálvez, F. (2013). Anti-NMDA receptor encephalitis: two paediatric cases. *Revista de neurologia*, *57*(11), 504-508.

Goodman, R., Ford, T., Corbin, T., & Meltzer, H. (2004). Using the Strengths and Difficulties Questionnaire (SDQ) multi-informant algorithm to screen looked-after children for psychiatric disorders. *European child & adolescent psychiatry*, *13*(2), ii25-ii31.

Gordon-Lipkin, E., Yeshokumar, A. K., Saylor, D., Arenivas, A., & Probasco, J. C. (2017). Comparative outcomes in children and adults with anti-N-methyl-d-aspartate (anti-NMDA) receptor encephalitis. *Journal of child neurology*, *32*(11), 930-935.

Gramfort, A., Papadopoulo, T., Olivi, E., & Clerc, M. (2010). OpenMEEG: opensource software for quasistatic bioelectromagnetics. *Biomedical engineering online*, *9*(1), 1-20.

Granerod, J., Ambrose, H. E., Davies, N. W., Clewley, J. P., Walsh, A. L., Morgan, D., ... & Ward, K. N. (2010). Causes of encephalitis and differences in their clinical presentations in England: a multicentre, population-based prospective study. *The Lancet infectious diseases*, *10*(12), 835-844.

Graus, F., Titulaer, M. J., Balu, R., Benseler, S., Bien, C. G., Cellucci, T., ... & Glaser, C. A. (2016). A clinical approach to diagnosis of autoimmune encephalitis. *The Lancet Neurology*, *15*(4), 391-404.

Greve, D. N., & Fischl, B. (2018). False positive rates in surface-based anatomical analysis. *Neuroimage*, *171*, 6-14.

Griffith, S. P., Malpas, C. B., Alpitsis, R., O'Brien, T. J., & Monif, M. (2020). The neuropsychological spectrum of anti-LGI1 antibody mediated autoimmune encephalitis. *Journal of Neuroimmunology*, 577271.

Haberlandt, E., Bast, T., Ebner, A., Holthausen, H., Kluger, G., Kravljanac, R., ... & Tuschen-Hofstätter, E. (2011). Limbic encephalitis in children and adolescents. *Archives of disease in childhood*, *96*(2), 186-191.

Hacohen, Y., & Vincent, A. (2018). Autoimmune neurological disorders-does the age matter?. *European Journal of Paediatric Neurology*, *22*(3), 341-343.

Hacohen, Y., Wright, S., Gadian, J., Vincent, A., Lim, M., Wassmer, E., & Lin, J. P. (2016). N-methyl-d-aspartate (NMDA) receptor antibodies encephalitis mimicking an autistic regression. *Developmental Medicine & Child Neurology*, *58*(10), 1092-1094.

Hacohen, Y., Wright, S., Waters, P., Agrawal, S., Carr, L., Cross, H., ... & Lim, M. J. (2013). Paediatric autoimmune encephalopathies: clinical features, laboratory investigations and outcomes in patients with or without antibodies to known central nervous system autoantigens. *Journal of Neurology, Neurosurgery & Psychiatry*, *84*(7), 748-755.

Hahn, C. D., Miles, B. S., MacGregor, D. L., Blaser, S. I., Banwell, B. L., & Hetherington, C. R. (2003). Neurocognitive outcome after acute disseminated encephalomyelitis. *Paediatric neurology*, *29*(2), 117-123.

Hahn, K., Schildmann, E. K., Baumeister, C., Seggern, I. V., & Schielke, E. (2012). Cognitive impairment after acute encephalitis: an ERP study. *International Journal of Neuroscience*, *122*(11), 630-636.

Hallquist, M. N., & Hillary, F. G. (2018). Graph theory approaches to functional network organization in brain disorders: A critique for a brave new small-world. *Network neuroscience*, *3*(1), 1-26.

Hamid, S. H., Whittam, D., Saviour, M., Alorainy, A., Mutch, K., Linaker, S., ... & Appleton, R. (2018). Seizures and encephalitis in myelin oligodendrocyte glycoprotein IgG disease vs aquaporin 4 IgG disease. *JAMA neurology*, *75*(1), 65-71.

Haneef, Z., & Chiang, S. (2014). Clinical correlates of graph theory findings in temporal lobe epilepsy. *Seizure*, *23*(10), 809-818.

Haneef, Z., Levin, H. S., & Chiang, S. (2015). Brain graph topology changes associated with anti-epileptic drug use. *Brain connectivity*, *5*(5), 284-291.

Hari, R., Baillet, S., Barnes, G., Burgess, R., Forss, N., Gross, J., ... & Nakasato, N. (2018). IFCN-endorsed practical guidelines for clinical magnetoencephalography (MEG). *Clinical Neurophysiology*, *129*(8), 1720-1747.

Harmony, T. (2013). The functional significance of delta oscillations in cognitive processing. *Frontiers in integrative neuroscience*, *7*, 83.

Heine, J., Kopp, U.A., Klag, J., Ploner, C.J., Prüss, H. and Finke, C. (2021), Long-Term Cognitive Outcome in Anti–N-Methyl-D-Aspartate Receptor Encephalitis. *Ann Neurol. 00*(1-13). https://doi.org/10.1002/ana.26241

Heine, J., Prüss, H., Bartsch, T., Ploner, C. J., Paul, F., & Finke, C. (2015). Imaging of autoimmune encephalitis–relevance for clinical practice and hippocampal function. *Neuroscience*, *309*, 68-83.

Heine, J., Prüss, H., Kopp, U. A., Wegner, F., Bergh, F. T., Münte, T., ... & Finke, C. (2018). Beyond the limbic system: disruption and functional compensation of large-scale brain networks in patients with anti-LGI1 encephalitis. *Journal of Neurology, Neurosurgery & Psychiatry*, *89*(11), 1191-1199.

Henderson, S. E., Sugden, D. A., & Barnett, A. L. (2007). *Movement assessment battery for children* (Vol. 26). London: Harcourt Assessment.

Hill, R. M., Boto, E., Rea, M., Holmes, N., Leggett, J., Coles, L. A., ... & Brookes, M. J. (2020). Multi-channel whole-head OPM-MEG: Helmet design and a comparison with a conventional system. *NeuroImage*, *219*, 116995.

Hillebrand, A., Singh, K. D., Holliday, I. E., Furlong, P. L., & Barnes, G. R. (2005). A new approach to neuroimaging with magnetoencephalography. *Human brain mapping*, *25*(2), 199-211.

Hipp, J. F., Hawellek, D. J., Corbetta, M., Siegel, M., & Engel, A. K. (2012). Large-scale cortical correlation structure of spontaneous oscillatory activity. *Nature neuroscience*, *15*(6), 884-890.

Honkaniemi, J., Dastidar, P., Kähärä, V., & Haapasalo, H. (2001). Delayed MR imaging changes in acute disseminated encephalomyelitis. *American journal of neuroradiology*, *22*(6), 1117-1124.

Horstmann, M. T., Bialonski, S., Noennig, N., Mai, H., Prusseit, J., Wellmer, J., ... & Lehnertz, K. (2010). State dependent properties of epileptic brain networks: Comparative graph–theoretical analyses of simultaneously recorded EEG and MEG. *Clinical Neurophysiology*, *121*(2), 172-185.

Hsiao, F. J., Yu, H. Y., Chen, W. T., Kwan, S. Y., Chen, C., Yen, D. J., ... & Lin, Y. Y. (2015). Increased intrinsic connectivity of the default mode network in temporal lobe epilepsy: evidence from resting-state MEG recordings. *PLoS One*, *10*(6), e0128787.

Huganir, R. L., & Nicoll, R. A. (2013). AMPARs and synaptic plasticity: the last 25 years. *Neuron*, *80*(3), 704-717.

Ibrahim, G. M., Cassel, D., Morgan, B. R., Smith, M. L., Otsubo, H., Ochi, A., ... & Doesburg, S. (2014). Resilience of developing brain networks to interictal epileptiform discharges is associated with cognitive outcome. *Brain*, *137*(10), 2690-2702.

Iizuka, T., Kaneko, J., Tominaga, N., Someko, H., Nakamura, M., Ishima, D., ... & Kanazawa, N. (2016). Association of progressive cerebellar atrophy with long-term outcome in patients with anti-N-methyl-D-aspartate receptor encephalitis. *JAMA neurology*, *73*(6), 706-713.

Irani, S. R., Michell, A. W., Lang, B., Pettingill, P., Waters, P., Johnson, M. R., ... & Somerville, E. R. (2011). Faciobrachial dystonic seizures precede Lgi1 antibody limbic encephalitis. *Annals of neurology*, *69*(5), 892-900.

Irani, S. R., Stagg, C. J., Schott, J. M., Rosenthal, C. R., Schneider, S. A., Pettingill, P., ... & Cardoso, M. J. (2013). Faciobrachial dystonic seizures: the influence of immunotherapy on seizure control and prevention of cognitive impairment in a broadening phenotype. *Brain*, *136*(10), 3151-3162.

Iype, M., Anish, T. S., Kunju, P. M., Saradakutty, G., Sreedharan, M., & Ahamed, S. M. (2018). Factors Related to Long Term Motor, Behavioral, and Scholastic Outcome in Children with Acute Disseminated Encephalomyelitis. *Pediatric neurology*, *89*, 49-57.

Jacobs, R. K., Anderson, V. A., Neale, J. L., Shield, L. K., & Kornberg, A. J. (2004). Neuropsychological outcome after acute disseminated encephalomyelitis: impact of age at illness onset. *Paediatric neurology*, *31*(3), 191-197.

Jeannin-Mayer, S., André-Obadia, N., Rosenberg, S., Boutet, C., Honnorat, J., Antoine, J. C., & Mazzola, L. (2019). EEG analysis in anti-NMDA receptor encephalitis: Description of typical patterns. *Clinical Neurophysiology*, *130*(2), 289-296.

Johnson, B. W., & He, W. (2019). MEG studies on the connectivity of brain networks in children. *Magnetoencephalography: From signals to dynamic cortical networks*, 733-756.

Kalita, J., Misra, U. K., & Srivastava, A. (2009). Cognitive impairment in encephalitis: P3 and MRI correlation. *Electromyography and clinical neurophysiology*, *49*(1), 27-33.

Kalnins, A. (2018). Multicollinearity: How common factors cause Type 1 errors in multivariate regression. *Strategic Management Journal*, *39*(8), 2362-2385.

Kalnins, A. (2022). When does multicollinearity bias coefficients and cause type 1 errors? A reconciliation of Lindner, Puck, and Verbeke (2020) with Kalnins (2018). *Journal of International Business Studies*, *53*(7), 1536-1548.

Kanmaz, S., Köse, S., Eraslan, C., Şimşek, E., Serin, H. M., Yılmaz, S., ... & Gökben, S. (2020). Neuropsychological outcome in cases with acute disseminated encephalomyelitis. *Turkish Journal of Pediatrics*, *62*(4).

Karakaş, S. (2020). A review of theta oscillation and its functional correlates. *International Journal of Psychophysiology*, *157*, 82-99.

Kataoka, H., Furiya, Y., & Ueno, S. (2008). Limbic encephalitis with involvement of prefrontal cortices and persistent amnesia. *The neurologist*, *14*(4), 255-257.

Khan, H., Sami, M. B., & Litvak, V. (2021). The utility of Magnetoencephalography in multiple sclerosis-A systematic review. *NeuroImage: Clinical*, 102814.

Kheirkhah, M., Baumbach, P., Leistritz, L., Witte, O. W., Walter, M., Gilbert, J. R., ... & Klingner, C. M. (2021). The Right Hemisphere Is Responsible for the Greatest Differences in Human Brain Response to High-Arousing Emotional versus Neutral Stimuli: A MEG Study. *Brain sciences*, *11*(8), 960.

King, D. J., Ellis, K. R., Seri, S., & Wood, A. G. (2019). A systematic review of cross-sectional differences and longitudinal changes to the morphometry of the brain following paediatric traumatic brain injury. *NeuroImage: Clinical*, *23*, 101844.

King, D. J., Seri, S., Beare, R., Catroppa, C., Anderson, V. A., & Wood, A. G. (2020). Developmental divergence of structural brain networks as an indicator of future cognitive impairments in childhood brain injury: Executive functions. *Developmental cognitive neuroscience*, *42*, 100762.

Klapwijk, E. T., Van De Kamp, F., Van Der Meulen, M., Peters, S., & Wierenga, L. M. (2019). Qoala-T: A supervised-learning tool for quality control of FreeSurfer segmented MRI data. *Neuroimage*, *189*, 116-129.

Koerte, I. K., Hufschmidt, J., Muehlmann, M., Lin, A. P., & Shenton, M. E. (2016). Advanced neuroimaging of mild traumatic brain injury. In *Translational research in traumatic brain injury*. CRC Press/Taylor and Francis Group.

Kornbluh, A. B., Bradstreet, L. E., Hutchinson, M. L., & Wilson, C. S. (2020). Serial neuropsychological testing in MOG antibody-associated disease to improve understanding of outcomes. *Multiple Sclerosis and Related Disorders*, *44*, 102316.

Kruskal, J. B. (1956). On the shortest spanning subtree of a graph and the traveling salesman problem. *Proceedings of the American Mathematical society*, *7*(1), 48-50.

Kühn, S., Schubert, F., & Gallinat, J. (2010). Reduced thickness of medial orbitofrontal cortex in smokers. *Biological psychiatry*, *68*(11), 1061-1065.

Kuni, B. J., Banwell, B. L., & Till, C. (2012). Cognitive and behavioral outcomes in individuals with a history of acute disseminated encephalomyelitis (ADEM). *Developmental neuropsychology*, *37*(8), 682-696.

Kurtzke, J. F. (1983). Rating neurologic impairment in multiple sclerosis: an expanded disability status scale (EDSS). *Neurology*, *33*(11), 1444-1444.

Kuznetsova, A., Nurislamova, Y., & Ossadtchi, A. (2021). Modified covariance beamformer for solving MEG inverse problem in the environment with correlated sources. *Neuroimage*, *228*, 117677.

Kybic, J., Clerc, M., Faugeras, O., Keriven, R., & Papadopoulo, T. (2006). Generalized head models for MEG/EEG: boundary element method beyond nested volumes. *Physics in Medicine & Biology*, *51*(5), 1333.

Lakhan, S. E. (2012). Teaching neuroimages: MRI time lag with acute disseminated encephalomyelitis. *Neurology*, *78*(22), e138-e139.

Lam, B. Y. H., Huang, Y., & Gao, Y. (2021). Gray matter asymmetry in the orbitofrontal cortex in relation to psychopathic traits in adolescents. *Journal of psychiatric research*, *132*, 84-96.

Lau, C. G., & Zukin, R. S. (2007). NMDA receptor trafficking in synaptic plasticity and neuropsychiatric disorders. *Nature Reviews Neuroscience*, *8*(6), 413.

Laurikainen, H., Isotupa, I., Nyman, M., Ilonen, T., Nummelin, T., Salokangas, R. K., & Hietala, J. (2019). Longitudinal brain morphology in anti-NMDA receptor encephalitis: a case report with controls. *BMC psychiatry*, *19*(1), 1-6.

Lee, C., Im, C. H., Koo, Y. S., Lim, J. A., Kim, T. J., Byun, J. I., ... & Jung, K. H. (2017). Altered network characteristics of spike-wave discharges in juvenile myoclonic epilepsy. *Clinical EEG and Neuroscience*, *48*(2), 111-117.

Lemon, J., Cooper, J., Defres, S., Easton, A., Sadarangani, M., Griffiths, M. J., ... & Kneen, R. (2019). Understanding parental perspectives on outcomes following paediatric encephalitis: A qualitative study. *PloS one*, *14*(9), e0220042.

Leypoldt, F., Armangue, T., & Dalmau, J. (2015). Autoimmune encephalopathies. *Annals of the New York Academy of Sciences*, *1338*(1), 94-114.

Li, C., Pang, X., Shi, K., Long, Q., Liu, J., & Zheng, J. (2021). The Insula Is a Hub for Functional Brain Network in Patients With Anti-N-Methyl-D-Aspartate Receptor Encephalitis. *Frontiers in neuroscience*, *15*, 143.

Li Hegner, Y. L., Marquetand, J., Elshahabi, A., Klamer, S., Lerche, H., Braun, C., & Focke, N. K. (2018). Increased functional MEG connectivity as a hallmark of MRI-negative focal and generalized epilepsy. *Brain topography*, *31*(5), 863-874.

Liuzzi, L., Gascoyne, L. E., Tewarie, P. K., Barratt, E. L., Boto, E., & Brookes, M. J. (2017). Optimising experimental design for MEG resting state functional connectivity measurement. *Neuroimage*, *155*, 565-576.

Loane, C., Argyropoulos, G. P., Roca-Fernández, A., Lage, C., Sheerin, F., Ahmed, S., ... & Butler, C. R. (2019). Hippocampal network abnormalities explain amnesia after VGKCC-Ab related autoimmune limbic encephalitis. *Journal of Neurology, Neurosurgery & Psychiatry*, *90*(9), 965-974.

López-Chiriboga, A. S., Klein, C., Zekeridou, A., McKeon, A., Dubey, D., Flanagan, E. P., ... & Gadoth, A. (2018). LGI1 and CASPR2 neurological autoimmunity in children. *Annals of neurology*, *84*(3), 473-480.

Lori, S., Portaccio, E., Zipoli, V., Giannini, M., Scarpelli, S., Goretti, B., & Amato, M. P. (2011). Cognitive impairment and event-related potentials in paediatric multiple sclerosis: 2-year study. *Neurological Sciences*, *32*(6), 1043-1046.

Macher, S., Zimprich, F., DeSimoni, D., Höftberger, R., & Rommer, P. S. (2018). Management of autoimmune encephalitis: an observational monocentric study of 35 patients. *Frontiers in immunology*, *9*, 2708.

Magara, S., Komatsubara, T., Hojo, M., Kobayashi, Y., Yoshino, M., Saitoh, A., & Tohyama, J. (2019). The association of epileptic focus estimated by magnetoencephalography with cognitive function in non-lesional epilepsy with continuous spikes and waves during slow wave sleep (ECSWS) children. *Brain and Development*, *41*(2), 163-172.

Magnotta, V. A., & Friedman, L. (2006). Measurement of signal-to-noise and contrast-to-noise in the fBIRN multicenter imaging study. *Journal of digital imaging*, *19*(2), 140-147.

Malinowska, U., Badier, J. M., Gavaret, M., Bartolomei, F., Chauvel, P., & Bénar, C. G. (2014). Interictal networks in magnetoencephalography. *Human brain mapping*, *35*(6), 2789-2805.

Mamashli, F., Khan, S., Bharadwaj, H., Michmizos, K., Ganesan, S., Garel, K. L. A., ... & Kenet, T. (2017). Auditory processing in noise is associated with complex patterns of disrupted functional connectivity in autism spectrum disorder. *Autism Research*, *10*(4), 631-647.

Marek, S., Tervo-Clemmens, B., Calabro, F. J., Montez, D. F., Kay, B. P., Hatoum, A. S., ... & Dosenbach, N. U. (2022). Reproducible brain-wide association studies require thousands of individuals. *Nature*, 1-7.

Masten, A. S., Roisman, G. I., Long, J. D., Burt, K. B., Obradović, J., Riley, J. R., ... & Tellegen, A. (2005). Developmental cascades: linking academic achievement and externalizing and internalizing symptoms over 20 years. *Developmental psychology*, *41*(5), 733.

Matlab. (2017). 9.2.0.538062 (R2017a). Natick, Massachusetts: The MathWorks Inc.

Matricardi, S., Patrini, M., Freri, E., Ragona, F., Zibordi, F., Andreetta, F., ... & Granata, T. (2016). Cognitive and neuropsychological evolution in children with anti-NMDAR encephalitis. *Journal of neurology*, *263*(4), 765-771.

Matsuzaki, J., Kagitani-Shimono, K., Sugata, H., Hanaie, R., Nagatani, F., Yamamoto, T., ... & Taniike, M. (2017). Delayed mismatch field latencies in autism spectrum disorder with abnormal auditory sensitivity: a magnetoencephalographic study. *Frontiers in Human Neuroscience*, *11*, 446.

Mayers, A. (2013). *Introduction to statistics and SPSS in psychology*. Edinburgh Gate, Harlow: Pearson Education Limited.

Mayer, A. R., Hanlon, F. M., & Ling, J. M. (2015). Gray matter abnormalities in pediatric mild traumatic brain injury. *Journal of Neurotrauma*, *32*(10), 723-730.

McGetrick, M. E., Varughese, N. A., Miles, D. K., Wang, C. X., McCreary, M., Monson, N. L., & Greenberg, B. M. (2021). Clinical features, treatment strategies, and outcomes in hospitalized children with immune-mediated encephalopathies. *Pediatric Neurology*, *116*, 20-26.

McKeon, G. L., Robinson, G. A., Ryan, A. E., Blum, S., Gillis, D., Finke, C., & Scott, J. G. (2018). Cognitive outcomes following anti-N-methyl-D-aspartate receptor encephalitis: a systematic review. *Journal of clinical and experimental neuropsychology*, *40*(3), 234-252.

McKeon, G. L., Scott, J. G., Spooner, D. M., Ryan, A. E., Blum, S., Gillis, D., ... & Robinson, G. A. (2016). Cognitive and social functioning deficits after anti-N-methyl-D-aspartate receptor encephalitis: an exploratory case series. *Journal of the International Neuropsychological Society: JINS*, *22*(8), 828-838.

McRobbie, D. W., Moore, E. A., Graves, M. J., & Prince, M. R. (2006). *MRI from protons to pictures*. Cambridge University Press.

Menary, K., Collins, P. F., Porter, J. N., Muetzel, R., Olson, E. A., Kumar, V., ... & Luciana, M. (2013). Associations between cortical thickness and general intelligence in children, adolescents and young adults. *Intelligence*, *41*(5), 597-606.

Miao, A., Shi, Y., Xiang, J., Wang, X., Ge, J., Chen, Q., ... & Wu, D. (2021). Using EEG and MEG to characterize extreme delta brush in a patient with anti-NMDA receptor encephalitis. *BMC neurology*, *21*(1), 1-5.

Miller, T. D., Chong, T. T. J., Aimola Davies, A. M., Ng, T. W., Johnson, M. R., Irani, S. R., ... & Kennard, C. (2017). Focal CA3 hippocampal subfield atrophy following LGI1 VGKC-complex antibody limbic encephalitis. *Brain*, *140*(5), 1212-1219.

Miller, T. D., Chong, T. T., Davies, A. M. A., Johnson, M. R., Irani, S. R., Husain, M., ... & Gowland, P. A. (2020). Human hippocampal CA3 damage disrupts both recent and remote episodic memories. *eLife*, *9*, e41836.

Montefusco-Siegmund, R., Maldonado, P. E., & Devia, C. (2013, November). *Effects of ocular artifact removal through ICA decomposition on EEG phase* [Conference presentation]. 2016th International IEEE/EMBS Conference on Neural Engineering (NER), San Diego, CA, United States. doi: 10.1109/NER.2013.6696198.

Moscato, E. H., Jain, A., Peng, X., Hughes, E. G., Dalmau, J., & Balice-Gordon, R. J. (2010). Mechanisms underlying autoimmune synaptic encephalitis leading to disorders of memory, behavior and cognition: insights from molecular, cellular and synaptic studies. *European Journal of Neuroscience*, *32*(2), 298-309.

Moscato, E. H., Peng, X., Jain, A., Parsons, T. D., Dalmau, J., & Balice-Gordon, R. J. (2014). Acute mechanisms underlying antibody effects in anti–N-methyl-D-aspartate receptor encephalitis. *Annals of neurology*, *76*(1), 108-119.

Mrabet, S., Achour, N. B., Kraoua, I., Benrhouma, H., Klaa, H., Rouissi, A., ... & Turki, I. B. Y. (2015). Anti-Ma2-encephalitis in a 2 year-old child: a newly diagnosed case and literature review. *European journal of paediatric neurology*, *19*(6), 737-742.

MRC Cognition and Brain Sciences Unit (8 March 2013). *Maxfilter Diagnostics*. MRC CBU Wiki, retrieved from https://imaging.mrc-cbu.cam.ac.uk/meg/maxdiagnost

Murray, B. J., Apetauerova, D., & Scammell, T. E. (2000). Severe acute disseminated encephalomyelitis with normal MRI at presentation. *Neurology*, *55*(8), 1237-1238.

Nahum, L., Ptak, R., Leemann, B., Lalive, P., & Schnider, A. (2010). Behaviorally spontaneous confabulation in limbic encephalitis: the roles of reality filtering and strategic monitoring. *Journal of the International Neuropsychological Society*, *16*(6), 995-1005.

Nakamura, B. J., Ebesutani, C., Bernstein, A., & Chorpita, B. F. (2009). A psychometric analysis of the child behavior checklist DSM-oriented scales. *Journal of Psychopathology and Behavioral Assessment*, *31*(3), 178-189.

Nasreddine, Z. S., Phillips, N. A., Bédirian, V., Charbonneau, S., Whitehead, V., Collin, I., ... & Chertkow, H. (2005). The Montreal Cognitive Assessment, MoCA: a brief screening tool for mild cognitive impairment. *Journal of the American Geriatrics Society*, *53*(4), 695-699.

Nauta, I. M., Kulik, S. D., Breedt, L. C., Eijlers, A. J., Strijbis, E. M., Bertens, D., ... & Schoonheim, M. M. (2021). Functional brain network organization measured with magnetoencephalography predicts cognitive decline in multiple sclerosis. *Multiple Sclerosis Journal*, *27*(11), 1727-1737.

Navarro, V., Kas, A., Apartis, E., Chami, L., Rogemond, V., Levy, P., ... & Honnorat, J. (2016). Motor cortex and hippocampus are the two main cortical targets in LGI1-antibody encephalitis. *Brain*, *139*(4), 1079-1093.

Nillo, R. M., Broce, I. J., Uzgil, B., Singhal, N. S., Glastonbury, C. M., Hess, C. P., Barkovich, J. A., Desikan, R. S., & Sugrue, L. P. (2021). Longitudinal analysis of regional brain changes in anti-NMDAR encephalitis: a case report. *BMC neurology*, *21*(1), 412. https://doi.org/10.1186/s12883-021-02446-8

Nygaard, G. O., Walhovd, K. B., Sowa, P., Chepkoech, J. L., Bjørnerud, A., Due-Tønnessen, P., ... & Harbo, H. F. (2015). Cortical thickness and surface area relate to specific symptoms in early relapsing–remitting multiple sclerosis. *Multiple Sclerosis Journal*, *21*(4), 402-414.

Obaid, S., Tucholka, A., Ghaziri, J., Jodoin, P. M., Morency, F., Descoteaux, M., ... & Nguyen, D. K. (2018). Cortical thickness analysis in operculo-insular epilepsy. *NeuroImage: Clinical*, *19*, 727-733.

Ogawa, R., Nakashima, I., Takahashi, T., Kaneko, K., Akaishi, T., Takai, Y., ... & Aoki, M. (2017). MOG antibody–positive, benign, unilateral, cerebral cortical encephalitis with epilepsy. *Neurology-Neuroimmunology Neuroinflammation*, *4*(2), e322.

Onugoren, M. D., Deuretzbacher, D., Haensch, C. A., Hagedorn, H. J., Halve, S., Isenmann, S., ... & Presslauer, S. (2015). Limbic encephalitis due to GABAB and AMPA receptor antibodies: a case series. *J Neurol Neurosurg Psychiatry*, *86*(9), 965-972.

Oostenveld, R., Fries, P., Maris, E., & Schoffelen, J. M. (2011). FieldTrip: open source software for advanced analysis of MEG, EEG, and invasive electrophysiological data. *Computational intelligence and neuroscience*, *2011*, 1-9.

Oswald, V., Zerouali, Y., Boulet-Craig, A., Krajinovic, M., Laverdiere, C., Sinnett, D., ... & Robaey, P. (2017). Spontaneous brain oscillations as neural fingerprints of working memory capacities: A resting-state MEG study. *Cortex*, *97*, 109-124.

Ozzoude, M., Ramirez, J., Raamana, P. R., Holmes, M. F., Walker, K., Scott, C. J., ... & Black, S. E. (2020). Cortical thickness estimation in individuals with cerebral small vessel disease, focal atrophy, and chronic stroke lesions. *Frontiers in Neuroscience*, *14*, 598868.

Paldino, M. J., Chu, Z. D., Chapieski, M. L., Golriz, F., & Zhang, W. (2017). Repeatability of graph theoretical metrics derived from resting-state functional networks in paediatric epilepsy patients. *The British journal of radiology*, *90*(1074), 20160656.

Pandolfi, V., Magyar, C. I., & Norris, M. (2014). Validity study of the CBCL 6–18 for the assessment of emotional problems in youth with ASD. *Journal of Mental Health Research in Intellectual Disabilities*, *7*(4), 306-322.

Paolilo, R. B., Deiva, K., Neuteboom, R., Rostásy, K., & Lim, M. (2020). Acute disseminated encephalomyelitis: current perspectives. *Children*, *7*(11), 210.

Pardoe, H. R., Abbott, D. F., Jackson, G. D., & Alzheimer's Disease Neuroimaging Initiative. (2013). Sample size estimates for well-powered cross-sectional cortical thickness studies. *Human brain mapping*, *34*(11), 3000-3009.

Pardoe, H. R., Hiess, R. K., & Kuzniecky, R. (2016). Motion and morphometry in clinical and nonclinical populations. *Neuroimage*, *135*, 177-185.

Peer, M., Prüss, H., Ben-Dayan, I., Paul, F., Arzy, S., & Finke, C. (2017). Functional connectivity of large-scale brain networks in patients with anti-NMDA receptor encephalitis: an observational study. *The Lancet Psychiatry*, *4*(10), 768-774.

Petit-Pedrol, M., Armangue, T., Peng, X., Bataller, L., Cellucci, T., Davis, R., ... & Ritacco, D. G. (2014). Encephalitis with refractory seizures, status epilepticus, and antibodies to the GABAA receptor: a case series, characterisation of the antigen, and analysis of the effects of antibodies. *The Lancet Neurology*, *13*(3), 276-286.

Phillips, O. R., Joshi, S. H., Narr, K. L., Shattuck, D. W., Singh, M., Di Paola, M., ... & Finke, C. (2018). Superficial white matter damage in anti-NMDA receptor encephalitis. *J Neurol Neurosurg Psychiatry*, *89*(5), 518-525.

Pohl, D., Alper, G., Van Haren, K., Kornberg, A. J., Lucchinetti, C. F., Tenembaum, S., & Belman, A. L. (2016). Acute disseminated encephalomyelitis: updates on an inflammatory CNS syndrome. *Neurology*, *87*(9 Supplement 2), S38-S45.

Polich, J. (2007). Updating P300: an integrative theory of P3a and P3b. *Clinical neurophysiology*, *118*(10), 2128-2148.

Polich, J. (2012). Neuropsychology of P300. In Luck, S. J., & Kappenman, E. S. (Eds.). *The Oxford handbook of event-related potential components* (pp.160–188). Oxford University Press.

Polich, J., Howard, L., & Starr, A. (1983). P300 latency correlates with digit span. *Psychophysiology*, *20*(6), 665-669.

Pravatà, E., Rocca, M. A., Valsasina, P., Riccitelli, G. C., Gobbi, C., Comi, G., ... & Filippi, M. (2017). Gray matter trophism, cognitive impairment, and depression in patients with multiple sclerosis. *Multiple Sclerosis Journal*, *23*(14), 1864-1874.

Pröbstel, A. K., Dornmair, K., Bittner, R., Sperl, P., Jenne, D., Magalhaes, S., ... & Derfuss, T. (2011). Antibodies to MOG are transient in childhood acute disseminated encephalomyelitis. *Neurology*, *77*(6), 580-588.

Proudfoot, M., Woolrich, M. W., Nobre, A. C., & Turner, M. R. (2014). Magnetoencephalography. *Practical neurology*, *14*(5), 336-343.

Quraan, M. A., McCormick, C., Cohn, M., Valiante, T. A., & McAndrews, M. P. (2013). Altered resting state brain dynamics in temporal lobe epilepsy can be observed in spectral power, functional connectivity and graph theory metrics. *PloS one*, *8*(7).

Raj, A., & Powell, F. (2018). Models of network spread and network degeneration in brain disorders. *Biological Psychiatry: Cognitive Neuroscience and Neuroimaging*, *3*(9), 788-797.

Ramanathan, S., Brilot, F., Irani, S. R., & Dale, R. C. (2023). Origins and immunopathogenesis of autoimmune central nervous system disorders. *Nature Reviews Neurology*, *19*(3), 172-190.

Rapaport, H., Seymour, R. A., Benikos, N., He, W., Pellicano, E., Brock, J., & Sowman, P. F. (2023). Investigating predictive coding in younger and older children using MEG and a multi-feature auditory oddball paradigm. *Cerebral Cortex*, *33*(12), 7489-7499.

R Core Team (2022). *R: A language and environment for statistical computing*. R Foundation for Statistical Computing, Vienna, Austria. https://www.R-project.org/.

Reindl, M., Di Pauli, F., Rostásy, K., & Berger, T. (2013). The spectrum of MOG autoantibody-associated demyelinating diseases. *Nature Reviews Neurology*, *9*(8), 455.

Rescorla, L., Ivanova, M. Y., Achenbach, T. M., Begovac, I., Chahed, M., Drugli, M. B., ... & Zhang, E. Y. (2012). International epidemiology of child and adolescent psychopathology II: integration and applications of dimensional findings from 44 societies. *Journal of the American Academy of Child & Adolescent Psychiatry*, *51*(12), 1273-1283.

Reuter, M., Tisdall, M. D., Qureshi, A., Buckner, R. L., van der Kouwe, A. J., & Fischl, B. (2015). Head motion during MRI acquisition reduces gray matter volume and thickness estimates. *Neuroimage*, *107*, 107-115.

Riggins, T., & Scott, L. S. (2020). P300 development from infancy to adolescence. *Psychophysiology*, *57*(7), e13346.

Roca, P., Presentación-Herrero, M. J., Miranda-Casas, A., Mulas, F., & Ortiz-Sanchez, P. (2014). The P300 component as a neurophysiological correlate of behavioural working

memory in adolescents with attention deficit hyperactivity disorder. *Revista de Neurologia*, *58*, S51-6.

Rosch, R. E., Wright, S., Cooray, G., Papadopoulou, M., Goyal, S., Lim, M., ... & Friston, K. J. (2018). NMDA-receptor antibodies alter cortical microcircuit dynamics. *Proceedings of the National Academy of Sciences*, *115*(42), E9916-E9925.

Rossor, T., Benetou, C., Wright, S., Duignan, S., Lascelles, K., Robinson, R., ... & Hacohen, Y. (2020). Early predictors of epilepsy and subsequent relapse in children with acute disseminated encephalomyelitis. *Multiple Sclerosis Journal*, *26*(3), 333-342.

Rossor, T., Benetou, C., Wright, S., Duignan, S., Lascelles, K., Robinson, R., ... & Lim, M. (2019). Early predictors of epilepsy and subsequent relapse in children with acute disseminated encephalomyelitis. *Multiple Sclerosis Journal*, 1352458518823486.

Routley, B., Shaw, A., Muthukumaraswamy, S. D., Singh, K. D., & Hamandi, K. (2020). Juvenile myoclonic epilepsy shows increased posterior theta, and reduced sensorimotor beta resting connectivity. *Epilepsy research*, *163*, 106324.

Rubinov, M., & Sporns, O. (2010). Complex network measures of brain connectivity: uses and interpretations. *Neuroimage*, *52*(3), 1059-1069.

Ryan, N. P., Catroppa, C., Beare, R., Silk, T. J., Crossley, L., Beauchamp, M. H., ... & Anderson, V. A. (2016). Theory of mind mediates the prospective relationship between abnormal social brain network morphology and chronic behavior problems after pediatric traumatic brain injury. *Social Cognitive and Affective Neuroscience*, *11*(4), 683-692.

Sakai, K., Yoshita, M., Samuraki, M., & Yamada, M. (2011). Acute disseminated encephalomyelitis with medial temporal lesions. *Clinical neurology and neurosurgery*, *113*(1), 72-74.

Salmond, C. H., Vargha-Khadem, F., Gadian, D. G., de Haan, M., & Baldeweg, T. (2007). Heterogeneity in the patterns of neural abnormality in autistic spectrum disorders: evidence from ERP and MRI. *Cortex*, *43*(6), 686-699.

Sargolzaei, S., Cabrerizo, M., Goryawala, M., Eddin, A. S., & Adjouadi, M. (2015). Scalp EEG brain functional connectivity networks in pediatric epilepsy. *Computers in biology and medicine*, *56*, 158-166.

Schimmel, M., Frühwald, M. C., & Bien, C. G. (2018). Limbic encephalitis with LGI1 antibodies in a 14-year-old boy. *European Journal of Paediatric Neurology*, *22*(1), 190-193.

Schmitt, S. E., Pargeon, K., Frechette, E. S., Hirsch, L. J., Dalmau, J., & Friedman, D. (2012). Extreme delta brush: a unique EEG pattern in adults with anti-NMDA receptor encephalitis. *Neurology*, *79*(11), 1094-1100.

Schölvinck, M. L., Leopold, D. A., Brookes, M. J., & Khader, P. H. (2013). The contribution of electrophysiology to functional connectivity mapping. *Neuroimage*, *80*, 297-306.

Schoonhoven, D. N., Fraschini, M., Tewarie, P., Uitdehaag, B. M., Eijlers, A. J., Geurts, J. J., ... & Strijbis, E. M. (2018). Resting-state MEG measurement of functional activation as a biomarker for cognitive decline in MS. *Multiple Sclerosis Journal*, 1352458518810260.

Shim, Y., Kim, S. Y., Kim, H., Hwang, H., Chae, J. H., Choi, J., ... & Lim, B. C. (2020). Clinical outcomes of pediatric Anti-NMDA receptor encephalitis. *European Journal of Paediatric Neurology*, *29*, 87-91.

Singh, K. D. (2012). Which “neural activity” do you mean? fMRI, MEG, oscillations and neurotransmitters. *Neuroimage*, *62*(2), 1121-1130.

Sled, J. G., Zijdenbos, A. P., & Evans, A. C. (1998). A nonparametric method for automatic correction of intensity nonuniformity in MRI data. *IEEE transactions on medical imaging*, *17*(1), 87-97.

Sosu, E. M., & Schmidt, P. (2017). Tracking emotional and behavioral changes in childhood: Does the Strength and Difficulties Questionnaire measure the same constructs across time?. *Journal of Psychoeducational Assessment*, *35*(7), 643-656.

Spilling, C. A., Jones, P. W., Dodd, J. W., & Barrick, T. R. (2019). Disruption of white matter connectivity in chronic obstructive pulmonary disease. *PloS one*, *14*(10), e0223297.

Sprawls, P. (2000). *Magnetic resonance imaging: principles, methods, and techniques*. Madison: Medical Physics Publishing.

Stam, C. J., & Reijneveld, J. C. (2007). Graph theoretical analysis of complex networks in the brain. *Nonlinear biomedical physics*, *1*(1), 3.

Stenroos, M., Hunold, A., & Haueisen, J. (2014). Comparison of three-shell and simplified volume conductor models in magnetoencephalography. *Neuroimage*, *94*, 337-348.

Steriade, C., Britton, J., Dale, R. C., Gadoth, A., Irani, S. R., Linnoila, J., ... & Bien, C. G. (2020). Acute symptomatic seizures secondary to autoimmune encephalitis and autoimmune-associated epilepsy: Conceptual definitions. *Epilepsia*, *61*(7), 1341-1351.

Stone, J. V. (2002). Independent component analysis: an introduction. *Trends in cognitive sciences*, *6*(2), 59-64.

Sundgren, M., Nikulin, V. V., Maurex, L., Wahlin, Å., Piehl, F., & Brismar, T. (2015). P300 amplitude and response speed relate to preserved cognitive function in relapsing–remitting multiple sclerosis. *Clinical Neurophysiology*, *126*(4), 689-697.

Symmonds, M., Moran, C. H., Leite, M. I., Buckley, C., Irani, S. R., Stephan, K. E., ... & Moran, R. J. (2018). Ion channels in EEG: isolating channel dysfunction in NMDA receptor antibody encephalitis. *Brain*, *141*(6), 1691-1702.

Tadel, F., Baillet, S., Mosher, J. C., Pantazis, D., & Leahy, R. M. (2011). Brainstorm: a user-friendly application for MEG/EEG analysis. *Computational intelligence and neuroscience*, *2011*, 1-13.

Tadel, F., Bock, E., Ramirez, R. R., Mosher, J. C., Leahy, R. M. (12 October 2021). *Tutorial 22: Source Estimation*. Retrieved 27 of June 2023 from https://neuroimage.usc.edu/brainstorm/Tutorials/SourceEstimation

Takahashi, T., Yamanishi, T., Nobukawa, S., Kasakawa, S., Yoshimura, Y., Hiraishi, H., ... & Kikuchi, M. (2017). Band-specific atypical functional connectivity pattern in childhood autism spectrum disorder. *Clinical Neurophysiology*, *128*(8), 1457-1465.

Tan, A., Hague, C., Greenberg, B. M., & Harder, L. (2018). Neuropsychological outcomes of paediatric demyelinating diseases: a review. *Child Neuropsychology*, *24*(5), 575-597.

Tanabe, T., Kashiwagi, M., Shimakawa, S., Fukui, M., Kadobayashi, K., Azumakawa, K., ... & Wakamiya, E. (2013). Behavioral assessment of Japanese children with epilepsy using SDQ (strengths and difficulties questionnaire). *Brain and Development*, *35*(1), 81-86.

Tardif, C. L., Collins, D. L., & Pike, G. B. (2009). Sensitivity of voxel-based morphometry analysis to choice of imaging protocol at 3 T. *Neuroimage*, *44*(3), 827-838.

Taulu, S., & Simola, J. (2006). Spatiotemporal signal space separation method for rejecting nearby interference in MEG measurements. *Physics in Medicine & Biology*, *51*(7), 1759.

Tenembaum, S., Chamoles, N., & Fejerman, N. (2002). Acute disseminated encephalomyelitis: a long-term follow-up study of 84 paediatric patients. *Neurology*, *59*(8), 1224-1231.

Tewarie, P., Schoonheim, M. M., Stam, C. J., van der Meer, M. L., van Dijk, B. W., Barkhof, F., ... & Hillebrand, A. (2013). Cognitive and clinical dysfunction, altered MEG resting-state networks and thalamic atrophy in multiple sclerosis. *PloS one*, *8*(7), e69318.

Tewarie, P., van Dellen, E., Hillebrand, A., & Stam, C. J. (2015). The minimum spanning tree: an unbiased method for brain network analysis. *Neuroimage*, *104*, 177-188.

Thatcher, R. W., Soler, E. P., North, D. M., & Otte, G. (2020). Independent Components Analysis "Artifact Correction" Distorts EEG Phase in Artifact Free Segments. *J Neurol Neurobiol*, *6*(4), 5-7.

Titulaer, M. J., McCracken, L., Gabilondo, I., Armangué, T., Glaser, C., Iizuka, T., ... & Aguilar, E. (2013). Treatment and prognostic factors for long-term outcome in patients with anti-NMDA receptor encephalitis: an observational cohort study. *The Lancet Neurology*, *12*(2), 157-165.

Trinka, E., Cock, H., Hesdorffer, D., Rossetti, A. O., Scheffer, I. E., Shinnar, S., ... & Lowenstein, D. H. (2015). A definition and classification of status epilepticus–Report of the ILAE Task Force on Classification of Status Epilepticus. *Epilepsia*, *56*(10), 1515-1523.

Uchigami, H., Arai, N., Sekiguchi, M., Ogawa, A., Yasuda, T., Seto, A., ... & Takeuchi, S. (2020). Anti-myelin oligodendrocyte glycoprotein antibody-positive acute disseminated encephalomyelitis mimicking limbic encephalitis: A case report. *Multiple sclerosis and related disorders*, *38*, 101500.

Uohashi, T., Kitamura, Y., Ishizu, S., Okamoto, M., Yamada, N., & Kuroda, S. (2006). Analysis of magnetic source localization of P300 using the multiple signal classification algorithm. *Psychiatry and clinical neurosciences*, *60*(6), 645-651.

van Dellen, E., Douw, L., Hillebrand, A., de Witt Hamer, P. C., Baayen, J. C., Heimans, J. J., ... & Stam, C. J. (2014). Epilepsy surgery outcome and functional network alterations in longitudinal MEG: a minimum spanning tree analysis. *Neuroimage*, *86*, 354-363.

van Dellen, E., Douw, L., Hillebrand, A., Ris-Hilgersom, I. H., Schoonheim, M. M., Baayen, J. C., ... & Reijneveld, J. C. (2012). MEG network differences between low-and high-grade glioma related to epilepsy and cognition. *PloS one*, *7*(11), e50122.

van der Ende, J., Verhulst, F. C., & Tiemeier, H. (2016). The bidirectional pathways between internalizing and externalizing problems and academic performance from 6 to 18 years. *Development and psychopathology*, *28*(3), 855-867.

van den Heuvel, M. P., de Lange, S. C., Zalesky, A., Seguin, C., Yeo, B. T., & Schmidt, R. (2017). Proportional thresholding in resting-state fMRI functional connectivity networks and consequences for patient-control connectome studies: Issues and recommendations. *Neuroimage*, *152*, 437-449.

van Dinteren, R., Arns, M., Jongsma, M. L., & Kessels, R. P. (2014). P300 development across the lifespan: a systematic review and meta-analysis. *PloS one*, *9*(2), e87347.

van Mierlo, P., Höller, Y., Focke, N. K., & Vulliemoz, S. (2019). Network perspectives on epilepsy using EEG/MEG source connectivity. *Frontiers in neurology*, *10*, 721.

van Sonderen, A., Arends, S., Tavy, D. L., Bastiaansen, A. E., De Bruijn, M. A., Schreurs, M. W., ... & Titulaer, M. J. (2018). Predictive value of electroencephalography in anti-NMDA receptor encephalitis. J Neurol Neurosurg Psychiatry, 89(10), 1101-1106.

Van Veen, B. D., Van Drongelen, W., Yuchtman, M., & Suzuki, A. (1997). Localization of brain electrical activity via linearly constrained minimum variance spatial filtering. *IEEE Transactions on biomedical engineering*, *44*(9), 867-880.

Venkatesan, A., & Jagdish, B. (2019). Imaging in encephalitis. In *Seminars in neurology* (Vol. 39, No. 03, pp. 312-321). Thieme Medical Publishers.

Verstraete, E., Veldink, J. H., Hendrikse, J., Schelhaas, H. J., van den Heuvel, M. P., & van den Berg, L. H. (2012). Structural MRI reveals cortical thinning in amyotrophic lateral sclerosis. *Journal of Neurology, Neurosurgery & Psychiatry*, *83*(4), 383-388.

Vinck, M., Oostenveld, R., Van Wingerden, M., Battaglia, F., & Pennartz, C. M. (2011). An improved index of phase-synchronization for electrophysiological data in the

presence of volume-conduction, noise and sample-size bias. *Neuroimage*, *55*(4), 1548-1565.

Vogrig, A., Joubert, B., André-Obadia, N., Gigli, G. L., Rheims, S., & Honnorat, J. (2019). Seizure specificities in patients with antibody-mediated autoimmune encephalitis. *Epilepsia*, *60*(8), 1508-1525.

Volz, M. S., Finke, C., Harms, L., Jurek, B., Paul, F., Flöel, A., & Prüss, H. (2016). Altered paired associative stimulation-induced plasticity in NMDAR encephalitis. *Annals of clinical and translational neurology*, *3*(2), 101-113.

von Schwanenflug, N., Krohn, S., Heine, J., Paul, F., Prüss, H., & Finke, C. (2022a). State-dependent signatures of anti-N-methyl-d-aspartate receptor encephalitis. *Brain communications*, *4*(1), fcab298.

von Schwanenflug, N., Ramirez-Mahaluf, J. P., Krohn, S., Romanello, A., Heine, J., Prüss, H., ... & Finke, C. (2022b). Reduced resilience of brain state transitions in anti-N-Methyl-D-Aspartate receptor encephalitis. *European Journal of Neuroscience*.

von Schwanenflug, N., Ramirez-Mahaluf, J. P., Krohn, S., Romanello, A., Heine, J., Prüss, H., ... & Finke, C. (2023). Reduced resilience of brain state transitions in anti-N-methyl-D-aspartate receptor encephalitis. *European Journal of Neuroscience*, *57*(3), 568-579.

Wagner, J., Weber, B., & Elger, C. E. (2015). Early and chronic gray matter volume changes in limbic encephalitis revealed by voxel-based morphometry. Epilepsia, 56(5), 754-761.

Wagstyl, K., & Lerch, J. P. (2018). Cortical thickness. In *Brain morphometry* (pp. 35-49). Humana Press, New York, NY.

Walker, D. A. (2003). JMASM9: converting Kendall's tau for correlational or meta-analytic analyses. *Journal of Modern Applied Statistical Methods*, *2*(2), 26.

Wang, K., Chen, Z., Wu, D., Ding, Q., Zheng, X., Wang, J., ... & Luo, B. (2019). Early second-line therapy is associated with improved episodic memory in anti-NMDA receptor encephalitis. *Annals of Clinical and Translational Neurology*, *6*(7), 1202-1213.

Wang, J., Duan, Y., Zhang, T., Huang, J., Ren, Z., Ye, J., ... & Liu, Y. (2021). Aberrant multimodal brain networks in patients with anti-NMDA receptor encephalitis. *CNS Neuroscience & Therapeutics*, *27*(6), 652-663.

Watson, C. G., DeMaster, D., & Ewing-Cobbs, L. (2019). Graph theory analysis of DTI tractography in children with traumatic injury. *NeuroImage: Clinical*, *21*, 101673.

Watson, C.G. (2020). brainGraph: Graph Theory Analysis of Brain MRI Data. R package version 3.0.0. https://github.com/cwatson/brainGraph

Wechsler, D. (2014). *Wechsler Intelligence Scale for Children (5th ed.)*. San Antonio, TX: NCS Pearson.

Wells, E., Hacohen, Y., Waldman, A., Tillema, J. M., Soldatos, A., Ances, B., ... & Gaillard, W. (2018). Neuroimmune disorders of the central nervous system in children in the molecular era. *Nature Reviews Neurology*, *14*(7), 433-445.

Whelan, R., Lonergan, R., Kiiski, H., Nolan, H., Kinsella, K., Bramham, J., ... & Tubridy, N. (2010). A high-density ERP study reveals latency, amplitude, and topographical differences in multiple sclerosis patients versus controls. *Clinical neurophysiology*, *121*(9), 1420-1426.

Whittle, S., Vijayakumar, N., Simmons, J. G., & Allen, N. B. (2020). Internalizing and externalizing symptoms are associated with different trajectories of cortical development during late childhood. *Journal of the American Academy of Child & Adolescent Psychiatry*, *59*(1), 177-185.

Wilde, E. A., Merkley, T. L., Bigler, E. D., Max, J. E., Schmidt, A. T., Ayoub, K. W., ... & Chu, Z. D. (2012). Longitudinal changes in cortical thickness in children after traumatic brain injury and their relation to behavioral regulation and emotional control. *International Journal of Developmental Neuroscience*, *30*(3), 267-276.

Williams, V. J., Juranek, J., Cirino, P., & Fletcher, J. M. (2018). Cortical thickness and local gyrification in children with developmental dyslexia. *Cerebral Cortex*, *28*(3), 963-973.

Winkler, A. M., Kochunov, P., Blangero, J., Almasy, L., Zilles, K., Fox, P. T., ... & Glahn, D. C. (2010). Cortical thickness or grey matter volume? The importance of selecting the phenotype for imaging genetics studies. *Neuroimage*, *53*(3), 1135-1146.

Witton, C., Furlong, P. L., & Seri, S. (2019). Technological challenges of paediatric MEG and potential solutions: the aston experience. *Magnetoencephalography: From Signals to Dynamic Cortical Networks*, 757-768.

Wright S. & Vincent A. (2019). Autoimmune epilepsies and encephalopathies. In M. Bureau, P. Genton, C. Dravet, A.V. Delgado-escueta, R. Guerrini, C.A. Tassinari, P. Thomas & P. Wolf (Eds.), *Epileptic Syndromes in Infancy*, Childhood and Adolescence 6th ed (pp. 497-511). London: John Libbey Eurotext.

Wu, C., Xiang, J., Jiang, W., Huang, S., Gao, Y., Tang, L., ... & Wang, X. (2017). Altered effective connectivity network in childhood absence epilepsy: a multi-frequency MEG study. *Brain topography*, *30*(5), 673-684.

Xu, J., Guo, Y., Li, J., Lv, X., Zhang, J., Zhang, J., ... & Tian, Y. (2022). Progressive cortical and sub-cortical alterations in patients with anti-N-methyl-d-aspartate receptor encephalitis. *Journal of Neurology*, *269*(1), 389-398.

Xu, N., Shan, W., Qi, J., Wu, J., & Wang, Q. (2021). Presurgical Evaluation of Epilepsy Using Resting-State MEG Functional Connectivity. *Frontiers in Human Neuroscience*, *15*, 649074.

Yang, J. C., Simon, C., Niu, Y. Q., Bogost, M., Schneider, A., Tassone, F., ... & Olichney, J. M. (2013). Phenotypes of hypofrontality in older female fragile X premutation carriers. *Annals of neurology*, *74*(2), 275-283.

Yeo, B. T., Krienen, F. M., Sepulcre, J., Sabuncu, M. R., Lashkari, D., Hollinshead, M., ... & Fischl, B. (2011). The organization of the human cerebral cortex estimated by intrinsic functional connectivity. *J. Neurophysiol*, *106*, 1125–1165.

Yeshokumar, A., Gordon-Lipkin, E., Arenivas, A., Rosenfeld, M., Patterson, K., Blum, R., ... & Probasco, J. (2022). Younger age at onset is associated with worse long-term behavioral outcomes in anti-NMDA receptor encephalitis. *Neurology-Neuroimmunology Neuroinflammation*, *9*(5).

Yeshokumar, A. K., Coughlin, A., Fastman, J., Psaila, K., Harmon, M., Randell, T., ... & Jette, N. (2021). Seizures in autoimmune encephalitis—A systematic review and quantitative synthesis. *Epilepsia*, *62*(2), 397-407.

Yeshokumar, A. K., Gordon-Lipkin, E., Arenivas, A., Cohen, J., Venkatesan, A., Saylor, D., & Probasco, J. C. (2017). Neurobehavioral outcomes in autoimmune encephalitis. *Journal of neuroimmunology*, *312*, 8-14.

Youssofzadeh, V., Agler, W., Tenney, J. R., & Kadis, D. S. (2018). Whole-brain MEG connectivity-based analyses reveals critical hubs in childhood absence epilepsy. *Epilepsy research*, *145*, 102-109.

Youthinmind (2016, June 20). Scoring the Strengths & Difficulties Questionnaire for age 4-17 or 18+. Retrieved 26 June 2021 from https://www.sdqinfo.org/py/sdqinfo/b3.py?language=Englishqz(UK)

Zalesky, A., Fornito, A., & Bullmore, E. T. (2010). Network-based statistic: identifying differences in brain networks. *Neuroimage*, *53*(4), 1197-1207.

Zhang, T., Duan, Y., Ye, J., Xu, W., Shu, N., Wang, C., ... & Liu, Y. (2018). Brain MRI characteristics of patients with anti-N-methyl-D-aspartate receptor encephalitis and their associations with 2-year clinical outcome. *American Journal of Neuroradiology*, *39*(5), 824-829.

Zhang, J., Feng, J., Zhang, Y., Mo, S., Dong, J., Zhu, H., ... & Chen, D. (2021). Resting-State MEG Source Space Network Metrics Associated with the Duration of Temporal Lobe Epilepsy. *Brain topography*, *34*(6), 731-744.

Zhou, D., Lebel, C., Evans, A., & Beaulieu, C. (2013). Cortical thickness asymmetry from childhood to older adulthood. *Neuroimage*, *83*, 66-74

Appendix 2.1

Clinical data of the encephalitis group in Chapter 2

ID	Diagnosis	Age at MRI (year:month)	Disease onset (age in year)	Gender	Antibody positive	mRS at scan	Medication at time of MRI
1	ADEM w/ ON	11:03	6	F	MOG	0	None
2	ADEM w/ Focal epilepsy, ASD, ADHD, Dyspraxia	15:09	2	M	No	1	Keppra
3	NMDAR AE, Learning difficulties, ASD	15:07	1	F	NMDA	3	Keppra, Clobazam
4	ADEM	8:06	3	F	No	0	None
5	ADEM w/Epilepsy	13:04	5	F	No	0	None
6	ADEM	12:07	4	F	MOG	1	None
7	ADEM	7:04	3	M	No	1	None
9	ADEM	9:10	7	F	No	1	None
10	ADEM w/ ON	6:10	2	F	MOG	1	Prednisolone
11	Antibody negative AE	15:04	3	M	No	2	Keppra, methylphenidate
13	RDEM	10:08	8	F	MOG	1	None
14	Brainstem encephalitis, atypical ADEM	6:02	3	M	No	0	None

Note. ADEM = Acute disseminated encephalomyelitis; RDEM = Recurrent disseminated encephalomyelitis ; ON = Optic Neuritis; ASD = Autism spectrum disorder; ADHD = attention deficit hyperactivity disorder; AE = Autoimmune Encephalitis. mRS = modified Rankin Scale.

Appendix 2.2

Qoala-T quality assessment output

The table below outlines the output obtained from the Qoala-T shinyapp after running a first standard pipeline in FreeSurfer, before manual edits were added, for the participants that were not discarded.

Participant ID	Group	MRI scanner	Qoala-T score
1	Encephalitis	Siemens Triotim	Exclude (45.11)
2	Encephalitis	Siemens Triotim	Include(53.29)
3	Encephalitis	Siemens Triotim	Include (79.44)
4	Encephalitis	Siemens Triotim	Exclude (32.73)
5	Encephalitis	Siemens Triotim	Exclude (15.17)
6	Encephalitis	Siemens Triotim	Exclude (49.90)
7	Encephalitis	Siemens Triotim	Exclude (21.56)
9	Encephalitis	Siemens Magnetom prisma	Exclude (15.17)
10	Encephalitis	Siemens Magnetom prisma	Include (66.67)
11	Encephalitis	Siemens Magnetom prisma	Include (53.69)
13	Encephalitis	Siemens Avanto	Exclude (27.54)
14	Encephalitis	Siemens Triotim	Exclude (20.76)
1	Healthy Control	Siemens Magnetom prisma	Include (54.29)
2	Healthy Control	Siemens Magnetom prisma	Include (67.47)
3	Healthy Control	Siemens Magnetom prisma	Include (72.85)
4	Healthy Control	Siemens Magnetom prisma	Include (79.24)
5	Healthy Control	Siemens Magnetom prisma	Include (59.88)
6	Healthy Control	Siemens Magnetom prisma	Include (61.48)
7	Healthy Control	Siemens Magnetom prisma	Include (73.25)
8	Healthy Control	Siemens Magnetom prisma	Exclude (28.34)
9	Healthy Control	Siemens Magnetom prisma	Include (58.88)
10	Healthy Control	Siemens Magnetom prisma	Include (86.83)
11	Healthy Control	Siemens Magnetom prisma	Exclude (48.10)
12	Healthy Control	Siemens Triotim	Exclude (31.74)
13	Healthy Control	Philips Achieva (BCH)	Include (66.87)
14	Healthy Control	Philips Achieva (BCH)	Exclude (42.71)
15	Healthy Control	Philips Achieva (BCH)	Include (52.30)
15	Healthy Control	Philips Achieva (BCH)	Include (56.29)
16	Healthy Control	Philips Achieva (BCH)	Include (63.87)
17	Healthy Control	Philips Achieva (BCH)	Include (68.46)
18	Healthy Control	Philips Achieva (BCH)	Include (48.90)
19	Healthy Control	Philips Achieva (BCH)	Include (66.87)

20	Healthy Control	Philips Achieva (BCH)	Include (56.89)
21	Healthy Control	Philips Achieva (BCH)	Include (50.90)
22	Healthy Control	Philips Achieva (BCH)	Include (66.67)
23	Healthy Control	Philips Achieva (BCH)	Include (49.50)
24	Healthy Control	Philips Achieva (BCH)	Exclude (45.71)
25	Healthy Control	Siemens Triotim	Exclude (19.56)
26	Healthy Control	Siemens Triotim	Exclude (17.37)
27	Healthy Control	Siemens Triotim	Exclude (17.76)
28	Healthy Control	Siemens Triotim	Exclude (24.95)
29	Healthy Control	Siemens Triotim	Exclude (29.74)
30	Healthy Control	Siemens Triotim	Exclude (22.55)
31	Healthy Control	Siemens Triotim	Include (51.10)
32	Healthy Control	Siemens Triotim	Exclude (39.72)
33	Healthy Control	Siemens Triotim	Include (80.24)
34	Healthy Control	Siemens Triotim	Exclude (39.72)
35	Healthy Control	Siemens Triotim	Include (75.45)
36	Healthy Control	Siemens Triotim	Include (60.08)
37	Healthy Control	Siemens Triotim	Include (72.65)
38	Healthy Control	Siemens Triotim	Excluded (45.51)
39	Healthy Control	Siemens Triotim	Include (77.05)
40	Healthy Control	Siemens Triotim	Include (80.04)
41	Healthy Control	Siemens Triotim	Exclude (49.90)
42	Healthy Control	Siemens Triotim	Exclude (18.36)
43	Healthy Control	Siemens Triotim	Exclude (34.13)
44	Healthy Control	Siemens Triotim	Exclude (35.13)
45	Healthy Control	Siemens Triotim	Exclude (30.94)
46	Healthy Control	Siemens Triotim	Exclude (26.35)
47	Healthy Control	Siemens Triotim	Exclude (25.35)

Appendix 3.1

Clinical data of the sample in Chapter 3

ID	Group	Diagnosis	Age at MEG (year)	Disease duration (year)	Gender	Antibody positive	Medication at time of MEG
1	Encephalitis	ADEM w/ ON	11	5	F	MOG	NA
2	Encephalitis	ADEM w/ Focal epilepsy, ASD, ADHD, Dyspraxia	15	13	M	No	Keppra
3	Encephalitis	NMDAR AE, Learning difficulties, ASD	15	14	F	NMDA	Keppra, Clobazam
4	Encephalitis	ADEM	8	5	F	No	NA
5	Encephalitis	ADEM w/Epilepsy	13	8	F	No	NA
6	Encephalitis	ADEM	12	8	F	MOG	NA
7	Encephalitis	ADEM	7	4	M	No	NA
8	Encephalitis	MOGab AE	15	2	M	MOG	Keppra
9	Encephalitis	ADEM	9	3	F	No	NA
10	Encephalitis	ADEM w/ ON	6	4	F	MOG	Prednisolone
11	Encephalitis	Antibody negative AE	15	12	M	No	Keppra, methylphenidate
12	Encephalitis	ADEM	8	3	M	MOG	NA
		Etiology					
1	Epilepsy	DNET	8	7	M	NA	Topiramate, Valproate
2	Epilepsy	FCD	14	10	F	NA	Phenytoin, Valproate, Clobazam
3	Epilepsy	FCD	17	12	F	NA	Parampanel, Lamotrigine, Clobazam, Melatonin
4	Epilepsy	MTS	12	12	M	NA	Topiramate, Lamotrigine, Rufinamide
5	Epilepsy	TS	15	6	M	NA	NA
6	Epilepsy	FCD	16	4	F	NA	Levetiracetam, Tegratol
7	Epilepsy	TS	14	7	F	NA	Lamotrigine, Oxcarbazepine, Clobazam

8	Epilepsy	Stroke	16	16	F	NA	Zonisamide, Carbamazipine, Ketogenic diet
9	Epilepsy	FCD	15	3	F	NA	Oxcarbazepine
10	Epilepsy	FCD	17	7	F	NA	Carbamazepine, Clobazam, Parampanel
11	Epilepsy	FCD	10	3	M	NA	Valproate, Oxcarbazepine
12	Epilepsy	Unknown	18	14	M	NA	Levetiracetam, Oxcarbazepine
13	Epilepsy	FCD	7	2	M	NA	Carbamazepine, Lamotrigine, Clobazam
14	Epilepsy	Left temporal abnormality	9	6	M	NA	Carbamazepine, Keppra
15	Epilepsy	Left posterior parietal-occipital gliosis	14	12	M	NA	Phenobarbital, Lamotrigine, Parampanel
16	Epilepsy	Bilateral gliosis with left insular cortex atrophy	15	15	F	NA	Lamotrigine, Valproate, Ketogenic diet
17	Epilepsy	Central white matter loss with left hemisphere infarct	5	2	M	NA	Prednisolone, Keppra, Carbamazepine
18	Epilepsy	Left posterior quadrant epilepsy	10	8	F	NA	Lamotrigine, Zonisamide

Note. ADEM = Acute disseminated encephalomyelitis; ON = Optic Neuritis; ASD = Autism spectrum disorder; ADHD = Attention deficit hyperactivity disorder; AE = Autoimmune Encephalitis; DNET = Dysembroplastic neuroepithelial tumour; FCD = Focal cortical dysplasia; MTS = Mesial temporal sclerosis; TS = Tuberous sclerosis.

Appendix 3.2

Exploratory network analyses in alpha and beta frequency oscillations

A.3.2.1 Comparison of network measures between Epilepsy and Control groups

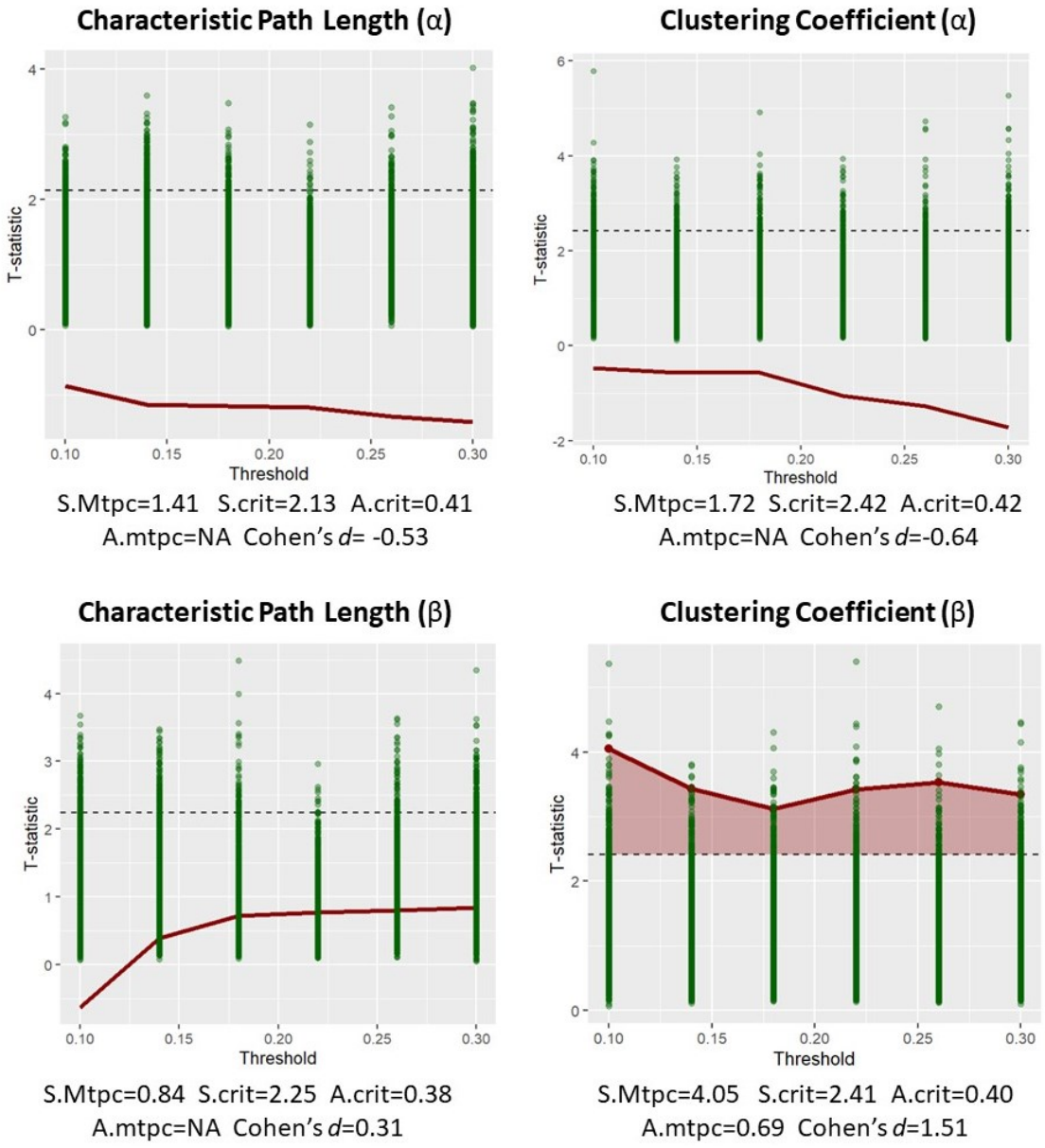

Note. S.mtpc = maximum observed statistic; S.crit = critical value of the null max. statistic; A.crit = mean of the supra-critical null AUCs; A.mtpc = AUC value of supracritical cluster.
Each graph depicts the network contrast of the Epilepsy group in reference to the Control group. The green dots are the maximum null *t* statistics of the 5000 permutations. Red dots are the observed *t* statistics. The dashed line is the critical null statistic (S.crit, top 95th percentile of the null distribution of maximum *t* statistics). The red shaded areas represent clusters of observed statistics above the critical value, whose area-under-the-curve (A.mtpc) is also greater than the mean areas-under-the-curve of the supracritical permuted statistics (A.crit). This means that a higher shaded red bar is a significantly higher network measure compared to the Control group (at $p < .05$). Non-shaded bars are non-significant. The effect size *d* is only that of the threshold with the largest difference.

A.3.2.2 Comparison of network measures between Epilepsy and Autoimmune Encephalitis

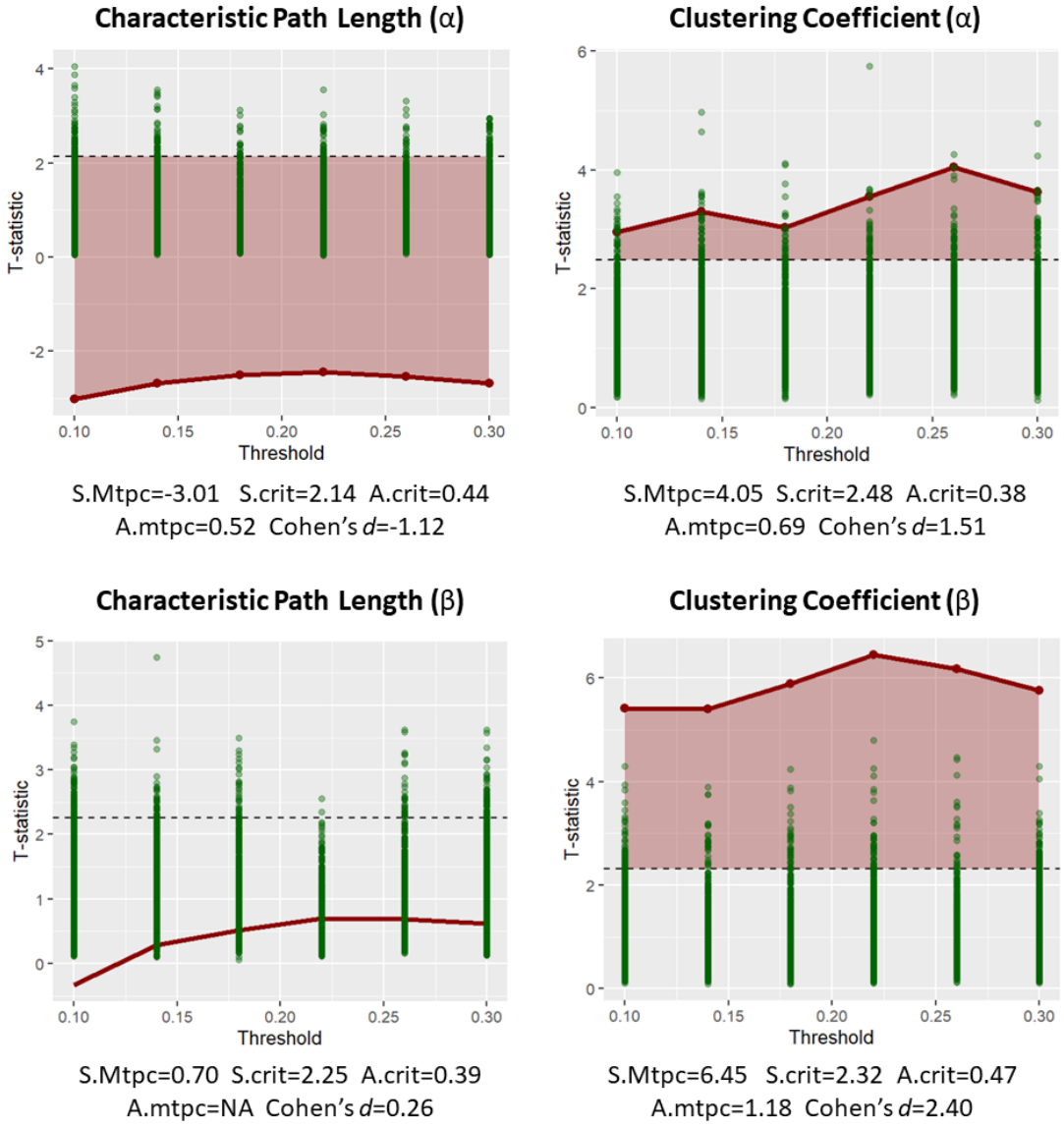

Note. S.mtpc = maximum observed statistic; S.crit = critical value of the null max. statistic; A.crit = mean of the supra-critical null AUCs; A.mtpc = AUC value of supracritical cluster.
Each graph depicts the network contrast of the Epilepsy group in reference to the AE group. The green dots are the maximum null *t* statistics of the 5000 permutations. Red dots are the observed *t* statistics. The dashed line is the critical null statistic (S.crit, top 95th percentile of the null distribution of maximum *t* statistics). The red shaded areas represent clusters of observed statistics above the critical value, whose area-under-the-curve (A.mtpc) is also greater than the mean areas-under-the-curve of the supracritical permuted statistics (A.crit). This means that a lower shaded red bar is a significantly lower network measure compared to the AE group and a higher shaded red bar is a significantly higher network measure compared to the AE group (at $p < .05$). The effect size *d* is only that of the threshold with the largest difference.

A.3.2.3 Comparison of network measures between Autoimmune Encephalitis and Control groups

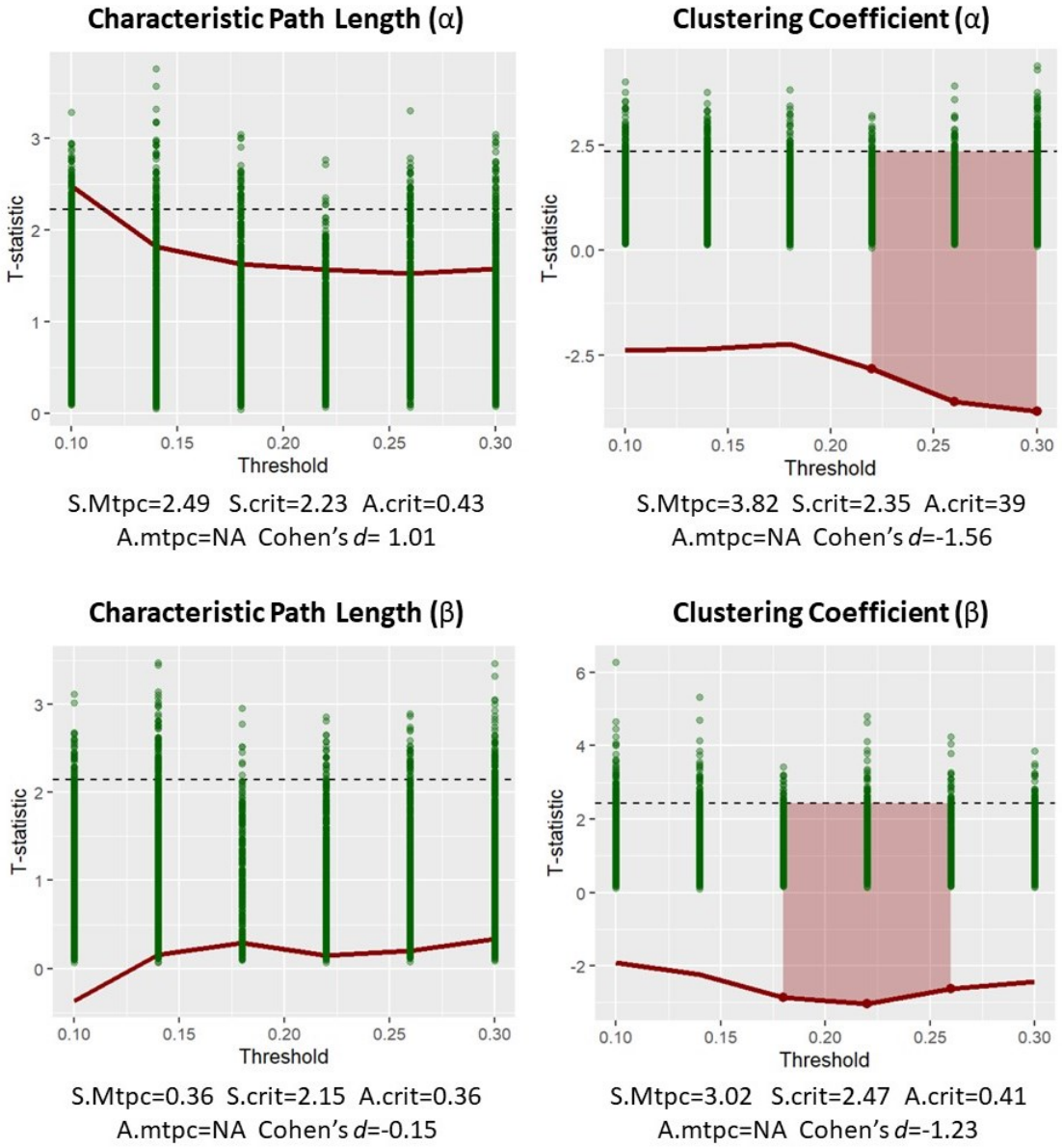

Note. S.mtpc = maximum observed statistic; S.crit = critical value of the null max. statistic; A.crit = mean of the supra-critical null AUCs; A.mtpc = AUC value of supracritical cluster.
Each graph depicts the network contrast of the AE group in reference to the Control group. The green dots are the maximum null *t* statistics of the 5000 permutations. Red dots are the observed *t* statistics. The dashed line is the critical null statistic (S.crit, top 95th percentile of the null distribution of maximum *t* statistics). The red shaded areas represent clusters of observed statistics above the critical value. Note however that here, the area-under-the-curve (A.mtpc) was not returned in the shaded clusters because it was not greater than the mean area-under-the-curve of the supracritical permuted statistics (A.crit). This means network measure compared to the Control group (at $p < .05$) do not have a stable difference across the thresholds despite the clusters of significant differences. The effect size *d* is only that of the threshold with the largest difference.

Appendix 4

Clinical data of the sample in Chapter 4

ID	Group	Diagnosis	Age (years)	Age of onset (years)	Gender	mRS	Antibody positive
401	AE	ADEM, pre-existing communication disorder	5	2	M	2	No
402	AE	RDEM	4	2	F	0	MOG
403	AE	ADEM w/ ON	16	13	F	0	MOG
404	AE	Recurring AE	15	7	F	0	MOG
405	AE	ADEM	10	6	F	1	No
406	AE	ADEM w/Epilepsy	11	3	M	1	No
407	AE	AE w/ON and Epilepsy	14	13	F	1	MOG
408	AE	AE w/ON	8	8	F	0	MOG
409	AE	ADEM	7	6	F	1	No
410	AE	Hashimoto encephalopathy	21	15	F	1	No
411	AE	ADEM	4	3	F	3	No
412	AE	NMDAR-ab AE	11	4	M	5	NMDA
4C1	Control	Recurrent ON	14	9	M	0	No
4C2	Control	Facial pain, headaches, anxiety	17	13	F	1	NA
4C3	Control	Multiple sclerosis	17	12	F	1	NA
4C4	Control	Childhood absence epilepsy	13	9	F	0	NA
4C5	Control	Functional movement disorder	15	14	F	1	NA
4C6	Control	Left hemifacial atrophy, linear scleroderma, right sided focal seizures	5	0	F	1	NA

4C7	Control	Guillain-Barré syndrome	2	11	F	1	NA
4C8	Control	Left frontal AVM rupture, resulting in collapse, migraines	13	11	M	2	NA
4C9	Control	Left middle cerebral artery infarction	4	3	M	2	NA
4C10	Control	SYNGAP-1 related intellectual disability	8	0	F	2	NA
4C11	Control	Dopamine responsive dystonia Segawa syndrome	6	6	F	1	NA
4C12	Control	Paroxysmal symptoms of unknown aetiology, likely functional, ASD, depression	16	15	F	1	NA
4C13	Control	Epilepsy, developmental coordination disorder	13	6	F	1	NA
4C14	Control	Benign tremor	12	3	M	1	NA
4C15	Control	Headaches	11	10	F	0	NA
4C16	Control	Epilepsy since infancy	10	1	M	3	NA
4C17	Control	Global developmental delay, myopathy, seizures	4	0	F	3	NA
4C18	Control	Developmental delay, mainly motor, hypotonia	7	0	F	4	NA
4C19	Control	Williams syndrome, epilepsy	14	0	F	3	NA
4C20	Control	Cerebral palsy secondary to preterm birth at 31 weeks	6	0	M	3	NA
4C21	Control	Cerebral palsy secondary to hypoxic brain injury, severe dev delay, seizures	6	0	M	4	NA
4C22	Control	Generalised epilepsy with myoclonic seizures, developmental delay	6	2	M	3	NA
4C23	Control	Developmental delay, spastic diplegia	5	0	F	3	NA

Note. AE = Autoimmune Encephalitis; ADEM = Acute disseminated encephalomyelitis; RDEM = Recurrent disseminated encephalomyelitis ; ON = Optic Neuritis; ASD = autism spectrum disorder; mRS = modified Rankin Scale; AVM = arteriovenous malformation.

Appendix 5

Clinical data of the encephalitis group in Chapter 5

ID	Diagnosis	Age (year:month)	Disease onset (age in year)	Gender	Antibody positive	mRS at scan	Medication at time of study
1	ADEM w/ ON	11:03	6	F	MOG	0	None
2	ADEM w/Focal epilepsy, ASD, ADHD, Dyspraxia	15:09	2	M	No	1	Keppra
3	NMDAR AE, Learning difficulties, ASD	15:07	1	F	NMDA	3	Keppra, Clobazam
4	ADEM	8:06	3	F	No	0	None
5	ADEM w/Epilepsy	13:04	5	F	No	0	None
6	ADEM	12:07	4	F	MOG	1	None
7	ADEM	7:04	3	M	No	1	None
8	MOGab AE	15:06	13	M	MOG	1	Keppra
9	ADEM	9:10	7	F	No	1	None
10	ADEM w/ ON	6:10	2	F	MOG	1	Prednisolone
11	Antibody negative AE	15:04	3	M	No	2	Keppra, methylphenidate
12	ADEM	8:09	5	M	MOG	0	None
13	RDEM	10:08	8	F	MOG	1	None

Note. ADEM = Acute disseminated encephalomyelitis; RDEM = Recurrent disseminated encephalomyelitis ; ON = Optic Neuritis; ASD = autism spectrum disorder; ADHD = Attention deficit hyperactivity disorder; AE = Autoimmune Encephalitis. mRS = modified Rankin Scale

Appendix 6

Abstract presented orally for the Encephalitis Conference 2021

https://acnr.co.uk/conference-reports/encephalitis-conference-2021/

Investigating long-term neuropsychological outcomes in paediatric autoimmune encephalitis using magnetoencephalography

Authors: Mr Charly Billaud, Dr Daniel King, Prof Evangeline Wassmer, Dr Elaine Foley, Ms. Lydiah Makusha, Prof. Klaus Kessler, Prof. Amanda Wood, Dr Sukhvir Wright

Paediatric autoimmune encephalitis is an inflammatory brain disease that causes cognitive deficits, psychiatric symptoms, seizures, altered mental status, MRI and EEG abnormalities. A subset of patients also experience residual cognitive or behavioural difficulties months to years after onset. There is a need to identify factors which can predict children at risks of such long-term difficulties.

Magnetoencephalography (MEG) is a functional neuroimaging modality which measures magnetic flux on the surface of the head associated with underlying neuronal electrical currents with high temporal resolution and (when combined with structural MRI) reasonable spatial resolution. Although its clinical use has been identified in paediatric conditions such as epilepsy, MEG has received little attention in research about pediatric immune-mediated encephalitis. MEG could enable us to understand the effect of autoimmune encephalitis on the still-developing cortical networks of the pediatric brain.

A cohort of n=20 children with a diagnosis of autoimmune encephalitis (including anti-NMDA encephalitis and ADEM) is currently being recruited from the Birmingham Children's Hospital (UK), at least two years after initial presentation. Participants undergo MEG recordings both at rest (resting-state MEG) and during tasks (auditory oddball and visuomotor paradigms). Participants will also undergo MRI and will complete neuropsychological assessments of educational attainment, behaviour and cognition.

The overall aim of this research in progress is to better understand the relationship between autoimmune encephalitis, differences in the spatiotemporal dynamics of brain networks using MEG and residual neuropsychological impairment. This will enable us to provide an initial assessment of the benefit of MEG in identifying factors which can predict children with autoimmune encephalitis at risks of such long-term difficulties.